BIOMIMETIC NANOCLAY SCAFFOLDS FOR BONE TISSUE ENGINEERING

A Dissertation
Submitted to the Graduate Faculty
of the
North Dakota State University
of Agriculture and Applied Science

By

Avinash Harishchandra Ambre

In Partial Fulfillment of the Requirements
for the Degree of
DOCTOR OF PHILOSOPHY

Major Program:
Materials and Nanotechnology

May 2014

Fargo, North Dakota

North Dakota State University
Graduate School

Title

BIOMIMETIC NANOCLAY SCAFFOLDS FOR BONE TISSUE ENGINEERING

By

Avinash Harishchandra Ambre

The Supervisory Committee certifies that this ***disquisition*** complies with North Dakota State University's regulations and meets the accepted standards for the degree of

DOCTOR OF PHILOSOPHY

SUPERVISORY COMMITTEE:

Dr. Kalpana S. Katti
Co-Chair

Dr. Dinesh R. Katti
Co-Chair

Dr. Sivapalan Gajan

Dr. Anna Grazul-Bilska

Approved:

November 14, 2014
Date

Dr. Erik K. Hobbie
Department Chair

ABSTRACT

Tissue engineering offers a significant potential alternative to conventional methods for rectifying tissue defects by evoking natural regeneration process via interactions between cells and 3D porous scaffolds. Imparting adequate mechanical properties to biodegradable scaffolds for bone tissue engineering is an important challenge and extends from molecular to macroscale. This work focuses on the use of sodium montmorillonite (Na-MMT) to design polymer composite scaffolds having enhanced mechanical properties along with multiple interdependent properties.

Materials design beginning at the molecular level was used in which Na-MMT clay was modified with three different unnatural amino acids and further characterized using Fourier Transform Infrared (FTIR) spectroscopy, X-ray diffraction (XRD). Based on improved bicompatibility with human osteoblasts (bone cells) and intermediate increase in d-spacing of MMT clay (shown by XRD), 5-aminovaleric acid modified clay was further used to prepare biopolymer (chitosan-polygalacturonic acid complex) scaffolds. Osteoblast proliferation in biopolymer scaffolds containing 5-aminovaleric acid modified clay was similar to biopolymer scaffolds containing hydroxyapatite (HAP).

A novel process based on biomineralization in bone was designed to prepare 5-aminovaleric acid modified clay capable of imparting multiple properties to the scaffolds. Bone-like apatite was mineralized in modified clay and a novel nanoclay-HAP hybrid (*in situ* HAPclay) was obtained. FTIR spectroscopy indicated a molecular level organic-inorganic association between the intercalated 5-aminovaleric acid and mineralized HAP. Osteoblasts formed clusters on biopolymer composite films prepared with different weight percent compositions of *in situ* HAPclay. Human MSCs formed mineralized nodules on composite films

and mineralized extracellular matrix (ECM) in composite scaffolds without the use of osteogenic supplements.

Polycaprolactone (PCL), a synthetic polymer, was used for preparing composites (films and scaffolds) containing *in situ* HAPclay. Composite films showed significantly improved nanomechanical properties. Human MSCs formed mineralized ECM on films in absence of osteogenic supplements and were able to infiltrate the scaffolds. Atomic force microscopy imaging of mineralized ECM formed on composite films showed similarities in dimensions, arrangement of collagen and apatite with their natural bone counterparts.

This work indicates the potential of *in situ* HAPclay to impart polymeric scaffolds with osteoinductive, osteoconductive abilities and improve their mechanical properties besides emphasizing nanoclays as cell-instructive materials.

ACKNOWLEDGEMENTS

I would like to begin by thanking my advisor, Prof. Kalpana S. Katti, for her continuous guidance, support and encouragement throughout the course of my research. Also, I would like to thank her for constantly motivating me to put in my best and work hard persistently. Next, I would also like to acknowledge and thank my co-advisor, Prof. Dinesh R. Katti, for his advice and support during my thesis work. I am grateful to other committee members Prof. Sivapalan Gajan and Prof. Anna Grazul-Bilska for their invaluable suggestions, helpful discussions and feedback. I would like to thank North Dakota EPSCoR for awarding me a Doctoral Dissertation Fellowship. I appreciate the Department of Civil Engineering, NDSU for providing me funding and resources for my doctoral research.

I highly appreciate cell culture laboratory facilities in the Department of Civil Engineering without which it would have been difficult to successfully perform cell culture experiments during my research. I am grateful to all staff members, especially Jan and Milka for their support and help for ordering daily laboratory supplies. I would also like to extend my heartfelt gratitude to all past and present group members for being cooperative and helpful. I would like to thank Scott Payne at NDSU Electron Microscopy Center for his assistance with electron microscopy.

Finally and most importantly, I owe special gratitude to all my family members, especially my mother for encouragement, patience and unconditional support.

TABLE OF CONTENTS

LIST OF TABLES

LIST OF FIGURES

LIST OF ABBREVIATIONS

AFM……Atomic Force Microscopy

ALP…….Alkaline Phosphatase

ANOVA……..Analysis of Variance

BMPs…….....Bone Morphogenetic Proteins

Chi…….....Chitosan

CNTs……..Carbon Nanotubes

DMEM……...Dulbecco's Modified Eagle Medium

ECM……...Extracellular Matrix

FTIR……...Fourier Transform Infrared

hMSCs……Human Mesenchymal Stem Cells

HAP……....Hydroxyapatite

ICAM……..Intercellular adhesion molecule

IGF……..Insulin Growth Factor

Na-MMT…….Sodium Montmorillonite

MSCs.....Mesenchymal Stem Cells

PCL…….Polycaprolactone

PCNs……...Polymer Clay Nanocomposites

PDGF……..Platelet derived growth factor

PPF……..Poly (propylene fumarate)

PEG…….....Poly (ethylene glycol)

PgA……..Polygalacturonic acid

PLLA……...Poly (L-lactic acid)

SEM…….Scanning Electron Microscopy

SSEA……...Stage-specific embryonic antigen

TCPS……...Tissue Culture Polystyrene

VCAM…….Vascular cell adhesion molecule

XRD…….X-ray diffraction

CHAPTER 1. INTRODUCTION[1]

This chapter presents an introduction to tissue engineering and discusses significant factors responsible for the use of 3D scaffolds in tissue engineering studies. It also describes different materials and methods used for fabricating tissue engineering scaffolds. Further, this chapter presents a discussion about cells used for bone tissue engineering and gives a review of mesenchymal stem cells (MSCs). Also, it discusses the potential of polymer clay nanocomposites (PCNs) in bone tissue engineering and choice of materials used for this doctoral research. The contents of this chapter (sections 1.3. & 1.4. including figures) have been published in book chapter by Kalpana S. Katti, Dinesh R. Katti, Avinash H. Ambre, Nanocomposites for Bone Tissue Engineering, Nanomaterials for Life Sciences Vol.8: Nanocomposites, Edited by Challa S.S.R. Kumar, Wiley-VCH Verlag GmbH & Co., 2010. Contents of sections 1.5.1., 1.5.2. and 1.5.3. have been published in book chapter by Kalpana S. Katti, Avinash H. Ambre, Dinesh R. Katti, Mesenchymal Stem Cells in Tissue Regeneration, Integrated Biomaterials in Tissue Engineering, Edited by M. Ramalingam, Z. Haidar, S. Ramakrishna, H. Kobayashi, Y. Haikel, Wiley, Scrivener, 2012. These contents have been modified to accommodate additional information wherever required for presentation in this dissertation.

1.1. Tissue Engineering

Tissue engineering, a continuously evolving interdisciplinary field, gained momentum in the early 1990s when Langer and Vacanti [1] perspicuously described it as an alternative approach having advantages over conventional methods to treat tissue defects and involving

[1] The contents of this chapter [sections 1.3., 1. 4., 1.5.1, 1.5.2., 1.5.3.] were co-authored by Avinash Ambre and Drs. Kalpana Katti and Dinesh Katti. Avinash Ambre conducted literature search, review for these sections and also wrote, revised these sections. Drs. Kalpana Katti and Dinesh Katti assisted in discussion, compilation and proofreading of these sections.

combined use of cells, scaffolds and growth factors for tissue regeneration. There have been reports related to experiments based on concepts similar to tissue engineering from the early 1930s. In one of these early experiments murine tumor cells enclosed in a polymer membrane showed survival after being implanted in the abdominal cavity of chick embryos [2]. Another study involved culture of murine pancreatic beta cells on synthetic polymer (silicone polycarbonate) capillaries to study their sensitivity to glucose and insulin release behavior [3]. Following these studies "artificial skin" made of collagen and chondroitin 6 sulfate serving as host for migrated fibroblast cells was used to treat skin burn injuries [4]. Extensive research focused on the regeneration of different types of tissues started after Langer and Vacanti [1] described the potential benefits of tissue engineering for tissue regeneration. Tissue engineering research has shown rapid progress, expansion due to the realization of its potential over the years for other therapeutic applications and as a platform for studying different diseases.

Conventional treatment methods to repair tissue defects such as autografts, allografts, xenografts and metallic implants are considered to have limitations. Autograft transplant procedures involving procurement of tissue from a patient's own own body have limitations related to availability of such tissue grafts and injury to the site from where the tissue was obtained. It becomes extremely difficult to use autografts in cases where larger volumes of tissue are required for rectifying the defect. Allograft transplant procedures that involve obtaining tissue from other healthy donor for a patient have risks associated with immune rejection, pathogen transfer and immune rejection. Xenograft transplantations involving use of tissue from an animal donor are limited by immune rejection and pathogen transfer. Metallic implants have been associated with problems such as stress shielding that weakens the surrounding bone, corrosion and their limited functional life (10-15 years). Ceramic implants being brittle may fail

suddenly and polymeric implants may weaken over time due to degradation. Tissue engineering has significant potential to overcome these limitations since it makes use of cell-scaffold interactions to stimulate new tissue formation via natural regeneration process. Besides this, there is a good possibility that the new tissue generated using tissue engineering approach has structural and functional characteristics similar to a natural, healthy tissue.

Scaffolds, cells and growth factors are the key components of tissue engineering (Figure 1.1). Each of these components has been the genesis of several interesting research problems encompassing different science and engineering disciplines. Scaffolds and cells have been the major focus of numerous studies over the course of evolution of tissue engineering since the early 1990s and these studies have laid the foundation for expansion of tissue engineering concepts beyond tissue regeneration. The studies presented in this dissertation deal with the design of polymer composite scaffolds for bone tissue engineering. Experimental investigations related to interactions of human osteoblasts (bone cells), human mesenchymal stem cells (hMSCs) with these scaffolds or scaffold materials also forms a part of these studies.

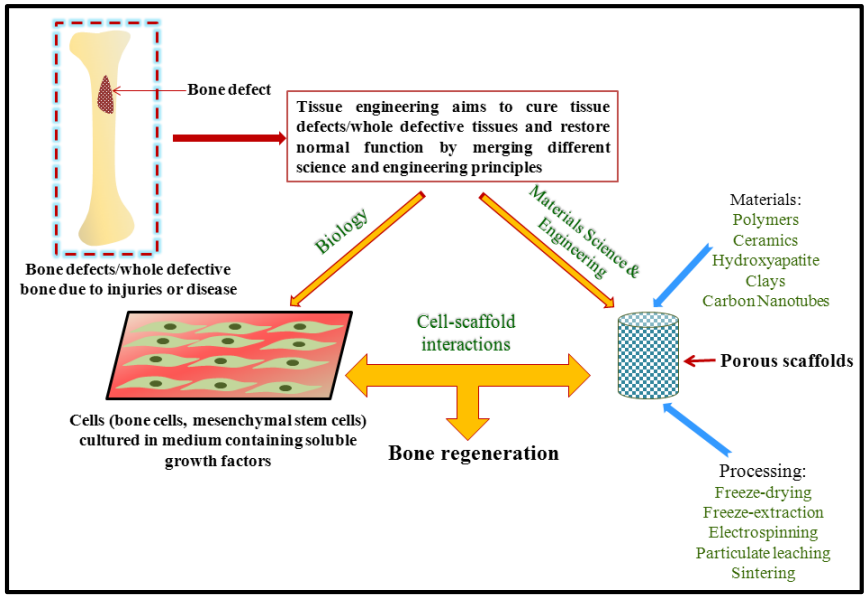

Figure 1.1. Schematic depicting the concept of tissue (e.g. bone) engineering

Tissues are composed of cells and extracellular matrix (ECM). Proteins and polysaccharides constituting the ECM show remarkable diversity and are arranged as a non-woven mesh in close association with the cells that produce them. Differences in the relative amounts of these ECM macromolecules and also in their arrangement give rise to diverse structural forms. Each of these structural forms suit the tissue-specific functional requirements. ECM is considered to be a dynamic, hierarchically organized (molecular scale to macroscale) nanocomposite that provides mechanical support to the cells [5]. It also presents a highly interactive environment to the cells in addition to performing an important role in cellular functions such as adhesion, migration, proliferation, differentiation and morphogenesis. Protein fibers (including both structural and functional) present in the ECM have nanoscale dimensions (10 to several hundred nanometers). An environment consisting of components having nanoscale dimensions is thus thought to be highly conducive to influence cell behavior. Protrusive cellular structures (filopodia and lamellipodia) having nanoscale dimensions are considered to complement such environmental components with nanoscale dimensions [6]. This leads to increase in sensitivity of cells to nanodimensional components or nanoscale features in their surrounding environment. Cells are also responsive to the mechanical and chemical cues from their surrounding environment. Therefore one of the major focus areas in tissue engineering is the development of three dimensional porous scaffolds that have structural and functional traits similar to those of the ECM present in a certain tissue.

Bone is considered a complex nanocomposite having a hierarchical structure extending from nanoscale to macroscale [7]. Besides performing important functions such as protection of vital internal organs, storage of calcium and phosphate based minerals and facilitating movement, bone also provides structural support. The mechanical properties of bone have been

attributed to its hierarchical structure. A major challenge in bone tissue engineering is designing scaffolds with mechanical properties adequate to support biomechanical loads at defect site for restoring mechanical function while the new tissue forms, matures in the scaffolds. Scaffolds need to provide appropriate microenvironment to the cells for tissue formation and also need to satisfy requirements related to porosity, pore size, biodegradability that further enhances the difficulty of designing scaffolds for bone tissue engineering. Among the multiple cues from their surrounding microenvironment cells are known to respond to mechanical cues by converting them in to biochemical signals [8].The mechanical properties required at macroscale to support the biomechanical loads can be different from those required at the sub-micron/molecular scale to influence cell behavior. Mechanical properties of bone tissue engineering scaffolds should be thus enough to provide appropriate mechanical cues to the cells for bone tissue formation and supporting biomechanical loads at the defect site in vivo or the regenerating bone (in case of in vitro bone regeneration). Thus the challenge related to mechanical properties of scaffolds seems to extend from molecular to macroscale.

The following sections in this chapter give a brief overview of the significant reasons for using 3D scaffolds also presents reasons for using 2D substrates (films) for tissue engineering. A description of different materials and methods used for fabricating tissue engineering scaffolds is also presented in these sections. Polymer clay nanocomposites (PCNs) and their potential for bone tissue engineering applications along with major reasons for the choice/selection of materials used for this doctoral research are also presented in the following sections. Further, this chapter discusses cells used for bone tissue engineering and presents a review of mesenchymal stem cells (MSCs).

1.2. Scaffolds: Significance in Tissue Engineering

Scaffolds for tissue engineering are expected to provide a microenvironment to the cells similar to the one cells experience in the extracellular matrix (ECM) under in vivo conditions. Designing scaffolds with a microenvironment similar to the ECM existing in a natural, healthy tissue in vivo can assist in providing cells with appropriate cues useful for regenerating (or engineering) the desired tissue. Compared to two-dimensional (2D) substrates, scaffolds used for tissue engineering studies are considered to provide a more physiological environment to the cells. Recently, fundamental characteristics of three-dimensional (3D) scaffolds apart from their dimensionality factor that make these scaffolds capable of presenting a more physiological environment have been identified and discussed extensively [9]. Cells exhibit relatively different morphology, organization (polarity) when cultured in 3D environment that can directly affect cellular functions. Effect of cell spreading, cell geometry on cellular functions has been well-studied in case of 2D substrates but have been proposed to have dissimilarities with those observed under 3D environment. These dissimilarities arise due to the steric constraints in 3D environment that cells need to overcome for spreading/extension, migration unlike on 2D substrates which are relatively unrestricted. Moreover, local mechanical properties and topography are likely to influence the adhesion between the cells and the surrounding matrix under 3D environment. This may further be responsible for the variations in cell-matrix adhesions under 3D environment. The ways in which the force in transmitted to the cells in 3D environment can differ compared to 2D substrates since cells in 3D environment experience physical constraints during deformation and have different morphology and organization. Cells cultured in a 3D environment are also more likely to experience diffusion dependent gradients of soluble factors in media and oxygen. 3D environment of scaffolds can also provide opportunities

for storage of soluble factors and synchronizing the timing of their release with their spatial presentation to the cells [9]. Although studies performed using 3D scaffolds are more significant in tissue engineering, use of 2D substrates have constituted an important part of several tissue engineering studies. Limitations and difficulties related to currently available experimental techniques (e.g. imaging of non-planar samples) to study specific cell-matrix interactions (e.g., cell adhesions, migration) in 3D environment have contributed to the use of 2D substrates. Besides this, fabrication methods having a control over surface morphology (at subcellular scale to nanoscale) of 3D scaffolds are still in the developmental stage [9] and this has contributed to the limited use of 3D scaffolds for studies related to understanding of specific factors affecting cell behavior. In tissue engineering studies involving materials design, 2D substrates are used to understand the effect of the designed material on cell behavior (e.g., biocompatibility, tissue formation ability) rather than the complex effects of 3D environment. Besides this, materials characterization in case of 2D substrates also involves relatively lesser experimental difficulties.

Design of tissue engineering scaffolds having the required properties is dependent on factors such as materials used for scaffold preparation and the processing routes used for scaffold fabrication. The following sections will thus elaborate on materials and processing routes used for fabricating scaffolds.

1.3. Materials for Scaffold Fabrication

Various organic and inorganic materials are used in the design of bone tissue engineering scaffolds. The organic materials that can be used for developing composite scaffolds are natural or synthetic polymers whereas commonly used inorganic materials are nanohydroxyapatite, silicates and carbon nanotubes. The success of these materials is dependent on whether they are able to mimic the nuances of the natural extracellular matrix.

1.3.1. Hydroxyapatites

Hydroxyapatite (HAP) is the major component of inorganic phase of bone and its natural or synthetic forms are known to be bioactive, osteoconductive, non-toxic, non-immunogenic with a crystal structure that is similar to the HAP present in bone tissue. It has been found that HAP at the nanoscale (nano-HAP) is functionally more effective as compared to HAP at the microscale that can be due to its improved surface properties such as higher surface roughness, lower contact angles and reduced pore size. These characteristics of nano-HAP are known to improve cell adhesion, differentiation and growth by increased adsorption of specific proteins [7, 10]. Nano-HAP is more active in influencing the unfolding of adhesive proteins to a greater extent and increase the number of available arginine-glycine-aspartic (RGD) acid sequences present in adhesive proteins for the cell surface receptors [10]. Many methods that have been used for synthesizing nano-HAP are solid-state, wet-chemical, hydrothermal, mechanochemical, pH shockwave and microwave techniques. Nano-HAP has been used in various studies for preparing nanocomposites for bone tissue engineering. In some of the recent studies, nano-HAP has been incorporated in polymers such as chitosan [11-13], poly-2-hydroxyethylmethacrylate-polycaprolactone (PHEMA/PCL) [14], poly (lactic acid) [15], poly(3-hydroxybutyrate-co-3-hydroxyvalerate) [16], polycaprolactone [17], and poly(propylene fumarate) [18]. All these studies demonstrate the utility of nano-HAP for developing nanocomposites for bone tissue engineering.

1.3.2. Silicates

Very few studies involving cell-material interactions [12, 19-23] have been conducted regarding the use of silicates, such as montmorillonite (MMT) clays, for the purpose of bone tissue engineering. MMT clays have been used for the purpose of preparing nanocomposites with

improved mechanical properties, decreased gas permeability and flammability and improved biodegradability [24]. The development of scaffolds with adequate mechanical properties that can withstand the rigors of the in-vivo environment after implantation, without adversely affecting the functions of the surrounding tissue, represents one of the major challenges of bone tissue engineering. The potential of MMT clays to improve the mechanical properties of the composites can be exploited in the case of scaffolds used for bone tissue engineering. Studies have suggested that MMT clays possess medicinal properties [25-28] and over the past few years have shown the potential of MMT clays to improve the mechanical properties of composites used in bone tissue engineering applications [12, 29-31].

1.3.3. Carbon Nanotubes

Carbon nanotubes (CNTs), which are members of the fullerene family of carbon allotropes, have mechanical properties in the gigapascal range, possess high surface area and are also known to be internalized by the cells. Functionalized carbon nanotubes have been used for studies related to cancer treatment [32], scaffolds for neurite growth [33], antiseptic bandages [34] and as biosensors for insulin detection [35]. The exceptional mechanical properties and surface area of CNTs can prove to be useful for bone tissue engineering applications and several studies have been conducted in this respect. For example, Shi et al. [36] prepared nanocomposite scaffolds using functionalized and non-functionalized ultra-short single walled carbon nanotubes (SWCNTs) and poly(propylene fumarate) (PPF). The functionalized ultra-short carbon nanotubes were found to be more effective in increasing the compressive properties of the scaffolds, on which rat bone mesenchymal stem cells (MSCs) were able to attach and proliferate. In another study, injectable nanocomposites of poly(propylene fumarate) and single walled carbon nanotubes were fabricated that not only had improved compressive and flexural

properties but also showed that the dispersion of CNTs was affected by their concentration in the nanocomposites [37]. Similar type of nanocomposites were prepared by Sitharam et al. [38], using PPF, SWCNTs and ultra-short SWCNTs. Notably, the rheological properties of the nanocomposites that affect their injectability was dependent on the size of the CNTs whereas the mechanical properties were dependent on the surface area of the CNTs. In another study, Sitharam et al. [39] assessed the in vivo biocompatibility of scaffolds made up of ultra-short CNTs and PPF/propylene fumarate diacrylate. It was found that bone growth was relatively faster on PPF/propylene fumarate diacrylate/CNT scaffolds than on scaffolds not containing carbon nanotubes. This suggested that composite scaffolds containing CNTs were osteoconductive and promoted osteogenesis. There have also been several other studies involving the use of CNTs based on composite systems such as chitosan/multi-walled CNTs [40] HAP/CNTs [41, 42], poly(carbonate)urethane/multi-walled CNTs [43] and poly(L-lactide)/magnetic multiwalled CNTs [44] and these studies have emphasized CNTs as useful bone tissue engineering materials.

1.3.4. Bioactive Glass

Bioactive glass, as an inorganic material can be used in the preparation of nanocomposites for bone tissue engineering applications. These glasses are characterized by rapid formation of hydroxycarbonate apatite layer on their surface that promotes their adhesion to the bone apatite. Apatite layer formation on bioactive glasses is observed when they are in contact with fluids identical or similar to human plasma [45]. In addition, they have a faster bonding rate with bone and stimulate osteogenic cells upon dissolution due to release of Si, Ca, P and Na ions. Notably, bioactive glasses prepared using the sol-gel method are nanostructured as opposed to those prepared by melt method [46, 47]. Bioactive glasses prepared by using sol-gel

method are more bioactive as compared to -those prepared by melt-method [48-50]. There was an emergence of interest a few years ago in using bioactive glass nanoparticles for preparing composites useful for bone tissue engineering. For example, Hong et al. [51] showed how bioactive glass ceramic nanoparticles can be prepared by combining sol-gel and coprecipitation method. The bioactivity of these nanoparticles was confirmed by formation of hydroxyapatite on these particles through FTIR and XRD experiments. In another study, Hong et al. [52] prepared nanocomposites scaffolds by incorporating bioactive glass nanoparticles in poly(L-lactic acid) that exhibited an increase in compressive strength, compressive modulus with an increase in the bioactive glass nanoparticle content. These scaffolds were bioactive and in vitro degradation rate of the scaffolds in PBS was more as compared to scaffolds without the bioactive glass nanoparticles due to the hydrophilic nature of bioactive glass. Liu et al. [53] modified the bioactive glass nanoparticles with low molecular weight poly(L-lactide) and further used these modified nanoparticles for preparing poly(L-lactide) composite scaffolds that showed an improvement in tensile strength up to 6 wt % loading. Biocompatibility studies using marrow stromal cells from rabbit on these scaffolds showed that the composites with unmodified bioactive glass nanoparticles had better initial cell adhesion and proliferation as compared to scaffolds with the modified particles but the trends were reversed after 7 days**.** Couto et al. [54] developed hydrogel composites using chitosan and bioactive glass nanoparticles with an aim to prepare injectable nanocomposites useful for tissue engineering. Rheological and in-vitro studies to determine the bioactivity of these hydrogel composites showed that they could prove useful for bone tissue regeneration. Mansur et al. [55] prepared nanocomposite scaffolds based on poly (vinyl alcohol) and bioactive glass that had interconnected macroporous structure with pores in the 10-500 μm range along and a mesoporous structure in the nanometer range. The compressive

properties of these scaffolds were found to be affected by the poly (vinyl alcohol) content and its degree of hydrolysis.

1.3.5. Polymers

Bone is considered to be a nanocomposite with the inorganic phase as its major component and hence it may be argued that in order to develop nanocomposites with appropriate mechanical properties mimicking those of bone, the inorganic phase would be relatively significant while designing nanocomposites in bone tissue engineering. But it is important to consider that the mechanical properties of bone are due to its hierarchical structure. It is very difficult to mimic this structural hierarchy during the preparation of nanocomposites in bone tissue engineering. Therefore proper selection of the organic phase becomes equally important for preparing nanocomposites in bone tissue engineering. Besides being able to mimic the features of the extracellular matrix (ECM), the organic phase is expected to have appropriate biodegradation rate that leads to successful tissue regeneration. In addition, the organic phase may have biodegradation products that cause changes in local pH but should be excreted from the body without affecting the pH dependent enzymatic reactions simultaneously taking place within the cells and their environment. It should also possess adequate mechanical properties to support the growing tissue in the dynamic in vivo environment without triggering an immune response. Natural and synthetic polymers can constitute the organic phase of composite scaffolds used for bone regeneration.

Natural polymers are obtained from natural sources such as animals and plants. These type of polymers possess biomolecules or sequences of biomolecules that are favorable for cell attachment and differentiation [56]. These polymers can be degraded by enzymes or by hydrolysis, are similar to biological macromolecules and may not trigger an immune response

due to their similarity with the extracellular matrix [57]. But some of their key disadvantages are uncontrolled biodegradation rate, variation in mechanical properties from batch to batch, scale up difficulties [56], possibility of infections in case of polymers derived from animal source such as collagen. Moreover, it is difficult to predict or estimate the in vivo biodegradation rate in these polymers because of different extent of enzymatic activity in different individuals. In case of synthetic polymers, it is possible to control their biodegradation rate properties by introducing appropriate functional groups in the polymeric chain by grafting or by choosing appropriate monomers while preparing these polymers. The mechanical properties of synthetic polymers are dependent on their molecular weight and can be controlled by using the proper polymer synthesis method such as addition polymerization, condensation polymerization and ring opening polymerization. But these polymers pose problems such as chronic inflammation, lack of desired cell response since they do not have the natural biomolecule sequences that promote cell attachment and uncertainties involved in complete removal of solvents during the processing of some synthetic polymers that can have an effect on the cell response. The following sections will discuss the natural and synthetic polymers that are used for bone tissue engineering.

1.3.5.1. Natural Polymers

Collagen is present in most connective tissues (bone, cartilage, tendon, cornea, blood vessels and skin) and known to be deposited by fibroblasts or by connective tissue cells in the extracellular matrix. Collagen is an important component of extracellular matrix (ECM) and is responsible for maintaining its structural integrity besides performing biological functions. The collagen superfamily is known to consist of 28 members/types. Types I, II, III and V considered to be main types of collagen are present in bone, cartilage, skin and muscle respectively [58]. Collagen (type I) is known to be extensively used for tissue engineering applications and can be

extracted/isolated from animal or human tissues such as skin, tendons and ligaments. It exhibits good biocompatibility, low immune response, good mechanical strength and can be crosslinked, hence helping control its mechanical and degradation properties [57]. Kikuchi et al [59] used glutaraldehyde for preparing crosslinked collagen/hydroxyapatite nanocomposites and found that the mechanical strength of these composites improved with glutaraldehyde content. In vivo studies involving the implantation of these crosslinked nanocomposites in to rabbit tibia indicated that the osteoclastic resorption of these composites decreased with the increasing glutaraldehyde content without any adverse reactions. Kim et al. [60] developed microspheres of collagen-apatite nanocomposites and studied the in vitro response of rat bone marrow stem cells on these microspheres. The in vitro studies showed that the rat bone marrow stem cells were able to attach and grow on these nanocomposite microspheres, which indicated that they can be used for bone tissue regeneration. There have also been several other studies involving use of collagen that emphasize its importance in bone tissue engineering [61-65].

Chitosan is another important biopolymer and is an incompletely deacetylated form of chitin that has been studied extensively for bone tissue engineering applications. It is known to be biocompatible, shows antimicrobial activity, is capable of activating macrophages and promotes the proliferation of fibroblasts [66]. There has been a sustained interest in chitosan based nanocomposites for bone tissue engineering. Thein-Han et al. prepared biomimetic chitosan-nanohydroxyapatite scaffolds that showed that the mechanical properties and the response of pre-osteoblasts improved and the degradation rate decreased by addition of nano-hydroxyapatite [11]. Their studies also suggested that the mechanical properties of the scaffolds were affected by the molecular weight and degree of deacetylation of chitosan. Zhang et al**.** studied nanofibrous scaffolds made up of chitosan and hydroxyapatite with attributes similar to

the extracellular matrix and found that these scaffolds favored the formation of bone tissue [67]. Kong et al. used chitosan for preparing chitosan/nanohydroxyapatite scaffolds and found that the biocompatibility and bioactivity of chitosan was further enhanced by adding nano-hydroxyapatite [68]. Li et al. prepared hybrid scaffolds of chtosan-alginate that had improved Young's modulus, improved shape retention in solutions of wide pH range, better cell proliferation as compared to pure chitosan scaffolds [69]. In one of the recent studies, Cai et al. developed nanocomposites based on chitosan, polylactic acid and hydroxyapatite with highly improved elastic modulus and compressive strength that were dependent on polylactic acid content [70]. The polylactic acid used in these composites was responsible for the rod-like shape of hydroxyapatite in these nanocomposites. Although there have been many studies based on chitosan for bone tissue engineering applications, it still remains the major component of most present studies because of presence of amino groups and its tunable degree of deacetylation that can have an effect on its ability to form complexes with other polyelectrolyte molecules and its mechanical properties. The amino groups of chitosan are protonated in acidic media and can form complexes with other polymeric molecules having functional groups with a complementary charge on them. This has increased the chances of developing novel nanocomposite systems involving the use of chitosan. For example, Verma et al. developed nanosfibrous polyelectrolyte scaffolds based on chitosan, polygalacturonic acid and hydroxyapatite that had better osteoblast cell adhesion compared to the scaffolds without hydroxyapatite [71].

Cellulose is a natural polymer that is found in plants such as cotton, wood, straw and produced by microbes such as acetobacter xylinum. It is convertible into different derivative forms such as carboxymethylcellulose, cellulose nitrate, cellulose acetate and cellulose xanthate and can be moulded or processed into fibers. It cannot be degraded enzymatically which is one

of its disadvantages but can be made degradable by altering its higher order structure [57]. Bacterial cellulose is superior to plant cellulose in aspects such as mechanical properties (tensile strength and modulus), surface area, water holding capacity and crystallinity [72]. Wan et al. studied the prospects of cellulose as a useful bone tissue engineering material by preparing nanocomposites based on hydroxyapatite and bacterial cellulose [72]. The prepared nanocomposites had 3-dimensional network structure with formation of carbonated hydroxyapatite after soaking in simulated body fluid. Li et al**.** oxidized bacterial cellulose with sodium periodate to obtain 2,3-dilaldehyde bacterial cellulose which is a biodegradable and biocompatible form of bacterial cellulose [73]. Although these studies did not involve the preparation of composites, it was interesting to note that the 2, 3-dilaldehyde bacterial cellulose scaffolds were able to degrade both in SBF and PBS and were able to form a microporous structure that was in a range useful for cell growth. Jiang et al. found that the microstructure, mechanical properties, degradation and bioactivity of nano- hydroxyapatite /chitosan/carboxymethyl cellulose scaffolds was suitable for bone tissue engineering applications [74]. Studies by Muller et al**.** [75] and Svensson et al. [76] have also shown that cellulose can be a useful material for tissue engineering applications.

Starch is a natural polymer found in plants such as corn, rice, potato, wheat and capable of being crosslinked, acetylated, converted into thermoplastic and blended with synthetic polymers to improve its mechanical properties [57]. Salgado et al. developed scaffolds based on starch/cellulose acetate blends and found that these scaffolds showed compressive properties that were adequate for bone tissue engineering [77]. Moreover, these scaffolds favored cell proliferation, formation of extracellular matrix and mineralization that suggested the utility of starch based materials in bone tissue engineering. Marques et al. studied composites of

hydroxyapatite and corn starch blended with polymers such as ethylene vinyl alcohol, cellulose acetate and polycaprolactone [78]. Their studies demonstrated the suitability of starch for bone tissue engineering and also explained that the importance of surface roughness, miscibility of the blend systems used and hydroxyapatite on osteoblast cell behavior. There have been few other studies [79-81] that imply that starch can be a useful bone tissue engineering material.

Hyaluronic acid is a natural polymer that consists of disaccharide units of α-1,4-D-glucoronic acid and β-1,3-N-acetyl-D-glucosamine that is found in connective tissues such as umbilical cord, synovial fluid and vitreous [82] It is also known to be present in the extracellular matrix and participates in maintaining the structure of the extracellular matrix, morphogenesis, wound repair and metastasis [83]. Hyaluronic acid has been used in studies related to bone tissue engineering. Lisignoli et al. used esterified hyaluronic acid based scaffolds having non-woven, micron-sized fibrous structures to study the differentiation and mineralization of rat bone marrow stromal cells in the presence and absence of basic fibroblast growth factor (bFGF) [84]. It was found that bFGF enhanced the mineralization rate and expression of differentiation markers such as osteocalcin and osteopontin. Their studies concluded that the hyaluronic acid based scaffolds were capable of supporting bone growth before implanatation. As an extension of these in vitro studies, Lisignoli et al. further implanted the hyaluronic acid based scaffolds cultured with rat bone marrow stromal cells in rats with defects in their forearm bones and found that these scaffolds showed bone growth trends that were similar to those found in their in vitro studies [85]. Ji et al**.** prepared hyaluronic acid based scaffolds by electrospinning and found them suitable for cell attachment and spreading [82]. Kim et al**.** used hyaluronic acid based scaffolds seeded with human mesenchymal stem cells for curing bone defects in rats that supported

formation of new bone tissue that was more enhanced in the presence of bone morphogenic protein (BMP-2) [83].

Silk fibroin polymers obtained from animal sources such as spiders (e.g. Nephila clavipes) and worms (e.g. Bombyx mori) that consist of secondary β-sheet structures formed due to the specific arrangement of hydrophobic and hydrophilic domains composed of specific amino acid sequences have also been investigated for nanocomposites design. The hydrophobic domains form the β-sheet structure (ordered) and their combination with the less ordered hydrophilic structures is responsible for the mechanical properties of silk. Silk fibroin obtained from B. Mori consists of light and heavy protein chains that are linked by disulfide bonds and coated with sericins. It is biocompatible, enzymatically degradable, has good mechanical properties with an advantage that its properties can be altered according to the requirements by using different processing routes.

1.3.5.2. Synthetic Polymers

Aliphatic polyesters such as poly (glycolic acid) (PGA), poly (lactic acid) (PLA), poly (lactic-co-glycolic acid) (PLGA) and polycaprolactone (PCL) are a class of synthetic polymers that can be used for bone tissue engineering applications. The differences in the properties of the polymers that fall under this category depend upon their monomer units.

PGA is characterized by moderate crystallinity, high melting point, low solubility in organic solvents and ability to undergo hydrolytic degradation. It has been suggested that PGA can be used in situations in which an initially faster degradation rate is needed, although the possibility of local pH variations due to its degradation products necessitates the consideration of its use in regions that have a buffering capacity or a mechanism for rapid removal of the degradation wastes.

PLA can be prepared either as D or L isomeric forms, denoted as PLLA or PDLA respectively. Since the degradation product of PLLA (i.e. is L-lactic acid) is found in the human metabolic, its use may be preferable. The higher solubility of PLA as compared to PGA in organic solvents can prove to be advantageous for electrospinning. The properties of PLGA can be controlled by adjusting the lactic acid/glycolic acid ratio.

PCL is semicrystalline, has good solubility in organic solvents and low melting point with a degradation rate lower than PGA and PLGA. Aliphatic polyesters have been used in numerous studies related to bone tissue engineering. Lee et al**.** [86] prepared PLLA/MMT scaffolds with improved mechanical properties and porosity that was suitable for bone tissue engineering. Liu et al. [87] showed that the extent of decrease in pH due to degradation of PLGA can be decreased by incorporating titania nanaoparticles in PLGA. The titania nanoparticles acted as a buffer to control the reduction in pH that further enhanced the significance of these nanocomposites [88] in relation to the behavior of osteoblasts on PLGA/titania nanocomposites. Nejati et al. [89] prepared PLLA/HAP nanocomposites with microstructure and compressive strength that was close to that of cancellous bone. Serrano et al. [90] studied the biocompatibility of PCL using murine fibroblasts. Their studies showed that PCL served as a good substrate for fibroblast adhesion and also increased the mitochondrial activity of the fibroblasts. Shor et al. [91] developed PCL/HAP scaffolds with a controlled microstructure (by using an extrusion technique) that showed an ability for mineralization upon seeding with fetal bovine osteoblasts. Erisken et al. [92] prepared graded nanocomposites scaffolds using PCL and β-tricalcium phosphate with spatial variation in structure and composition and ability to form extracellular mineralized extracellular matrix (ECM). There have also been several other studies [15, 93-98] illustrating aliphatic polyesters as a useful bone tissue engineering material.

Polyphosphazene is a synthetic polymer with a backbone of alternating phosphorous and nitrogen atoms with each phosphorous atom linked to two organic side groups. The degradation of polyphosphazene can be modulated by making changes in the side groups. This gives polyphosphazene an advantage over aliphatic polyesters that require changes in their backbone structure for controlling their degradation rate [99, 100]. The incorporation of side groups such as imidazolyl, amino acid esters, glycolate esters and lactate esters causes polyphosphazene to become sensitive to hydrolysis and release non-toxic products. Bhattacharya et al. [101] prepared polyphosphazene-nanohydroxyapatite composite nanofibers as a potential material system for bone tissue engineering application. Nukavarapu et al. [102] synthesized prepared three different types of polyphosphazene with different side groups and further used phenylalanine ethyl ester substituted polyphosphazene having glass transition temperature higher than 37ºC (physiological temperature) for developing scaffolds with nanohydroxyapatite. These scaffolds showed compressive strength close to human cancellous bone and also proved favorable for osteoblast cell adhesion and proliferation.

Poly (propylenefumarate) (PPF) is an unsaturated linear polyester capable of being crosslinked by using crosslinking agents such as methyl methacrylate, N-vinyl pyrrolidinone and PPF-diacrylate and poly (ethylene glycol)-diacrylate [18, 103]. Degradation products of poly (propylenefumarate) are non-toxic that makes it useful from tissue engineering perspective. Horch et al. [104] used alumoxane nanoparticles for making PPF composites with improved flexural properties for bone tissue engineering applications. Lee et al. [18] found that PPF/HAP nanocomposite system was suitable for attachment and proliferation of murine pre-osteoblast cells and could serve as suitable system for bone tissue engineering. Several other studies [105-108] have also reported the suitability of PPF for bone tissue engineering applications. One of

these studies demonstrated an interesting possibility of developing injectable nanocomposites made up of PPF and single-walled carbon nanotubes (SWCNTs) [106]. It was found that functionalization of the carbon nanotubes (CNTs) played an important role in the rheological behavior and degree of crosslinking in these nanocomposites that are important in case of developing injectable nanocomposites. Studies related to injectable nanocomposites are important for tissue engineering because these composites provide us with an option of minimizing complex surgical procedures, developing scaffolds for curing defects having unusual shapes and delivering cells, bioactive molecules to the defect sites along with the nanocomposite solution.

A wide variety of synthetic polymers can be developed and used for designing nanocomposites useful for tissue engineering applications. The improvement in the understanding of the polymerization mechanisms over the years has increased the possibilities of developing synthetic polymer systems according to the requirements of bone tissue engineering. Other than some of the synthetic polymers discussed in the preceding paragraphs, the synthetic polymer systems that have been developed and studied for bone tissue engineering are poly(ester urethane) [109], poly(urethane) [110-112] and poly(vinyl alcohol) [113, 114].

1.4. Methods of Scaffold Fabrication

The fact that nanoscale features have an important effect on cell behavior emphasizes the importance of nanocomposites in bone tissue engineering. In order to obtain appropriate nanoscale features or nanostructure in the final nanocomposite, it is necessary to use appropriate processing methods. There are some challenges associated with the preparation of these nanocomposites. One of them is the need to conserve the intrinsic properties of the materials used for preparation of the nanocomposites. The processing method used might affect the

conformation of the polymer chains in case of polymers or the distribution of the nanosized inorganic materials in the form of particles while preparing the nanocomposites. The changes in conformation of polymer chains in case of natural polymers may affect the available biomolecule sequences and cell behavior. In addition to this, the properties of polymeric materials such as melting point, glass transition temperature, viscosity and their resistance to solvents used during processing may also limit the number of routes by which they can be processed. For bone regeneration it is necessary to develop nanocomposites with structural features that mimic or at least resemble the structural features of the extracellular matrix (ECM). In this context, at present there are a number of processing routes used for developing nanocomposites for bone tissue engineering and these are discussed in the following sections.

1.4.1. Electrospinning

Electrospinning is a simple technique that can be used to produce fibers having diameter in the nanometer range. This makes it useful for mimicking the structure of the extracellular matrix proteins. Besides this, the fibers produced by electrospinning have high surface area to mass ratio (40 to 100 m^2/g), superior stiffness and tensile strength [115, 116]. Also, the possibilities of spinning fibers at room temperature from a variety of polymers, producing aligned nanofibers, and spinning fibers simultaneously from separate solutions to generate layered scaffold structures emphasize its attractiveness in bone tissue engineering [115, 117]. Electrospinning apparatus consists of a high voltage supply, a capillary tube containing a polymer solution connected to a needle or a pipette and a grounded metallic collector. A schematic of this process is shown in Figure 1.2. The needle and the metallic collector act as two electrodes between which a high voltage (several tens of KV) is applied. Application of a high voltage supply generates an electric field between the two electrodes that produces electrostatic

forces (generated by electrostatic repulsion between the surface charges on the droplet and Columbic force exerted by the external electric field) in the spherical droplet liquid (polymer solution) at the needle tip and opposes the surface tension forces in the liquid droplet. This results in the deformation of the spherical droplet to a conical shape known as "Taylor cone." When the electric field surpasses a critical value the electrostatic force overcomes the surface tension forces that results in the ejection of an electrically charged jet from the tip of the Taylor cone. The electrically charged jet interacts with the externally applied electric field that makes it unstable, causes it to bend as it moves towards the grounded collector and thus produce long ultrafine fibers (produced by the splitting of the jet due to repulsive forces) in the form of a non-woven structure [118]. The evaporation of the solvent from the charged jet takes place as it moves towards the collector. Different types of collectors such as plate-type, cylinder-type, disc-type and frame-type can be used to control the alignment of the electrospun fibers [119]. The electrospinning process and thus the dimensions of the electrospun fibers are affected by a number of factors such as viscosity, conductivity, surface tension, the magnitude of the applied voltage, the distance between the needle and the collector, solution flow rate and solution temperature. There are also some limitations associated with the electrospinning process such as use of organic solvents and difficulty in generation of controlled, three-dimensional pore structure. In case of natural polymers that are categorized as proteins, the electrospinning process may alter the structure of such polymers that can further affect the cell behavior on the scaffolds. Also, chemical crosslinking may be necessary for some electrospun polymers to prevent them from dissolving in aqueous media [5]. In relation to bone tissue engineering, electrospinning process has been used in a number of studies for developing polymer or polymer nanocomposite scaffolds. Some examples of polymer and polymer nanocomposite systems in the form of

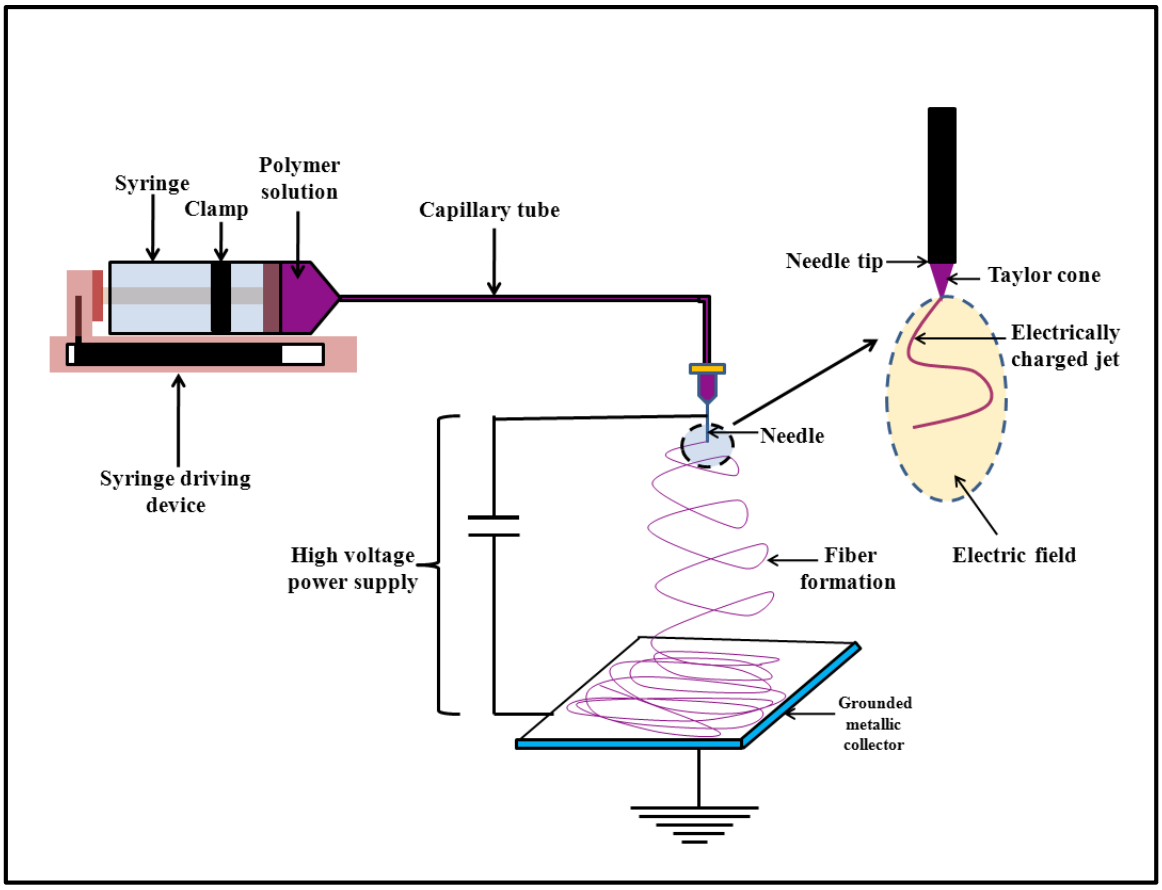

Figure 1.2. Schematic of electrospinning process

eletrospun scaffolds that have been investigated for bone tissue regeneration applications are polycaprolactone/nanohydroxyapatite/collagen [120], polyphosphazene/nanohydroxyapatite [101], carboxymethyl chitin/poly(vinyl alcohol) [121], poly(D,L-lactide-co-glycolide)/nano-hydroxyapatite [122], silk fibroin/bone morphogenetic/nanohydroxyapatite [123], poly(lactide-co-glycolide/amorphous tricalcium phosphate [124], and thiolated hyaluronic acid derivative [82].

1.4.2. Phase Separation

Phase separation is a thermodynamic process that is used for preparing interwoven, nano-fibrous scaffolds in bone tissue engineering. The thermally induced phase separation method is

the common method for phase separation but it is also possible to use a non-solvent to the polymer for inducing phase separation. A schematic showing this process is shown in Figure 1.3.

Thermally induced phase separation is of two types; viz., solid-liquid phase separation and liquid-liquid phase separation depending on the crystallization temperature (freezing point) of the solvent used. In case of solid-liquid phase separation, the crystallization temperature of the solvent used is higher than the liquid-liquid phase separation temperature that makes the solvent to crystallize and the polymer to separate when the temperature of the polymer solution is lowered. The crystallized solvent is further removed by freeze-drying (sublimation) that leaves behind pores having morphology similar to the solvent crystallites. Thus, it is possible to control the pore structure and the type of phase separation by using solvents having different crystallization (freezing) properties.

For liquid-liquid phase separation to take place, the crystallization temperature of the solvent used is lower than the liquid-liquid phase separation temperature that makes the polymer to separate in to polymer-rich and polymer-lean phase. This type of phase separation is affected by the upper or a lower critical solution temperature of the polymers involved and is posited to take place either due to spinodal liquid-liquid phase separation or nucleation and growth mechanism.

Phase separation by nucleation and growth mechanism is supposed to take place in the metastable region of the temperature-composition phase diagram where the solution is stable with respect to the small fluctuations in composition. The polymer concentration under the metastable region controls the structure of the polymer solid that is obtained after the removal of the solvent with low polymer concentration resulting in a powder like polymer solid and high concentration resulting in a closed pore structure of the polymer solid. The spinodal region is unstable and small variations in polymer concentration cause a decrease in free energy that

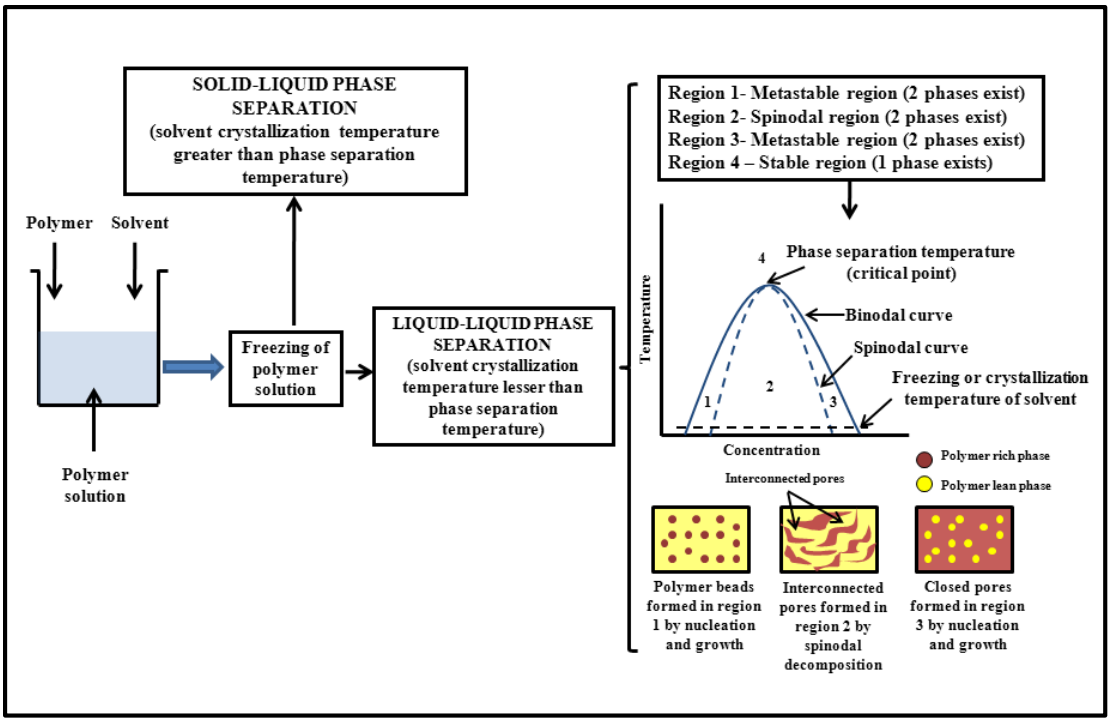

Figure 1.3. Schematic of phase separation process

results in a wave of concentration fluctuations in the polymer solution. These further result in the formation of interconnected polymer-rich and polymer-lean (mostly solvent) phases to give a scaffold having a continuous pore network after the removal of the polymer-lean phase. It is also possible to induce phase separation at room temperature by adding a non-solvent to the polymer solution to obtain a gel from which the solvent is then extracted by using water. The gel is further cooled below the glass transition temperature of the polymer and freeze dried to get a nanofibrous scaffold.

One of the advantages of the phase separation technique is that the morphology of the scaffold can be controlled by changing the parameters such as polymer type and concentration, polymer type, freezing temperature and using different types of porogens. Further, this technique can also be useful for preparing scaffolds of different shapes according to the requirement and maintaining batch-to-batch consistency. In spite of being a simple technique, phase separation

remains a laboratory scale technique limited to a few polymers. Phase separation technique has been used in preparing scaffolds based on polymer systems such as PEG/PLLA[125], polylactide-dextran blend [126], PLLA [127], PLGA [128], hydroxyapatite/poly (hydroxyabutyrate-co-hydroxyvalerate) [129], and hydroxyapatite/chitosan-gelatin [130].

1.4.3. Freeze Drying

Freeze drying technique is used for the removal of the solvent after phase separation of the polymer solution by lowering the temperature or by adding a non-solvent to the polymer. During freeze-drying, the temperature is maintained low enough so that remixing of the phase separated polymer solution is prevented. A schematic showing the freeze drying methodology is shown in Figure 1.4. It has been used in several studies related to bone tissue regeneration for developing scaffolds based on polymers such as PLLA [131], chitosan [71, 132], gelatin [133], carboxymethyl cellulose [134], poly(ether ester) [135], silk fibroin/hyaluronan [136, 137]. There have also been studies involving the use of nanocomposite scaffolds prepared by using the phase separation technique for bone tissue engineering applications. Few examples of polymer nanocomposite scaffolds that have been fabricated by using the freeze drying technique are poly (L-lactic acid)/nanohydroxyapatite [138], collagen/hydroxyapatite [139], chitosan/hydroxyapatite [11, 140], gelatin/hydroxyapatite [141, 142], PDLLA/PLGA/bioglass [143]. Also, polyelectrolyte complex (PEC) fibrous scaffolds for tissue engineering have been synthesized and scaffolds are fabricated using the freeze drying methodology [71]. The design parameters that are typically optimized are temperature ranges, and time as well as the concentrations of the polymer solutions.

1.4.4. Particulate Leaching

The particulate leaching technique is a relatively simple technique used to prepare porous scaffolds by using porogens that are soluble in water or non-toxic solvents. Porogens such as sugar, sodium chloride and saccharose are used to generate the pores. A polymer solution with the porogens dispersed in it is cast in to a mold followed by removal of the solvent by evaporation and subsequent leaching of the porogen to produce a porous scaffold. A schematic showing this process is shown in Figure 1.5. Effective control of pore size and porosity by varying the size and amount of porogens is the main advantage of this technique. Incomplete removal of solvents from the polymer solution by evaporation, lack of interconnectivity and open pore structure in scaffolds requiring low porosity due to decrease in the number of contact points between the porogens due to reduction in the number of porogens and suitability of this technique to mostly thin scaffolds are the limitations of this technique. This technique has been used in combination with other techniques but lack of complete interconnectivity is still its one of the major limitations**.** Liu et al. [144] prepared gelatin/apatite nanofibrous scaffolds by combining thermally induced phase separation and particulate (porogen) leaching technique.

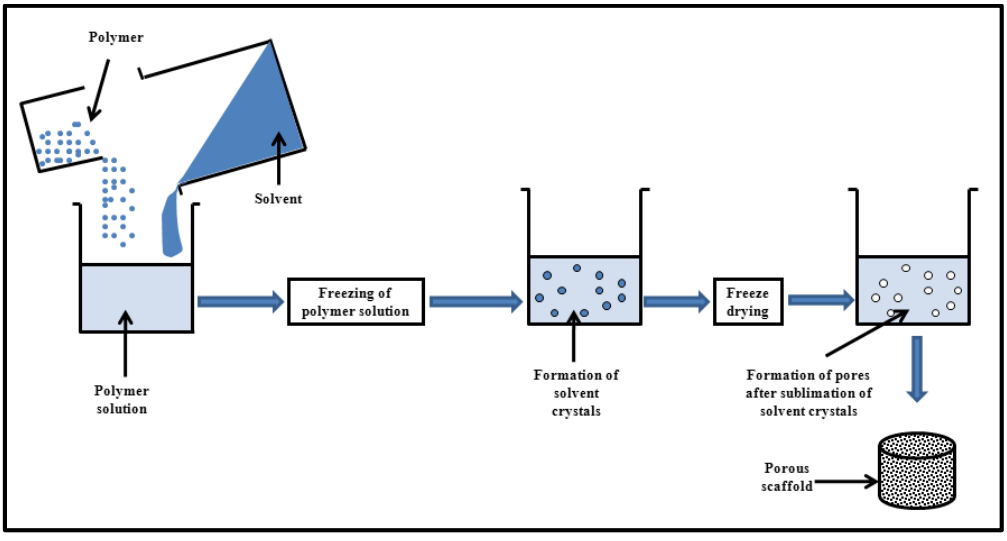

Figure 1.4. Schematic of freeze drying process

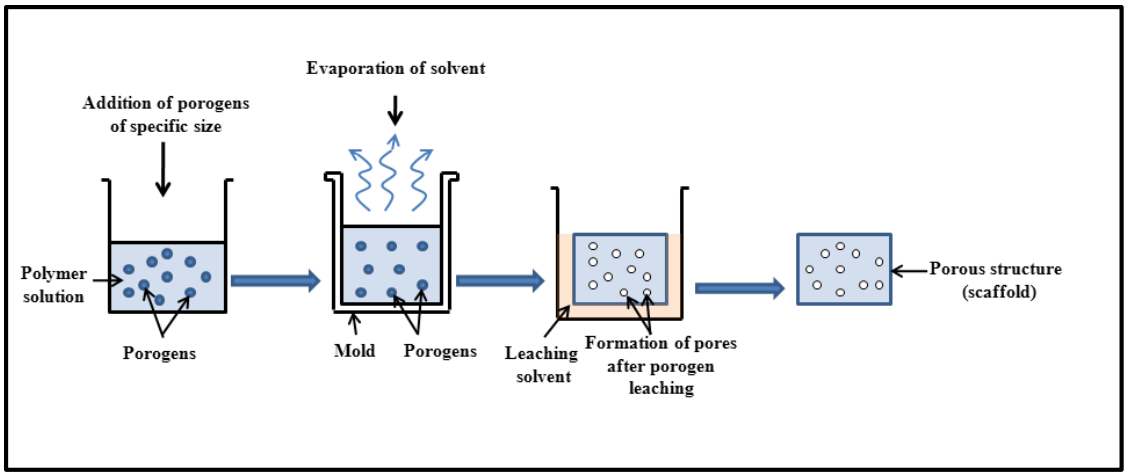

Figure 1.5. Schematic of particulate leaching process

They employed preheating of the mold to develop interconnectivity in between the particulates and thus between the pores of the scaffold. The interconnected pores in the scaffold were helpful in distribution of the cells throughout the scaffold. Several studies related to bone tissue generation have been carried out using scaffolds prepared by using the particulate leaching technique and the recent trend has been to further improve this technique [126, 145-149].

1.5. Cells for Bone Tissue Engineering

Cells have a key role in tissue engineering, especially in case of critical size tissue defects where the size of the defect presents difficulties related to the number of cells required. In addition to this, the cells used for tissue engineering also need to satisfy other requirements. Cells must be capable of differentiating into desired phenotype [150] upon being stimulated by appropriate signals (chemical, mechanical and electrical). They must be capable of organization through structural support from the surrounding environment (e.g. scaffolds) and also producing a properly organized extracellular matrix (ECM) [150, 151]. Cells also need to produce the required cytokines (or cell signaling molecules) [151], show mechanical and structural confirmity with the surrounding native cells and integrate with the surrounding cells to minimize

the risks of immune rejection [150]. Cells for tissue engineering can be obtained from autologous (patient's own) sources, allogenic (from human donor excluding the patient) and xenogenic (from animal donor) sources that have limitations. Autologous cells are considered the most appropriate for use due to low possibilities of immune rejection but have limitations in case of critical size tissue defects due to difficulties in obtaining sufficient cell numbers without affecting the donor site. Allogenic and xenogenic cells are associated with risks of immune rejection and pathogen transfer. Primary (mature) cells obtained from tissue explants have limited proliferation, tissue formation abilities and may show improper phenotype expression [151]. In case of bone tissue engineering, cell-related factors such as osteogenic and vasculogenic potential of cells, ability to control differentiation into osteogenic lineage, stable expression of osteogenic phenotype to avoid "non-specific" tissue formation [152] are considered important for bone formation. Extensive and emerging research over the past few years has shown that mesenchymal stem cells (MSCs), embryonic stem cells and induced pluripotent stem cells are promising alternatives to conventional cell types. This research work involves the use of osteoblasts (from bone tissue) and human mesenchymal stem cells (hMSCs). Since relevant characteristics of mature cells obtained from tissues having been already mentioned, the following sections will discuss mesenchymal stem cells (MSCs) in detail considering them as one of the major cell source for bone tissue engineering applications.

1.5.1. Mesenchymal Stem Cells

The term "mesenchymal" in mesenchymal stem cells is related to the embryological germ layer known as "mesoderm" or "mesenchyme." This germ layer is supposed to be capable of differentiating into different types of tissues such as bone, cartilage, blood, cartilage, vascular, tendons and ligaments. However, the term "mesenchymal stem cells" is mostly used to describe

cells that are known to give rise to connective tissue cells except the blood. Hematopoietic stem cells are known to be responsible for giving rise to blood cells. A proper definition for the "mesenchymal stem cells" seems to be in an emerging state. Many studies describe mesenchymal stem cells as a concept that developed on the basis of work carried out by Friedenstein and his co-workers. They noticed adherent colony forming units (CFUs) of fibroblastic nature during the culture of bone marrow cells [153, 154] and through further studies demonstrated that these cells were capable of differentiating into osteogenic and chondrogenic lineage [154]. Similar observations were made in subsequent studies carried out by other groups [155, 156]. MSCs can be distinguished from hematopoietic stem cells by their ability to rapidly adhere to tissue culture plastic and the fibroblastic appearance of their progeny. The International Society for Cellular Therapy has set up criteria for the identification of MSCs and these are as follows [157]:

a. MSCs must adhere to plastic during cell culture
b. MSCs must express specific surface antigens. Greater than 95 percent of the MSC population should express surface antigens such as CD73, CD90 and CD105. Also, the percentage of cells expressing antigens such as CD34, CD45 should be less than 2 percent.
c. MSCs must show ability to differentiate into osteogenic, chondrogenic and adipogenic lineages. The ability to differentiate into different lineages can be demonstrated by accepted staining methods.

Despite the criteria set up by the International Society for Cellular Therapy, studies suggest that these may be subjected to change due to the constantly evolving understanding of mesenchymal stem cells. MSCs are being scrutinized with respect to their self-renewal ability,

heterogeneity, in vitro and in vivo identity, differentiation potential and similarities or differences between the MSCs derived from different types of tissues. These points of scrutiny related to MSCs would be briefly discussed in the following sections.

1.5.1.1. Self-renewal of MSCs

Self-renewal is one of the important characteristics of MSCs and can take place through symmetric and asymmetric cell divisions[158]. The self-renewal ability of MSCs has been under question in several studies. Present understanding of the MSCs has been through extensive experiments related to their ex vivo culture. Adequate evidence regarding the self-renewal ability of the MSCs in the in vivo environment is still lacking that makes it difficult to validate the definition of MSCs. There may be a possibility that the self-renewal ability of MSCs seen during culture may be an effect of the culture conditions and not their inherent nature. Lack of evidence regarding the self-renewal ability of MSCs has been attributed to the difficulty in identifying a specific phenotype marker for MSCs in vivo [159]. Very few studies have attempted to address this problem. Simmons et al [160] developed an antibody known as STRO1 to identify the cell surface antigens present in MSCs from bone marrow. STRO1 is capable for identifying a population of bone marrow cells that are clonogenic, have ability to form colony forming unit (CFU) fibroblasts and differentiate into specialized cell types. In order to further improve the process of identifying MSC rich population, it was proposed that markers such as VCAM/CD106 can be used along with STRO1. But the binding ability of STRO1 to erythrocyte progenitor cells can limit its use [161]. In a recent study, markers such as SSEA-1 and SSEA-4 have been reported for identifying the mesenchymal stem cells in vivo [162]. Despite this, there seems to be a need for extensively characterizing the MSCs in vivo like the hematopoietic stem cells. The issue of finding a specific marker for the MSCs in vivo is complicated further due to the loss of

the in vivo markers during the in vitro cell culture that creates difficulties during interpretation of results [161]. Besides the lack of adequate evidence for specific markers in MSCs for in vivo characterization, the mode of cell division (symmetric or asymmetric) utilized by the MSCs for self-renewal is uncertain [157, 158]. The concept of self-renewal related with the MSCs seems to drift towards uncertainty due to the accumulation of mutations during each round of DNA replication during cell division. Thus, there would be some differences between the parent cell and the daughter cell and this has been often ignored for practical reasons [163].

1.5.1.2. Heterogeneity of MSCs

The heterogeneity of MSC population has been reported widely in literature. MSC populations cultured both ex vivo and in vivo have been reported for their heterogeneity on the basis of MSC colonies having differences in growth rates, cell morphology, multipotentiality and phenotype [164]. The difference in multipotentiality of the stem cells in a MSC population is linked to the question regarding the true stem cell nature of the MSCs. There is a possibility that the "clonal expansion" of MSCs can be interpreted as self-renewal but in reality MSCs can be said to have true stem cell nature if they also are able to show the same multipotentiality as their parent cells during their expansion [157]. This has further given rise to the methods that can be used for assaying the true stem cell nature of the MSCs. For the purpose of assaying the true stem cell nature of the MSCs, researchers have proposed the development of in vivo assays at the single cell level [159, 165]. Assaying self-renewal ability and multipotentiality at the single cell level in vivo would be a more accurate way of examining the true stem cell nature of the MSCs. These types of assays have been already well-established for the hematopoietic stem cells. The low frequency of MSCs and their requirement in large numbers further adds to the difficulty of developing methods to assess their true stem cell nature in vivo [165].

1.5.1.3. MSCs from Different Types of Tissues

There have been reports that MSCs are also present in different types of tissues such as adipose, umbilical cord blood, pancreas and synovial tissue. For the purpose of tissue regeneration there is a requirement for a considerable number of MSCs. Presence of MSCs in other tissues in addition to the bone marrow seems encouraging with respect to the prospect of tissue regeneration. The low frequency of MSCs in the bone marrow also makes it important to study the other tissues consisting MSCs. Comparative studies between the MSCs found in bone marrow and other tissues would be helpful in finding whether MSCs from different sources can fall under the same category. This is a difficult task since no definite phenotypic markers for identifying MSCs in vivo have been established. Despite this, there have been studies suggesting that there may be differences in the differentiation capacity of the MSCs from different tissues under the same culture conditions [166]. Studies have also found that the MSCs from different tissues have same morphology and phenotype but were different with respect to the ease of isolation, proliferation and differentiation capacity [159].

1.5.1.4. MSCs, Progenitor Cells and Precursor Cells

The difficulties in the identification of MSCs appear to be further increased due to the similarities between the MSCs and the supporting cells in their environment [167]. For example, there are similarities in the morphology and phenotype between the MSCs and the adventitial reticular cells in the bone marrow. Also, similarities exist between the MSCs and the pericytes (cells in close proximity to the endothelial cells in blood vessels) related to their differentiation potential and the capacity to preserve their multipotentiality after several cell culture passages. The pericytes and also the bone lining cells express the same surface markers as the MSCs. Another facet of confusion related to MSCs is the presence of progenitor and precursor cells in

different types of tissues containing MSCs. These cells are representative of different levels of differentiation. The progenitors have less differentiation compared to the MSCs and the precursors have the least differentiation potential since they represent a stage just before a complete differentiation. Progenitors and precursors have also been categorized as the "transit amplifying cells." The transit amplifying cells are known to arise from the stem cells and undergo limited number of cell divisions before they lose their self-renewal ability and then differentiate terminally [168].

1.5.1.5. Differentiation Potential of MSCs

The supposed ability of the MSCs to differentiate into different lineages has contributed immensely to their importance in tissue regeneration applications. Studies focused on studying the differentiation potential of MSCs have shown that they are able to differentiate into cells of mesodermal origin such as the osteoblasts, chondrocytes and the adipocytes and also into non-mesodermal cell lineages such as the neurons, skin cells and hepatocytes [157, 169]. Some of these studies involved in vitro experiments whereas in some studies also involved in vivo experiments. In addition to this, there are also reports related to the differentiation of MSCs into more cell types of mesodermal origin such as the endothelial cells, muscle cells and cardiac cells. In one of the studies, it was shown that the MSCs show pluripotent behavior both in vitro and in vivo [170]. This has raised questions whether the MSCs can be known as pluripotent cells and also whether the term "mesenchymal" associated with the MSCs is appropriate [169]**.** Therefore, there seems to be a need for assessing the MSCs for pluripotency and the repeatability of the pluripotent behavior by stringent assays. The differentiation of the MSCs can be affected by using growth factors and cytokines such as fibroblast growth factor, transforming growth factor-β, bone morphogenetic protein (BMP-2), harmones such as dexamethasone, vitamins such as

ascorbic acid and also chemicals such as β-glycerophosphate. Besides this, signaling pathways such as Wnt, Notch and regulation of factors such as runt homology domain transcription factor (Runx)2 are involved in the process of MSC differentiation [166, 169]. For the purpose of studying the differentiation potential of the MSCs, cell assays involving nonclonal cell strains are used. Such assays involve stains such as alizarin red (for osteogenesis), oil red O (for adipogenesis), alcian blue (for chondrogeneis). Although these assays have been used extensively for studying the differentiation of MSCs, there are difficulties in comparing these in vitro assays with the in vivo assays. The use of nonclonal cell strains in these assays gives results that are not a precise measure of the multipotentiality of the MSCs.

1.5.1.6. Dedifferentiation and Transdifferentiation of MSCs

The MSCs also show ability to dedifferentiate and transdifferentiate in addition to their ability to differentiate into different lineages. Dedifferentiation is a process in which completely differentiated cells are able to reverse their developmental process and convert into a less differentiated state (precursor or progenitor cells) [171, 172]. During this process, reversal is observed in the cells at the “genetic level”, “protein level”, in terms of morphology and at the “functional level” [172]. Reversal at the genetic level can be identified by the changes in gene expression profile and reversal at the protein level can be identified by increase in protein production related to a less differentiated state of the cell. At the morphological level, the dedifferentiated cells appear to be smaller in size than the completely differentiated cells, possess less cell organelles and higher “karyoplasmic ratio”. Also, at the “functional level” the differentiated cells get back their ability to proliferate. In case of transdifferentiation, differentiated cells change into cells of a completely different phenotype. It can also be said to switching of a cell committed to a specific lineage to a cell committed to a different lineage and

can be a result of reprogramming at the genetic level [173]. Transdifferentiation may involve two stages. During the first stage, the differentiated cells are converted back to a cell having stem cell or progenitor cell phenotype. In the second stage, the cells resulting from the conversion of the differentiated cells redifferentiate into new, differentiated cells. This suggests that dedifferentiation may be a part of transdifferentiation. Studies have shown that completely differentiated osteoblasts obtained from MSCs dedifferentiated into a less differentiated state resembling a stem cell like stage. These cells derived from the differentiated osteoblasts then differentiated into chondrocytes and adipocytes [173]. In a similar manner, differentiated adipocytes and chondrocytes were also able to transdifferentiate into other cell types of mesenchymal origin. In some of the other studies, it has been shown that MSCs were able to transdifferentiate into cardiomyocytes and epithelial cells [174]. The dedifferentiation capacity of the MSCs has increased the difficulty in understanding their direct role in tissue repair. It may be possible that during tissue repair, the already existing differentiated cells derived from the MSCs may dedifferentiate into a less differentiated state, get back their stem cell like properties and then differentiate into a specific lineage. It is thus possible that not only the MSCs but also the new differentiated cells obtained by transdifferentiation of the already existing differentiated cells may play a role in tissue repair [161]. Transdifferentiation of MSCs can be advantageous for tissue engineering where a considerable number of cells are required for tissue regeneration. In order to extend the use of cells obtained by transdifferentiation, extensive studies are required to assess their long-term stability.

1.5.2. Understanding the Mesenchymal Stem Cells (MSCs)

Development in the understanding of factors at different length and time scales that affect the behavior of the MSCs can provide the impetus for regenerating tissues ready for clinical applications. But this seems to be a difficult task and depends on the present understanding of the mesenchymal stem cell (MSC) components, molecules involved in adhesion of MSCs, niche (in vivo microenvironment of the MSCs), migration ability of MSCs, immunomodulatory effect of MSCs and stimuli necessary for MSC differentiation. The following sections of the chapter would make an attempt to discuss these topics briefly. Also, the present cell culture methods, differentiation assays and characterization methods related to MSCs would also be discussed in the remaining part of this chapter. Besides this, the present and the potential use of MSCs for bone tissue engineering applications would be discussed.

1.5.2.1. Integrins and Their Role in Mesenchymal Stem Cells (MSCs)

For tissue engineering applications, the cells seeded on the porous scaffolds need to adhere to the scaffold substrate and also migrate to the interior parts of the scaffold. Adhesion and migration have an effect on different cellular processes involved in tissue formation. Integrins and focal adhesions play an important role in the adhesion and migration of the cells. Integrins constitute a large family of receptors and are known to take part in cell-extracellular matrix adhesion and cell-cell adhesion. In tissue engineering, the scaffold is designed so that it provides an environment similar to the extracellular matrix and therefore integrins become important for cell-scaffold adhesion.

Integrins are known as “heterodimeric” receptors since they consist of non-covalently bonded α and β subunits[159]. These subunits are type 1 transmembrane glycoproteins and each of them has a comparatively long extracellular domain and a short cytoplasmic domain. There

are 18 α and 8 β subunits in case of mammalian integrins and these subunits combine together in different ways to create 24 different types of heterodimeric integrins. These integrins can bind to a range of ligands on the cell surface and the extracellular matrix [159]. The extracellular domains bind to the extracellular proteins and the cytoplasmic domains bind to the intracellular domains. The intracellular domain and ligand link serves as a connection between the receptor, the signaling pathways and the cytoskeletal system. The binding of the receptors to the extracellular and intracellular domains gives the receptors an ability to transmit signals from the inside to the outside of the cell and vice versa. Important events such as cell morphology, cell migration, cell proliferation, cell differentiation and cell death are dependent on the interactive signaling between the cells and the extracellular matrix. Fibronectin, laminin, collagens, tenascin, vitronectin, osteopontin and bone sialoprotein are some of the ligands for the integrins that are present in the extracellular matrix. Adhesion between the cells is supposed to take place by binding of the integrins to the cell membrane receptors. Counter receptors such as vascular cell adhesion molecule (VCAM-1), inter-cellular cell adhesion molecules ICAM-1 and ICAM-2 are involved in these types of intercellular adhesions. Additionally, the integrins promote the adhesion between the cells through soluble, multivalent molecules. The binding of the extracellular domain of the integrins with the extracellular matrix ligands is followed by binding of the cytoplasmic domain to the anchor proteins inside the cell such as catenin, talin and actinin. These anchor proteins connect the integrins to the actin filaments that constitute a part of the cytoskeleton. The link formed between the integrins and the actin filaments by the anchor proteins can cause clustering of integrins under favorable conditions. These integrins clusters are known as the focal adhesion between the cell and the extracellular matrix [175]. Focal adhesions are also important for cell polarization, cell migration, cell growth and cell survival [176].

Integrins through their involvement in the focal adhesions affect cell morphology and control cell migration. Studies seem to suggest that integrins indirectly control cell migration by their participation in the signaling related to the matrix metalloproteinases (MMPs) expression [159]. MMPs are proteolytic enzymes that degrade the extracellular matrix proteins at specific sites and thus help in cell migration. Regulation of some of the proteins from the cyclin family by integrins is suggestive of their role in cell proliferation.

Components of integrins such as α1, α2, α3, α5, α6, β1, β3, β4 for human mesenchymal stem cells (MSCs) have been identified by fluorescence activated cell sorting method. Additionally, integrins such as ICAM-1, ICAM-2, VCAM-1, CD72 and LFA3 have also been identified for MSCs [177]. Integrins are also known to play a role in the differentiation of MSCs and keeping in mind their use for bone tissue engineering applications, an overview of their role in osteogenic differentiation would be given in the following paragraph. Studies have shown that the integrin β1 significantly affects the adhesion, proliferation and the differentiation of the MSCs [159, 177-179]. It has also been found that integrins such as α11, α2 and integrin linked kinase (ILK) are upregulated during osteogenic differentiation. Increase in glycoprotein levels such as tenascin during osteogenic differentiation has been linked to the hypothesis of reduction in MSC motility during osteogenic differentiation. Also, binding between the upregulated integrin α2β1 with type I collagen has been identified as one of the events involved in regulation of osteogenic differentiation. Phosphorylation of focal adhesion kinase (FAK) in MSCs has also been suggested as one of the possible reasons for the increase in osteogenic gene expression during osteogenic differentiation.

1.5.2.2. Mesenchymal Stem Cell (MSC) Niche

In addition to insufficient information on the in vivo behavior of the MSCs, the specific location of the MSCs in vivo also seems to be characterized insufficiently. Recent studies seem to support the concept of "niche" put forth in the 1970s [180]. The niche is supposed to be composed of "microenvironmental cells" that support the stem cells and also help the stem cells to maintain tissue homeostasis [181]. The supporting cells can be non-stem cells. These along with the extracellular matrix and soluble molecules are the niche components. Niche helps in maintaining the stem cells in an undifferentiated state and provides them a protective environment from different types of stimuli to maintain this undifferentiated state. Besides this, niche protects the stem cells from uncontrolled cell division and occasionally allows differentiation of stem cells through certain cues on requirement. The microenvironment of the niche is dynamic and it has been proposed that the concept of niche can be also applicable to MSCs in the bone marrow [157]. Studies have indicated that the MSCs are located in a perivascular niche in the adult tissues [157, 182]. MSCs have been found lining the blood vessels and have also been hypothesized to be pericytes. The MSCs and pericytes have been found to express surface markers representative of both cell types and also show similar multipotentiality. The location of the MSCs in the perivascular niche is implicative that the MSCs can migrate to distant tissues in response to injuries or disease.

1.5.2.3. Immunomodulatory Effect of MSCs

MSCs have been reported for their ability to avoid allogenic rejection in humans and animals [166]. Specific reasons for this ability of MSCs have yet not been clearly understood, but one of the possible reasons suggested is the lack of major histocompatibility complex (MHC)-II in MSCs. Mechanisms similar to those involved in avoiding the rejection of a foetal

allograft by the maternal immune system have also been suggested in relation to the immunomodulatory behavior of MSCs. MSCs have also been found to inhibit proliferation and activation of T cells when they are subjected to mitogenic or allogenic stimulation in vitro [183]. Examples of immunomodulatory effects of MSCs have been reported. In case of animals, the injection of MSCs delayed the rejection of dissimilar skin grafts. Results have also been encouraging in case of use of MSCs for treatment of severe graft versus host disease. Immunomodulatory effect of MSCs in tissue engineering can possibly be useful for avoiding the problem of immune rejection in case of engineered tissues developed from MSCs.

1.5.3. Mesenchymal Stem Cell (MSC) Culture

Despite the lack of complete understanding of the MSC behavior in vivo as mentioned earlier, MSCs have been isolated, expanded and have been induced to differentiate into different lineages to corroborate their utility for tissue engineering and other therapeutic applications. The present in vitro methods for isolation and expansion of MSCs from bone marrow and some of the issues related to their in vitro culture would be discussed in brief under this section. Differentiation of the MSCs through the components of the cell culture medium would also be discussed briefly.

1.5.3.1. Mesenchymal Stem Cell (MSC) Isolation

MSCs can be isolated from the bone marrow aspirates collected from superior iliac crest of the pelvis, tibia and femur in case of humans [184]. In case of animals, MSCs can be isolated from the same bone sites as in humans. Percoll density centrifugation is a common technique for the centrifugation of MSCs. It involves use of solutions with high density but low viscosity and low osmotic pressure. Mononucleated cells obtained from bone marrow by this technique are seeded on the tissue culture polystyrene dish with the required changes of cell culture medium

composed of basal medium, growth supplements (e.g. L-glutamine) and antibiotic. During the process of cell culture medium, non-adherent cells considered to be hematopoetic cells are removed and the adherent cells are the mesenchymal stem cells (MSCs) [185]. An alternative to this technique is the enzyme digestion technique that can be used to isolate MSCs from solid tissues such as bone and cartilage. In enzyme digestion technique, collagenase enzyme is used to cleave the collagen present in these solid tissues to release the cells and the released cells are then collected by washing and centrifugation. The MSCs obtained by enzyme digestion of tissues are similar to those obtained from bone marrow aspirates with respect to their differentiation potential and phenotype. Although the enzyme digestion technique has been found to give a high yield of MSCs, this technique has not been standardized [186]. The purity of the MSC population obtained by both these techniques has been under question and this has led to development of other techniques of to get an enriched population of MSCs. Techniques such as isolation of MSCs based on their cell surface markers, magnetic bead sorting and fluorescence-activated cell sorting have been developed for the purpose of MSC enrichment [186].

1.5.3.2. Mesenchymal Stem Cell (MSC) Expansion

Requirement of MSCs in considerable numbers for bone tissue engineering and other clinical applications has made MSC expansion important. Due to their low numbers in the bone marrow and also some of the other tissue sources, they need to be cultured by using appropriate methods to get the required numbers without having an effect on their capabilities. Factors such as the culture media and its components need to be considered in this case.

Cell culture medium for MSC culture consists of two important components; viz. basal medium and the serum. Basal medium contains glucose, amino acids and inorganic ions such as calcium, magnesium, potassium, sodium and phosphate. The yield of MSCs during their

expansion is affected by components of cell culture medium, cell plating density and also the surface quality of the tissue culture plastic used for their expansion [186]**.** It has been reported that culture medium containing alpha Modified Eagle's Medium (α-MEM) as the basal medium is more favorable for MSC expansion. Also, culture medium containing DMEM, low glucose levels and L-alanyl-L-glutamine (Glutamax) has been reported to be conducive for better proliferation of MSCs. Greater stability of L-alanyl-L-glutamine as compared to L-glutamine has been cited as the reason for the better proliferation of MSCs [186, 187]. The nature of the serum also has an effect on the expansion of MSCs and several comparative studies have been performed between animal sera (fetal calf serum and fetal bovine serum) and human serum. Considering the different results from these studies, it is difficult to draw definite conclusions regarding the most suitable serum for in vitro MSC expansion. Besides this, questions exist over the use of MSCs cultured in medium containing animal serum since they can trigger immune reactions when used for clinical applications. Growth factors such as basic fibroblast growth factor (bFGF), platelet derived growth factor (PDGF), epidermal growth factor (EGF) and insulin growth factors (IGF) are added to culture medium for MSC expansion. bFGF is the most common growth factor that is used in culture medium for MSC expansion and maintaining their multipotentiality. Antibiotics are also added to the cell culture medium to avoid contamination in very low concentrations (up to one percent).

1.5.3.3. Media for Inducing Osteogenic Differentiation in MSCs

For bone tissue engineering applications, it is necessary that the MSCs differentiate into an osteogenic lineage. One of the ways to induce osteogenic differentiation in MSCs derived from bone marrow is to add supplements to the cell culture medium containing the basal medium, serum and antibiotics. Supplements such as dexamethasone, L-ascorbic acid 2

phosphate and β-glycerophosphate are commonly added to the cell culture medium for the purpose of osteogenic differentiation. The quantity of dexamethasone can have an effect on whether the MSCs undergo osteogenic differentiation or differentiate into other lineage [185]. Ascorbic acid alone can also be used as a supplement in place of L-ascorbic acid 2 phosphate but has been found to be relatively unstable under cell culture conditions (37°C and neutral pH). Use of ascorbic acid in high concentrations can prove toxic for the cells and using β-glycerophosphate is important for calcium phosphate matrix deposition by the differentiated MSCs. Other external factors added to culture medium such as recombinant human bone morphogenetic proteins and parathyroid hormone related peptides are also known to induce osteogenic differentiation. In case of MSCs derived from the umbilical cord blood and adipose tissue, the osteogenic supplements used are the same as in the case of MSCs obtained from bone marrow. Additional external factors can be added in case of MSCs derived from umbilical cord blood and adipose tissue sources. For example, external factors such as vitamin D_3 and fibroblast growth factor can be used in case of MSCs from umbilical cord blood and polyamine spermine can be added in case of MSCs derived from adipose tissue [188].

Senescence is one of the issues associated with the in vitro expansion of MSCs and has been widely reported. To be more specific, replicative senescence in MSCs is associated with permanent arrest of cell division. Under the condition of senescence, the MSCs remain alive and enter into a permanent growth arrest phase during their cell cycle [189]. Due to senescence, MSCs undergo a limited number (30-40) of population doublings in vitro. Senescence is also known to be accompanied by loss of multipotentiality. Reduction in the length of the telomeres during successive cell divisions has been linked to MSC senescence. Telomerase enzyme known for its role in synthesis of telomeres can have an effect on the proliferation and differentiation

abilities of MSCs. Methods need to be developed to activate and maintain telomerase activity in MSCs for their in vitro expansion.

1.5.3.4. MSCs in Bone remodeling, Fracture repair and Their Use in Bone Tissue Engineering Applications

MSCs are known to play an indirect role in bone remodeling since they can give rise to osteoblast progenitor cells [161].The opposing action of the osteoblasts and osteoclasts are important for bone tissue homeostasis. The differentiation of the osteoclasts from their precursors depends on the molecules expressed by the osteoblasts. Osteoblast receptors such as receptor activator of nuclear factor-kB (RANK), RANK ligand and decoy receptor osteoprotegerin interact with each other and thus regulate the formation of osteoclasts (osteoclastogenesis) along with bone resorption. The indirect role of MSCs in bone remodeling has been suggested through experiments showing expression of RANKL and osteoprotegerin in vitro cultured MSCs. MSCs cultured in presence of supplements such as dexamethasone used to promote osteogenic differentiation have been found to have increased OPG expression.

Fracture healing has been classified as indirect or direct fracture healing. In case of direct fracture healing, MSCs from the perivascular regions are known to contribute more as compared to the MSCs from the periosteum. In case of indirect fracture healing, both intramembranous and endrochondral bone formation are known to take place. For intramembranous fracture healing, MSCs from the periosteum differentiate into osteoblasts and form bone. For endrochondral fracture healing, chondroprogenitors form a cartilagenous callus that is followed by entry of blood vessels, recruitment of chondroclasts and osteoprogenitors to form a woven bone.

Knowledge about the role of MSCs in bone remodeling and fracture repair alongwith its properties discussed in the previous sections encourage its use for bone tissue engineering

applications. MSCs have been used in studies related to tissue engineering using scaffolds made up of different materials such as chitosan [190], poly(L-lactic acid) [191], collagen [192], polycaprolactone [193] and alginate [194]. In addition to development of materials for use of MSCs in bone regeneration, it is becoming increasingly important to study the different types of stimuli affecting MSC differentiation. Identifying the role of different types of stimuli in MSC differentiation can also help in designing better material systems and improving the present tissue engineering approach.

1.6. Polymer Clay Nanocomposites (PCNs) and Potential of Na-MMT Clay for Bone Tissue Engineering

Research on PCNs was spurred by reports of significant enhancement in mechanical properties of PCNs by Toyota research group in 1990 [195]. Since then several studies have reported the effect of addition of sodium-montmorillonite (Na-MMT) nanoclay on permeability [196-198], flammability [199, 200] and biodegradability [201] of PCNs besides the significant enhancement in mechanical properties [24]. Extensive simulation [202-204] and experimental studies [205, 206] performed by our group led to the development of "altered phase model" for PCNs according to which a significant volume of the polymer is affected by molecular level interactions between the constitutents of PCNs that causes change in crystallinity of the polymer in the altered zone around the intercalated clay particles [207]. This change in crystallinity is responsible for significant enhancement in nanomechanical properties of PCNs.

The reinforcing ability of Na-MMT clay can be used to enhance the mechanical properties of polymeric scaffolds used in tissue engineering. Besides this our previous studies have shown that Na-MMT clay intercalated with organic molecules (modifiers) affects the nanomechanical properties and polymer crystallinity. Ability of Na-MMT clay to affect

nanomechanical properties can be useful to influence cell behavior since the cells are responsive to mechanical cues from their surrounding environment. Effect on crystallinity of PCNs due to addition of Na-MMT clay can be useful to influence degradation of polymeric scaffolds since change in polymer crystallinity affects ingress of the surrounding medium and thus the degradation of the polymer under physiological (aqueous) environment. Following factors were also considered for the use of MMT clay in this work:

1. Reported use of Na-MMT clay for drug-delivery and drug-release applications [30, 208, 209].
2. Ability of MMT clays to be excreted from the body [28].
3. Medicinal use of MMT clay to treat disorders such as ulcers, diarrhea and hyperthyroidism [210].
4. The nanoscale dimension of MMT sheet can be used for affecting the cell response since the cell protrusions (filopodia and lamellipodia) are more responsive to nanoscale features [6].
5. The human bone also consists of ions such as sodium, magnesium, silicon, zinc and carbonate in addition to the mineral apatite. Silicon is known to affect bone formation rate, pattern [10] and also involved in early stages of bone calcification [211]. MMT clay consists of ions such as silicon, magnesium, aluminum and therefore can be useful for bone tissue engineering studies

Use of Na-montmoriilonite (Na-MMT) nanoclay for designing polymer composite scaffolds for bone tissue engineering is a major focus of this work. Na-MMT clay was used in this work to design polymer composite scaffolds based on the hypothesis that Na-MMT clays are capable of enhancing mechanical properties of polymer based scaffolds. The problem of

imparting mechanical properties to bone tissue engineering scaffolds extends across different scales (molecular to macroscale). Besides this, studies have indicated that designing polymer-clay nanocomposites (PCNs) at molecular level can be useful to have better control over their physical properties across higher length scales. Therefore a materials design strategy beginning at the molecular level was used in which Na-MMT clay was modified with unnatural amino acids and this modified MMT clay was further used for experimental investigations involving Fourier Transform Infrared (FTIR) spectroscopy, X-ray diffraction and biocompatibility assessment. Based on these investigations, 5-aminovaleric acid modified MMT clay was used to prepare chitosan-polygalacturonic acid (ChiPgA) bipolymer composite scaffolds and these scaffolds were studied for their suitability for bone tissue engineering applications that also included studies related to the response of osteoblasts (bone cells) to ChiPgA scaffolds containing modified MMT clay compared to ChiPgA scaffolds containing hydroxyapatite (a material known for its favorable cell response). Chitosan was used on the basis of its known bicompatibility, wound healing ability, antimicrobial properties and minimal foreign body reaction. Polygalacturonic acid (PgA) is a de-esterified form of pectin. Pectin has been reported for its use in food industry and for producing drugs. Besides this, pectin has also been reported for its favorable effect on proliferation of osteoblasts [212]. Considering multiple requirements of bone tissue engineering scaffolds, especially osteoinductivity and osteoconductivity, bone-like apatite was mineralized in 5-aminovaleric acid clay using a processing route based on biomineralization in bone to obtain a novel three-component nanoclay-hydroxyapatite hybrid (in situ HAPclay). This nanoclay-HAP hybrid was used to prepare ChiPgA composites (films and scaffolds) and response of osteoblasts, hMSCs in the absence of osteogenic supplements to these composites was comprehensively studied using biological assays and imaging. In situ HAPclay

was also used to prepare synthetic polymer composites (films and scaffolds). Polycaprolactone (PCL), a synthetic and an aliphatic polyester, was used for this purpose considering its versatility, lesser complexities compared to biopolymers and immense prospects for tissue engineering applications. Apart from studying the response of hMSCs to these synthetic composites, the effect of incorporation of in situ HAPclay on the nanomechanical properties, in vitro degradation and scaffold microstructure was studied. Sub-micron scale morphology of the mineralized ECM formed on these synthetic PCL composites was studied using atomic force microscopy (AFM) and the mineralized ECM components (mineral, collagen) were compared to their natural bone counterparts for similarities in dimensions, arrangement.

1.7. Objectives of Research

The specific objectives of this research are as follows:

1. To modify and thus intercalate Na-MMT clay with unnatural amino acids.
2. To characterize the modified Na-MMT clays using experimental techniques such as FTIR spectroscopy, XRD and assess the biocompatibility of the modified clays using relevant cells (osteoblasts).
3. To fabricate chitosan-polygalacturonic (ChiPgA) biopolymer complex based composite scaffolds containing unnatural amino acid modified Na-MMT clay and perform comparative studies using these scaffolds related to their biocompatibility with osteoblasts, microstructure, porosity, swelling properties and their spectroscopic characterization (FTIR spectroscopy).
4. To mineralize bone-like apatite in Na-MMT clay intercalated with unnatural amino acid using a processing route based on biomineralization in bone and thus make this clay more

effective for imparting bone formation ability and improved mechanical properties to bone tissue engineering composites (films and scaffolds).

5. To characterize the nanoclay-hydroxyapatite (HAP) hybrid (also known as in situ HAPclay) using FTIR spectroscopy, XRD, transmission electron microscopy (TEM) and scanning electron microscopy (SEM).
6. To prepare ChiPgA biopolymer complex based composites (films and scaffolds) containing in situ HAPclay and study the response of osteoblasts and human mesenchymal stem cells (hMSCs) to these composites without the use of osteogenic supplements.
7. To study the microstructure of ChiPgA/in situ HAPclay scaffold, surface morphology of ChiPgA/in situ HAPclay films and determine the porosity, swelling ratios of ChiPgA/in situ HAPclay scaffolds.
8. To perform a unique two-stage cell seeding experiment using hMSCs as a strategy to enhance tissue (bone) formation under in vitro conditions on polymer composites containing in situ HAPclay.
9. To fabricate synthetic polymer (polycaprolactone) composite films and scaffolds containing in situ HAPclay and perform studies related to the response of hMSCs to these composites, scaffold microstructure, surface morphology (for films), nanomechanical properties (for films) and in vitro degradation under accelerated conditions (for scaffolds).
10. To study cell-dependent bone mineral formation mechanisms on PCL/in situ HAPclay films (an engineered synthetic polymer composite based substrate) using scanning electron microscopy (SEM) and SEM-EDS (energy dispersive spectroscopy)

1.8. Organization of Dissertation

This dissertation is organized into different chapters as follows:

1) Chapter 1: This chapter give an introduction to tissue engineering**.** It also gives a brief overview of the significant factors related to the use of 3D scaffolds and also presents reasons for using 2D substrates (films) for tissue engineering. It further describes different materials and methods used for fabricating tissue engineering scaffolds. This chapter also discusses polymer clay nanocomposites (PCNs) and their potential for bone bone tissue engineering and presents factors considered while selecting materials used for this research work.
2) Chapter 2: This chapter presents design of organomodified clays using unnatural amino acids and discusses these clays as potential biomaterials for bone tissue engineering
3) Chapter 3: Studies related to fabrication of ChiPgA biopolymer composite scaffolds containing unnatural amino acid modified nanoclay and indicating their suitability for bone tissue engineering are presented in this chapter
4) Chapter 4: This chapter describes the preparation, characterization of nanoclay-hydroxyapatite (HAP) hybrid (also known as in situ HAPclay) based on biomineralization in bone and presents results related to response of osteoblasts (bone cells) to ChiPgA biopolymer composites containing in situ HAPclay
5) Chapter 5: This chapter describes preparation of ChiPgA/in situ HAPclay composites using two different methods and the response of human mesenchymal stem cells (hMSCs) to these composites along with other studies indicating their suitability for bone tissue engineering

6) Chapter 6: This chapter discusses the fabrication of synthetic polymer (polycaprolactone) composites (films and scaffolds) containing in situ HAPclay and presents results from experimental investigations related to response of hMSCs to these composites, characterization of these composites using different imaging techniques and nanoindentation, ultrastructure of mineralized ECM formed on these composites and in vitro biodegradation studies (for scaffolds)
7) Chapter 7: This chapter discusses cell dependent bone mineral formation mechanisms in brief and presents observations from experiments involving cell dependent mineral formation on engineered synthetic polymer (polycaprolactone) composites
8) Chapter 8: This chapter presents summary and important conclusions of the research presented in this dissertation
9) Chapter 9: This chapter attempts to present future directions for bone tissue engineering research and closely related fields

1.9. References

[1] Langer R, Vacanti JP. Tissue Engineering. Science. 1993;260:920-6.

[2] Stock U, Vacanti J. Tissue Engineering: Current State and Prospects. Annual Review of Medicine. 2001;52:443-51.

[3] Chick W, Like A, Lauris V. Beta cell culture on synthetic capillaries: an artificial endocrine pancreas. Science. 1975;187:847-9.

[4] Burke JF, Yannas IV, Quinby WCJ, Bondoc CC, Jung WK. Successful Use of a Physiologically Acceptable Artificial Skin in the Treatment of Extensive Burn Injury. Annals of Surgery. 1981;194:413-28.

[5] Goldberg M, Langer R, Jia XQ. Nanostructured materials for applications in drug delivery and tissue engineering. Journal of Biomaterials Science-Polymer Edition. 2007;18:241-68.

[6] Stevens MM, George JH. Exploring and Engineering the Cell Surface Interface. Science. 2005;310:1135-8.

[7] Murugan R, Ramakrishna S. Development of nanocomposites for bone grafting. Composites Science and Technology. 2005;65:2385-406.

[8] Buxboim A, Ivanovska IL, Discher DE. Matrix elasticity, cytoskeletal forces and physics of the nucleus: how deeply do cells 'feel' outside and in? Journal of Cell Science. 2010;123:297-308.

[9] Baker BM, Chen CS. Deconstructing the third dimension – how 3D culture microenvironments alter cellular cues. Journal of Cell Science. 2012;125:3015-24.

[10] Chan CK, Kumar TSS, Liao S, Murugan R, Ngiam M, Ramakrishman S. Biomimetic nanocomposites for bone graft applications. Nanomedicine. 2006;1:177-88.

[11] Thein-Han WW, Misra RDK. Biomimetic chitosan-nanohydroxyapatite composite scaffolds for bone tissue engineering. Acta Biomaterialia. 2009;5:1182-97.

[12] Katti KS, Katti DR, Dash R. Synthesis and characterization of a novel chitosan/montmorillonite/hydroxyapatite nanocomposite for bone tissue engineering. Biomedical Materials. 2008;3:12.

[13] Cai X, Tong H, Shen X, Chen W, Yan J, Hu J. Preparation and characterization of homogeneous chitosan-polylactic acid/hydroxyapatite nanocomposite for bone tissue engineering and evaluation of its mechanical properties. Acta Biomaterialia. 2009;5:2693-703.

[14] Huang J, Lin YW, Fu XW, Best SM, Brooks RA, Rushton N, et al. Development of nano-sized hydroxyapatite reinforced composites for tissue engineering scaffolds. 2007. p. 2151-7.

[15] Kothapalli CR, Shaw MT, Wei M. Biodegradable HA-PLA 3-D porous scaffolds: Effect of nano-sized filler content on scaffold properties. Acta Biomaterialia. 2005;1:653-62.

[16] Cool SM, Kenny B, Wu A, Nurcombe V, Trau M, Cassady AI, et al. Poly(3-hydroxybutyrate-co-3-hydroxyvalerate) composite biomaterials for bone tissue regeneration: In vitro performance assessed by osteoblast proliferation, osteoclast adhesion and resorption, and macrophage proinflammatory response. Journal of Biomedical Materials Research Part A. 2007;82A:599-610.

[17] Lee HJ, Kim SE, Choi HW, Kim CW, Kim KJ, Lee SC. The effect of surface-modified nano-hydroxyapatite on biocompatibility of poly([epsilon]-caprolactone)/hydroxyapatite nanocomposites. European Polymer Journal. 2007;43:1602-8.

[18] Lee K-W, Wang S, Yaszemski MJ, Lu L. Physical properties and cellular responses to crosslinkable poly(propylene fumarate)/hydroxyapatite nanocomposites. Biomaterials. 2008;29:2839-48.

[19] Katti KS, Ambre AH, Peterka N, Katti DR. Use of unnatural amino acids for design of novel organomodified clays as components of nanocomposite biomaterials. Philosophical Transactions of THE ROYAL SOCIETY A 2010;368:1963-80.

[20] Ambre AH, Katti KS, Katti DR. Nanoclay Based Composite Scaffolds for Bone Tissue Engineering Applications. Journal of Nanotechnology in Engineering and Medicine. 2010;1:031013-9.

[21] Ambre A, Katti KS, Katti DR. In situ mineralized hydroxyapatite on amino acid modified nanoclays as novel bone biomaterials. Materials Science and Engineering: C. 2011;31:1017-29.

[22] Ambre AH, Katti DR, Katti KS. Nanoclays mediate stem cell differentiation and mineralized ECM formation on biopolymer scaffolds. Journal of Biomedical Materials Research Part A. 2013;101:2644-60.

[23] Mieszawska AJ, Llamas JG, Vaiana CA, Kadakia MP, Naik RR, Kaplan DL. Clay enriched silk biomaterials for bone formation. Acta Biomaterialia. 2011;7:3036-41.

[24] Sinha Ray S, Okamoto M. Polymer/layered silicate nanocomposites: a review from preparation to processing. Progress in Polymer Science. 2003;28:1539-641.

[25] Viseras C, Aguzzi C, Cerezo P, Lopez-Galindo A. Uses of clay minerals in semisolid health care and therapeutic products. Applied Clay Science. 2007;36:37-50.

[26] Wen-Fu Lee, Yao-Tsung Fu. Effect of montmorillonite on the swelling behavior and drug-release behavior of nanocomposite hydrogels. Journal of Applied Polymer Science. 2003;89:3652-60.

[27] Dong Y, Feng S-S. Poly(d,l-lactide-co-glycolide)/montmorillonite nanoparticles for oral delivery of anticancer drugs. Biomaterials. 2005;26:6068-76.

[28] Carretero MI. Clay minerals and their beneficial effects upon human health. A review. Applied Clay Science. 2002;21:155-63.

[29] Zheng JP, Wang CZ, Wang XX, Wang HY, Zhuang H, Yao KD. Preparation of biomimetic three-dimensional gelatin/montmorillonite-chitosan scaffold for tissue engineering. Reactive and Functional Polymers. 2007;67:780-8.

[30] Depan D, Kumar AP, Singh RP. Cell proliferation and controlled drug release studies of nanohybrids based on chitosan-g-lactic acid and montmorillonite. Acta Biomaterialia. 2009;5:93-100.

[31] Marras SI, Kladi KP, Tsivintzelis I, Zuburtikudis I, Panayiotou C. Biodegradable polymer nanocomposites: The role of nanoclays on the thermomechanical characteristics and the electrospun fibrous structure. Acta Biomaterialia. 2008;4:756-65.

[32] Shvedova AA, Kisin ER, Porter D, Schulte P, Kagan VE, Fadeel B, et al. Mechanisms of pulmonary toxicity and medical applications of carbon nanotubes: Two faces of Janus? Pharmacology & Therapeutics. 2009;121:192-204.

[33] Marianna F, Mukasa B. Carbon nanotubes as functional excipients for nanomedicines: I. pharmaceutical properties. Nanomedicine : the official journal of the American Academy of Nanomedicine. 2008;4:173-82.

[34] Simmons TJ, Lee SH, Park TJ, Hashim DP, Ajayan PM, Linhardt RJ. Antiseptic single wall carbon nanotube bandages. Carbon. 2009;47:1561-4.

[35] Wang Y, Li J. A carbon nanotubes assisted strategy for insulin detection and insulin proteolysis assay. Analytica Chimica Acta. 2009;650:49-53

[36] Shi XF, Sitharaman B, Pham QP, Liang F, Wu K, Billups WE, et al. Fabrication of porous ultra-short single-walled carbon nanotube nanocomposite scaffolds for bone tissue engineering. Biomaterials. 2007;28:4078-90.

[37] Shi XF, Hudson JL, Spicer PP, Tour JM, Krishnamoorti R, Mikos AG. Rheological behaviour and mechanical characterization of injectable poly(propylene fumarate)/single-walled carbon nanotube composites for bone tissue engineering. 2005. p. S531-S8.

[38] Sitharaman B, Shi XF, Tran LA, Spicer PP, Rusakova I, Wilson LJ, et al. Injectable in situ cross-linkable nanocomposites of biodegradable polymers and carbon nanostructures for bone tissue engineering. Journal of Biomaterials Science-Polymer Edition. 2007;18:655-71.

[39] Sitharaman B, Shi X, Walboomers XF, Liao H, Cuijpers V, Wilson LJ, et al. In vivo biocompatibility of ultra-short single-walled carbon nanotube/biodegradable polymer nanocomposites for bone tissue engineering. Bone. 2008;43:362-70.

[40] Abarrategi A, Gutiérrez MC, Moreno-Vicente C, Hortigüela MJ, Ramos V, López-Lacomba JL, et al. Multiwall carbon nanotube scaffolds for tissue engineering purposes. Biomaterials. 2008;29:94-102.

[41] Xu JL, Khor KA, Sui JJ, Chen WN. Preparation and characterization of a novel hydroxyapatite/carbon nanotubes composite and its interaction with osteoblast-like cells. Materials Science and Engineering: C. 2009;29:44-9.

[42] Balani K, Anderson R, Laha T, Andara M, Tercero J, Crumpler E, et al. Plasma-sprayed carbon nanotube reinforced hydroxyapatite coatings and their interaction with human osteoblasts in vitro. Biomaterials. 2007;28:618-24.

[43] Khang D, Kim SY, Liu-Snyder P, Palmore GTR, Durbin SM, Webster TJ. Enhanced fibronectin adsorption on carbon nanotube/poly(carbonate) urethane: Independent role of surface nano-roughness and associated surface energy. Biomaterials. 2007;28:4756-68.

[44] Feng J, Sui J, Cai W, Wan J, Chakoli AN, Gao Z. Preparation and characterization of magnetic multi-walled carbon nanotubes-poly(l-lactide) composite. Materials Science and Engineering: B. 2008;150:208-12.

[45] Burg KJL, Porter S, Kellam JF. Biomaterial developments for bone tissue engineering. Biomaterials. 2000;21:2347-59.

[46] Rezwan K, Chen QZ, Blaker JJ, Boccaccini AR. Biodegradable and bioactive porous polymer/inorganic composite scaffolds for bone tissue engineering. Biomaterials. 2006;27:3413-31.

[47] Mahony O, Jones JR. Porous bioactive nanostructured scaffolds for bone regeneration: a sol-gel solution. Nanomedicine. 2008;3:233-45.

[48] Pereira MM, Hench LL. Mechanisms of hydroxyapatite formation on porous gel-silica substrates. Journal of Sol-Gel Science and Technology. 1996;7:59-68.

[49] R. Li, A. E. Clark, L. L. Hench. An investigation of bioactive glass powders by sol-gel processing. Journal of Applied Biomaterials. 1991;2:231-9.

[50] Pilar Sepulveda, Julian R. Jones, Larry L. Hench. Characterization of melt-derived 45S5 and sol-gel-derived 58S bioactive glasses. Journal of Biomedical Materials Research. 2001;58:734-40.

[51] Hong Z, Liu A, Chen L, Chen X, Jing X. Preparation of bioactive glass ceramic nanoparticles by combination of sol-gel and coprecipitation method. Journal of Non-Crystalline Solids. 2009;355:368-72.

[52] Hong Z, Reis RL, Mano JF. Preparation and in vitro characterization of scaffolds of poly(l-lactic acid) containing bioactive glass ceramic nanoparticles. Acta Biomaterialia. 2008;4:1297-306.

[53] Liu A, Hong Z, Zhuang X, Chen X, Cui Y, Liu Y, et al. Surface modification of bioactive glass nanoparticles and the mechanical and biological properties of poly(l-lactide) composites. Acta Biomaterialia. 2008;4:1005-15.

[54] Couto DS, Hong Z, Mano JF. Development of bioactive and biodegradable chitosan-based injectable systems containing bioactive glass nanoparticles. Acta Biomaterialia. 2009;5:115-23.

[55] Mansur HS, Costa HS. Nanostructured poly(vinyl alcohol)/bioactive glass and poly (vinyl alcohol)/chitosan/bioactive glass hybrid scaffolds for biomedical applications. Chemical Engineering Journal. 2008;137:72-83.

[56] Langer, Robert. Tissue Engineering:A New Field and Its Challenges. 1997;14:840-1.

[57] Mano JF, Silva GA, Azevedo HS, Malafaya PB, Sousa RA, Silva SS, et al. Natural origin biodegradable systems in tissue engineering and regenerative medicine: present status and some moving trends. Journal of The Royal Society Interface. 2007;4:999-1030.

[58] Cen L, Liu W, Cui L, Zhang W, Cao Y. Collagen Tissue Engineering: Development of Novel Biomaterials and Applications. Pediatr Res. 2008;63:492-6.

[59] Kikuchi M, Matsumoto HN, Yamada T, Koyama Y, Takakuda K, Tanaka J. Glutaraldehyde cross-linked hydroxyapatite/collagen self-organized nanocomposites. Biomaterials. 2004;25:63-9.

[60] Kim HW, Gu HJ, Lee HH. Microspheres of collagen-apatite nanocomposites with osteogenic potential for tissue engineering. Tissue Engineering. 2007;13:965-73.

[61] Venugopal J, Low S, Choon AT, Kumar TSS, Ramakrishna S. Mineralization of osteoblasts with electrospun collagen/hydroxyapatite nanofibers. Journal of Materials Science-Materials in Medicine. 2008;19:2039-46.

[62] Lode A, Bernhardt A, Gelinsky M. Cultivation of human bone marrow stromal cells on three-dimensional scaffolds of mineralized collagen: influence of seeding density on colonization, proliferation and osteogenic differentiation. Journal of Tissue Engineering and Regenerative Medicine. 2008;2:400-7.

[63] Ngiam M, Liao S, Patil AJ, Cheng Z, Chan CK, Ramakrishna S. The fabrication of nano-hydroxyapatite on PLGA and PLGA/collagen nanofibrous composite scaffolds and their effects in osteoblastic behavior for bone tissue engineering. Bone. 2009;45:4-16.

[64] Sotome S, Uemura T, Kikuchi M, Chen J, Itoh S, Tanaka J, et al. Synthesis and in vivo evaluation of a novel hydroxyapatite/collagen-alginate as a bone filler and a drug delivery carrier of bone morphogenetic protein. 2004. p. 341-7.

[65] Tsai SW, Hsu FY, Chen PL. Beads of collagen-nanohydroxyapatite composites prepared by a biomimetic process and the effects of their surface texture on cellular behavior in MG63 osteoblast-like cells. Acta Biomaterialia. 2008;4:1332-41.

[66] Krayukhina MA, et al. Polyelectrolyte complexes of chitosan: formation, properties and applications. Russian Chemical Reviews. 2008;77:799.

[67] Zhang Y, Venugopal JR, El-Turki A, Ramakrishna S, Su B, Lim CT. Electrospun biomimetic nanocomposite nanofibers of hydroxyapatite/chitosan for bone tissue engineering. Biomaterials. 2008;29:4314-22.

[68] Kong L, Gao Y, Lu G, Gong Y, Zhao N, Zhang X. A study on the bioactivity of chitosan/nano-hydroxyapatite composite scaffolds for bone tissue engineering. European Polymer Journal. 2006;42:3171-9.

[69] Li Z, Ramay HR, Hauch KD, Xiao D, Zhang M. Chitosan-alginate hybrid scaffolds for bone tissue engineering. Biomaterials. 2005;26:3919-28.

[70] Cai X, Tong H, Shen X, Chen W, Yan J, Hu J. Preparation and characterization of homogeneous chitosan-polylactic acid/hydroxyapatite nanocomposite for bone tissue engineering and evaluation of its mechanical properties. Acta Biomaterialia. 2009;5:2693-03

[71] Verma D, Katti KS, Katti DR. Polyelectrolyte-complex nanostructured fibrous scaffolds for tissue engineering. Materials Science and Engineering: C. 2009;29:2079-84.

[72] Wan YZ, Hong L, Jia SR, Huang Y, Zhu Y, Wang YL, et al. Synthesis and characterization of hydroxyapatite-bacterial cellulose nanocomposites. Composites Science and Technology. 2006;66:1825-32.

[73] Li J, Wan Y, Li L, Liang H, Wang J. Preparation and characterization of 2,3-dialdehyde bacterial cellulose for potential biodegradable tissue engineering scaffolds. Materials Science and Engineering: C. 2009;29:1635-42.

[74] Jiang L, Li Y, Wang X, Zhang L, Wen J, Gong M. Preparation and properties of nano-hydroxyapatite/chitosan/carboxymethyl cellulose composite scaffold. Carbohydrate Polymers. 2008;74:680-4.

[75] Müller FA, Müller L, Hofmann I, Greil P, Wenzel MM, Staudenmaier R. Cellulose-based scaffold materials for cartilage tissue engineering. Biomaterials. 2006;27:3955-63.

[76] Svensson A, Nicklasson E, Harrah T, Panilaitis B, Kaplan DL, Brittberg M, et al. Bacterial cellulose as a potential scaffold for tissue engineering of cartilage. Biomaterials. 2005;26:419-31.

[77] Salgado AJ, Gomes ME, Chou A, Coutinho OP, Reis RL, Hutmacher DW. Preliminary study on the adhesion and proliferation of human osteoblasts on starch-based scaffolds. Materials Science and Engineering: C. 2002;20:27-33.

[78] Marques AP, Reis RL. Hydroxyapatite reinforcement of different starch-based polymers affects osteoblast-like cells adhesion/spreading and proliferation. Materials Science and Engineering: C. 2005;25:215-29.

[79] Santos MI, Fuchs S, Gomes ME, Unger RE, Reis RL, Kirkpatrick CJ. Response of micro- and macrovascular endothelial cells to starch-based fiber meshes for bone tissue engineering. Biomaterials. 2007;28:240-8.

[80] Gomes ME, Godinho JS, Tchalamov D, Cunha AM, Reis RL. Alternative tissue engineering scaffolds based on starch: processing methodologies, morphology, degradation and mechanical properties. Materials Science and Engineering: C. 2002;20:19-26.

[81] Neves NM, Kouyumdzhiev A, Reis RL. The morphology, mechanical properties and ageing behavior of porous injection molded starch-based blends for tissue engineering scaffolding. Materials Science and Engineering: C. 2005;25:195-200.

[82] Ji Y, Ghosh K, Shu XZ, Li B, Sokolov JC, Prestwich GD, et al. Electrospun three-dimensional hyaluronic acid nanofibrous scaffolds. Biomaterials. 2006;27:3782-92.

[83] Kim J, Kim IS, Cho TH, Lee KB, Hwang SJ, Tae G, et al. Bone regeneration using hyaluronic acid-based hydrogel with bone morphogenic protein-2 and human mesenchymal stem cells. Biomaterials. 2007;28:1830-7.

[84] Lisignoli G, Zini N, Remiddi G, Piacentini A, Puggioli A, Trimarchi C, et al. Basic fibroblast growth factor enhances in vitro mineralization of rat bone marrow stromal cells grown on non-woven hyaluronic acid based polymer scaffold. Biomaterials. 2001;22:2095-105.

[85] Lisignoli G, Fini M, Giavaresi G, Nicoli Aldini N, Toneguzzi S, Facchini A. Osteogenesis of large segmental radius defects enhanced by basic fibroblast growth factor activated bone marrow stromal cells grown on non-woven hyaluronic acid-based polymer scaffold. Biomaterials. 2002;23:1043-51.

[86] Lee JH, Park TG, Park HS, Lee DS, Lee YK, Yoon SC, et al. Thermal and mechanical characteristics of poly(-lactic acid) nanocomposite scaffold. Biomaterials. 2003;24:2773-8.

[87] Liu H, Slamovich EB, Webster TJ. Less harmful acidic degradation of poly(lactic-co-glycolic acid) bone tissue engineering scaffolds through titania nanoparticle addition. International Journal of Nanomedicine. 2006;1:541-5.

[88] Liu H, et al. Increased osteoblast functions on nanophase titania dispersed in poly-lactic-co -glycolic acid composites. Nanotechnology. 2005;16:S601.

[89] Nejati E, Mirzadeh H, Zandi M. Synthesis and characterization of nano-hydroxyapatite rods/poly(l-lactide acid) composite scaffolds for bone tissue engineering. Composites Part A: Applied Science and Manufacturing. 2008;39:1589-96.

[90] Serrano MC, Pagani R, Vallet-Regí M, Peña J, Rámila A, Izquierdo I, et al. In vitro biocompatibility assessment of poly([var epsilon]-caprolactone) films using L929 mouse fibroblasts. Biomaterials. 2004;25:5603-11.

[91] Shor L, Güçeri S, Wen X, Gandhi M, Sun W. Fabrication of three-dimensional polycaprolactone/hydroxyapatite tissue scaffolds and osteoblast-scaffold interactions in vitro. Biomaterials. 2007;28:5291-7.

[92] Erisken C, Kalyon DM, Wang HJ. Functionally graded electrospun polycaprolactone and beta-tricalcium phosphate nanocomposites for tissue engineering applications. Biomaterials. 2008;29:4065-73.

[93] Yang Y, Yan SF, Li XX, Yin JB, Chen XS. Preparation of Poly(L-lactide)/Surface-Grafting Silica Nanocomposites and Their Surface Induction of Bone-like Apatite in Simulated Body Fluid. Chemical Journal of Chinese Universities-Chinese. 2008;29:2294-8.

[94] Karp J M SMSaDJE. Bone formation on two-dimensional poly(DL-lactide- co -glycolide) (PLGA) films and three-dimensional PLGA tissue engineering scaffolds in vitro. 2003;64a:388.

[95] Jose M, Thomas V, Johnson K, Dean D, Nyairo E. Aligned PLGA/HA nanofibrous nanocomposite scaffolds for bone tissue engineering. Acta Biomaterialia. 2009;5:305-15.

[96] X CVJaMP. Nano-fibrous poly(L-lactic acid) scaffolds with interconnected spherical macropores. 2004;25:2065.

[97] Verma D, Katti K, Katti D. Bioactivity in in situ hydroxyapatite-polycaprolactone composites. Journal of Biomedical Materials Research Part A. 2006;78A:772-80.

[98] Lei Y, Rai B, Ho KH, Teoh SH. In vitro degradation of novel bioactive polycaprolactone--20% tricalcium phosphate composite scaffolds for bone engineering. Materials Science and Engineering: C. 2007;27:293-8.

[99] Krogman NR, Weikel AL, Kristhart KA, Nukavarapu SP, Deng M, Nair LS, et al. The influence of side group modification in polyphosphazenes on hydrolysis and cell adhesion of blends with PLGA. Biomaterials. 2009;30:3035-41.

[100] Lee, Yong K. Design Parameters of Polymers for Tissue Engineering Applications. Macromolecular Research. 2005;13:277-84.

[101] Bhattacharyya S, Kumbar SG, Khan YM, Nair LS, Singh A, Krogman NR, et al. Biodegradable Polyphosphazene-Nanohydroxyapatite Composite Nanofibers: Scaffolds for Bone Tissue Engineering. Journal of Biomedical Nanotechnology. 2009;5:69-75.

[102] Nukavarapu SP, Kumbar SG, Brown JL, Krogman NR, Weikel AL, Hindenlang MD, et al. Polyphosphazene/Nano-Hydroxyapatite Composite Microsphere Scaffolds for Bone Tissue Engineering. Biomacromolecules. 2008;9:1818-25.

[103] Wang S, Lu L, Yaszemski MJ. Bone-Tissue-Engineering Material Poly(propylene fumarate): Correlation between Molecular Weight, Chain Dimensions, and Physical Properties. Biomacromolecules. 2006;7:1976-82.

[104] Horch RA, Shahid N, Mistry AS, Timmer MD, Mikos AG, Barron AR. Nanoreinforcernent of poly(propylene fumarate)-based networks with surface modified alumoxane nanoparticles for bone tissue engineering. Biomacromolecules. 2004;5:1990-8.

[105] Mistry AS, Cheng SH, Yeh T, Christenson E, Jansen JA, Mikos AG. Fabrication and in vitro degradation of porous fumarate-based polymer/alumoxane nanocomposite scaffolds for bone tissue engineering. Journal of Biomedical Materials Research Part A. 2009;89A:68-79.

[106] Shi XF, Hudson JL, Spicer PP, Tour JM, Krishnamoorti R, Mikos AG. Injectable nanocomposites of single-walled carbon nanotubes and biodegradable polymers for bone tissue engineering. Biomacromolecules. 2006;7:2237-42.

[107] Wang S, Kempen DHR, Yaszemski MJ, Lu L. The roles of matrix polymer crystallinity and hydroxyapatite nanoparticles in modulating material properties of photo-crosslinked composites and bone marrow stromal cell responses. Biomaterials. 2009;30:3359-70.

[108] Cai Z-Y, Yang D-A, Zhang N, Ji C-G, Zhu L, Zhang T. Poly(propylene fumarate)/(calcium sulphate/[beta]-tricalcium phosphate) composites: Preparation, characterization and in vitro degradation. Acta Biomaterialia. 2009;5:628-35.

[109] Boissard CIR, Bourban PE, Tami AE, Alini M, Eglin D. Nanohydroxyapatite/poly(ester urethane) scaffold for bone tissue engineering. Acta Biomaterialia.In Press, Corrected Proof.

[110] Zhao C-X, Zhang W-D. Preparation of waterborne polyurethane nanocomposites: Polymerization from functionalized hydroxyapatite. European Polymer Journal. 2008;44:1988-95.

[111] Dong Z, Li Y, Zou Q. Degradation and biocompatibility of porous nano-hydroxyapatite/polyurethane composite scaffold for bone tissue engineering. Applied Surface Science. 2009;255:6087-91.

[112] Zanetta M, Quirici N, Demarosi F, Tanzi MC, Rimondini L, Farè S. Ability of polyurethane foams to support cell proliferation and the differentiation of MSCs into osteoblasts. Acta Biomaterialia. 2009;5:1126-36.

[113] Mansur HS, Costa HS. Nanostructured poly(vinyl alcohol)/bioactive glass and poly(vinyl alcohol)/chitosan/bioactive glass hybrid scaffolds for biomedical applications. Chemical Engineering Journal. 2008;137:72-83.

[114] Srivastava VK, Rastogi A, Goel SC, Chukowry SK. Implantation of tricalcium phosphate-polyvinyl alcohol filled carbon fibre reinforced polyester resin composites into bone marrow of rabbits. Materials Science and Engineering: A. 2007;448:335-9.

[115] Huang Z-M, Zhang YZ, Kotaki M, Ramakrishna S. A review on polymer nanofibers by electrospinning and their applications in nanocomposites. Composites Science and Technology. 2003;63:2223-53.

[116] Desai K, Kit K, Li J, Zivanovic S. Morphological and Surface Properties of Electrospun Chitosan Nanofibers. Biomacromolecules. 2008;9:1000-6.

[117] Barnes CP, Sell SA, Boland ED, Simpson DG, Bowlin GL. Nanofiber technology: Designing the next generation of tissue engineering scaffolds. Advanced Drug Delivery Reviews. 2007;59:1413-33.

[118] Geng X, Kwon O-H, Jang J. Electrospinning of chitosan dissolved in concentrated acetic acid solution. Biomaterials. 2005;26:5427-32.

[119] Murugan R, Huang ZM, Yang F, Ramakrishna S. Nanofibrous scaffold engineering using electrospinning. 2007. p. 4595-603.

[120] Venugopal J, Vadgama P, Kumar TSS, Ramakrishna S. Biocomposite nanofibres and osteoblasts for bone tissue engineering. Nanotechnology. 2007;18.

[121] Shalumon KT, Binulal NS, Selvamurugan N, Nair SV, Menon D, Furuike T, et al. Electrospinning of carboxymethyl chitin/poly(vinyl alcohol) nanofibrous scaffolds for tissue engineering applications. Carbohydrate Polymers. 2009;77:863-9.

[122] Jose MV, Thomas V, Johnson KT, Dean DR, Nyairo E. Aligned PLGA/HA nanofibrous nanocomposite scaffolds for bone tissue engineering. Acta Biomaterialia. 2009;5:305-15.

[123] Li C, Vepari C, Jin H-J, Kim HJ, Kaplan DL. Electrospun silk-BMP-2 scaffolds for bone tissue engineering. Biomaterials. 2006;27:3115-24.

[124] Schneider OD, Weber F, Brunner TJ, Loher S, Ehrbar M, Schmidlin PR, et al. In vivo and in vitro evaluation of flexible, cottonwool-like nanocomposites as bone substitute material for complex defects. Acta Biomaterialia. 2009;5:1775-84.

[125] Kim HD, Bae EH, Kwon IC, Pal RR, Nam JD, Lee DS. Effect of PEG-PLLA diblock copolymer on macroporous PLLA scaffolds by thermally induced phase separation. Biomaterials. 2004;25:2319-29.

[126] Cai Q, Yang J, Bei J, Wang S. A novel porous cells scaffold made of polylactide-dextran blend by combining phase-separation and particle-leaching techniques. Biomaterials. 2002;23:4483-92.

[127] He L, Zhang Y, Zeng X, Quan D, Liao S, Zeng Y, et al. Fabrication and characterization of poly(l-lactic acid) 3D nanofibrous scaffolds with controlled architecture by liquid-liquid phase separation from a ternary polymer-solvent system. Polymer. 2009;50:4128-38.

[128] Hua FJ, Park TG, Lee DS. A facile preparation of highly interconnected macroporous poly(,-lactic acid-co-glycolic acid) (PLGA) scaffolds by liquid-liquid phase separation of a PLGA-dioxane-water ternary system. Polymer. 2003;44:1911-20.

[129] Jack KS, Velayudhan S, Luckman P, Trau M, Grøndahl L, Cooper-White J. The fabrication and characterization of biodegradable HA/PHBV nanoparticle-polymer composite scaffolds. Acta Biomaterialia. 2009;5:2657-67.

[130] Zhao F, Yin Y, Lu WW, Leong JC, Zhang W, Zhang J, et al. Preparation and histological evaluation of biomimetic three-dimensional hydroxyapatite/chitosan-gelatin network composite scaffolds. Biomaterials. 2002;23:3227-34.

[131] Kim J-W, Taki K, Nagamine S, Ohshima M. Preparation of poly(L-lactic acid) honeycomb monolith structure by unidirectional freezing and freeze-drying. Chemical Engineering Science. 2008;63:3858-63.

[132] Ho M-H, Kuo P-Y, Hsieh H-J, Hsien T-Y, Hou L-T, Lai J-Y, et al. Preparation of porous scaffolds by using freeze-extraction and freeze-gelation methods. Biomaterials. 2004;25:129-38.

[133] Wu X, Liu Y, Li X, Wen P, Zhang Y, Long Y, et al. Preparation of Aligned Porous Gelatin Scaffolds by Unidirectional Freeze-drying Method. Acta Biomaterialia.In Press, Accepted Manuscript.

[134] Yuan N-Y, Lin Y-A, Ho M-H, Wang D-M, Lai J-Y, Hsieh H-J. Effects of the cooling mode on the structure and strength of porous scaffolds made of chitosan, alginate, and carboxymethyl cellulose by the freeze-gelation method. Carbohydrate Polymers. 2009;78:349-56.

[135] Deschamps AA, Claase MB, Sleijster WJ, de Bruijn JD, Grijpma DW, Feijen J. Design of segmented poly(ether ester) materials and structures for the tissue engineering of bone. Journal of Controlled Release. 2002;78:175-86.

[136] Garcia-Fuentes M, Meinel AJ, Hilbe M, Meinel L, Merkle HP. Silk fibroin/hyaluronan scaffolds for human mesenchymal stem cell culture in tissue engineering. Biomaterials. 2009;30:5068-76.

[137] Mandal BB, Kundu SC. Cell proliferation and migration in silk fibroin 3D scaffolds. Biomaterials. 2009;30:2956-65.

[138] Wei G, Ma PX. Structure and properties of nano-hydroxyapatite/polymer composite scaffolds for bone tissue engineering. Biomaterials. 2004;25:4749-57.

[139] Yunoki S, Marukawa E, Ikoma T, Sotome S, Fan HS, Zhang XD, et al. Effect of collagen fibril formation on bioresorbability of hydroxyapatite/collagen composites. 2007. p. 2179-83.

[140] Oliveira JM, Rodrigues MT, Silva SS, Malafaya PB, Gomes ME, Viegas CA, et al. Novel hydroxyapatite/chitosan bilayered scaffold for osteochondral tissue-engineering applications: Scaffold design and its performance when seeded with goat bone marrow stromal cells. Biomaterials. 2006;27:6123-37

[141] Kim HW, Kim HE, Salih V. Stimulation of osteoblast responses to biomimetic nanocomposites of gelatin-hydroxyapatite for tissue engineering scaffolds. Biomaterials. 2005;26:5221-30.

[142] Landi E, Valentini F, Tampieri A. Porous hydroxyapatite/gelatine scaffolds with ice-designed channel-like porosity for biomedical applications. Acta Biomaterialia. 2008;4:1620-6.

[143] Maquet V, Boccaccini AR, Pravata L, Notingher I, Jérôme R. Porous poly([alpha]-hydroxyacid)/Bioglass® composite scaffolds for bone tissue engineering. I: preparation and in vitro characterisation. Biomaterials. 2004;25:4185-94.

[144] Liu X, Smith LA, Hu J, Ma PX. Biomimetic nanofibrous gelatin/apatite composite scaffolds for bone tissue engineering. Biomaterials. 2009;30:2252-8.

[145] Gong Y, Zhou Q, Gao C, Shen J. In vitro and in vivo degradability and cytocompatibility of poly(l-lactic acid) scaffold fabricated by a gelatin particle leaching method. Acta Biomaterialia. 2007;3:531-40.

[146] Hou Q, Grijpma DW, Feijen J. Porous polymeric structures for tissue engineering prepared by a coagulation, compression moulding and salt leaching technique. Biomaterials. 2003;24:1937-47.

[147] Oh SH, Kang SG, Kim ES, Cho SH, Lee JH. Fabrication and characterization of hydrophilic poly(lactic-co-glycolic acid)/poly(vinyl alcohol) blend cell scaffolds by melt-molding particulate-leaching method. Biomaterials. 2003;24:4011-21.

[148] Reignier J, Huneault MA. Preparation of interconnected poly([epsilon]-caprolactone) porous scaffolds by a combination of polymer and salt particulate leaching. Polymer. 2006;47:4703-17.

[149] Kim S-S, Sun Park M, Jeon O, Yong Choi C, Kim B-S. Poly(lactide-co-glycolide)/hydroxyapatite composite scaffolds for bone tissue engineering. Biomaterials. 2006;27:1399-409.

[150] Kim KM, Evans GRD. Tissue Engineering:The Future of Stem Cells. Topics in Tissue Engineering. 2005;2:1-21.

[151] Polak JM, Bishop AE. Stem Cells and Tissue Engineering: Past, Present, and Future. Annals of the New York Academy of Sciences. 2006;1068:352-66.

[152] Marolt D, Knezevic M, Vunjak-Novakovic G. Bone tissue engineering with human stem cells. Stem Cell Research & Therapy. 2010;1:10.

[153] Friedenstein AJ, Chailakhjan RK, Lalykina KS. The Development of Fibroblast Colonies in Monolayer Cultures of Guinea-Pig Bone Marrow and Spleen Cells. Cell Proliferation. 1970;3:393-403.

[154] Friedenstein AJ, Chailakhyan RK, Gerasimov UV. Bone marrow osteogenic stem cells: in vitro cultivation and transplantation in diffusion chambers. Cell Proliferation. 1987;20:263-72.

[155] Caplan A. Mesenchymal Stem Cells. J Orthop Res. 1991;6:641-50.

[156] Pittenger M F MAM, Beck S C, Jaiswal R K, Douglas R and Mosca J D. Multilineage potential of adult human mesenchymal stem cells. Science. 1999;284:143.

[157] Kuhn NZ, Tuan RS. Regulation of stemness and stem cell niche of mesenchymal stem cells: Implications in tumorigenesis and metastasis. Journal of Cellular Physiology. 2010;222:268-77.

[158] Morrison SJ, Kimble J. Asymmetric and symmetric stem-cell divisions in development and cancer. Nature. 2006;441:1068-74.

[159] Docheva D, Popov C, Mutschler W, Schieker M. Human mesenchymal stem cells in contact with their environment: surface characteristics and the integrin system. Journal of Cellular and Molecular Medicine. 2007;11:21-38.

[160] Simmons P, Torok-Storb B. Identification of stromal cell precursors in human bone marrow by a novel monoclonal antibody, STRO-1. Blood. 1991;78:55-62.

[161] Bielby R, Jones E, McGonagle D. The role of mesenchymal stem cells in maintenance and repair of bone. Injury. 2007;38:S26-S32.

[162] da Silva Meirelles L, Caplan AI, Nardi NB. In Search of the In Vivo Identity of Mesenchymal Stem Cells. Stem Cells. 2008;26:2287-99.

[163] Tajbakhsh S. Stem cell: what's in a name? 2009.

[164] Bianco P, Riminucci M, Gronthos S, Robey PG. Bone Marrow Stromal Stem Cells: Nature, Biology, and Potential Applications. STEM CELLS. 2001;19:180-92.

[165] Bianco P, Robey PG, Simmons PJ. Mesenchymal Stem Cells: Revisiting History, Concepts, and Assays. Cell stem cell. 2008;2:313-9.

[166] Vaananen H. Mesenchymal Stem Cells. Annals of Medicine. 2005;37:469-79.

[167] Jones E, McGonagle D. Human bone marrow mesenchymal stem cells in vivo. Rheumatology. 2008;47:126-31.

[168] Gregorio G, Yamamoto M, Ali A, Abe E, Roberson P, Manolagas S, et al. Attenuation of the self-renewal of transit-amplifying osteoblast progenitors in the murine bone marrow by 17β-estradiol. J Clin Invest. 2001;107:803-12.

[169] Godara P, Nordon RE, McFarland CD. Mesenchymal stem cells in tissue engineering. Journal of Chemical Technology & Biotechnology. 2008;83:397-407.

[170] Jiang Y, Jahagirdar BN, Reinhardt RL, Schwartz RE, Keene CD, Ortiz-Gonzalez XR, et al. Pluripotency of mesenchymal stem cells derived from adult marrow. Nature. 2002;418:41-9.

[171] Cai SA, Fu X, Sheng Z. Dedifferentiation: A New Approach in Stem Cell Research. BioScience. 2007;57:655-62.

[172] Odelberg SJ. Inducing cellular dedifferentiation: a potential method for enhancing endogenous regeneration in mammals. Seminars in Cell & Developmental Biology. 2002;13:335-43.

[173] Song L, Tuan RS. Transdifferentiation potential of human mesenchymal stem cells derived from bone marrow. The FASEB Journal.

[174] Hwang NS, Zhang C, Hwang Y-S, Varghese S. Mesenchymal stem cell differentiation and roles in regenerative medicine. Wiley Interdisciplinary Reviews: Systems Biology and Medicine. 2009;1:97-106.

[175] Alberts B, Johnson A, Lewis J, Raff M, Roberts K, Walter P. Molecular Biology of the Cell. Fourth Edition ed: Garland Science,Taylor & Francis Group; 2002.

[176] Brakebusch C, Fassler R. The integrin-actin connection, an eternal love affair. EMBO J. 2003;22:2324-33.

[177] Majumdar M, Keane-Moore M, Buyaner D, Hardy W, Moorman M, McIntosh K, et al. Characterization and functionality of cell surface molecules on human mesenchymal stem cells. Journal of Biomedical Science. 2003;10:228-41.

[178] Walsh S, Jordan GR, Jefferiss C, Stewart K, Beresford JN. High concentrations of dexamethasone suppress the proliferation but not the differentiation or further maturation of human osteoblast precursors in vitro: relevance to glucocorticoid-induced osteoporosis. Rheumatology. 2001;40:74-83.

[179] Klees RF, Salasznyk RM, Kingsley K, Williams WA, Boskey A, Plopper GE. Laminin-5 Induces Osteogenic Gene Expression in Human Mesenchymal Stem Cells through an ERK-dependent Pathway. Mol Biol Cell. 2005;16:881-90.

[180] Schofield R. The relationship between the spleen colony-forming cell and the haemopoetic stem cell. Blood Cells. 1978;4:7-25.

[181] Moore KA, Lemischka IR. Stem Cells and Their Niches. Science. 2006;311:1880-5.

[182] Kolf C, Cho E, Tuan R. Mesenchymal stromal cells. Biology of adult mesenchymal stem cells: regulation of niche, self-renewal and differentiation. Arthritis Research & Therapy. 2007;9:204.

[183] Chanda D, Kumar S, Ponnazhagan S. Therapeutic potential of adult bone marrow-derived mesenchymal stem cells in diseases of the skeleton. Journal of Cellular Biochemistry. 2010;111:249-57.

[184] Barry FP, Murphy JM. Mesenchymal stem cells: clinical applications and biological characterization. The International Journal of Biochemistry & Cell Biology. 2004;36:568-84.

[185] Marion NW, Mao JJ. Mesenchymal Stem Cells and Tissue Engineering. In: Irina Klimanskaya and Robert L, editor. Methods in Enzymology: Academic Press; 2006. p. 339-61.

[186] Pountos I, Corscadden D, Emery P, Giannoudis PV. Mesenchymal stem cell tissue engineering: Techniques for isolation, expansion and application. Injury. 2007;38:S23-S33.

[187] Sotiropoulou PA, Perez SA, Salagianni M, Baxevanis CN, Papamichail M. Characterization of the Optimal Culture Conditions for Clinical Scale Production of Human Mesenchymal Stem Cells. STEM CELLS. 2006;24:462-71.

[188] Seong J, Kim B-C, Park J-H, Kwon I, Mantalaris A, Hwang Y-S. Stem Cells in bone tissue engineering. Biomedical Materials. 2010;5:062001.

[189] Sethe S, Scutt A, Stolzing A. Aging of mesenchymal stem cells. Ageing Research Reviews. 2006;5:91-116.

[190] García Cruz DM, Gomes M, Reis RL, Moratal D, Salmerón-Sánchez M, Gómez Ribelles JL, et al. Differentiation of mesenchymal stem cells in chitosan scaffolds with double micro and macroporosity. Journal of Biomedical Materials Research Part A. 2010;95A:1182-93.

[191] Dong J-L, Li L-X, Mu W-D, Wang Y-H, Zhou D-S, Wei Hao, et al. Bone Regeneration with BMP-2 Gene-modified Mesenchymal Stem Cells Seeded on Nano-hydroxyapatite/Collagen/ Poly(L-Lactic Acid) Scaffolds. Journal of Bioactive and Compatible Polymers. 2010;25:547-66.

[192] Kim TG, Park S-H, Chung HJ, Yang D-Y, Park TG. Microstructured scaffold coated with hydroxyapatite/collagen nanocomposite multilayer for enhanced osteogenic induction of human mesenchymal stem cells. Journal of Materials Chemistry. 2010;20:8927-33.

[193] Shokrollahi P, Mirzadeh H, Scherman OA, Huck WTS. Biological and mechanical properties of novel composites based on supramolecular polycaprolactone and functionalized hydroxyapatite. Journal of Biomedical Materials Research Part A. 2010;95A:209-21.

[194] Yang C, Frei H, Rossi FM, Burt HM. The differential in vitro and in vivo responses of bone marrow stromal cells on novel porous gelatin–alginate scaffolds. Journal of Tissue Engineering and Regenerative Medicine. 2009;3:601-14.

[195] Okada A, Kawasumi M, Usuki A, Kojima Y, Kurauchi T, Kamigaito O. Synthesis and properties of nylon-6/clay hybrids. In Polymer based molecular composites MRS SymposiumProceedings (eds D W Schaefer & J E Mark). 1990;171:45-50.

[196] Yano K, Usuki A, Okada A, Kurauchi T, Kamigaito O. Synthesis and properties of polyimide-clay hybrid. Journal of Polymer Science Part A: Polymer Chemistry. 1993;31:2493-8.

[197] Bharadwaj RK. Modeling the Barrier Properties of Polymer-Layered Silicate Nanocomposites. Macromolecules. 2001;34:9189-92.

[198] Messersmith PB, Giannelis EP. Synthesis and barrier properties of poly(ϵ-caprolactone)-layered silicate nanocomposites. Journal of Polymer Science Part A: Polymer Chemistry. 1995;33:1047-57.

[199] Gilman JW. Flammability and thermal stability studies of polymer layered-silicate (clay) nanocomposites. Applied Clay Science. 1999;15:31-49.

[200] Gilman JW, Jackson CL, Morgan AB, R. H. Flammability Properties of Polymer−Layered-Silicate Nanocomposites. Polypropylene and Polystyrene Nanocomposites. Chemistry of Materials. 2000;12:1866-73.

[201] Sinha Ray S, Yamada K, Okamoto M, Ueda K. Polylactide-Layered Silicate Nanocomposite: A Novel Biodegradable Material. Nano Letters. 2002;2:1093-6.

[202] Sikdar D, Katti K, Katti D. Molecular Interactions Alter Clay and Polymer Structure in Polymer Clay Nanocomposites. Journal of Nanoscience and Nanotechnology. 2008;8:1638-57.

[203] Sikdar D, Katti DR, Katti KS. The role of interfacial interactions on the crystallinity and nanomechanical properties of clay-polymer nanocomposites: A molecular dynamics study. Journal of Applied Polymer Science. 2008;107:3137-48.

[204] Katti KS, Sikdar D, Katti DR, Ghosh P, Verma D. Molecular interactions in intercalated organically modified clay and clay-polycaprolactam nanocomposites: Experiments and modeling. Polymer. 2006;47:403-14.

[205] Sikdar D, Katti D, Katti K, Mohanty, Bedabibhas. Effect of Organic Modifiers on Dynamic and Static Nanomechanical Properties and Crystallinity of Intercalated Clay–Polycaprolactam Nanocomposites. Journal of Applied Polymer Science. 2007;105:790-802.

[206] Sikdar D, Katti D, Katti K, Mohanty, Bedabibhas. Influence of backbone chain length and functional groups of organic modifiers on crystallinity and nanomechanical properties of intercalated clay-polycaprolactam nanocomposites. International Journal of Nanotechnology. 2009;6:468-92.

[207] Sikdar D, Pradhan SM, Katti DR, Katti KS, Mohanty B. Altered Phase Model for Polymer Clay Nanocomposites. Langmuir. 2008;24:5599-607.

[208] Takahashi T, Yamada Y, Kataoka K, Nagasaki Y. Preparation of a novel PEG-clay hybrid as a DDS material: Dispersion stability and sustained release profiles. Journal of Controlled Release. 2005;107:408-16.

[209] des Rieux A, Fievez V, Garinot M, Schneider Y-J, Préat V. Nanoparticles as potential oral delivery systems of proteins and vaccines: A mechanistic approach. Journal of Controlled Release. 2006;116:1-27.

[210] Long L-H, Zhang Y-T, Wang X-F, Cao Y-X. Montmorillonite adsorbs urea and accelerates urea excretion from the intestine. Applied Clay Science. 2009;46:57-62.

[211] Carlisle EM. Silicon: A Possible Factor in Bone Calcification. Science. 1970;167:279-80.

[212] Liu L, Won YJ, Cooke PH, Coffin DR, Fishman ML, Hicks KB, et al. Pectin/poly(lactide-co-glycolide) composite matrices for biomedical applications. Biomaterials. 2004;25:3201-10.

CHAPTER 2. DESIGN OF ORGANOMODIFIED NANOCLAYS USING UNNATURAL AMINO ACIDS AS BIOMATERIALS FOR BONE TISSUE ENGINEERING[2]

This chapter presents studies related to design of organomodified clays using unnatural amino acids for bone tissue engineering applications. The contents of this chapter have been published in Katti, K.S., Ambre, A.H., Katti, D. R. Use of unnatural amino acids for design of novel organomodified clays as components of nanocomposite biomaterials. Philosophical Transactions of The Royal Society A. 2010; 368:1963-1980.

2.1. Introduction

Tissue engineering is "an interdisciplinary field of research that applies the principles of engineering and life sciences towards the development of biological substitutes that restore, maintain, or improve tissue function" [1]. The main focus of tissue engineering is the development of materials with adequate mechanical properties that favor tissue formation, differentiation and regeneration. In this regard, there has been a continuous thrust in recent years for developing composite systems using polymers and fillers in the micrometer-nanometer range that can satisfy the requirements such as biocompatibility, biodegradability, surface properties and mechanical properties needed for materials used for tissue engineering.

In addition, extensive research on polymer-clay nanocomposites (PCNs) since 1990 when Toyota research group [2] reported significant findings for nylon/clay nanocomposites has paved the way for developing advanced composite materials based on polymer-clay composite systems.

[2]The contents of this chapter were co-authored by Avinash Ambre (second author) and Drs. Kalpana Katti and Dinesh Katti. Avinash Ambre conducted literature review, performed all experiments, drew conclusions and wrote, revised all the sections in this chapter. Drs. Kalpana Katti and Dinesh Katti assisted in discussion and proofreading of all the sections.

Polymer-clay nanocomposites (PCNs) are composites that consist of clay particles having at least one of their dimensions in nanometer range dispersed in a polymer matrix [3]. PCNs show significant improvement in properties as compared to neat polymer and polymers containing micron-size fillers. Several studies have reported that PCNs show improvement in mechanical properties [2, 4-11], decrease in gas permeability [12-15] and flammability [16, 17] and also affect the biodegradability of biodegradable polymers [18]. There has also been a considerable interest in modeling & simulation and development of new theories for PCNs. A recent simulation study has reported the development of an altered phase concept for PCNs [19]. According to this study, molecular-level interactions between polymer and clay in PCNs create an "altered polymer phase" with different elastic properties as compared to the neat polymer. This "altered polymeric phase" was responsible for the increase in mechanical properties of PCNs. In another simulation study related to PCNs, it was found that the properties of the clay and polymer and the interactions at the interfaces between them change the properties of both the polymer and clay that played an important role in the mechanical behavior of PCNs [20].

Montmorillonite (MMT) clay has been an important constituent of PCNs that is responsible for their significantly improved or changed properties. Sodium montmorillonite (Na-MMT) is a layered silicate from the family of 2:1 phyllosilicates [3, 21, 22]. There is one octahedral alumina sheet between two silica tetrahedral sheets in each layer of MMT (Figure 2.1.). The thickness of each layer is in the nanometer range and its lateral dimension is in micrometer range. Isomorphic substitutions take place in the layers of Na-MMT that generate negative charge, which is balanced by the exchangeable cations such as sodium, calcium and magnesium present in the interlayer spacing. Pure MMT clay is hydrophilic and can be made organophilic by exchanging the cations present in the interlayer with cationic surfactants such as

alkylammonium or alkylphosphonium ions. The cationic surfactants may also increase the interlayer spacing and thus facilitate the intercalation of the polymeric species in the interlayer [3, 21-23].

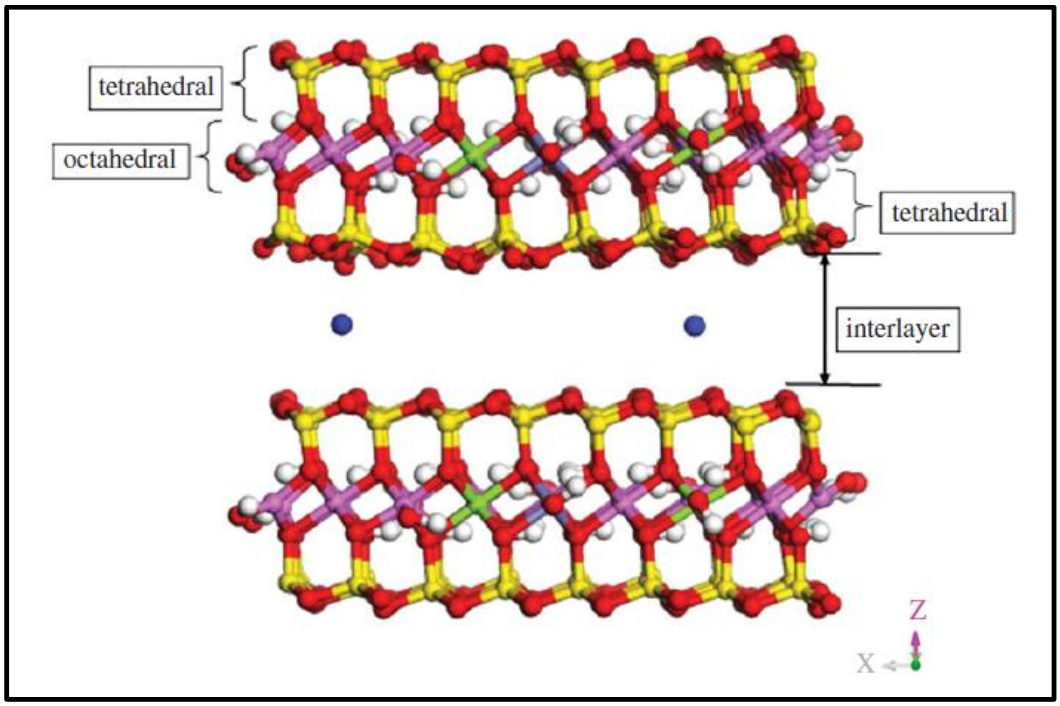

Figure 2.1. Model of the atomic structure of Na-MMT clay

Although MMT clay has medicinal properties and several studies involving the use of MMT clay for drug release and drug delivery applications have been carried out till date, a limited number of studies related to the utilization of MMT for structural application in biomaterials have been reported. Few studies related to the use of chitosan and MMT have been reported [24-27]. Xu et al. prepared chitosan/MMT nanocomposite films with an improved tensile strength [28]. Wang et al. [26] prepared exfoliated-intercalated chitosan/MMT nanocomposites and found that the presence of MMT clay improved the thermal properties and increased the hardness and elastic modulus of the composites. Lin et al**.** [29] developed chitosan/clay nanocomposites that showed an improvement in tensile strength and a decrease in

in vitro degradation. In our previous work, we synthesized a novel chitosan/ MMT/hydroxyapatite (HAP) nanocomposite that showed significant increase in nanomechanical property as compared to the chi/HAP and chi/MMT composites [30]. Also, polycaprolactone/MMT nanocomposites were prepared by electrospinning that exhibited improved stiffness as compared to neat polycaprolactone without any significant decrease in the ductility of the polymer [31]. Zheng et al. [32] developed a gelatin/MMT-chitosan scaffold that showed an improvement in mechanical properties due to the addition of MMT and also found that the degradation rate was affected by the MMT clay content.

Modification of clays plays an important role in the preparation of nanocomposites since it can affect the final properties of the nanocomposites. The extent of intercalation of the polymer in the interlayer spacing of clay is affected by the interactions between the polymer and the functional groups of the modifier used for clay modification. Our prior simulation study in using amino acids to intercalate clays has indicated that clays may be intercalated with amino acids [33]. In addition, our work involving PCNs indicated the role of chain length and functionality of a modifier on the ability to intercalate the clay [34]. Hence, we chose amino acids with longer chains as modifiers in this work. Molecular dynamics simulation studies related to PCNs have shown the importance of the effect of interactions between polymer, organic modifiers and clay on the crystallinity and nanomechanical properties of PCNs [35]. Also, we found that organic modifiers affect the crystallinity and nanomechanical properties of the prepared PCNs [36]. Therefore, it is essential to use an appropriate modifier to obtain the required properties in the composites. In order to use MMT clay for structural application in biomaterials, it is necessary to increase its interlayer spacing and simultaneously maintain or improve its biocompatibility. Unnatural amino acids possess the potential to be used as modifiers that can increase the

interlayer spacing of clay and also maintain or improve its biocompatibility. These are the "non-genetically coded amino acids" [37] that are either natural or synthetic and are gaining significance in drug research. They find use as chiral building blocks, molecular scaffolds in constructing combinatorial libraries and molecular probes for better understanding of biological systems [37, 38]. In this work, we hypothesize that MMT clays modified using unnatural amino acids based on molecular level materials design approach are biocompatible and have potential to be used as biocompatible constituents for increasing mechanical properties of bone tissue engineering scaffolds. Modifying/intercalating sodium montmorillonite (Na-MMT) clay with unnatural amino acids, characterization of Na-MMT clay modified with unnatural amino acids using X-ray diffraction (XRD) and Fourier transform infrared spectroscopy (FTIR) and studying the bicompatibility of unnatural amino acid Na-MMT clays with osteoblasts (bone cells) were the objectives of this study. Three different unnatural amino acids (Figure 2.2.) were used for modifying MMT clay. X-ray diffraction (XRD) was used to study the intercalation of amino acids in the MMT clay. The modified clays were also characterized by Fourier transform infrared (FTIR) spectroscopy and the biocompatibility of the modified MMT clay was assessed through cell culture experiments.

2.2. Materials

Na-Montmorillonite (Swy-2, Crook County, WY) with a cationic exchange capacity of 76.4 mequiv/100g was obtained from the Clay Minerals Repository at the University of Missouri, Columbia, Missouri. The three amino acids, viz.: (±2) Aminopimelic acid, 5-Aminovaleric acid, DL-2- Aminocaprylic acid were obtained from Sigma-Aldrich. Silver nitrate (0.1 N) was purchased from Anachemia chemicals and 1 N hydrochloric acid (HCL) was purchased purchased from VWR International. Chitosan (> 85% deacetylated) and

polygalacturonic acid (~95 % enzymatic) were obtained from Sigma-Aldrich. In order to perform cell culture experiments, HyQ Dulbecco's Modified Eagle's Medium (DMEM)—12 (1:1) from Hyclone, G418 solution (antibiotic) from JR Scientific were used. Osteoblast cells (cell line number CRL-11372) and fetal bovine serum (FBS) were purchased from American Type Culture Collection (ATCC).

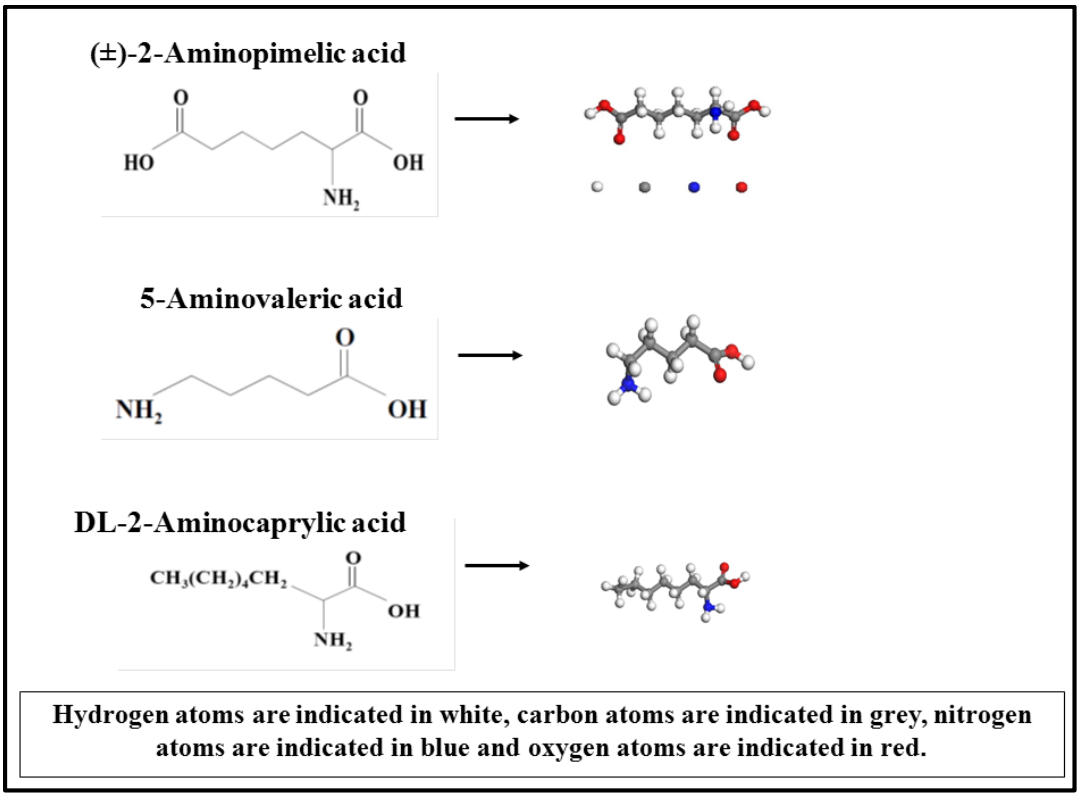

Figure 2.2. Molecular structure of unnatural amino acids

2.3. Experiments

2.3.1. Preparation of Modified Montmorillonite (MMT) Clays

Sodium montmorillonite (Na-MMT) was ground into fine powder and then screened through # 325 sieve (45 µm). Five grams of this fine and sieved sodium MMT was placed in an oven for heating for 12 hours at 60ºC. Sodium MMT was then dispersed into 400 ml deionized (DI) water preheated to 60ºC. In another beaker, 1.9 grams of amino acid was added to 100 ml

DI water preheated to 60ºC. The pH of the amino acid solution used was maintained at 1.8 by adding 0.1 N HCL. The amino acid solution was then added to the MMT clay suspension and the resulting solution was stirred vigorously for 1 hour under pH of 1.8 at 60ºC. The modified montmorillonite (MMT) was separated by centrifuging and further washed several times with DI water until the Cl^- ions were completely removed from the clay. The filtrate obtained after centrifuging was titrated with 0.1 N silver nitrate. The titration procedure was repeated until no white precipitate was formed that indicated the complete removal of chloride ions. Finally, the modified clay was placed in an oven for 24 hours at 70ºC for 24 hours. The modified clay was then ground and passed through # 325 sieve (45 µm). The aforementioned method of preparation of modified clays was used for preparation of modified clays with the three amino acids used in this study.

2.3.2 Preparation of Chitosan-PgA-HAP-MMT Composite Films

Chitosan (Chi) and polygalacturonic acid (PgA) solutions were prepared separately by dissolving 1 gram each of chitosan and polygalacturonic acid to 100 ml deionized water. Acetic acid was used for dissolving chitosan in deionized water and diluted sodium hydroxide solution was used for dissolving polygalacturonic acid in deionized water. Chitosan solution was added dropwise to polygalacturonic acid solution and the resulting mixture was sonicated to obtain ChiPgA polyelectrolyte complex solution. Hydroxyapatite (HAP) was prepared by using wet precipitation method [39]. HAP (20 wt %) and MMT clay modified with 5-aminovaleric acid (10 wt %) were dispersed in deionized water by sonication separately and added to the ChiPgA polyelectrolyte complex solution. The resulting mixture was sonicated for proper mixing of HAP and modified clay. Films were prepared by adding the ChiPgAHAPMMT solution (1: 10 dilution) to tissue culture polystyrene Petri dishes (60 mm OD x 15 mm H) and subsequent

evaporation under atmospheric conditions. These films were used for determining biocompatibility through cell culture.

2.3.3. XRD Characterization

The XRD experiments on powdered clay samples were done by using X-ray diffractometer (model Philips X'pert, Almelo, Netherlands) equipped with secondary monochromator and Cu-tube using CuKα radiation of wavelength 1.54056 Å. The d-spacing of clay structure was calculated from the XRD data using Bragg's diffraction law. The scan range used was $2\theta = 2\text{-}30^{o}$ and the scan rate used was 2°/min. Powdered MMT clay and modified clay samples were placed in an aluminum mount prior to performing the XRD scan.

2.3.4. FTIR Characterization

FTIR experiments were conducted using a Thermonicolet, Nexus, 870 spectrometer with a KBr beam splitter in the range of 4000-400 cm^{-1} at a spectral resolution of 4 cm^{-1} and mirror velocity of 0.158 cm s^{-1}. FTIR experiments were performed by using transmission technique. Samples for FTIR experiments in the form of pellets were prepared from mixture of KBr and powdered clay. The samples were placed in the universal sample holder for conducting the FTIR experiments.

2.3.5. Cell Culture

Powdered MMT and modified clays (1.5 mg each) were placed in tissue culture polystyrene Petri dishes and then sterilized by placing these Petri dishes for 2.5 hours under ultraviolet (UV) light. Tissue culture polystyrene Petri dishes without clay samples were also sterilized under UV light. 40,000 osteoblast cells (passage # 7) were then seeded in to these Petri dishes (60 mm OD x 15 mm H) having actual growth area of 19.5 cm^2. Cells in the Petri dishes were then allowed to grow in the presence of 1.5 ml cell culture medium that consisted of 90 %

HyQ DMEM-12 (1:1), 10 % FBS and 0.6 % G418 solution (antibiotic) for each sample. The Petri dishes containing the samples were then placed in an incubator at 37º C and at 5 % CO_2. The growth of the cells in Petri dishes containing the clays was investigated by taking photographs after 48 hours of seeding the cells on the powdered clay samples by using an inverted microscope. Two Petri dishes (duplicates) were used for each type of modified clay and also the unmodified clay. Twenty photographs were taken for each type of clay from these duplicates and number of cells in each of these twenty photographs were used for calculating the cell density.

For determining the biocompatibility of the ChiPgAHAPMMT films, osteoblast cells were seeded on these films in the Petri dishes. Osteoblast cells [CRL 11372, American Type Culture Collection (ATCC)] at 95 % confluence were obtained from T-flasks. 0.5 ml cell solution was added to the Petri dishes containing the films along with 1.5 ml cell culture medium. The attachment of osteoblast cells on the films was observed under an inverted microscope.

2.3.6. Statistical Analysis

One-way ANOVA was used for performing statistical analysis with Minitab software and probability values less than 0.05 ($p < 0.05$) were considered statistically significant.

2.4. Results and Discussion

2.4.1. XRD Results

The XRD patterns of MMT clay and MMT clay modified with the three amino acids used in this study are shown in Figures 2.3. (a, b & c).The peak corresponding to d_{001} plane of pure MMT clay is observed at $2\theta = 8.842º$. The d_{001} spacing at this value of 2θ is 9.992 Å. In case of MMT clay modified with (±2) aminopimelic acid, the peak appears at $2\theta = 7.943º$, which

corresponds to a b d_{001} spacing of 11.121 Å. For MMT clay modified with 5-aminovaleric acid, the peak appears at 2θ= 6.912º that corresponds to a d_{001} spacing of 12.771 Å. The peak for MMT clay modified with DL-2-aminocaprylic acid is seen at 2θ= 6.757º that corresponds to d_{001} spacing of 13.070 Å. Thus, the d_{001} spacing of MMT clay shows an increase after modification with amino acids that indicates the formation of an intercalated structure. Figure 4 shows the comparative increase in interlayer spacing of MMT clay after modification with the amino acids. It is observed that the increase in interlayer spacing is the highest in case of MMT clay modified with DL-2-aminocaprylic acid. The difference in the extent of increase in interlayer spacing may be due to difference in the positions or number of the –COOH and $–NH_2$ groups in the three amino acids. DL-2-aminocaprylic acid has one extra $–CH_2$- group besides the methyl $–CH_3$ group as compared to (±2) aminopimelic acid and 5-aminovaleric acid. This suggests that the increase in d-spacing of the MMT clay can be affected by the length of the hydrocarbon chain and the position of the functional groups in the intercalating molecule.

2.4.2. FTIR Results of (±2) Aminopimelic Acid, 5-Aminovaleric Acid, DL-2-Aminocaprylic Acid, MMT Clay and MMT Clay Modified with (±2) Aminopimelic Acid, 5-Aminovaleric Acid, DL-2- Aminocaprylic Acid

Figures 2.4. (a,b) show the FTIR spectra for the three amino acids within the 4000-400 cm^{-1} region and 2000-1260 cm^{-1} region respectively. Table 2.1. shows the band assignments of the bands seen in this region. The bands in the 1680-1682 cm^{-1} region are due to the intramolecular hydrogen bonding due to the carboxylic groups in the three amino acids. Figure 2.5. (a-c) shows the FTIR spectra for MMT clay and MMT clay modified with the three amino acids. The corresponding band assignments are given in Table 2.2. Further discussion about the FTIR spectra shown in figure 2.5. (a-c) is given in following paragraphs under this section.

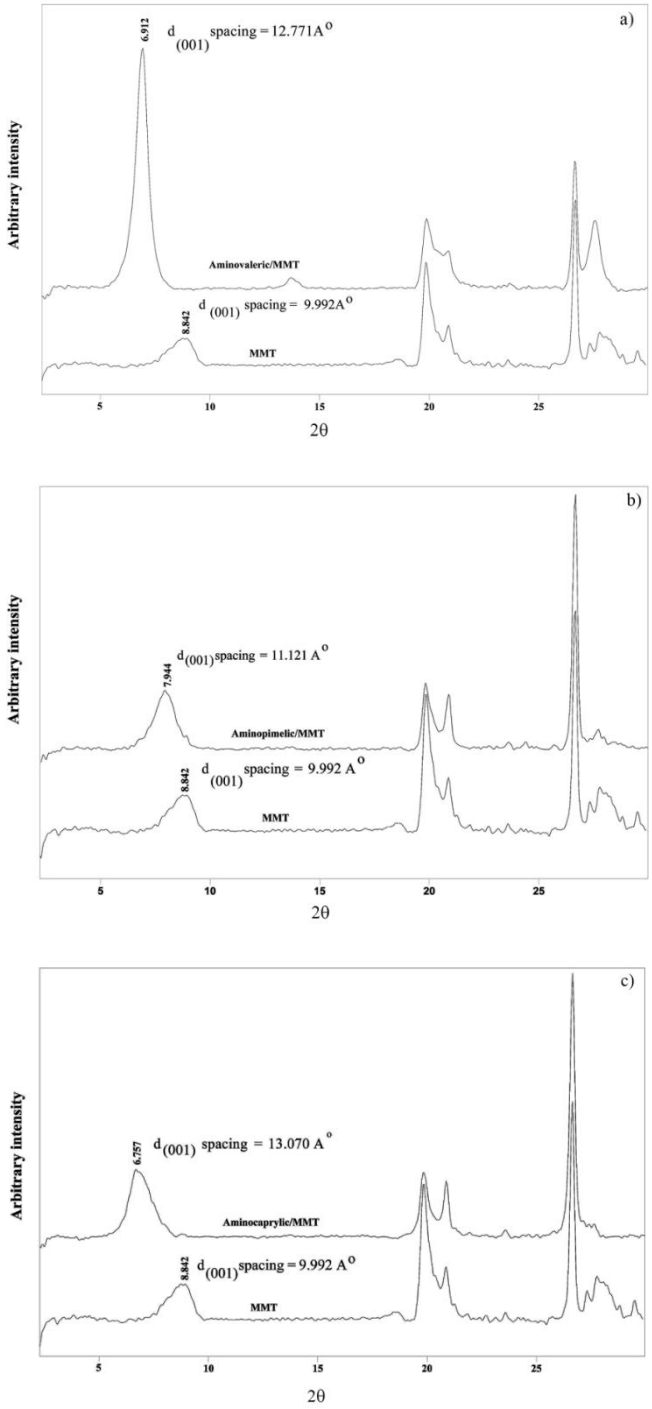

Figure 2.3. XRD pattern of a) MMT and MMT modified with 5-aminovaleric acid, b) XRD pattern of MMT and MMT modified with (±)-2-aminopimelic acid, c) XRD pattern of MMT and MMT modified with DL-2-aminocaprylic acid

Figure 2.5. (a) shows the FTIR spectra of the modified clays within the 4000-400 cm^{-1} range. Figure 2.5. (b) shows the spectra for the clays modified with the three amino acids within the 3800-2100 cm^{-1} range. The clays modified with amino acids show a shift in the band position corresponding to the structural OH group as compared to pure MMT clay. In Figure 2.5. (c), it is observed that there are differences in the FTIR spectra of the modified clays and the pure MMT clay. In case of the clays modified with the amino acids, bands are seen at 1733 cm^{-1}, 1716 cm^{-1} and 1731 cm^{-1} that indicate the presence of the amino acids in the modified clays. These bands are attributed to the C=O stretching bands of the carboxylic group in the amino acid. There is a shift in the position of the C=O stretching band to a lower frequency by 16 cm^{-1} in case of MMT clay modified with5-aminovaleric acid that suggests hydrogen bonding interactions between 5-aminovaleric acid and MMT clay. Figure 2.5. (c) also shows that there is a shift in the band positions associated with H-O-H deformation in case of clays modified with the three amino acids. Also, the bands in the 1681-1680 cm^{-1} region observed in case of the three amino acids are absent in case of all the three modified clays that indicates that the intramolecular hydrogen bonding of the three amino acids is broken due to the possible interaction of the amino acids with the clay. Figure 2.6. (a) shows the second derivative spectrum of the modified clays in the 1645-1600 cm^{-1} region. It is seen that in case of clays modified with 5-aminovaleric acid and DL-2-aminocaprylic acid, there is an overlap of two bands in this region. The bands near the 1616 cm^{-1} in case of clays modified with 5-aminovaleric acid and DL-2-aminocaprylic acid may be due to the N-H deformation vibrations that arise due to the presence of these acids in MMT clay. The absence of N-H deformation in near 1616 cm^{-1} in case of clay modified with (±2) aminopimelic acid may be attributed to the presence of two carboxylic groups that may mask the effect of presence of the amine group of (±2) aminopimelic acid. Figure 2.6. (b) shows the FTIR spectra

of modified and unmodified clays within the 1394-835 cm^{-1} region. The corresponding second derivative spectrum for this region is given in figure 2.6. (c). The band assignments for this region are given in Table 2.2. There are shifts in the Si-O stretching vibrations in case of clays modified with the amino acids. These shifts may be attributed to the interaction between the protonated amine group and the surface oxygen of silica tetrahedral. Also, the band at 1210 cm^{-1} position observed in case of pure MMT clay seems to be absent in case of clays modified with 5-aminovaleric acid and DL-2-aminocaprylic acid. This may be an implication that the crystal structure of MMT clay has changed due to intercalation of amino acids in MMT clay. Therefore, the unpolarized infrared beam is unable to cause Si-O out-of-plane stretching vibration in case of the modified clays.

2.4.3. Cell Culture Results

The number of osteoblast cells grown in the presence of MMT clay and MMT clay modified with amino acids was counted manually from the images taken with an inverted microscope after 48 hours of seeding the osteoblast cells. The cell density (cells/mm^2) for the modified clay samples was calculated and plotted as shown in Figure 2.7. (a & b). The images in Figure 2.8. shows that the osteoblast cells are attached and grow in the presence of MMT clay and MMT clay modified with the amino acids. The growth of osteoblast cells is comparatively high in case of MMT clay modified with 5-aminovaleric acid and comparatively low in case of MMT clay modified with DL-2-aminocaprylic acid. Among the modified MMT clays, MMT clay modified with 5-aminovaleric acid showed relatively higher biocompatibility.

Figure 2.9. shows that osteoblast cells were able to attach on the ChiPgAHAPMMT films. This indicates that the MMT clay modified with 5-aminovaleric acid has potential for biomaterial applications.

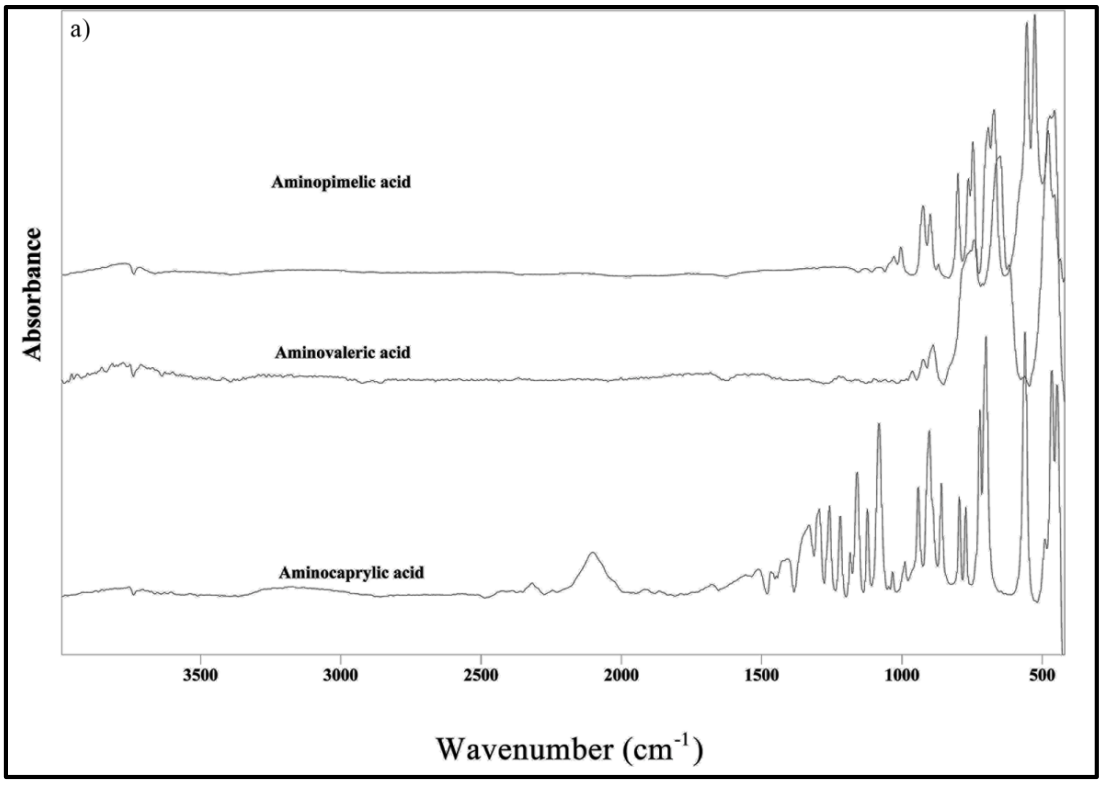

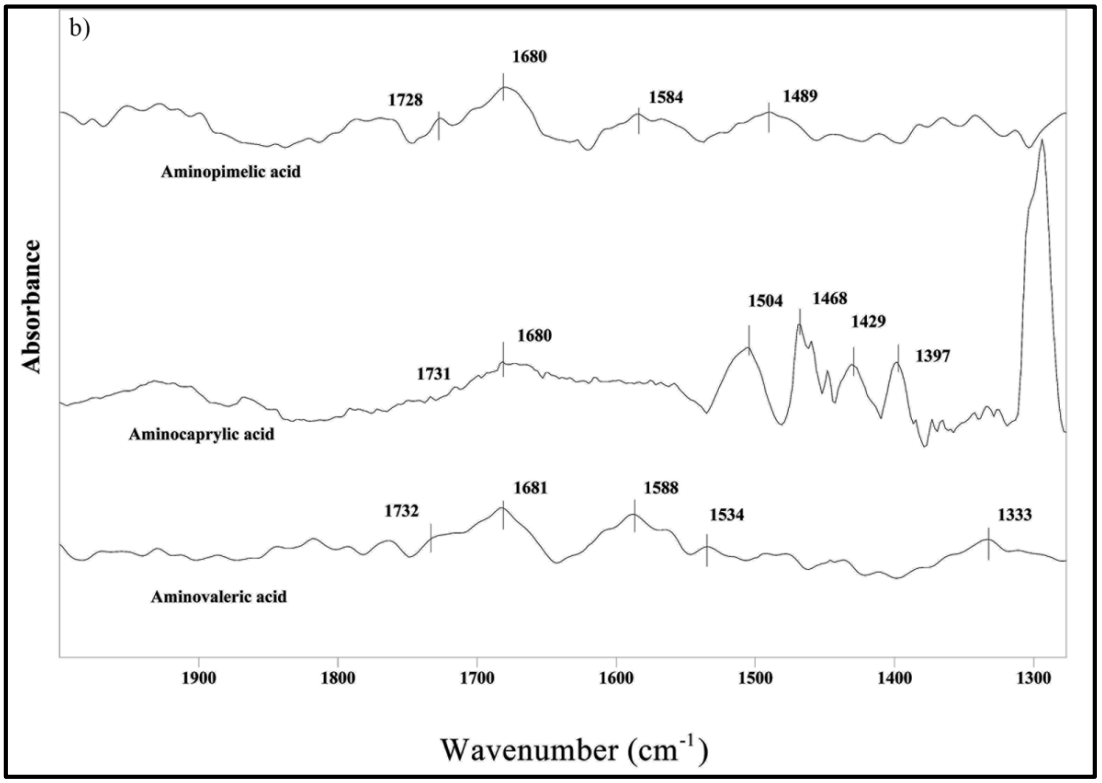

Figure 2.4. FTIR spectra of the three unnatural amino acids within the a) 4000-400 cm^{-1} range and b) 2000-1260 cm^{-1} range

Table 2.1. Band assignment for amino acids

Band position (cm^{-1})	Band assignment
3777, 3754, 3752	O-H and N-H stretching
3723, 3713, 3706	O-H and N-H stretching
2369, 2338, 2319	$N-H^{+}$ stretching
1681, 1680	C=O stretching vibration (intramolecular hydrogen bonding in carboxylic acids)
1732, 1731, 1728	C=O stretching
1584, 1588	$R-COO^{-}$ symmetric stretching
1534, 1504, 1489, 1468	N-H vibrations

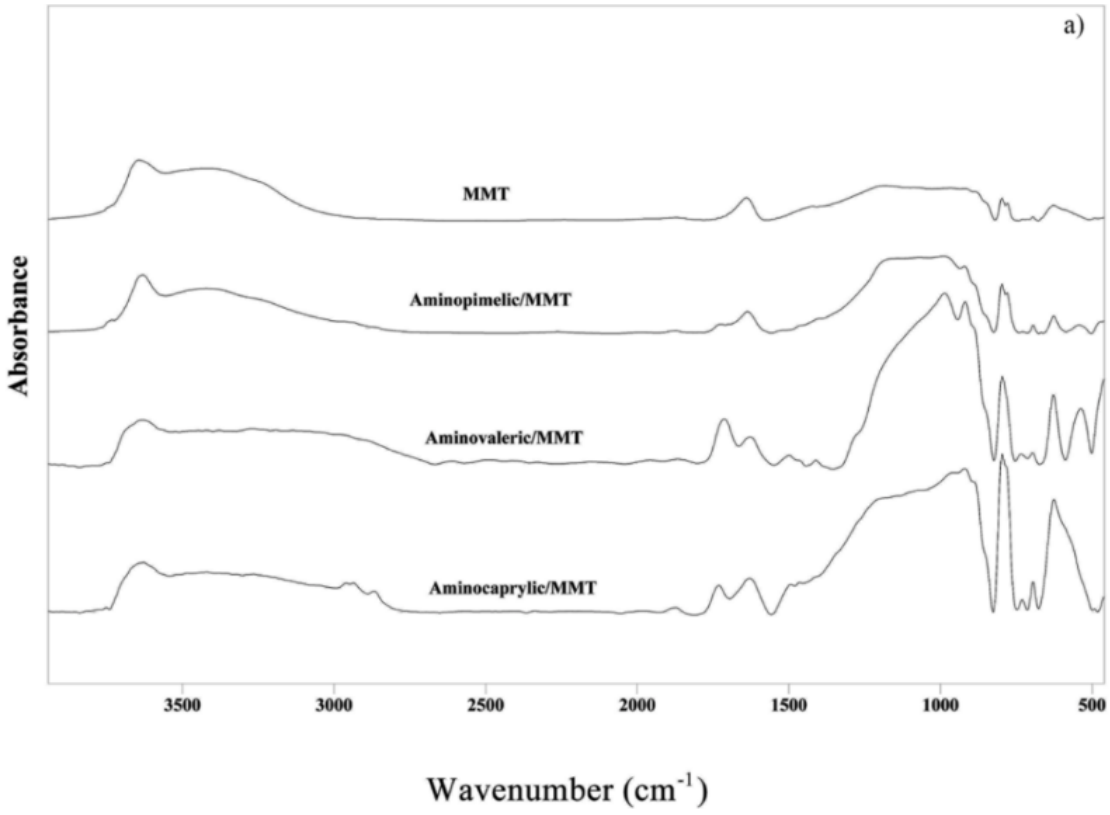

Figure 2.5. FTIR spectra of MMT clay modified with amino acids within the a) 4000-400 cm^{-1} range, b) 3800-2100 cm^{-1} range, c) 2040-1535 cm^{-1} range

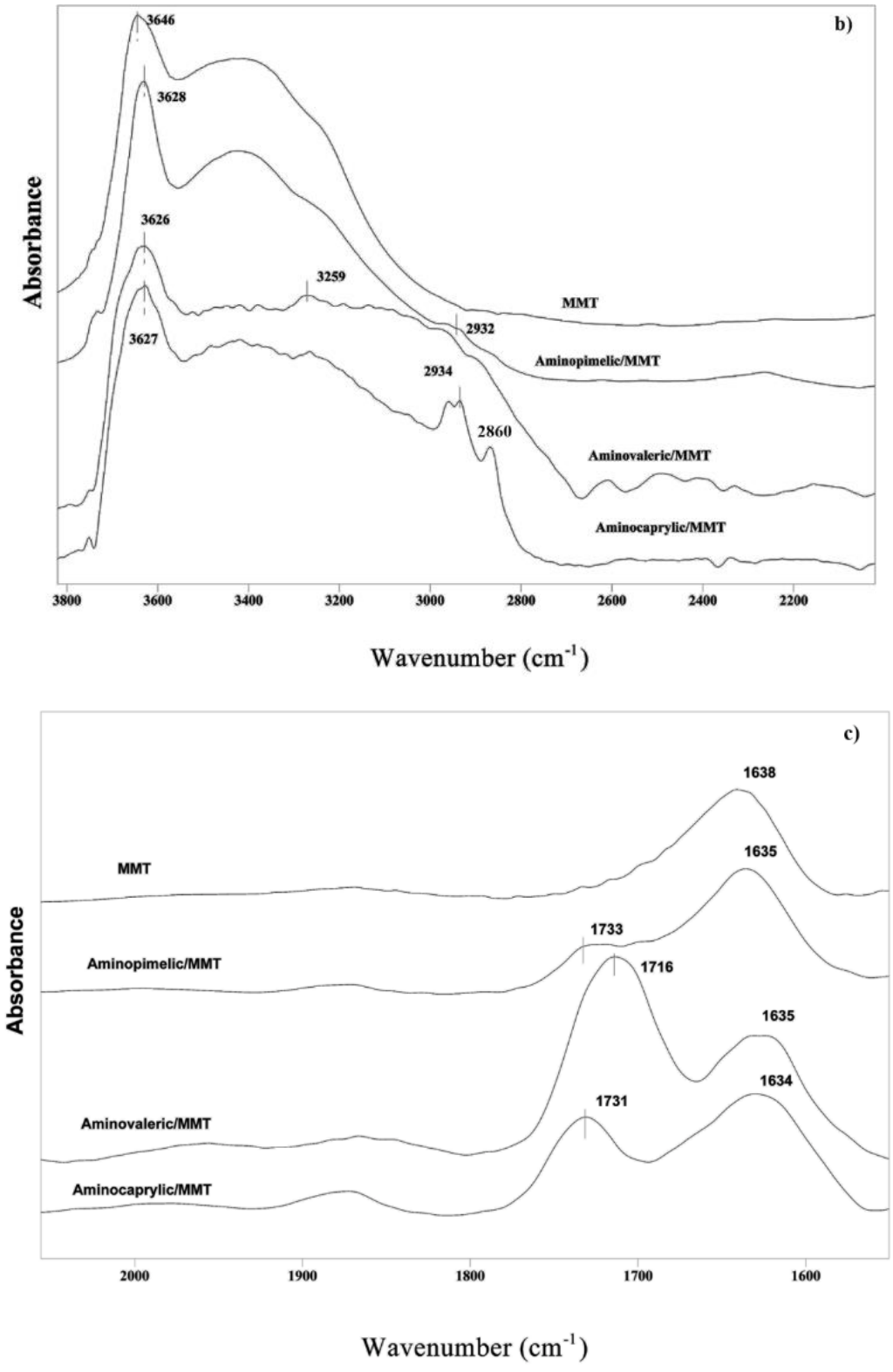

Figure 2.5. FTIR spectra of MMT clay modified with amino acids within the a) 4000-400 cm^{-1} range, b) 3800-2100 cm^{-1} range, c) 2040-1535 cm^{-1} range (continued)

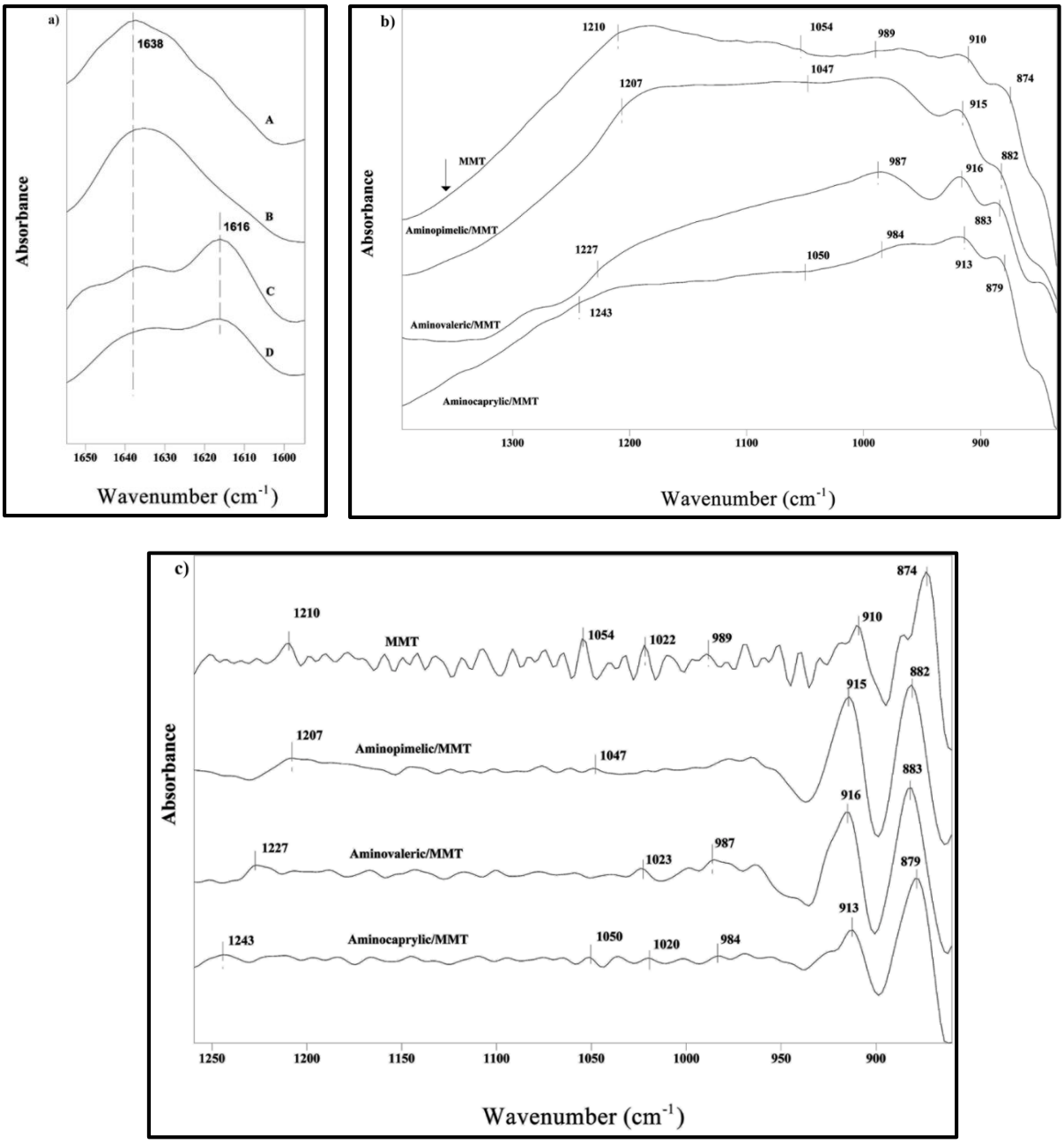

Figure 2.6. Second derivative FTIR spectra of MMT clay modified with amino acids within the a) 1655-1595 cm^{-1} range, c) 1394-835 cm^{-1} range and FTIR spectra of clay modified with amino acids within the b) 1394-835 cm^{-1} range

Table 2.2. Band assignment for MMT clay and MMT clay modified with amino acids

Band position (cm^{-1})	**Sample**	**Band assignment**
3646	MMT clay	O-H stretching of structural OH group
1638		H-O-H deformation
1211		Si-O out-of- plane stretching
1179,1054, 989		Si-O stretching
910		Al-OH deformation
874		Al-FeOH deformation
3628	MMT clay modified with (±2) aminopimelic acid	O-H stretching of structural OH group
2932		Asymmetric C-H stretching
1635		H-O-H deformation
1207		Si-O out-of- plane stretching
1047		Si-O stretching
915		Al-OH deformation
882		Al-FeOH deformation
3626	MMT clay modified with 5-aminovaleric acid	O-H stretching of structural OH group
3259		N-H symmetric stretching
1716		C=O stretching
1635		H-O-H deformation
1616		N-H deformation
987		Si-O stretching
916		Al-OH deformation
883		Al-FeOH deformation
3627	MMT clay modified with DL-2-aminocaprylic acid	O-H stretching of structural OH group
2934		Asymmetric C-H stretching
2860		Symmetric C-H stretching
1731		C=O stretching
1634		H-O-H deformation
1615		N-H deformation
1050, 984		Si-O stretching
914		Al-OH deformation
879		Al-FeOH deformation

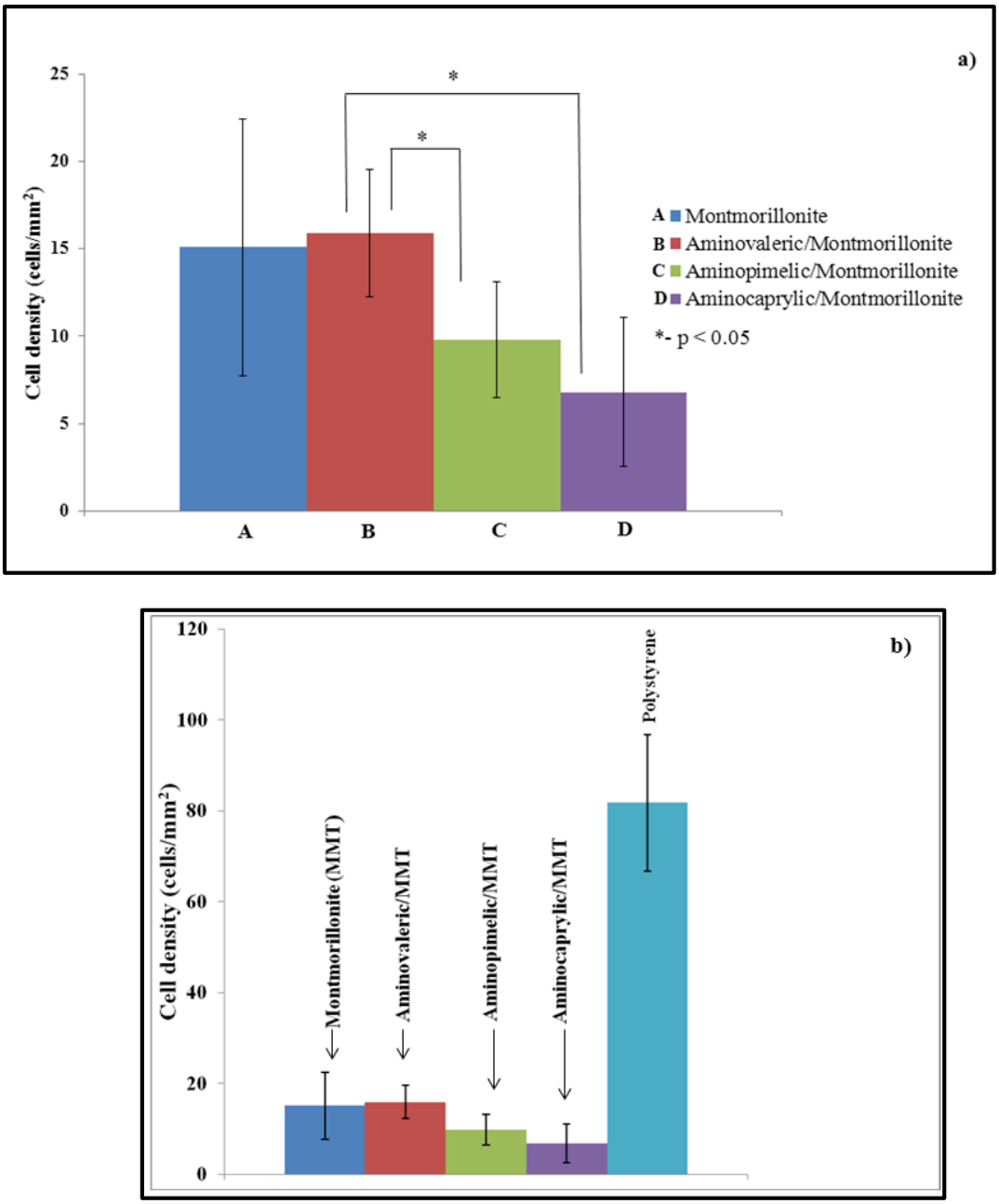

Figure 2.7. Comparative cell density data after 48 hours for a) MMT clay and MMT clay modified with the three amino acids, b) MMT clay, MMT clay modified with the three amino acids and tissue culture polystyrene Petri dishes ($p < 0.05$). Statistically significant differences in cell density were observed in case of modified MMT clays and polystyrene Petri dishes

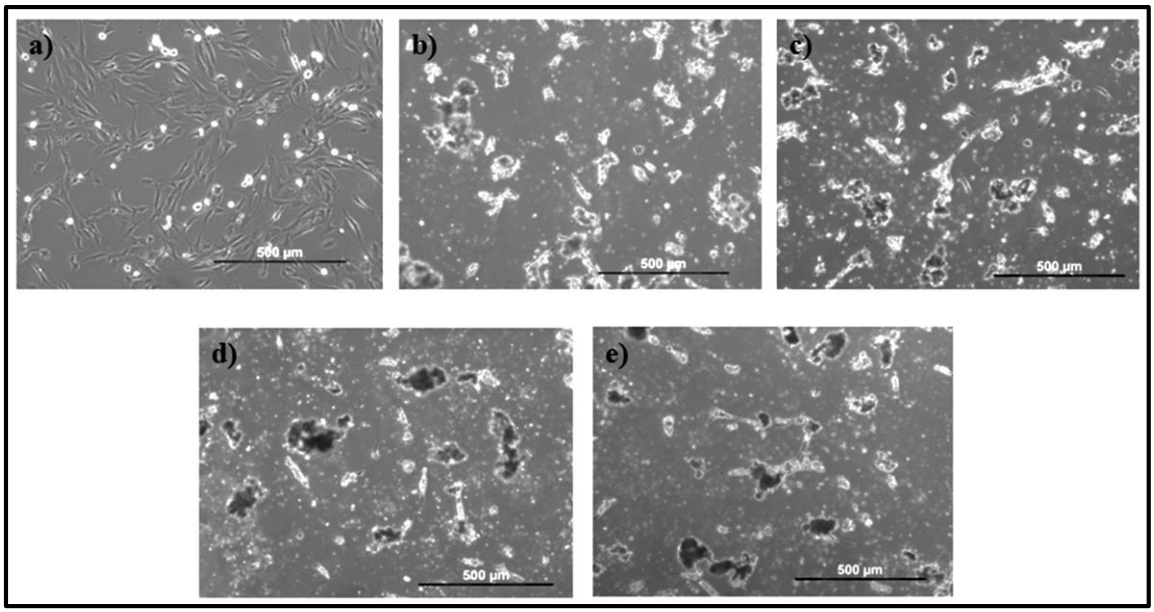

Figure 2.8. Inverted microscope images of osteoblasts cultured in a) tissue culture polystyrene (TCPS) Petri dishes, b) TCPS Petri dishes containing MMT clay, c) TCPS Petri dishes containing MMT clay modified with aminovaleric acid, d) TCPS Petri dishes containing MMT clay modified with aminocaprylic acid, e) TCPS Petri dishes containing MMT clay modified with aminopimelic acid. Scale bars (a-e) – 500 µm

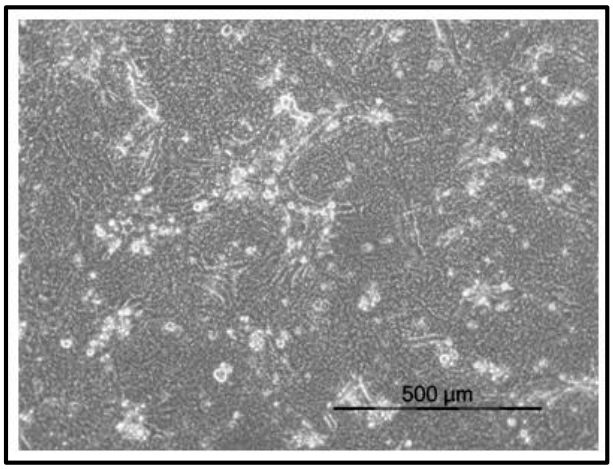

Figure 2.9. Inverted microscope image of osteoblast cells seeded on ChiPgAHAPMMT films after 4 days. Scale bar-500 µm

2.5. Conclusions

MMT clay was intercalated with three unnatural amino acids: (±2) Aminopimelic acid, 5-Aminovaleric acid and DL-2-Aminocaprylic acid. The intercalation of the clays by all the three amino acids was confirmed by XRD. Transmission FTIR experiments of clays modified with the three amino acids showed shifts in band positions of C=O vibration that were indicative of interactions between the amino acids and MMT clay. Our prior work on molecular dynamics simulations of interactions between constituents of PCNs indicates that significant non-bonded interactions, such as here observed between clay and modifier, have a large impact on the final mechanical response of the nanocomposite. Cell culture experiments showed that all the three modified clays were biocompatible. Thus, the MMT clays modified with the three amino acids used in this study show potential for structural application in biomaterials as indicated by the cell behavior on the ChiPgAHAPMMT films prepared by using the modified clay.

2.6. References

[1] Langer R, Vacanti JP. Tissue Engineering. Science. 1993;260:920-6.

[2] Okada A, Kawasumi M, Usuki A, Kojima Y, Kurauchi T, Kamigaito O. Synthesis and properties of nylon-6/clay hybrids. In Polymer based molecular composites MRS SymposiumProceedings (eds D W Schaefer & J E Mark). 1990;171:45-50.

[3] Alexandre M, Dubois P. Polymer-layered silicate nanocomposites: preparation, properties and uses of a new class of materials. Materials Science and Engineering: R: Reports. 2000;28:1-63.

[4] Giannelis EP. Polymer Layered Silicate Nanocomposites. Advanced Materials. 1996;8:29-35.

[5] Maiti P, Yamada K, Okamoto M, Ueda K, Okamoto K. New Polylactide/Layered Silicate Nanocomposites: Role of Organoclays. Chemistry of Materials. 2002;14:4654-61.

[6] Pramanik M, Srivastava SK, Samantaray BK, Bhowmick AK. Rubber-clay nanocomposite by solution blending. Journal of Applied Polymer Science. 2003;87:2216-20.

[7] Lim ST, Lee CH, Choi HJ, Jhon MS. Solidlike transition of melt-intercalated biodegradable polymer/clay nanocomposites. Journal of Polymer Science Part B: Polymer Physics. 2003;41:2052-61.

[8] Park H-M, Lee W-K, Park C-Y, Cho W-J, Ha C-S. Environmentally friendly polymer hybrids Part I Mechanical, thermal, and barrier properties of thermoplastic starch/clay nanocomposites. Journal of Materials Science. 2003;38:909-15.

[9] Chen GX, Hao GJ, Guo TY, Song MD, Zhang BH. Structure and mechanical properties of poly(3-hydroxybutyrateco-3-hydroxyvalerate) (PHBV)/clay nanocomposites. Journal of Materials Science Letters. 2002;21:1587-9.

[10] Ma C-CM, Kuo C-T, Kuan H-C, Chiang C-L. Effects of swelling agents on the crystallization behavior and mechanical properties of polyamide 6/clay nanocomposites. Journal of Applied Polymer Science. 2003;88:1686-93.

[11] Wang S, Hu Y, Wang Z, Yong T, Chen Z, Fan W. Synthesis and characterization of polycarbonate/ABS/montmorillonite nanocomposites. Polymer Degradation and Stability. 2003;80:157-61.

[12] Xu R, Manias E, Snyder AJ, Runt J. New Biomedical Poly(urethane urea)−Layered Silicate Nanocomposites. Macromolecules. 2000;34:337-9.

[13] Bharadwaj RK. Modeling the Barrier Properties of Polymer-Layered Silicate Nanocomposites. Macromolecules. 2001;34:9189-92.

[14] Messersmith PB, Giannelis EP. Synthesis and barrier properties of poly(ϵ-caprolactone)-layered silicate nanocomposites. Journal of Polymer Science Part A: Polymer Chemistry. 1995;33:1047-57.

[15] Yano K, Usuki A, Okada A, Kurauchi T, Kamigaito O. Synthesis and properties of polyimide-clay hybrid. Journal of Polymer Science Part A: Polymer Chemistry. 1993;31:2493-8.

[16] Gilman JW. Flammability and thermal stability studies of polymer layered-silicate (clay) nanocomposites. Applied Clay Science. 1999;15:31-49.

[17] Gilman JW, Jackson CL, Morgan AB, R. H. Flammability Properties of Polymer−Layered-Silicate Nanocomposites. Polypropylene and Polystyrene Nanocomposites. Chemistry of Materials. 2000;12:1866-73.

[18] Sinha Ray S, Yamada K, Okamoto M, Ueda K. Polylactide-Layered Silicate Nanocomposite: A Novel Biodegradable Material. Nano Letters. 2002;2:1093-6.

[19] Sikdar D, Pradhan SM, Katti DR, Katti KS, Mohanty B. Altered Phase Model for Polymer Clay Nanocomposites. Langmuir. 2008;24:5599-607.

[20] Sikdar D, Katti K, Katti D. Molecular Interactions Alter Clay and Polymer Structure in Polymer Clay Nanocomposites. Journal of Nanoscience and Nanotechnology. 2008;8:1638-57.

[21] Pavlidou S, Papaspyrides CD. A review on polymer–layered silicate nanocomposites. Progress in Polymer Science. 2008;33:1119-98.

[22] Sinha Ray S, Okamoto M. Polymer/layered silicate nanocomposites: a review from preparation to processing. Progress in Polymer Science. 2003;28:1539-641.

[23] de Paiva LB, Morales AR, Valenzuela Díaz FR. Organoclays: Properties, preparation and applications. Applied Clay Science. 2008;42:8-24.

[24] Günister E, Pestreli D, Ünlü CH, Atıcı O, Güngör N. Synthesis and characterization of chitosan-MMT biocomposite systems. Carbohydrate Polymers. 2007;67:358-65.

[25] Darder M, Colilla M, Ruiz-Hitzky E. Chitosan–clay nanocomposites: application as electrochemical sensors. Applied Clay Science. 2005;28:199-208.

[26] Wang SF, Shen L, Tong YJ, Chen L, Phang IY, Lim PQ, et al. Biopolymer chitosan/montmorillonite nanocomposites: Preparation and characterization. Polymer Degradation and Stability. 2005;90:123-31.

[27] Wang X, Du Y, Luo J, Lin B, Kennedy JF. Chitosan/organic rectorite nanocomposite films: Structure, characteristic and drug delivery behaviour. Carbohydrate Polymers. 2007;69:41-9.

[28] Xu Y, Ren X, Hanna MA. Chitosan/clay nanocomposite film preparation and characterization. Journal of Applied Polymer Science. 2006;99:1684-91.

[29] Lin K-F, Hsu C-Y, Huang T-S, Chiu W-Y, Lee Y-H, Young T-H. A novel method to prepare chitosan/montmorillonite nanocomposites. Journal of Applied Polymer Science. 2005;98:2042-7.

[30] Katti KS, Katti DR, Dash R. Synthesis and characterization of a novel chitosan/montmorillonite/hydroxyapatite nanocomposite for bone tissue engineering. Biomedical Materials. 2008;3:12.

[31] Marras SI, Kladi KP, Tsivintzelis I, Zuburtikudis I, Panayiotou C. Biodegradable polymer nanocomposites: The role of nanoclays on the thermomechanical characteristics and the electrospun fibrous structure. Acta Biomaterialia. 2008;4:756-65.

[32] Zheng JP, Wang CZ, Wang XX, Wang HY, Zhuang H, Yao KD. Preparation of biomimetic three-dimensional gelatin/montmorillonite-chitosan scaffold for tissue engineering. Reactive and Functional Polymers. 2007;67:780-8.

[33] Katti DR, Ghosh P, Schmidt S, Katti KS. Mechanical Properties of the Sodium Montmorillonite Interlayer Intercalated with Amino Acids. Biomacromolecules. 2005;6:3276-82.

[34] Sikdar D, Katti D, Katti K, Mohanty, Bedabibhas. Influence of backbone chain length and functional groups of organic modifiers on crystallinity and nanomechanical properties of intercalated clay-polycaprolactam nanocomposites. International Journal of Nanotechnology. 2009;6:468-92.

[35] Sikdar D, Katti DR, Katti KS. The role of interfacial interactions on the crystallinity and nanomechanical properties of clay-polymer nanocomposites: A molecular dynamics study. Journal of Applied Polymer Science. 2008;107:3137-48.

[36] Sikdar D, Katti D, Katti K, Mohanty, Bedabibhas. Effect of Organic Modifiers on Dynamic and Static Nanomechanical Properties and Crystallinity of Intercalated Clay–Polycaprolactam Nanocomposites. Journal of Applied Polymer Science. 2007;105:790-802.

[37] Ma JS. Unnatural amino acids in drug discovery. Chimica Oggi-Chemistry Today2003. p. 65-8.

[38] Dougherty DA. Unnatural amino acids as probes of protein structure and function. Current Opinion in Chemical Biology. 2000;4:645-52.

[39] Katti KS, Turlapati P, Verma D, Bhowmik R, Gujjula PK, Katti DR. Static and Dynamic Mechanical Behavior of Hydroxyapatite-Polyacrylic Acid Composites Under Simulated Body Fluid. American Journal of Biochemistry and Biotechnology. 2006 2:73-9.

CHAPTER 3. BIOPOLYMER COMPOSITE SCAFFOLDS CONTAINING NANOCLAY FOR BONE TISSUE ENGINEERING

Fabrication of chitosan-polygalacturonic acid (ChiPgA) composite scaffolds containing 5-aminovaleric acid (an unnatural amino acid) modified clay and studies showing their suitability for bone tissue engineering applications are presented in this chapter. The contents of this chapter have been published in Ambre, A.H., Katti, K.S., Katti, D.R. Nanoclay Based Composite Scaffolds for Bone Tissue Engineering Applications, ASME Journal of Nanotechnology for Engineering and Medicine. 2010, 1, 031013

3.1. Introduction

Extensive studies have been done in the field of tissue engineering since early 1990s when Langer and Vacanti introduced tissue engineering as an interdisciplinary field that combines the principles of engineering and life sciences to develop constructs useful for improving, maintaining or restoring the function of a tissue [1]. In the hindsight it can be realized that most of these studies are concerned with maintaining or restoring the function of a tissue and have corroborated that cells, scaffold and growth factors are the three important and basic components of tissue engineering. Bone tissue engineering constitutes an important area in the field of tissue engineering. The importance of bone tissue engineering has been augmented by the functional traits of bone such as providing structural support to the body, protecting the vital internal organs, facilitating body movement and acting as a reservoir of calcium and phosphate based minerals [2, 3]. Also, the increase in the number of knee and hip replacement surgeries over the past few years together with the limitations of current treatment methods such as autografts, allografts, metallic and ceramic implants have contributed to the increase in the importance of bone tissue engineering [4].

As mentioned earlier, cells, scaffold and growth factors are the three basic and important components of tissue engineering. As far as bone tissue engineering studies are concerned, the cells that can be used are differentiated cells such as osteoblasts or undifferentiated cells such as mesenchymal stem cells. Bone morphogenetic proteins (BMPs), transforming growth factor beta (TGF-β), fibroblast growth factors (FGFs), insulin growth factor I and II (IGF I/II) and platelet derived growth factors (PDGF) are some examples of growth factors that have been used for bone tissue engineering studies [4]. Scaffolds are the three dimensional porous structures that form a critical part of tissue engineering studies. Although there have been studies involving the use of ceramics such as hydroxyapatite for the preparation of scaffolds, most of the bone tissue engineering studies involve the use of polymers (natural and synthetic) and fillers such as hydroxyapatite, bioactive glass for the preparation of composite scaffolds. Biocompatibility, biodegradability, high porosity, adequate pore size (100-500 μm), interconnected pores and adequate mechanical properties are the basic requirements of a scaffold for tissue engineering applications. On the basis of studies done in the past, it can be understood that biocompatibility and biodegradability can be controlled by the choice of polymers (natural or synthetic) whereas the scaffold architecture (porosity, pore size and interconnectivity of pores) can be controlled by the use of an appropriate processing technique. One of the most important challenges in bone tissue engineering is the development of scaffolds with appropriate mechanical properties. The mechanical properties of a scaffold are supposed to be an outcome of the combination of factors such as materials used in the fabrication of scaffolds and the scaffold architecture. The overall success of a scaffold for tissue engineering applications depends on attaining a balance of the basic requirements for a scaffold mentioned earlier that further adds to the challenges associated with tissue engineering.

The purpose of scaffold in tissue engineering is to create an environment that is similar to the in vivo environment that favors the growth of cells and subsequent formation of a tissue. These scaffolds are intended to mimic the structure of the extracellular matrix since the cells respond to the mechanical properties, chemical properties and the structural features of the extracellular matrix [5, 6]. As far as bone tissue is concerned, the osteoblasts are sensitive to the mechanical and chemical signals that are conveyed through the intercellular interactions and the interactions between the cells and the surrounding extracellular matrix. Further, the connections in between the osteocytes and between the osteoblasts and osteocytes are supposed to form a three dimensional network responsible for transduction of mechanical stimuli and thus affect bone homeostasis [7]. Since the cells are supposed to attach, grow and form a tissue on the scaffold, it is necessary that the proper mechanical signals are relayed between the cells and the substrate constituting the structural features of the scaffold for proper tissue regeneration. Besides this, the scaffold should have adequate overall mechanical properties for bearing the weight of the regenerating tissue. Thus, it appears that the mechanical properties of the scaffold should be adequate from a lower scale to a higher scale for its optimum performance.

It has already been mentioned that the mechanical properties of the scaffold can be modulated by the proper choice of the materials or the fabrication technique that affects the scaffold architecture. Polymeric materials of natural or synthetic origin can be used for the preparation of composite scaffolds. Natural polymers possess molecule sequences that are similar to the sequences found in the extracellular matrix macromolecules that favor cell attachment but are limited by possibilities of batch-to-batch variation and lack of control over their properties. On the other hand, the properties of synthetic polymers can be controlled by introducing proper functional groups using different synthesis routes but they lack the molecule

sequences that are found in the macromolecules present in the extracellular matrix [8, 9]. Some examples of natural polymers that have been used for bone tissue engineering studies are chitosan [10, 11], collagen [12, 13], cellulose [14, 15], starch [16, 17] and silk fibroin [18, 19]. Aliphatic polyesters such as poly (lactic-co-glycolic acid) (PLGA) [20] and poly (lactic acid) (PLA) [21], polycaprolactone [22], polyphosphazene [23], poly (propylenefumarate) [24] are some examples of synthetic polymers that have been used previously for studies related to bone tissue engineering. Hydroxyapatite and bioactive glass are the fillers that have been extensively used for the preparation of composite scaffolds used for bone tissue engineering studies due to their osteoconductive properties. Electrospinning, freeze-drying preceded by phase separation and particulate leaching are some of the methods that are used for the fabrication of scaffolds. The electrospinning process is useful for preparing fibers having dimensions that fall in the range of extracellular matrix proteins but is limited by the use of organic solvents and difficulties in producing a uniform porous structure. The freeze-drying method preceded by phase separation is useful for producing scaffolds of varying size and shape having morphologies that can be controlled by varying the freezing temperature and concentration of polymer solutions. Particulate leaching is useful for preparing scaffolds with specific pore size and porosity but involves use of organic solvents and difficulties in obtaining interconnected pores.

The challenge of developing scaffolds with adequate mechanical properties presents a unique problem in the field of tissue engineering due to the dependence of the mechanical properties of a scaffold on several factors mentioned earlier. There seem to be two possible ways to overcome this problem; viz., by creating hierarchical structures from the molecular scale to the macroscale same as those that are supposed to be present in the extracellular matrix or by using nanosized fillers to create polymer composite scaffolds [5, 25]. Due to the very low

probability of completely mimicking the hierarchical structures present in the extracellular matrix, strategies that involve the fabrication of nanofibrous composites containing nanosized fillers may prove useful. Electrospinning, polyelectrolyte complexation and self-assembly methods involving the use of nanosized fillers mixed with polymers may be used for this purpose. Various studies have suggested that polymer nanocomposites containing nanosized fillers can prove to be useful not only to get a favorable cell response but also for achieving adequate mechanical properties [5, 25, 26]. Polymer-clay nanocomposites (PCNs) seem to possess tremendous potential with regard to the aspect of achieving adequate mechanical properties. The work on the use of montmorillonite (MMT) clay for the preparation of PCNs was pioneered by the Toyota research group in 1990 when they reported significant improvement in mechanical properties of the PCNs composed of low MMT clay loadings [27]. Subsequently, MMT clay was used for the preparation of PCNs in various studies that reported increase in mechanical properties [28-33], decrease in gas permeability [34, 35] and flammability [36, 37] and effect on biodegradability [38] after the addition of MMT clay. MMT clay is a layered silicate with one octahedral sheet between two tetrahedral sheets in each layer and thickness of each layer in the nanometer range that contributes to its high aspect ratio [38]. According to the traditional view, the observed increase in the mechanical properties of nanocomposites has been attributed to the high aspect ratio of the MMT clay sheets that leads to the increase in polymer-filler interactions. Various experimental and simulation studies carried out in our group led to the development of an "altered phase model" that attributed the enhancement in the mechanical properties of the PCNs to the formation of "altered phase" having different crystallinity and elastic properties due to the molecular level interactions between the modifier, clay and the polymer [39]. In one of the previous simulation studies carried by our group, it was also found

that the attractive interactions between the functional groups of a modifier and the polymer accompanied by the repulsive interactions between the polymer backbone and the modifier were responsible for the change in crystallinity and an increase in the nanomechanical properties of PCNs [40].

Modifiers are organic molecules that are used to modify the clay to increase the miscibility of clay in the polymer. The backbone chain length and the functional groups present in the modifier affect the d-spacing of the clay [41]. Also, it was found in this study that the backbone chain length of the modifier has more influence on the d-spacing of the clay than the functional groups present in the modifier. In addition to this, the potential of intercalating MMT clay with amino acids was brought forth by previous simulation studies carried out in our group [41]. The medicinal property of MMT clay such as its ability to adsorb various types of toxins and its ability to cross the gastrointestinal barrier [42-46] along with its drug-carrying and drug-delivery abilities [47-51] encourage its use for tissue engineering applications. It has been reported that these clays are excreted from the body since they are unable to be absorbed by the intestinal tract and they can also be dissolved by the acids present in the stomach or the bowel [52] . In addition to this, clays have also been used as an oral laxative and as an antidiarrhoeal [52]. These findings imply that clay can be suitable for tissue engineering applications where it is necessary that the degradation products obtained from the scaffold materials are excreted without having any adverse effect on the normal body functions.

The modifiers used in our previous studies were used for modification of MMT clay that was further used for the preparation of PCNs intended for structural applications and hence they were not investigated for their biocompatibility. So, on the basis of the results obtained from our previous studies and reported antibacterial activity we chose three unnatural amino acids having

a longer backbone chain length as compared to the natural amino acids for modifying the MMT clay [53]. It was found that the three unnatural amino acids were able to intercalate the MMT clay and these unnatural amino acid modified clays were biocompatible. Further, it was observed that the MMT clay modified with 5-aminovaleric acid had better biocompatibility amongst the modified clays along with an increase in interlayer spacing of 2.779 Aº and therefore it was further used for preparing polymer composite films. It was found that the human osteoblast cells were able to adhere on these polymer composite films [53].

The use of montmorillonite clay for bone tissue engineering applications needs to be investigated further. Among the few studies that have been previously carried out earlier, MMT clay was used for preparing nanocomposites to study the effect of clay addition on the mechanical properties of polymers such as chitosan [54], polycaprolactone [55] and gelatin [56] to explore their potential for biomaterial applications. There have also been few studies focused on the use of MMT clay for preparing nanocomposites for tissue engineering applications [51, 57]. But the use of MMT clays modified with unnatural amino acids in the preparation of polymer composite scaffolds for bone tissue engineering does not seem to have been reported elsewhere.

In the present work, we used MMT clay modified with 5-aminovaleric acid for the preparation of polymer composite scaffolds for bone tissue engineering studies. The choice of the MMT clay modified with 5-aminovaleric acid was based on the results obtained from our previous studies that showed that MMT clay modified with 5-aminovaleric had increased d-spacing and slightly better biocompatibility than the other two modified MMT clays [53]. Polyelectrolyte system consisting of chitosan and polygalacturonic acid was used for the preparation of composite scaffolds based on the properties of these polymers that are favorable

for tissue engineering applications. Chitosan (Chi) is a natural polymer known for its biocompatibility, antimicrobial activity, wound healing ability and minimal foreign body reaction [58]. Polygalacturonic acid is a de-esterified form of pectin found in the cell walls of plants and is known to be favorable for cell adhesion and proliferation [59]. The choice of these polymers in the present study was also based on our previous studies related to chitosan-polygalacturonic-hydroxyapatite composite scaffolds [60, 61]. This study is based on the hypothesis that scaffolds containing unnatural amino acid modified clay are capable of providing a favorable environment for adhesion and proliferation of osteoblasts (bone cells) and can also have enhanced mechanical properties due to addition of modified MMT clay. Fabrication of ChiPgA scaffolds containing 5-aminovaleric acid modified clay, characterization of fabricated clay based scaffolds and studying the biocompatibility of these clay based scaffolds with osteoblasts were the objectives of this study. The polymer composite scaffolds fabricated in this study were studied for their biocompatibility using the MTT assay and were further characterized by scanning electron microscopy (SEM). FTIR studies, studies to determine the swelling ratio and porosity were also carried out to further characterize the composite scaffolds containing modified MMT clay.

3.2. Materials and Methods

3.2.1. Materials

Polymers such as chitosan (≥ 85 % deacetylated, molecular weight 190000-310000) and polygalacturonic acid (approx. 95 % enzymatic, molecular weight 25000-50000) were bought from Sigma Aldrich. 5-aminovaleric acid used for modifying the montmorillonite clay was also obtained from Sigma Aldrich. Na-montmorillonite (Na-MMT) (Swy-2, Crook County, WY) clay having a cationic exchange capacity of 76.4 mequiv/100g was procured from the Clay Minerals

Repository at the University of Missouri, Columbia, Missouri. The raw materials used for the preparation of synthetic hydroxyapatite (HAP) such as sodium phosphate (Na_2HPO_4) and clacium chloride ($CaCl_2$) were obtained from J.T. Baker and EM Sciences respectively. HyQ Dulbecco's modified Eagle's medium (DMEM)-12 (1:1) from Hyclone, G418 antibiotic from JR scientific and fetal bovine serum (FBS) from American Type Culture Collection (ATCC) were used for the preparation of cell culture medium. Human osteoblast cells (cell line number-CRL 11372) were also obtained from ATCC for cell culture experiments.

3.2.2. Modification of Na-MMT Clay

The detailed procedure for modifying Na-MMT clay with 5-aminovaleric acid has been documented elsewhere [53]. The procedure can be summarized as follows:

A suspension of Na-MMT clay was prepared by dispersing Na-MMT clay in deionized water at 60°C and a solution of 5-aminovaleric acid in deionized water having pH 1.8 was added to the Na-MMT clay suspension at 60°C. The resulting mixture of clay and amino acid solution was stirred vigorously for 1 hour followed by centrifuging, washing, drying, grinding and sieving to get a fine powder of MMT clay modified with 5-aminovaleric acid.

3.2.3. Preparation of Hydroxyapatite

Synthetic hydroxyapatite (HAP) was prepared by using a wet precipitation method described elsewhere [62]. According to this method, a liter of $CaCl_2$ solution (19.9 mM) was added to a liter of Na_2HPO_4 solution (11.9 mM) at a pH of 7.44 followed by stirring for 12 hours and subsequent drying of the precipitate obtained after centrifuging. The dried precipitate was further ground and then sieved to obtain a powder of synthetic hydroxyapatite.

3.2.4. Preparation of Chitosan/Polygalacturonic Acid (ChiPgA) Composite Scaffolds

The preparation of ChiPgA composite scaffolds was based on a method reported previously [60, 61]. Separate solutions of chitosan and polygalacturonic acid solutions were prepared in deionized water. Acetic acid and diluted sodium hydroxide solution were used for dissolving chitosan and polygalacturonic acid respectively. ChiPgA polyelectrolyte solution was prepared by adding chitosan solution dropwise to the polygalacturonic acid solution followed by sonication. This was followed by addition of MMT clay modified with 5-aminovaleric acid and synthetic HAP (both dispersed in deionized water separately by sonication) to the resultant ChiPgA polyelectrolyte solution to obtain the ChiPgA composite solution. The ChiPgA composite solution was then frozen at -20°C and then freeze dried at -85°C, 200 mtorr pressure. Porous scaffold was obtained after freeze drying of the ChiPgA composite scaffold. ChiPgA composite scaffolds having four different compositions were prepared;, viz., ChiPgA (0 wt % HAP + 0 wt % clay modified with 5-aminovaleric acid), ChiPgAHAP (20 wt % HAP + 0 wt % clay modified with 5-aminovaleric acid), ChiPgAMMT (0 wt% HAP + 10 wt % clay modified with 5-aminovaleric acid) and ChiPgAHAPMMT (20 wt % HAP + 10 wt % clay modified with 5-aminovaleric acid).

3.2.5. Characterization

3.2.5.1. MTT Assay

In MTT assay, a yellow colored dye known as (3-(4, 5 dimethylthiazol-2)-2, 5-diphenyltetrazolium bromide) is reduced by the action of a dehydrogenase enzyme to a purple colored product known as formazan. This purple colored formazan is solubilized and the intensity of this purple colored solubilized formazan is read by using a spectrophotometer. The intensity values obtained from the spectrophotometer indicate the number of live cells. For

performing MTT assay, scaffolds of four different compositions as mentioned earlier were used. Triplicate scaffold samples of each composition were separately placed in wells (e.g. 3 samples of scaffolds containing 10 wt % modified clay in 3 different wells) of 24-well polystyrene plates and sterilized under ultraviolet light for 2 hours. After sterilization, 0.4 ml cell culture medium was added to each well of the plate containing the scaffolds followed by incubation for 2 hours at 37°C, 5 % CO_2. 2 x 10^5 human osteoblast cells (passage # 6) were then seeded on these scaffolds and 0.4 ml of cell culture medium was subsequently added. The cell seeded scaffolds were then incubated at 37°C, 5 % CO_2 for a period of 3 days and 12 days. Then the scaffolds were washed with phosphate buffer saline (PBS) solution after the removal of cell culture medium. Subsequently, 600 µL fresh cell culture medium and 60 µL MTT solution (5 mg/mL PBS) were added followed by incubation at 37°C, 5 % CO_2 for 4 hours. The resulting medium was then replaced by 0.7 ml dimethyl sulfoxide (DMSO) followed by incubation at 37°C, 5 % CO_2 for 4 hours. Absorbance readings were then taken at 570 nm using a spectrophotometer. Three readings were obtained for each scaffold sample. The complete cell culture medium used for this assay was made by adding 0.6 ml G418 antibiotic to a mixture of HyQ DMEM (90 %) and FBS (10 %).

3.2.5.2. Fourier Transform Infrared (FTIR) Spectroscopy Studies

Photoacoustic FTIR experiments were carried out on ChiPgA composite scaffolds of four different compositions; viz. ChiPgA, ChiPgAHAP, ChiPgAMMT and ChiPgAHAPMMT mentioned earlier. ThermoNicolet, Nexus 870 spectroscopy instrument equipped with MTEC model 300 photoacoustic accessory was used for performing these experiments. Linear photoacoustic spectra was collected after 1000 scans in the range of 4000-400 cm^{-1} range at a mirror velocity of 0.15 cm/s.

3.2.5.3. Scanning Electron Microscopy (SEM) studies

Scanning electron microscopy (SEM) studies were carried out on dry ChiPgA, ChiPgAHAP, ChiPgAMMT and ChiPgAHAPMMT scaffolds to study the microstructure of the scaffolds using a JEOL JSM-6490LV scanning electron microscope. SEM imaging was also performed on the scaffolds seeded with human osteoblast cells. For this purpose, the cell-seeded scaffold samples after being incubated for the required time were washed with PBS and then the cells on these scaffolds were fixed using glutaraldehyde. The scaffold samples were then dehydrated in ethanol series (10, 30, 50, 70 and 100 % (v/v)) and then finally the 100% ethanol was substituted with hexamethyldisilazane (HMDS) before drying them. The dried scaffolds were then mounted, gold sputtered and imaged.

3.2.5.4. Swelling Studies

ChiPgA, ChiPgAHAP, ChiPgAMMT and ChiPgAHAPMMT scaffold samples (triplicates) were weighed and then immersed in phosphate buffer saline (PBS, pH 7.2). The scaffolds immersed in PBS were further incubated at 37°C for 6 hours, 12 hours and 24 hours. The scaffold samples were then removed and weighed. Three samples each were used for the scaffolds of four different compositions used in these studies. The swelling ratio was calculated according to the following formula:

swelling ratio = $(W-W_0) / W_0 \times 100$,

where, W= weight of dry scaffold, W_0= weight of wet scaffold

3.2.5.5. Determination of Porosity

The porosity of the scaffolds was determined by calculating the apparent density of the scaffold samples (quadruplicates) and the solid density of the composite. The apparent density of the scaffolds was calculated by measuring the mass and the density of the scaffolds and further

using the equation $\rho = mV^{-1}$, where m represents the mass of the scaffolds and V represents the volume of the scaffolds. The porosity of the scaffolds was further calculated by using the following formula:

Porosity = $(1- \rho /\rho_s)$, where ρ = apparent density, ρ_s= solid density

The values for density of the solid composite are shown in Table 3.2.

3.2.5.6. Mechanical Properties

For determining the compressive mechanical properties, the ChiPgA composite scaffold samples [sextuplicates (n = 6)] of different compositions were compressed at 1 mm/min using MTS 858 materials testing servo- mechanical test frame (Materials Testing Solutions, Eden Prairie, MN, USA). The scaffold samples used for compression testing had diameter of 10 mm and length 10 mm. The compressive elastic modulus for the scaffolds was calculated from the slope of the initial linear region of the stress-strain curve.

3.2.5.7. Statistical Analysis

One-way ANOVA was used for performing statistical analysis and probability values less than 0.05 ($p < 0.05$) were considered statistically significant. Analysis was performed using Minitab software.

3.3. Results and Discussion

3.3.1. MTT Assay

Figure 3.1. shows the results obtained from MTT assay done on ChiPgA, ChiPgAHAP, ChiPgAMMT and ChiPgAHAPMMT scaffolds. These results indicate that the human osteoblast cells are able to live and grow on the ChiPgA composite scaffolds. Interestingly, it can be seen from these results that the number of live cells (indicated by absorbance values) in case of ChiPgA scaffolds containing MMT clay modified with 5-aminovaleric acid is comparable to

ChiPgA scaffolds containing only hydroxyapatite (HAP) known for its osteoconductive properties. After 12 days culture, ChiPgA composite scaffolds containing modified MMT clay and hydroxyapatite (HAP) show statistically higher absorbance values (proportional to cell numbers) compared to ChiPgA scaffolds without modified clay or HAP. Absorbance values for scaffolds containing only modified MMT clay and only HAP were comparable with each other. ChiPgA scaffolds containing both modified MMT clay and HAP showed statistically higher absorbance values compared to ChiPgA scaffolds, ChiPgA scaffolds containing only modified MMT clay and only HAP. Differences between absorbance values observed after 3 days and 12 days culture were statistically significant except for ChiPgA scaffolds. The ChiPgA scaffolds containing MMT clay modified with 5-aminovaleric acid (ChiPgAMMT and ChiPgAHAPMMT) appear to be biocompatible and seem to provide an environment favorable for the growth of human osteoblast cells.

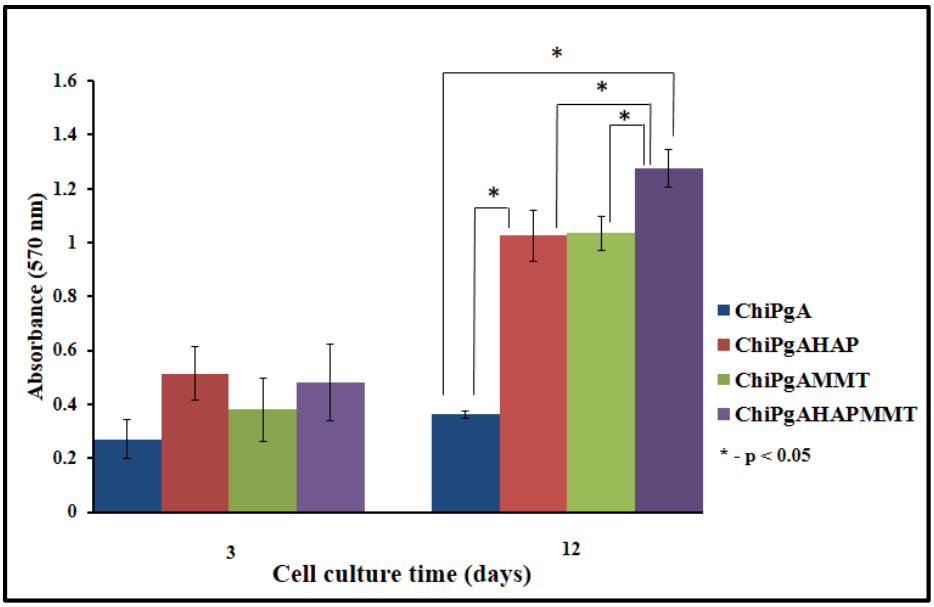

Figure 3.1. Comparative plot of results obtained from MTT assay on ChiPgA based composite scaffolds. (description of this plot given under section 3.3.1)

3.3.2. Photoacoustic Fourier Transform Infrared Spectroscopy (PA-FTIR)

Figure 3.2. (a,b) shows the spectra obtained from PA-FTIR experiments done on the ChiPgA composite scaffolds of four different compositions. Figure 3.2. (a) shows the spectra obtained in the 4000-400 cm^{-1} range from the scaffolds of different compositions. The bands from the functional groups present in chitosan (Chi) and polygalacturonic acid (PgA) and the bands from hydroxyapatite and MMT clay are supposed to be present in the lower region of the spectra and therefore spectral region from 1925-430 cm^{-1} wavenumber is presented in Figure 3.2. (b). Bands are observed close to the positions 1597 cm^{-1} and 1412 cm^{-1} in the PA-FTIR spectra of all ChiPgA composite scaffold samples that correspond to the asymmetric and symmetric stretching of dissociated carboxylic groups present in PgA. Also, bands are seen near the 1522 cm^{-1} position in the spectra of all the ChiPgA composite scaffolds that corresponds to the NH_3^+ vibration and appear to come from chitosan due to conversion of $–NH_2$ to $–NH_3^+$. The presence of bands corresponding to dissociated carboxylic groups and NH_3^+ vibration in the spectra of the ChiPgA composite scaffolds is indicative of formation of a polyelectrolyte complex between chitosan and polygalacturonic acid. The phosphate bands are known to be present in the region around 1000 cm^{-1} region, but these seem to be overlapped by the bands arising from vibrations of C-O-C glycosidic linkages in chitosan and polygalacturonic. This makes it is difficult to identify the phosphate bands from hydroxyapatite (HAP) in the ChiPgA composite scaffolds containing HAP. The bands seen near 566 cm^{-1} in case of ChiPgA composite scaffolds containing HAP are absent in case of ChiPgA composite scaffolds not containing HAP and are attributed to the OPO bending of phosphate present in HAP. Also, the bands around 527 cm^{-1} and 468 cm^{-1} present in case of ChiPgAMMT and ChiPgAHAPMMT scaffolds are not present in ChiPgA and ChiPgAHAP scaffolds and these band positions appear to correspond to the Si-O-Al and Si-O-Si

vibrations from MMT clay modified with 5-aminovaleric acid. From the PA-FTIR spectra of the scaffolds, it can be said that MMT clay modified with 5-aminovaleric acid was successfully incorporated in the ChiPgA polyelectrolyte based scaffold system. The band assignments for band positions shown in Figure 3.2. are shown in Table 3.1.

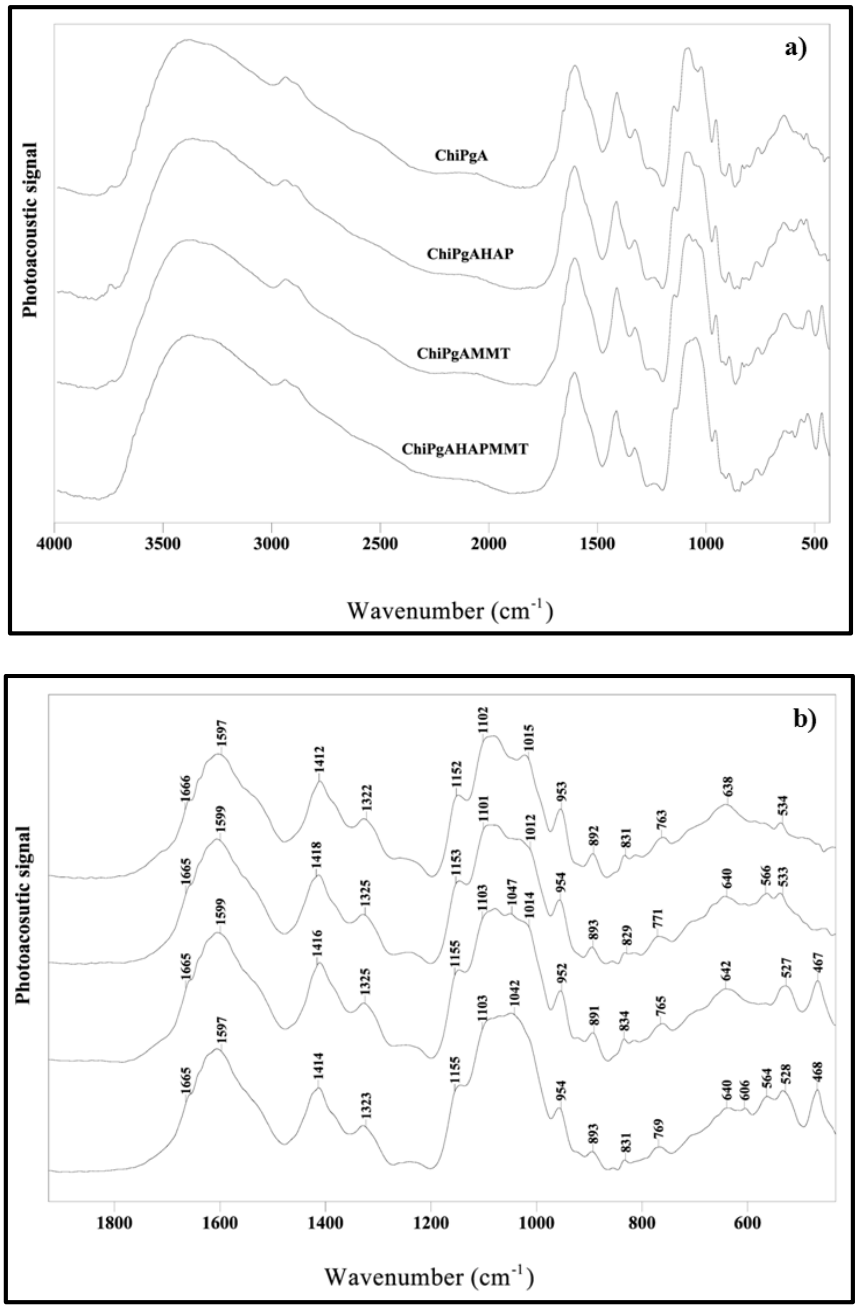

Figure 3.2. PA-FTIR spectra of ChiPgA based scaffolds: a) in the 4000-400 cm^{-1} region and b) in the 1925-430 cm^{-1} region

Table 3.1. PA-FTIR band assignments for ChiPgA composite scaffolds

Wavenumber (cm^{-1})				Band assignment
ChiPgA	**ChiPgAHAP**	**ChiPgAMMT**	**ChiPgAHAPMMT**	
1666	1665	1665	1665	Amide I bands from acetamide group of chitosan
1597	1599	1599	1597	Antisymmetric stretching of COO^{-1} group
1522	1524	1520	1524	Assymetric NH_3^+ deformation vibration
1412	1418	1416	1414	Symmetric stretching of carbonyl from COO^{-1} group
1322	1325	1325	1323	CH bending vibrations of the ring
1152	1153	1155	1155	C-O-C in glycosidic linkage
1102	1101	1103	1103	C-O-C in glycosidic linkage
1015	1012	1014	1014	Skeletal vibrations involving C-O stretching
953	954	952	954	Symmetrical ring vibration of pyranose
892	893	891	893	CH deformation vibration of β-pyranose
831	829	834	831	CH deformation vibration of pyranose
638	640	642	640	OH out of plane bending
-	566	-	564	γ_4 O-P-O bending
-	-	527	528	Si-O-Al vibration from clay
-	-	467	468	Si-O-Si bending from clay

3.3.3. Scanning Electron Microscopy (SEM) Studies

Figure 3.3. (a-d) show the scanning electron microscopy (SEM) images of ChiPgA, ChiPgAHAP, ChiPgAMMT and ChiPgAHAPMMT scaffolds. The microstructure of these scaffolds appears to be different from each other despite the same processing method being the same for the fabrication of these scaffolds. The SEM images of ChiPgAMMT and ChiPgAHAPMMT scaffolds show a different microstructure as compared to the microstructure of ChiPgA and ChiPgAHAP scaffolds. Compartment like features are seen in the microstructure of ChiPgAMMT and ChiPgAHAPMMT scaffolds. This implies that addition of MMT clay

modified with 5-aminovaleric acid has an effect on the microstructure of ChiPgA scaffolds. Figures 3.4. (a-d) show the SEM images of ChiPgA, ChiPgAHAP, ChiPgAMMT and ChiPgAHAPMMT scaffolds with human osteoblast cells. It can be seen from these images that the human osteoblast cells are able to grow in these scaffolds. In case of ChiPgA scaffolds, the cells appear to have a round morphology whereas the cells have a relatively flat morphology in case of ChiPgAHAP, ChiPgAMMT and ChiPgAHAPMMT scaffolds. In some cases, the cells are flat and also appear to take the shape of the substrate constituting the scaffold pore walls.

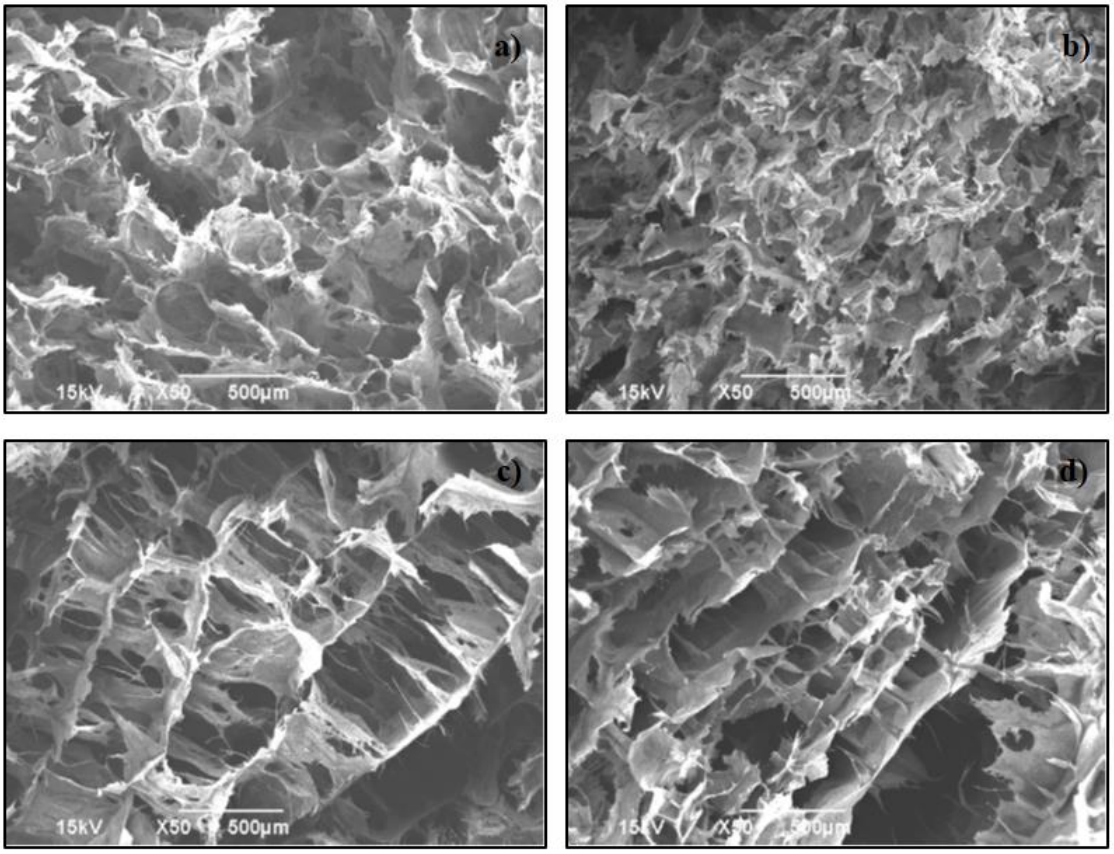

Figure 3.3. SEM image of a) dry ChiPgA scaffold, b) dry ChiPgAHAP scaffold, c) dry ChiPgAMMT scaffold, d) dry ChiPgAHAPMMT scaffold

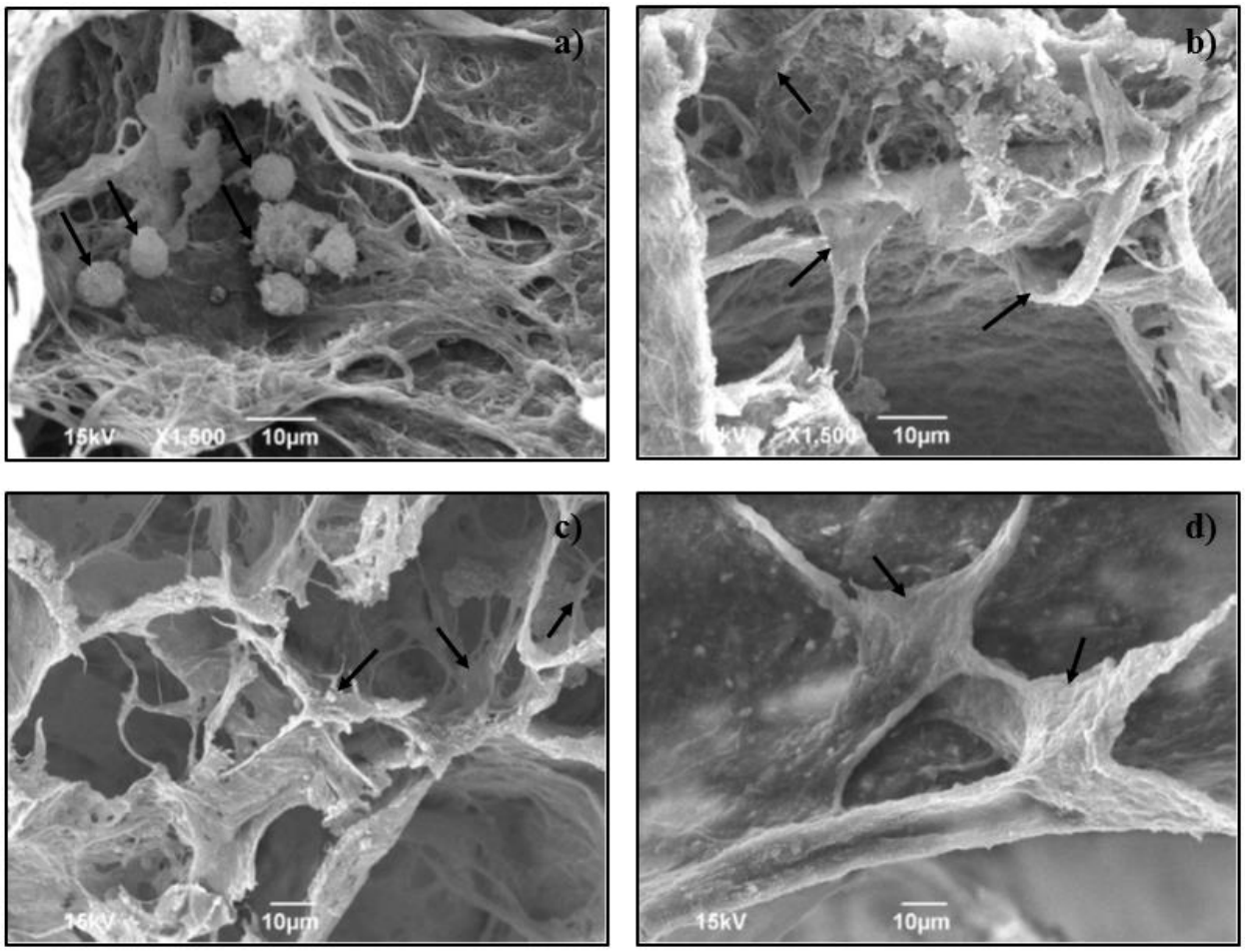

Figure 3.4. SEM image of a) ChiPgA scaffold seeded with human osteoblasts, b) ChiPgAHAP scaffold seeded with human osteoblasts, c) ChiPgAMMT scaffold seeded with human osteoblasts, d) ChiPgAHAPMMT scaffold seeded with human osteoblasts. Arrows (black color) indicate osteoblasts having spherical morphology and flat morphology (conforming to the scaffold pore walls and bridging the pores)

3.3.4. Swelling Studies

Figure 3.5. shows the plot of results obtained from swelling studies done on ChiPgA composite scaffolds. Statistically significant differences in swelling ratios were observed after 6 hours between ChiPgA scaffolds without any fillers (modified MMT clay, HAP) and ChiPgA composite scaffolds containing HAP, modified MMT clay or both. Swelling ratios for ChiPgA and ChiPgAHAP scaffolds after 12 hours showed statistically significant differences compared to swelling ratios obtained after 6 hours. Overall, it appears that the extent of change in the

swelling ratio is higher in case of ChiPgA and ChiPgAHAP scaffolds from 6 hours of immersion time to 12 hours of immersion time than the extent of change in swelling ratio from 12 hours of immersion time to 24 hours of immersion time. Also, it can be seen that the swelling ratio of ChiPgAHAPMMT scaffolds does not appear to change much over an immersion time of 24 hours as compared to the ChiPgA, ChiPgAHAP and ChiPgAMMT scaffolds. Besides this, the swelling ratio of ChiPgAMMT and ChiPgAHAPMMT scaffolds appears to be comparable to ChiPgA and ChiPgAHAP scaffolds after 12 hours and 24 hours of soaking time. This indicates that the addition of MMT clay known for its high swelling capacity does not affect much the swelling ratio of ChiPgAMMT and ChiPgAHAPMMT scaffolds after soaking time of 6 hours. The swelling capacity of the ChiPgA composite scaffolds indicates that the cells and the nutrients can reach the interior parts of these scaffolds.

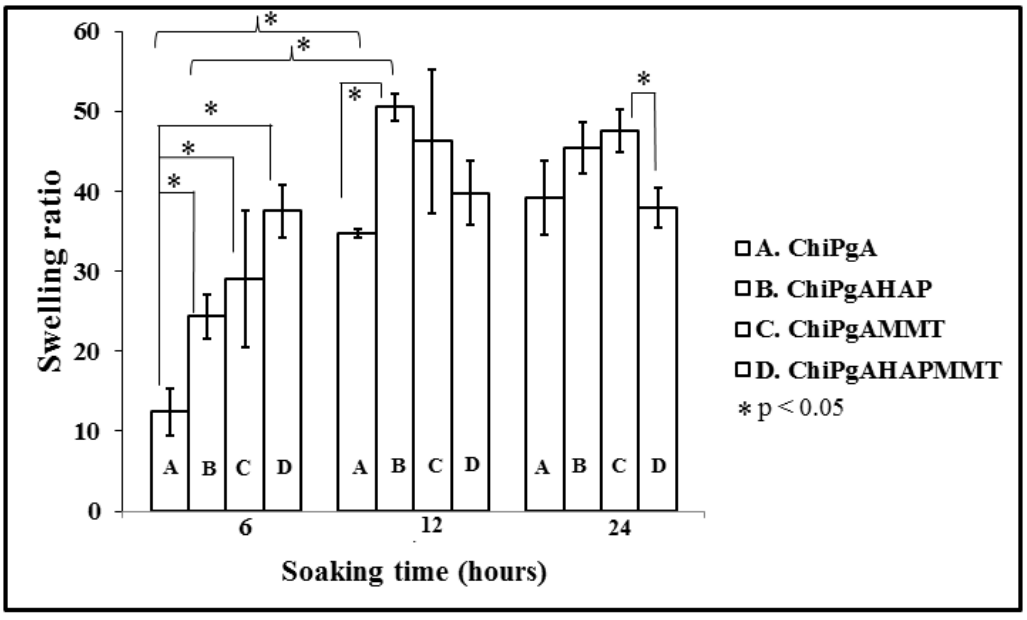

Figure 3.5. Comparative plot of results obtained from swelling studies on ChiPgA based scaffolds. (description for plot given under section 3.3.4.)

3.3.5. Porosity of Scaffolds

Figure 3.6. shows a comparative plot of the ChiPgA composite scaffolds. It can be seen from these plots that all the four different scaffolds have porosities greater than 90 percent. This satisfies the need of high porosity for scaffolds in tissue engineering applications. It is known that a scaffold needs to have high porosity for effective transport of nutrients throughout the scaffold and also for developing adequate vasculature around a regenerating tissue.

Table 3.2. Apparent and solid density values of ChiPgA composites

Property	ChiPgA	ChiPgAHAP	ChiPgAMMT	ChiPgAHAPMMT
Apparent density	0.02366 ± 0.00173	0.02385 ± 0.00112	0.02413 ± 0.00180	0.02434 ± 0.00257
Solid density	0.4651 ± 0.2031	0.4849 ± 0.1086	0.6166 ±0.0387	0.5335 ± 0.0114

3.3.6. Mechanical Properties of Scaffolds

Figure 3.7. represents a typical stress-strain curve obtained for ChiPgA, ChiPgAHAP, ChiPgAMMT and ChiPgAHAPMMT scaffolds. The stress-strain curve seems to have three regions; viz. initial linear region, a plateau region and densification region. According to Gibson and Ashby, such stress-strain curves are seen in the case of porous (cellular) materials [63]. They explained that the initial linear region is dependent on the bending of the cell (pore) walls. The plateau region results due to the collapse of the cells (pores). After the cells (pores) are completely collapsed, the opposing cell (pore) walls make contact with each other and further compress the solid that gives rise to the densification region where rapid stress increase is observed. Figure 3.8. shows a comparative plot of the compressive elastic moduli of ChiPgA based composite scaffolds. It can be seen that values of the compressive elastic modulus of ChiPgAHAP, ChiPgAMMT and ChiPgAHAPMMT scaffolds is in the 4-6 MPa range and higher

than that of ChiPgA scaffolds. Differences in elastic moduli values of ChiPgA and ChiPgA composite scaffolds were statistically significant. The high porosity of the ChiPgA composite scaffolds seems to have an effect on the mechanical properties of these scaffolds and hence the values of elastic moduli of the scaffolds are much less as compared to the compressive elastic modulus of cancellous bone (0.05-5 GPa).

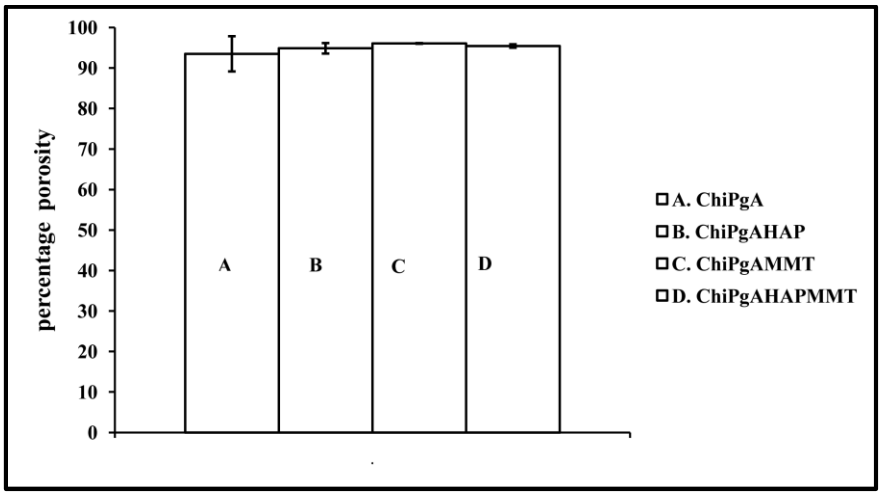

Figure 3.6. Comparative plot showing the percentage porosity of ChiPgA based scaffolds

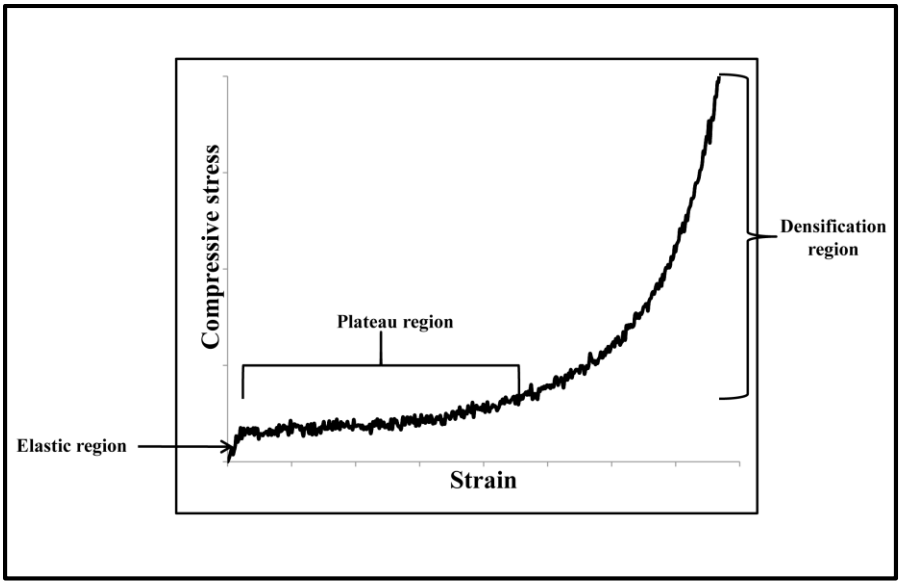

Figure 3.7. Typical stress-strain curve obtained from compression test on ChiPgA based scaffolds

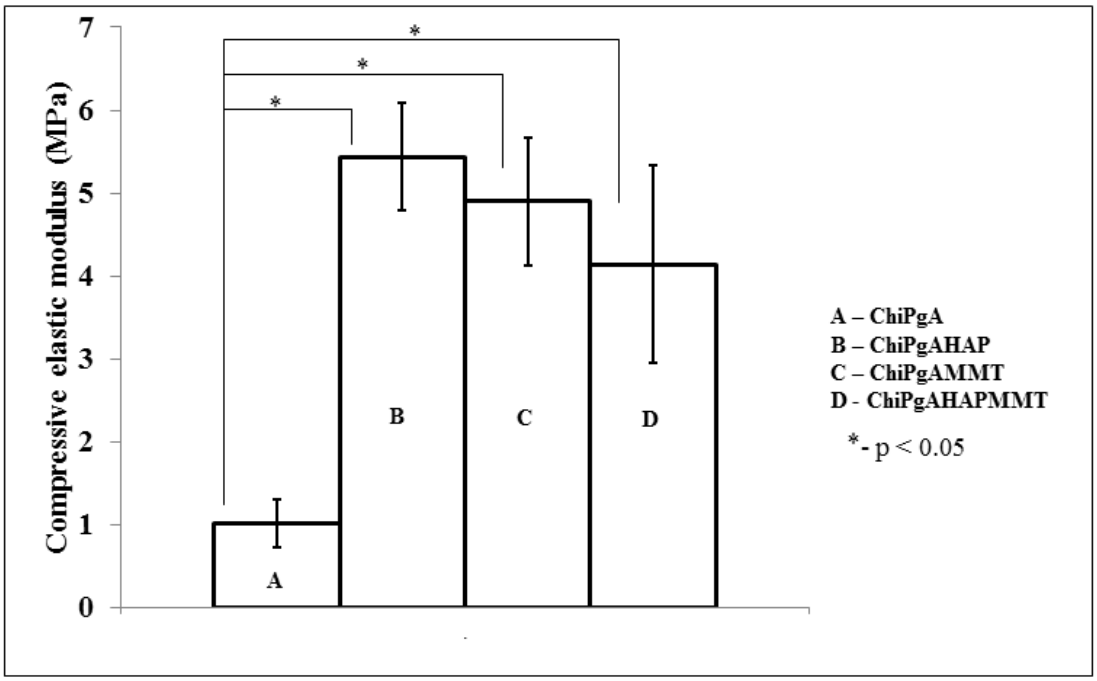

Figure 3.8. Comparative plot of the compressive elastic moduli of the ChiPgA based scaffolds. Differences in elastic moduli values of ChiPgA and ChiPgA composite scaffolds were statistically significant.

3.4. Conclusions

Scaffolds based on chitosan/polygalacturonic acid (ChiPgA) complex containing montmorillonite (MMT) clay modified with 5-aminovaleric acid were successfully prepared by freeze-drying technique. The microstructure of the scaffolds containing the modified MMT clay was affected due to the addition of this modified clay as seen in the scanning electron microscopy (SEM) images. This was despite the same processing technique being used for the fabrication of all the ChiPgA scaffolds of different composition. Experiments related to the biocompatibility of the ChiPgA composite scaffolds showed that human osteoblast cells were able to live and grow in them. The MTT assay also indicated that the number of osteoblast cells in ChiPgA scaffolds containing the modified clay was comparable to ChiPgA scaffolds containing hydroxyapatite (HAP) known for its osteoconductive properties. Overall, the ChiPgA composite scaffolds were found to be biocompatible. This was also indicated by the SEM images

of the ChiPgA composite scaffolds seeded with human osteoblast cells. Photoacoustic-FTIR (PA-FTIR) experiments on the ChiPgA composite scaffolds indicated formation of a polyelectrolyte complex between chitosan and polygalacturonic acid. PA-FTIR studies also showed that the MMT clay modified with 5-aminovaleric acid was successfully incorporated in the ChiPgA based scaffolds.

Swelling studies on ChiPgA composite scaffolds showed the swelling ability of the scaffolds that indicated that the cells and the nutrients would be able to reach the interior parts of the scaffolds. In addition to this, the ChiPgA scaffolds had a porosity greater than 90 percent that satisfies the requirement of high porosity for scaffolds used in tissue engineering studies. High porosity facilitates the nutrient transport throughout the scaffold and also plays a role in the development of adequate vasculature throughout the scaffold. Compressive mechanical tests on the scaffolds showed that the ChiPgA composite scaffolds had compressive elastic moduli in the range of 4-6 MPa and appear to be affected by the high porosity of the scaffolds.

It can be thus said that the ChiPgA composite scaffolds containing MMT clay modified with 5-aminovaleric acid are biocompatible. Also, the ChiPgA scaffolds containing the modified MMT clay appears to satisfy some of the basic requirements of scaffolds for tissue engineering applications. Although the compressive mechanical properties of the scaffold are lower as compared to cancellous bone, biocompatibility of the ChiPgA composite scaffolds containing MMT clay modified with 5-aminovaleric acid provides good scope for further optimizing the processing parameters to control the architecture of these scaffolds.

3.5. References

[1] Langer R, Vacanti JP. Tissue Engineering. Science. 1993;260:920-6.

[2] Murugan R, Ramakrishna S. Development of nanocomposites for bone grafting. Composites Science and Technology. 2005;65:2385-406.

[3] Dorozhkin SV. Calcium orthophosphates. Journal of Materials Science. 2007;42:1061-95.

[4] António J. Salgado, Olga P. Coutinho, Rui L. Reis. Bone Tissue Engineering: State of the Art and Future Trends. Macromolecular Bioscience. 2004;4:743-65.

[5] Goldberg M, Langer R, Jia XQ. Nanostructured materials for applications in drug delivery and tissue engineering. Journal of Biomaterials Science-Polymer Edition. 2007;18:241-68.

[6] Barnes CP, Sell SA, Boland ED, Simpson DG, Bowlin GL. Nanofiber technology: Designing the next generation of tissue engineering scaffolds. Advanced Drug Delivery Reviews. 2007;59:1413-33.

[7] Pirraco RP, Marques AP, Reis RL. Cell interactions in bone tissue engineering. Journal of Cellular and Molecular Medicine. 2010;14:93-102.

[8] Langer, Robert. Tissue Engineering:A New Field and Its Challenges. 1997;14:840-1.

[9] Mano JF, Silva GA, Azevedo HS, Malafaya PB, Sousa RA, Silva SS, et al. Natural origin biodegradable systems in tissue engineering and regenerative medicine: present status and some moving trends. Journal of The Royal Society Interface. 2007;4:999-1030.

[10] Zhang Y, Venugopal JR, El-Turki A, Ramakrishna S, Su B, Lim CT. Electrospun biomimetic nanocomposite nanofibers of hydroxyapatite/chitosan for bone tissue engineering. Biomaterials. 2008;29:4314-22.

[11] Kong L, Gao Y, Lu G, Gong Y, Zhao N, Zhang X. A study on the bioactivity of chitosan/nano-hydroxyapatite composite scaffolds for bone tissue engineering. European Polymer Journal. 2006;42:3171-9.

[12] Kikuchi M, Matsumoto HN, Yamada T, Koyama Y, Takakuda K, Tanaka J. Glutaraldehyde cross-linked hydroxyapatite/collagen self-organized nanocomposites. Biomaterials. 2004;25:63-9.

[13] Kim HW, Gu HJ, Lee HH. Microspheres of collagen-apatite nanocomposites with osteogenic potential for tissue engineering. Tissue Engineering. 2007;13:965-73.

[14] Svensson A, Nicklasson E, Harrah T, Panilaitis B, Kaplan DL, Brittberg M, et al. Bacterial cellulose as a potential scaffold for tissue engineering of cartilage. Biomaterials. 2005;26:419-31.

[15] Müller FA, Müller L, Hofmann I, Greil P, Wenzel MM, Staudenmaier R. Cellulose-based scaffold materials for cartilage tissue engineering. Biomaterials. 2006;27:3955-63.

[16] Santos MI, Fuchs S, Gomes ME, Unger RE, Reis RL, Kirkpatrick CJ. Response of micro- and macrovascular endothelial cells to starch-based fiber meshes for bone tissue engineering. Biomaterials. 2007;28:240-8.

[17] Sundaram J, Durance TD, Wang R. Porous scaffold of gelatin-starch with nanohydroxyapatite composite processed via novel microwave vacuum drying. Acta Biomaterialia. 2008;4:932-42.

[18] Hofmann S, Hagenmüller H, Koch AM, Müller R, Vunjak-Novakovic G, Kaplan DL, et al. Control of in vitro tissue-engineered bone-like structures using human mesenchymal stem cells and porous silk scaffolds. Biomaterials. 2007;28:1152-62.

[19] Mandal BB, Kundu SC. Non-mulberry silk gland fibroin protein 3-D scaffold for enhanced differentiation of human mesenchymal stem cells into osteocytes. Acta Biomaterialia. 2009;5:2579-90.

[20] Liu H, Slamovich EB, Webster TJ. Less harmful acidic degradation of poly(lactic-co-glycolic acid) bone tissue engineering scaffolds through titania nanoparticle addition. International Journal of Nanomedicine. 2006;1:541-5.

[21] Nejati E, Mirzadeh H, Zandi M. Synthesis and characterization of nano-hydroxyapatite rods/poly(l-lactide acid) composite scaffolds for bone tissue engineering. Composites Part A: Applied Science and Manufacturing. 2008;39:1589-96.

[22] Serrano MC, Pagani R, Vallet-Regí M, Peña J, Rámila A, Izquierdo I, et al. In vitro biocompatibility assessment of poly([var epsilon]-caprolactone) films using L929 mouse fibroblasts. Biomaterials. 2004;25:5603-11.

[23] Nukavarapu SP, Kumbar SG, Brown JL, Krogman NR, Weikel AL, Hindenlang MD, et al. Polyphosphazene/Nano-Hydroxyapatite Composite Microsphere Scaffolds for Bone Tissue Engineering. Biomacromolecules. 2008;9:1818-25.

[24] Mistry AS, Cheng SH, Yeh T, Christenson E, Jansen JA, Mikos AG. Fabrication and in vitro degradation of porous fumarate-based polymer/alumoxane nanocomposite scaffolds for bone tissue engineering. Journal of Biomedical Materials Research Part A. 2009;89A:68-79.

[25] Christenson EM, Anseth KS, van den Beucken L, Chan CK, Ercan B, Jansen JA, et al. Nanobiomaterial applications in orthopedics. Journal of Orthopaedic Research. 2007;25:11-22.

[26] Stevens MM, George JH. Exploring and Engineering the Cell Surface Interface. Science. 2005;310:1135-8.

[27] Okada A, Kawasumi M, Usuki A, Kojima Y, Kurauchi T, Kamigaito O. Synthesis and properties of nylon-6/clay hybrids. In Polymer based molecular composites MRS SymposiumProceedings (eds D W Schaefer & J E Mark). 1990;171:45-50.

[28] Giannelis EP. Polymer Layered Silicate Nanocomposites. Advanced Materials. 1996;8:29-35.

[29] Chen GX, Hao GJ, Guo TY, Song MD, Zhang BH. Structure and mechanical properties of poly(3-hydroxybutyrateco-3-hydroxyvalerate) (PHBV)/clay nanocomposites. Journal of Materials Science Letters. 2002;21:1587-9.

[30] Lim ST, Lee CH, Choi HJ, Jhon MS. Solidlike transition of melt-intercalated biodegradable polymer/clay nanocomposites. Journal of Polymer Science Part B: Polymer Physics. 2003;41:2052-61.

[31] Ma C-CM, Kuo C-T, Kuan H-C, Chiang C-L. Effects of swelling agents on the crystallization behavior and mechanical properties of polyamide 6/clay nanocomposites. Journal of Applied Polymer Science. 2003;88:1686-93.

[32] Park H-M, Lee W-K, Park C-Y, Cho W-J, Ha C-S. Environmentally friendly polymer hybrids Part I Mechanical, thermal, and barrier properties of thermoplastic starch/clay nanocomposites. Journal of Materials Science. 2003;38:909-15.

[33] Pramanik M, Srivastava SK, Samantaray BK, Bhowmick AK. Rubber-clay nanocomposite by solution blending. Journal of Applied Polymer Science. 2003;87:2216-20.

[34] Yano K, Usuki A, Okada A, Kurauchi T, Kamigaito O. Synthesis and properties of polyimide-clay hybrid. Journal of Polymer Science Part A: Polymer Chemistry. 1993;31:2493-8.

[35] Messersmith PB, Giannelis EP. Synthesis and barrier properties of poly(ϵ-caprolactone)-layered silicate nanocomposites. Journal of Polymer Science Part A: Polymer Chemistry. 1995;33:1047-57.

[36] Gilman JW, Jackson CL, Morgan AB, R. H. Flammability Properties of Polymer−Layered-Silicate Nanocomposites. Polypropylene and Polystyrene Nanocomposites. Chemistry of Materials. 2000;12:1866-73.

[37] Gilman JW. Flammability and thermal stability studies of polymer layered-silicate (clay) nanocomposites. Applied Clay Science. 1999;15:31-49.

[38] Sinha Ray S, Okamoto M. Polymer/layered silicate nanocomposites: a review from preparation to processing. Progress in Polymer Science. 2003;28:1539-641.

[39] Sikdar D, Pradhan SM, Katti DR, Katti KS, Mohanty B. Altered Phase Model for Polymer Clay Nanocomposites. Langmuir. 2008;24:5599-607.

[40] Sikdar D, Katti DR, Katti KS. The role of interfacial interactions on the crystallinity and nanomechanical properties of clay-polymer nanocomposites: A molecular dynamics study. Journal of Applied Polymer Science. 2008;107:3137-48.

[41] Katti DR, Ghosh P, Schmidt S, Katti KS. Mechanical Properties of the Sodium Montmorillonite Interlayer Intercalated with Amino Acids. Biomacromolecules. 2005;6:3276-82.

[42] Forni F, Iannuccelli V, Coppi G, Bernabei MT. Effect of Montmorillonite on Drug Release from Polymeric Matrices. Archiv der Pharmazie. 1989;322:789-93.

[43] Lee W-F, Fu Y-T. Effect of montmorillonite on the swelling behavior and drug-release behavior of nanocomposite hydrogels. Journal of Applied Polymer Science. 2003;89:3652-60.

[44] Dong Y, Feng S-S. Poly(d,l-lactide-co-glycolide)/montmorillonite nanoparticles for oral delivery of anticancer drugs. Biomaterials. 2005;26:6068-76.

[45] Lin F-H, Chen C-H, Cheng WTK, Kuo T-F. Modified montmorillonite as vector for gene delivery. Biomaterials. 2006;27:3333-8.

[46] Viseras C, Aguzzi C, Cerezo P, Lopez-Galindo A. Uses of clay minerals in semisolid health care and therapeutic products. Applied Clay Science. 2007;36:37-50.

[47] Takahashi T, Yamada Y, Kataoka K, Nagasaki Y. Preparation of a novel PEG-clay hybrid as a DDS material: Dispersion stability and sustained release profiles. Journal of Controlled Release. 2005;107:408-16.

[48] des Rieux A, Fievez V, Garinot M, Schneider Y-J, Préat V. Nanoparticles as potential oral delivery systems of proteins and vaccines: A mechanistic approach. Journal of Controlled Release. 2006;116:1-27.

[49] Sun B, Ranganathan B, Feng S-S. Multifunctional poly(d,l-lactide-co-glycolide)/montmorillonite (PLGA/MMT) nanoparticles decorated by Trastuzumab for targeted chemotherapy of breast cancer. Biomaterials. 2008;29:475-86.

[50] Wang X, et al. Biopolymer/montmorillonite nanocomposite: preparation, drug-controlled release property and cytotoxicity. Nanotechnology. 2008;19:065707.

[51] Depan D, Kumar AP, Singh RP. Cell proliferation and controlled drug release studies of nanohybrids based on chitosan-g-lactic acid and montmorillonite. Acta Biomaterialia. 2009;5:93-100.

[52] Carretero MI. Clay minerals and their beneficial effects upon human health. A review. Applied Clay Science. 2002;21:155-63.

[53] Katti KS, Ambre AH, Peterka N, Katti DR. Use of unnatural amino acids for design of novel organomodified clays as components of nanocomposite biomaterials. Philosophical Transactions of The Royal Society A 2010;368:1963-80.

[54] Lin K-F, Hsu C-Y, Huang T-S, Chiu W-Y, Lee Y-H, Young T-H. A novel method to prepare chitosan/montmorillonite nanocomposites. Journal of Applied Polymer Science. 2005;98:2042-7.

[55] Marras SI, Kladi KP, Tsivintzelis I, Zuburtikudis I, Panayiotou C. Biodegradable polymer nanocomposites: The role of nanoclays on the thermomechanical characteristics and the electrospun fibrous structure. Acta Biomaterialia. 2008;4:756-65.

[56] Zheng JP, Wang CZ, Wang XX, Wang HY, Zhuang H, Yao KD. Preparation of biomimetic three-dimensional gelatin/montmorillonite-chitosan scaffold for tissue engineering. Reactive and Functional Polymers. 2007;67:780-8.

[57] Katti KS, Katti DR, Dash R. Synthesis and characterization of a novel chitosan/montmorillonite/hydroxyapatite nanocomposite for bone tissue engineering. Biomedical Materials. 2008;3:12.

[58] Krayukhina MA, et al. Polyelectrolyte complexes of chitosan: formation, properties and applications. Russian Chemical Reviews. 2008;77:799.

[59] Verma D, Katti KS, Katti DR. Effect of Biopolymers on Structure of Hydroxyapatite and Interfacial Interactions in Biomimetically Synthesized Hydroxyapatite/Biopolymer Nanocomposites. Annals of Biomedical Engineering. 2008;36:1024-32.

[60] Verma D, Katti KS, Katti DR. Polyelectrolyte-complex nanostructured fibrous scaffolds for tissue engineering. Materials Science and Engineering: C. 2009;29:2079-84.

[61] Verma D, et al. Osteoblast adhesion, proliferation and growth on polyelectrolyte complex-hydroxyapatite nanocomposites. Philosophical Transactions of The Royal Society A Mathematical Physical and Engineering Sciences. 2010;368:2083.

[62] Verma D, Katti KS, Katti DR, Mohanty B. Mechanical response and multilevel structure of biomimetic hydroxyapatite/polygalacturonic/chitosan nanocomposites. Materials Science and Engineering: C. 2008;28:399-405.

[63] Gibson LJ, Ashby MF. Cellular solids : structure and properties. 2nd Edition ed. New York: Cambridge University Press; 1999.

CHAPTER 4. NANOCLAYS WITH BIOMINERALIZED HYDROXYAPATITE FOR BONE REGENERATION

This chapter presents the preparation of a novel three component nanoclay-hydroxyapatite (HAP) hybrid using a processing route based on biomineralization in bone. This hybrid (also known as *in situ* HAPclay) prepared by mineralizing HAP in modified clay was characterized and further used for preparing biopolymer composites for bone regeneration. Details about *in situ* HAPclay characterization, use of *in situ* HAPclay for preparing biopolymer composites and studies related to the use of these prepared composites for bone regeneration are also presented in this chapter. The contents of this chapter have been published in Ambre, A.H., Katti, K.S., Katti, D.R. In situ Mineralized Hydroxyapatite on Amino Acid Modified Nanoclays as Novel Bone Biomaterials. Materials Science and Engineering C. 2011; 31: 1017-1029

4.1. Introduction

The introduction of tissue engineering by Langer and Vacanti [1] in the early 1990s explained how an interdisciplinary approach can be used for generating tissues to replace or repair damaged tissues. Besides this, Langer and Vacanti also put forth the idea of placing cells on porous structures known as “scaffolds” that serve as a guiding “template” for the generation of vascularized tissues. Most of the studies till date report the use of scaffolds based on polymeric or polymeric composite materials. This can be attributed to the ability to control the properties in case of synthetic polymers and the presence of biomolecule sequences favoring cell attachment in case of natural polymers. Moreover, the possibilities of controlling mechanical properties, cell behavior and subsequent tissue formation by incorporating fillers in polymers have made polymer composites an interesting subject for studies in tissue engineering. In several studies related to bone tissue engineering, hydroxyapatite (HAP) has been used for the

preparation of polymer composite scaffolds due to its attributes such as osteoconductivity, non-toxicity and non-immunogenecity. Similarly, bioactive glass and other calcium phosphate based compounds with variable compositions of calcium and phosphate, variable crystallinity and phases have also been for studies related to tissue engineering. The human bone consists of ions such as carbonate, sodium, fluorine, magnesium, zinc, silicon and aluminum along with hydroxyapatite [2]. Ions such as magnesium are supposed to affect the mineralization of bone whereas silicon ions are supposed to affect the bone formation rate and pattern [2]. Studies involving bioactive glasses indicate that silicon affects their surface reactions [3] and can also instigate bone formation [4]. The effect of various types of ions on cell behavior and bone tissue formation can be investigated by using minerals or ceramics containing ions such as carbonate, sodium, silicon, fluorine, magnesium, zinc and aluminum. There have been studies on the preparation and use of silicon substituted hydroxyapatite discs, granules and compacted powders for studying their effect on osteoblasts [5], their in vivo behavior [3] and bioactivity [6]. These studies indicate that the presence of silicon affects the cell behavior and tissue formation. Keeping in mind the tissue engineering approach, incorporation of fillers containing silicon, carbonate, sodium, magnesium, zinc to prepare polymer composite scaffolds can prove useful for regeneration of bone tissue. Also, developing scaffolds with adequate nanoscale (for scaffold walls) and macroscale (for the scaffold architecture) mechanical properties favorable for bone regeneration constitutes an important part of tissue engineering. The use of montmorillonite (MMT) clays for preparing polymer composite scaffolds may prove useful in this respect.

Research related to polymer-clay nanocomposites (PCNs) since 1990 has shown that addition of MMT clay in small quantities can lead to an improvement in mechanical properties [7-10] and have an effect on properties such as gas permeability [11-13], flammability [14, 15]

and biodegradability. The effectiveness of MMT clay in affecting the various properties has been conventionally attributed to the high aspect ratio of MMT clay that increases the polymer-clay interactions. In order to get more insight into this effectiveness of MMT clay, several experimental and simulation studies done in our group led to the development of "altered phase" model. This model explains the formation of "altered phase" with different crystallinity and elastic properties as a result of molecular interactions between the three components; viz., polymer, clay and modifier [16]. A prior simulation study carried out in our group indicated that there are attractive interactions between the functional groups of a modifier and polymer. These interactions along with the repulsive interactions between the polymer backbone and the modifier affect the crystallinity and increase the nanomechanical properties of PCNs [17]. Besides this, the backbone chain length and the functional groups in modifiers (organic molecules) used to modify the clay have an effect on the d-spacing of clay and also the nanomechanical properties of PCNs [18].

The medicinal properties of MMT clay [19] and studies related to its pharmaceutical applications [20-22] suggest that MMT clay may prove useful for tissue engineering applications. In addition to this, its ability to be excreted from the body and to be dissolved by acids present in the stomach emphasize its possible utility for tissue engineering applications. Polymer-clay nanocomposites based on chitosan, polycaprolactone and gelatin studied for biomaterial applications highlight the effect of addition of clay on mechanical properties of the resulting PCNs [23-25]. Studies related to the effect of addition of MMT clay on the behavior of cells have been very few [26, 27]. Therefore, it is necessary to enhance our understanding on the effect of addition of MMT clay to PCNs on the behavior of cells to extend the use of PCNs for tissue engineering applications. In our previous work, we used three unnatural amino acids as

modifiers for MMT clay on the basis of their backbone chain length and previous reports of antibacterial activity. Results obtained from this work showed that amongst the clays intercalated with the three amino acids, MMT clay modified with 5-aminovaleric acid had improved biocompatibility [28]. The MMT clay modified with 5-aminovaleric acid was used for preparing chitosan/polygalacturonic acid (ChiPgA) composite scaffolds in another study [29]. It was found that human osteoblast cells were able to proliferate on the ChiPgA composite scaffolds and the overall properties of these scaffolds indicated that these scaffolds satisfied some of the important requirements for tissue engineering applications.

In case of bone tissue engineering, it is necessary to develop material systems that in addition to supporting the growth and proliferation of osteoblast cells also favor the formation of a bone tissue. Studies have indicated that materials with nanoscale features can be useful for eliciting a cellular response that would lead to bone formation [30]. Therefore, it is expected that the addition of nanosize fillers may prove advantageous for preparing polymer composites to be used for bone tissue engineering applications. The modification of nanosize MMT clay with organic molecules and its subsequent incorporation in PCNs has been found to be an effective method for improving the mechanical properties of PCNs. The use of HAP known for its osteoconductive properties for bone tissue regeneration has been demonstrated through several studies. Nanosize filler having properties of both MMT clay and HAP may prove useful for improving the mechanical properties and affecting the tissue regeneration capabilities of a polymer composite scaffold. As mentioned earlier, results from our previous study showed that polymer scaffolds containing modified MMT clay favored the growth of human osteoblast cells. In order to further improve the effectiveness of the modified clay for bone tissue engineering applications, synthesizing apatite or calcium phosphate based compound in the modified clay by

using the modified MMT clay as a kind of template may prove a useful approach. This approach can also be one of the ways of preparing nanosize fillers having properties of MMT clay and HAP. Non-collagenous proteins in bone such as osteocalcin, osteonectin, osteopontin, etc. are the possible sites of "biomineralization" in bone [31]. Likewise, the functional groups present in a modifier used for modifying MMT clay can possibly serve as sites for the growth of apatite or calcium phosphate based compound in clay. The schematic shown in Figure 4.1. explains the possible approach of growing apatite or calcium phosphate based compound in clay by using the functional groups of the modifier.

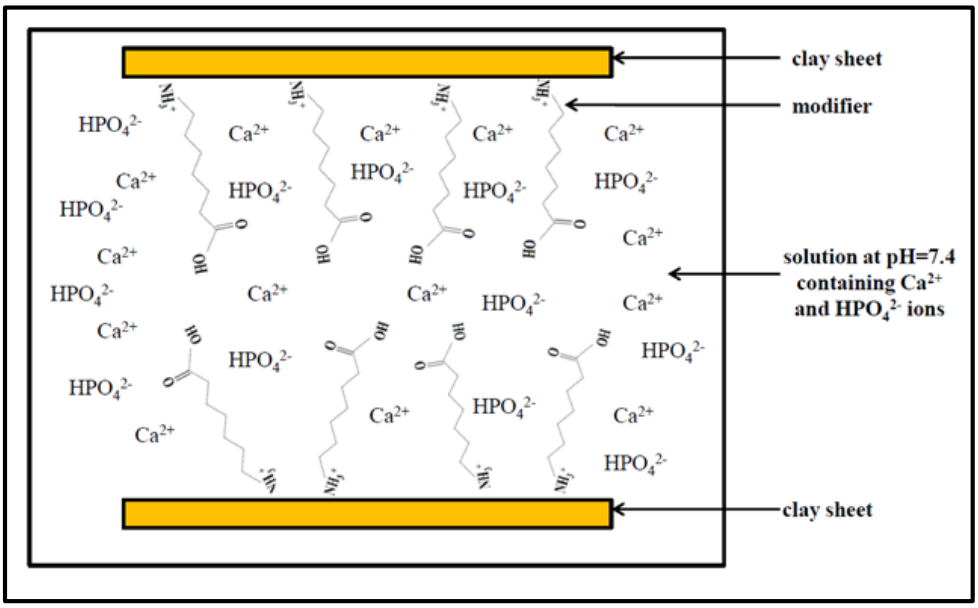

Figure 4.1. Schematic of the possible approach used for growing apatite or calcium phosphate based compound in modified clay by using the functional groups of the modifier

This work reports a novel method of synthesizing apatite using MMT clay modified with 5-aminovaleric acid. The modified MMT clay with mineralized apatite named as *in situ* HAPclay was characterized by Fourier Transform Infrared Spectroscopy (FTIR) and X-ray diffraction (XRD). The *in situ* HAPclay was then used in the preparation of chitosan/polygalacturonic acid (ChiPgA) composite films. The ChiPgA system has been previously investigated in our group for

bone tissue engineering [32-35]. The response of the human osteoblasts on these films was studied by using inverted optical microscopy. The ChiPgA films containing *in situ* HAPclay were also characterized by FTIR. We hypothesize that *in situ* HAPclay synthesized by a novel method based on biomineralization in bone is capable of enhancing the osteoconductive properties and mechanical properties of polymer composites containing *in situ* HAPclay. Thus, the overall objectives of this work were synthesis of in situ HAPclay, characterization of *in situ* HAPclay using XRD and infrared spectroscopy and assessing osteoconductive properties of polymer composites containing *in situ* HAPclay through cell culture experiments involving bone cells (osteoblasts).

4.2. Materials and Methods

4.2.1. Materials

SWy-2, Crook County, Wyoming sodium montmorillonite (Na-MMT) clay with a cation exchange capacity of 76.4 mequiv/100g from the Clay Minerals Repository at the University of Missouri, Columbia, Missouri was used in this study for experiments. The modifier 5-aminovaleric acid was purchased from Sigma Aldrich. Sodium phosphate (Na_2HPO_4) from J.T. Baker and calcium chloride ($CaCl_2$) from EM Sciences were used for preparing *in situ* HAPclay. Chitosan (≥ 85 % deacetylated, molecular weight 190000-310000) and polygalacturonic acid (approx. 95 % enzymatic, molecular weight 25000-50000) from Sigma Aldrich were used for the preparation of composite films. The complete cell culture medium was made from HyQ Dulbecco's modified eagle's medium (DMEM)-12 (1:1) from Hyclone, fetal bovine serum (FBS) from American Type Cell Culture Collection (ATCC) and G418 antibiotic from JR scientific. Human osteoblast cells (cell line number: CRL 11372) from ATCC were used for cell culture experiments.

4.2.2. Preparation of Modified MMT Clay

5-aminovaleric acid was used for modifying MMT clay according to the procedure described in our previous work [28]. To summarize, 5-aminovaleric acid solution in deionized water having pH 1.8 was added to the Na-MMT clay suspension in deionized water at 60°C and the mixture obtained was vigorously stirred for 1 hour. This was followed by centrifuging, washing of the modified clay separated from deionized water by centrifuging to remove chloride ions, drying at 70°C, grinding and sieving for obtaining a fine powder of modified MMT clay.

4.2.3. Synthesis of *In Situ* HAPclay and Hydroxyapatite (HAP)

MMT clay modified with 5-aminovaleric acid according to procedure described in 4.2.2. was dispersed in 23.8 mM solution of Na_2HPO_4 in deionized water by stirring for 2 hours. A 39.8 mM solution of $CaCl_2$ in deionized water was added to the modified clay - Na_2HPO_4 suspension. The pH of the resulting solution was maintained at 7.4 and this solution was further stirred for 8 hours. The subsequent precipitate obtained was allowed to settle for 24 hours and water over the settled precipitates was poured off. The water remaining in the precipitates was removed by centrifuging and the separated precipitate was further dried at 70°C. The dried precipitate was sieved through a 45 μm sieve after grinding to obtain a fine powder. This powder known as *in situ* HAPclay was used for further experiments.

HAP was prepared on the basis of wet precipitation method reported in our previous studies [36]. For preparing HAP, 39.8 mM solution of $CaCl_2$ was added to 23.8 mM solution of Na_2HPO_4. This was followed by stirring, settling of precipitates, centrifuging, drying and sieving to obtain HAP powder.

4.2.4. Preparation of Chitosan/Polygalacturonic Acid (ChiPgA) Composite Films Containing *In Situ* HAPclay

The method for ChiPgA composite films containing *in situ* HAPclay used in this work is based on the method of preparing ChiPgA composite polyelectrolyte complexes that were used in our previous studies for preparing scaffolds [29, 32, 33]. For preparing the ChiPgA composite films containing *in situ* HAPclay in the present study, changes were made in the sequence of addition of *in situ* HAPclay as compared to our previous studies. A schematic of the procedure for preparing films is shown in Figure 4.2. Chitosan and polygalacturonic acid solutions were prepared in deionized water by using acetic acid to dissolve chitosan and diluted sodium hydroxide solution to dissolve polygalacturonic acid. *In situ* HAPclay was dispersed in deionized water by sonication and added to chitosan solution. The solution obtained was added dropwise to the polygalacturonic acid solution. This final solution of chitosan, *in situ* HAP clay and polygalacturonic acid was sonicated to obtain a ChiPgA composite solution containing *in situ* HAPclay. Films of different compositions consisting *in situ* HAPclay in the range of 10 wt % to 20 wt % were prepared. For cell culture experiments, the ChiPgA composite solution was diluted with deionized water and the diluted solution was used for preparing composite films in tissue culture Petri dishes (60 mm OD x 15 mm H, growth area 19.5 cm^2) by air drying at room temperature.

4.2.5. Characterization

4.2.5.1. Transmission FTIR Spectroscopy Studies

Transmission FTIR spectroscopy studies were performed using powdered samples of MMT clay modified with 5-aminovaleric acid, *in situ* HAPclay and HAP. The powdered samples sandwiched between two silicon windows were placed in a universal sample holder for

performing the experiments. ThermoNicolet, Nexus, 870 spectrometer equipped with a KBr beam splitter was used for performing these experiments in the range of 4000-400 cm^{-1}. Spectral resolution of 4 cm^{-1} and a mirror velocity of 0.158 cm/s for collecting 100 scans was used for each sample in these experiments.

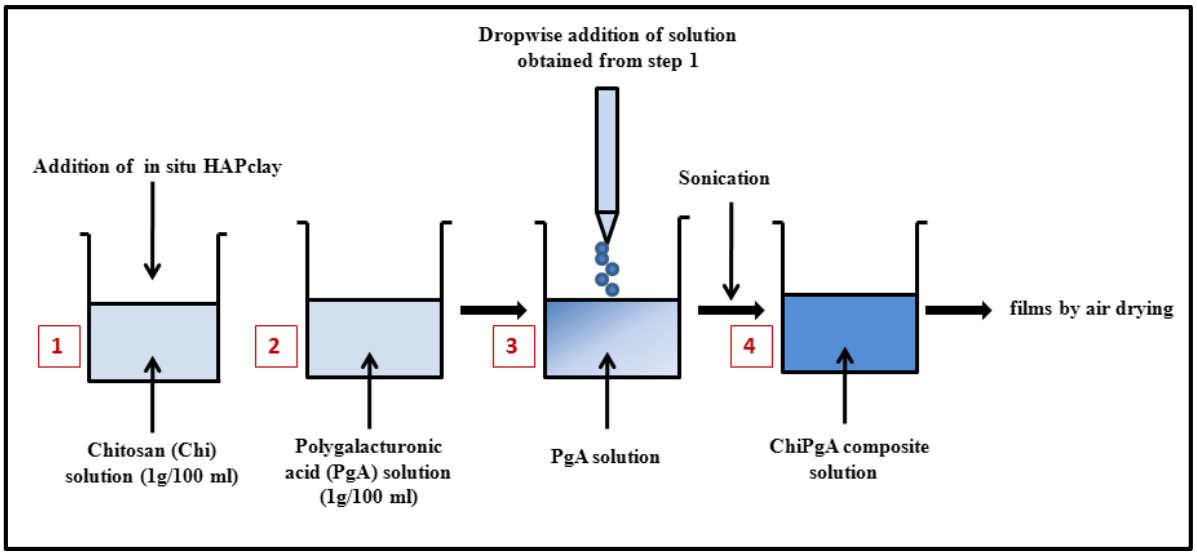

Figure 4.2. Schematic for preparing ChiPgA films containing *in situ* HAPclay (*In situ* HAPclay was prepared using MMT clay modified with 5-aminovaleric acid)

Transmission FTIR spectroscopy studies were also performed on chitosan/polygalacturonic acid (ChiPgA) and ChiPgA composite films containing 12.5 wt % *in situ* HAPclay using the same instrument and sample holder as for the FTIR experiments on powdered samples. The spectral resolution and mirror velocity was also the same as for the FTIR experiments on powdered samples.

4.2.5.2. X-ray Diffraction (XRD) Experiments

XRD experiments were performed on powdered samples of MMT clay modified with 5-aminovaleric acid, *in situ* HAPclay and HAP. X-ray diffractometer from Philips X'pert, Almelo, The Netherlands was used for these experiments. The diffractometer used for these experiments was equipped with a secondary monochromator and Cu-tube using CuKα radiation of

wavelength 1.54056 A°. The powdered samples were scanned in the range of 2θ= 2° to 60° at a scan rate of 0.3 min^{-1}.

4.2.5.3. Cell Culture Experiments

The ChiPgA composite films obtained by air-drying the composite solution in Petri dishes (growth area 19.5 cm^2) were sterilized by placing the Petri dishes with films (~ 4.986 cm diameter) under ultraviolet light for 1.5 hours. 3 x 10^5 human osteoblast cells (ATCC, CRL 11372, passage # 9) were seeded on these films and 3 ml of complete cell culture medium was then added. The Petri dishes containing films seeded with human osteoblasts were then incubated at 37°C, 5 % CO_2 for a cell culture period of 36 days (for films containing 10 wt % and 20 wt % *in situ* HAPclay). In case of osteoblast seeded films containing 12.5 wt % *in situ* HAPclay, cell culture period was 16 days and for osteoblast seeded films containing 15 wt % *in situ* HAPclay, cell culture period was 12 days. ChiPgA films containing different weight percent compositions of *in situ* HAPclay were used for cell culture studies considering the potential changes in mechanical properties (for films and scaffolds) and microstructure of scaffolds according to the content of *in situ* HAPclay. Mechanical properties and microstructure of scaffolds may have to be tailored according to the requirements at bone defect site by varying the *in situ* HAPclay content. Therefore ChiPgA films with different weight compositions of *in situ* HAPclay were used to show the suitability of films for cellular events favoring bone formation. The behavior (attachment, pattern/cluster formation) of the seeded cells was observed using an inverted microscope (Axiovert 40, Zeiss) after every 4 days during the cell culture period. Media was changed after every two days.

4.3. Results and Discussion

4.3.1. Transmission FTIR Spectroscopy

Figure 4.3. shows the transmission FTIR spectra of modified MMT clay, *in situ* HAPclay, mixture of modified MMT clay with HAP and hydroxyapatite (HAP) in the 4000-400 cm^{-1} range. For further analysis of these spectra, regions with data limits from 4000-2000 cm^{-1} and 2000-400 cm^{-1} were used. These regions of the spectra are shown in Figures 4.4. and 4.5.

In Figure 4.4.**,** it can be seen that the band positions 3568 cm^{-1} and 3571 cm^{-1} are seen in case of *in situ* HAPclay and HAP. These band positions correspond to the hydroxyl stretching bands observed in HAP [37]. The presence of the hydroxyl stretching band in *in situ* HAPclay indicates the formation of HAP in the modified MMT clay. The band positions at 3631 cm^{-1} and 3628 cm^{-1} seen in the modified MMT clay and the (HAP + modified MMT clay) mixture correspond to the stretching of the structural –OH groups present in modified MMT clay. It can be seen that the band corresponding to the stretching of the structural –OH groups of modified MMT clay is not distinctly visible in *in situ* HAPclay. This seems to be because the band corresponding to the structural –OH group in modified MMT clay are masked by the stretching of the hydroxyl ions and the stretching of –OH in the water adsorbed in the interstices of HAP formed in the *in situ* HAPclay. Figure 4.5. shows the spectra in the 2000-400 cm^{-1} region for the powdered samples mentioned previously. The purpose of obtaining a spectrum of a mixture of modified MMT clay and HAP was to make more obvious the changes in band positions and appearance or disappearance of bands in case of *in situ* HAPclay. The presence of band at 1702 cm^{-1} in modified MMT clay and at 1706 cm^{-1} in the (HAP + modified MMT clay) mixture can be attributed to the C=O stretching of the carboxylic group present in the amino acid. In the spectrum of *in situ* HAPclay, a broad band is seen around the 1623 cm^{-1} wavenumber position.

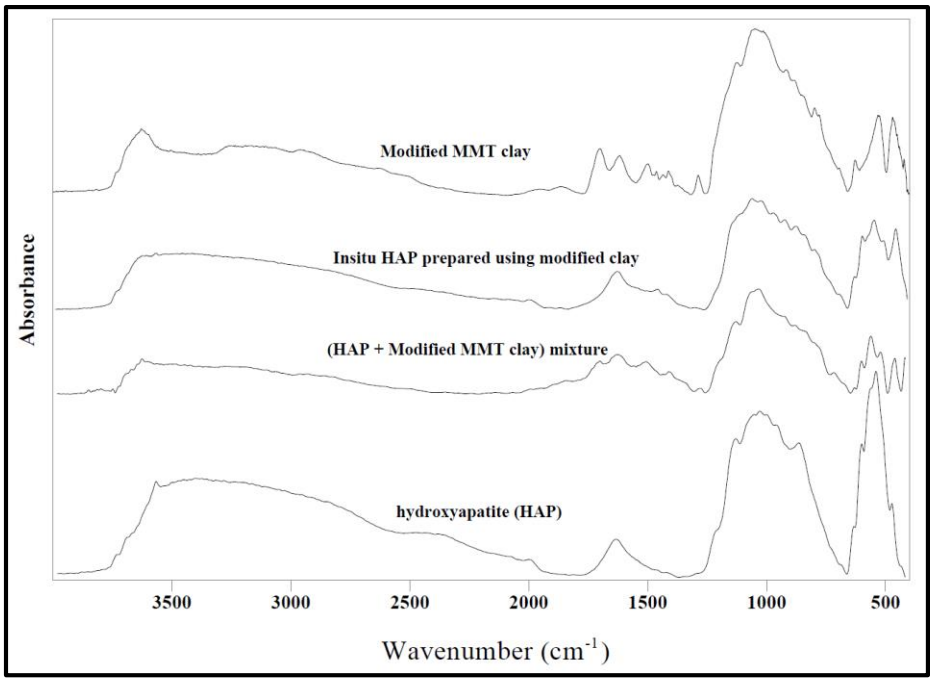

Figure 4.3. Transmission FTIR spectra of modified MMT clay, *in situ* HAPclay (*in situ* HAP prepared using modified clay), mixture of HAP and modified MMT clay and hydroxyapatite (HAP) in the 4000-400 cm^{-1} range

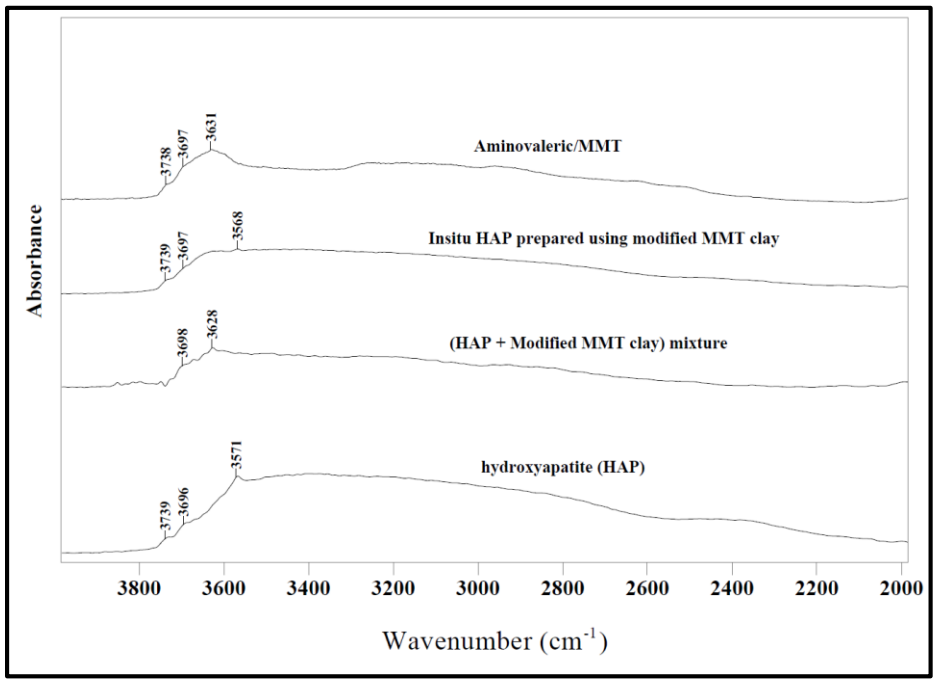

Figure 4.4. Transmission FTIR spectra of modified MMT clay, *in situ* HAPclay (*in situ* HAP prepared using modified MMT clay), mixture of HAP and modified MMT clay and hydroxyapatite (HAP) in the 4000-2000 cm^{-1} range

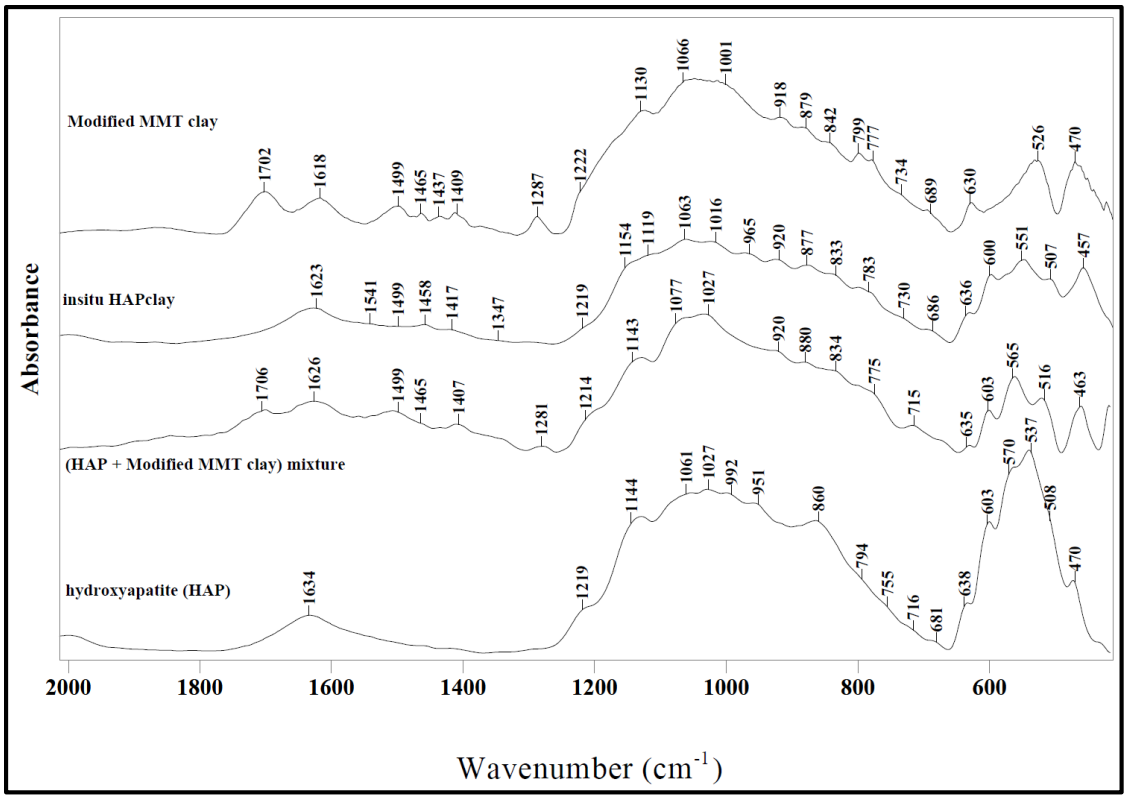

Figure 4.5. Transmission FTIR spectra of modified MMT clay, *in situ* HAPclay (*in situ* HAP prepared using modified MMT clay), mixture of HAP and modified MMT clay and hydroxyapatite (HAP) in the 2000-400 cm^{-1} range

The broad band around 1623 cm^{-1} indicates change in the chemical environment of the functional group that gives rise to the band at 1623 cm^{-1} and appears to overlap bands due to the vibrations of other functional groups in *in situ* HAPclay. The band at 1702 cm^{-1} that appears due to the C=O stretching of the carboxylic group seems to be shifted to a lower wavenumber position at 1541 cm^{-1} in case of *in situ* HAPclay. This shift is indicative of the dissociation of carboxylic group. Also, a band position at 1347 cm^{-1} is seen in case of *in situ* HAPclay. Band positions 1541 cm^{-1} and 1347 cm^{-1} can be attributed to the C=O asymmetric and symmetric vibrations in the dissociated carboxylic groups. During the preparation of *in situ* HAPclay the modified MMT clay is added to a solution of sodium phosphate that has a pH in the basic range. This possibly seems to favor the dissociation of the carboxylic group in the sodium phosphate

solution and these dissociated carboxylic groups seem to further interact with the calcium. The difference in the symmetric and asymmetric stretching vibration of the dissociated carboxylic group of 194 cm^{-1} in case of *in situ* HAPclay is an indication of chelation with calcium ions in the *in situ* HAPclay [38-40]. The presence of a free electron pair in the oxygen of dissociated carboxyl group and empty 3d orbitals in calcium ions favor chelation between the dissociated carboxyl group and calcium ions in the *in situ* HAPclay [41]. Also, the higher charge density of the calcium ions and greater tendency of the calcium ions to accept electrons favors chelation of these ions with the dissociated carboxyl group [42]**.** The formation of chelate between the carboxylate group and the calcium ions possibly plays an important role in the nucleation of hydroxyapatite [43]. A band position corresponding to the symmetric NH_3^+ deformation vibration in modified MMT clay and *in situ* HAPclay is seen at 1499 cm^{-1}. Thus, the NH_3^+ seems unlikely to be involved in interactions with calcium or phosphate in *in situ* HAPclay. The band positions seen in the spectra of modified MMT clay and mixture of modified MMT clay with HAP at 1287 cm^{-1} and 1281 cm^{-1} respectively are due to the OH deformation in the carboxylic group of amino acid. The absence of this band in the spectrum of *in situ* HAP clay is suggestive of further evidence of the dissociation of carboxylic group of amino acid. The vibrations associated with $-CH_2-$ deformation arising from the backbone of 5-aminovaleric acid are seen in the case of modified MMT clay in the 1465-1407 cm^{-1} region. These vibrations are also seen in case of mixture of modified MMT clay with HAP. In case of *in situ* HAPclay, these bands are also seen but are shifted to different wavenumber positions. These shifts indicate the involvement of 5-aminovaleric acid (modifier) in the formation of HAP in the modified MMT clay.

Band position 1634 cm^{-1} in HAP corresponds to the H-O-H deformation of adsorbed water in HAP. In case of *in situ* HAPclay, appearance of a band corresponding to the H-O-H deformation at 1634 cm^{-1} can thus be expected. But, it is seen that the band corresponding to H-O-H deformation appears at 1623 cm^{-1} in *in situ* HAPclay (second derivative of the *in situ* HAPclay spectrum in Figure 4.6.). This may be due to the overlap of different bands around the 1623 cm^{-1} region.

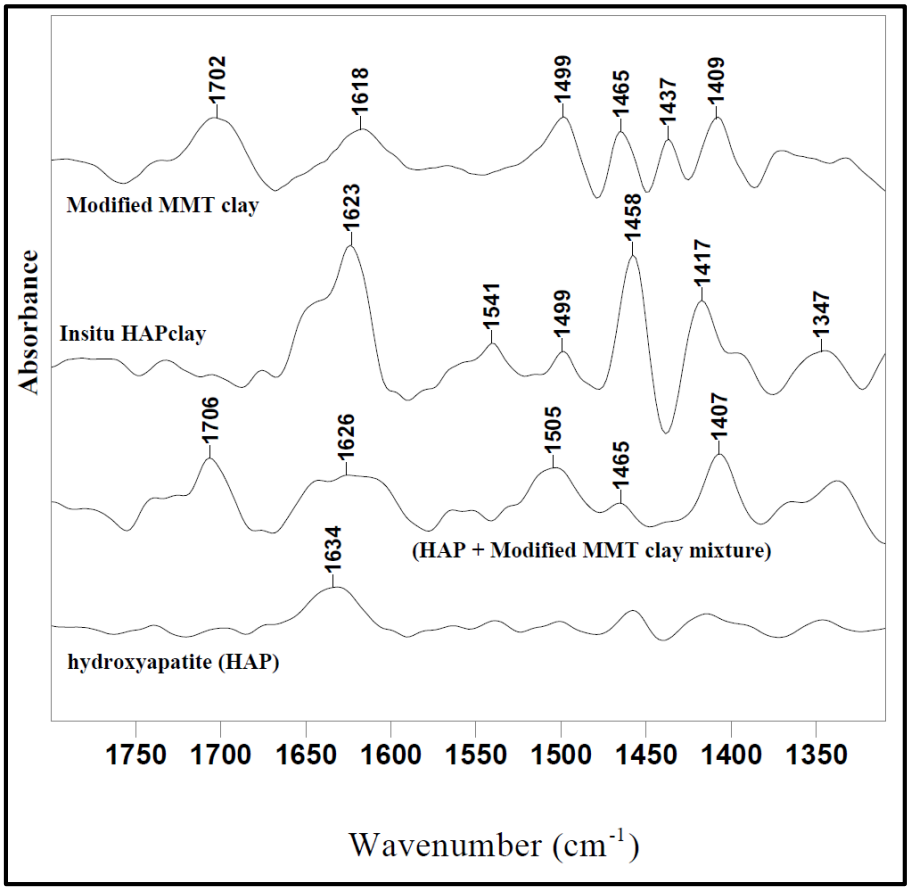

Figure 4.6. Second derivative spectra of modified MMT clay, *in situ* HAPclay (*in situ* HAP prepared using modified MMT clay), mixture of HAP and modified MMT clay and hydroxyapatite (HAP) in the 2000-400 cm^{-1} range

The region of the spectra from 1200 cm^{-1} to 400 cm^{-1} in Figure 4.5. shows spectral features that is useful for studying the changes that may take place in the Si-O vibrations of modified clay and also other vibrations such as Al-O, Al-Mg and Al-Fe vibrations. Also, this

region of the spectra provides information regarding the phosphate vibrations known to be present in hydroxyapatite. The bands at 1154 cm^{-1}, 1143 cm^{-1} and 1144 cm^{-1} in the spectra of *in situ* HAPclay, mixture of modified MMT clay with HAP and HAP respectively correspond to the γ_6 vibration of phosphate ion of HPO_4^{2-} in hydroxyapatite. HPO_4^{2-} has been found to enter into the crystal lattice of biological and synthetic apatites at specific sites in the lattice [36]. In case of *in situ* HAPclay, the position of the γ_6 vibration of phosphate ion is at a higher wavenumber that may be due to the greater interaction of HPO_4^{2-} with its neighboring chemical environment. This band corresponding to the γ_6 vibration of phosphate ion of HPO_4^{2-} is not seen in case of modified MMT clay. The band at 1130 cm^{-1} seen in modified MMT clay corresponds to the Si-O stretching vibration. This band appears to have shifted to a lower wavenumber position of 1119 cm^{-1} that may be due to the non-bonded interactions with the calcium or phosphate ions in *in situ* HAPclay. The bands at 920 cm^{-1}, 877 cm^{-1}, 730 cm^{-1} and 783 cm^{-1} in *in situ* HAPclay indicate the presence of modified MMT clay. The band at 1016 cm^{-1} in *in situ* HAPclay can be attributed to the γ_3 vibration of phosphate ion in HAP formed in *in situ* HAPclay. The band corresponding to the γ_3 vibration of phosphate ion in HAP is seen at 1027 cm^{-1}. The lower γ_3 vibration frequency of phosphate ion in *in situ* HAPclay also indicates difference in the nature of molecular interactions and chemical environment of the phosphate ion in *in situ* HAPclay. Also, this may also due to the different symmetry of the hydroxyapatite formed in *in situ* HAPclay. Band corresponding to the γ_4 phosphate vibration at 600 cm^{-1} in *in situ* HAPclay provides further evidence of presence of hydroxyapatite in *in situ* HAPclay. Presence of band corresponding to the γ_4 phosphate vibration at 551 cm^{-1} at a lower wavenumber position compared to the position of the same type of vibration in hydroxyapatite at 570 cm^{-1} further indicates the difference in symmetry of hydroxyapatite formed in *in situ* HAPclay and nature of interactions of phosphate

ions with its surroundings. In case of *in situ* HAPclay, the difference in the symmetry of HAP formed in it may be due to the differences in its formation process as compared to the formation of hydroxyapatite (HAP). In the modified MMT clay, the functional groups of the modifier used are supposed to provide the sites of nucleation and growth in it. The symmetry of HAP grown at these sites would thus depend on the orientation of the functional groups of the modifier in the modified MMT clay. Also, the different type of ions in this grown hydroxyapatite may experience different chemical environments that may have an effect on their vibration frequencies. It is difficult to assign the band position 457 cm^{-1} observed in *in situ* HAPclay to the γ_2 phosphate vibration since this band may be result of a shift of either the SiOSi deformation vibration (470 cm^{-1}) seen in modified MMT clay or may be result of shift of phosphate vibration seen in hydroxyapatite (470 cm^{-1}).

On comparing the different spectra shown in Figure 4.5., it can be thus said that there are molecular level interactions between the functional groups of the modifier and the inorganic ions of the hydroxyapatite formed in it. As explained earlier, the shift of the C=O stretching vibration due to dissociation of carboxylic group, disappearance of band associated with OH deformation of carboxylic group and difference in the vibration frequencies of the phosphate ions as compared to the modified clay-HAP mixture and HAP are some of the obvious indicators of the molecular level interactions in *in situ* HAPclay. Figure 4.7. shows the transmission FTIR spectra of ChiPgA and ChiPgA films containing *in situ* HAPclay. For the purpose of further analysis, spectra in the regions 4000-2000 cm^{-1} and 2000-400 cm^{-1} have been presented in Figures 4.8. and 4.9. In Figure 4.9., a shoulder band at 1743 cm^{-1} in case of ChiPgA film indicates the presence of some undissociated carboxylic groups from PgA whereas in case of ChiPgA film containing *in situ* HAPclay no band is seen around 1743 cm^{-1} region. This indicates that almost

all the carboxylic groups are dissociated in case of ChiPgA film containing *in situ* HAPclay. The bands 1618 cm^{-1} and 1622 cm^{-1} in case of ChiPgA and ChiPgA film containing *in situ* HAPclay arise from the asymmetric stretching of the dissociated carboxylate groups. The bands at 1413 cm^{-1} and 1429 cm^{-1} arise from the symmetric stretching of the dissociated carboxylate groups in ChiPgA and ChiPgA containing *in situ* HAPclay. The higher vibration frequency of symmetric stretching of the dissociated carboxylate groups in ChiPgA containing *in situ* HAPclay may be due to the interaction of these groups with *in situ* HAPclay. The occurrence of CH bending pyranose ring vibrations at 1331 cm^{-1} in case of ChiPgA film containing *in situ* HAPclay as compared to 1324 cm^{-1} in ChiPgA film also indicates interaction of the ChiPgA polyelectrolyte. Similarly, it is also observed that the pyranose ring vibration in ChiPgA film containing *in situ* HAPclay occurs at 772 cm^{-1} as compared to 760 cm^{-1} in ChiPgA which further implies presence of interactions between the polyelectrolyte and the *in situ* HAPclay. The overlap of the phosphate vibrations of *in situ* HAPclay expected to occur around the 1000 cm^{-1} region with the vibrations arising from the ring of ChiPgA polyelectrolyte makes band assignment of phosphate vibrations difficult in this region. The increase in the width of the band around 1000 cm^{-1} region in case of ChiPgA film containing *in situ* HAPclay as compared to the spectra of ChiPgA film seems to imply the overlap of bands arising from phosphate vibrations and the ring vibrations of the ChiPgA polyelectrolyte. Although, a weak band at 857 cm^{-1} in case of ChiPgA film *containing in situ* HAPclay is seen, it is difficult to say whether this band is due to the shift of the Mg-OH (877 cm^{-1}) or FeOH (833 cm^{-1}) vibration seen in case of *in situ* HAPclay. This band thus indicates the presence of *in situ* HAPclay. Similarly, the band at 466 cm^{-1} is also an indication of *in situ* HAPclay in the ChiPgA film. Tables 4.1.-4.4. give the FTIR band assignments.

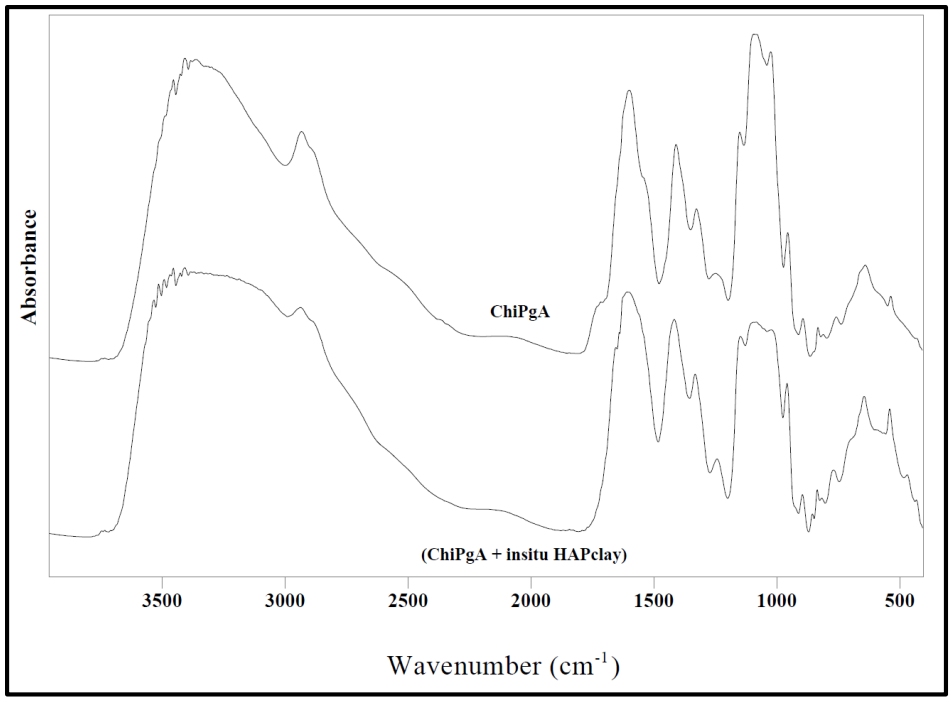

Figure 4.7. Transmission FTIR spectra of ChiPgA film and ChiPgA film containing *in situ* HAPclay in the 4000-400 cm^{-1} range

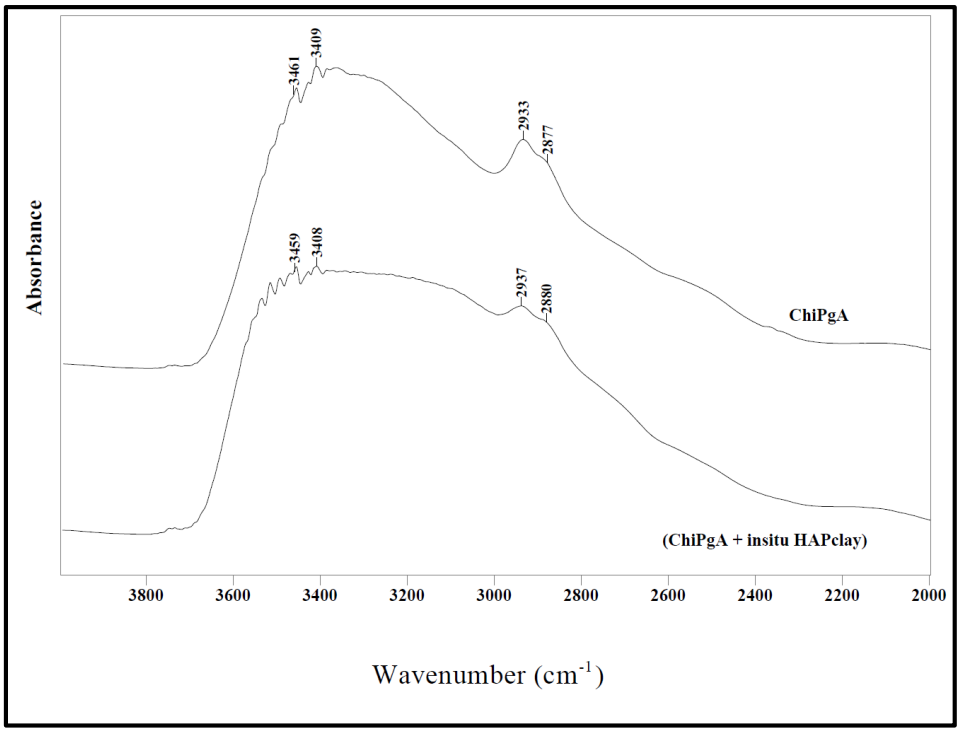

Figure 4.8. Transmission FTIR spectra of ChiPgA film and ChiPgA film containing *in situ* HAPclay in the 4000-2000 cm^{-1} range

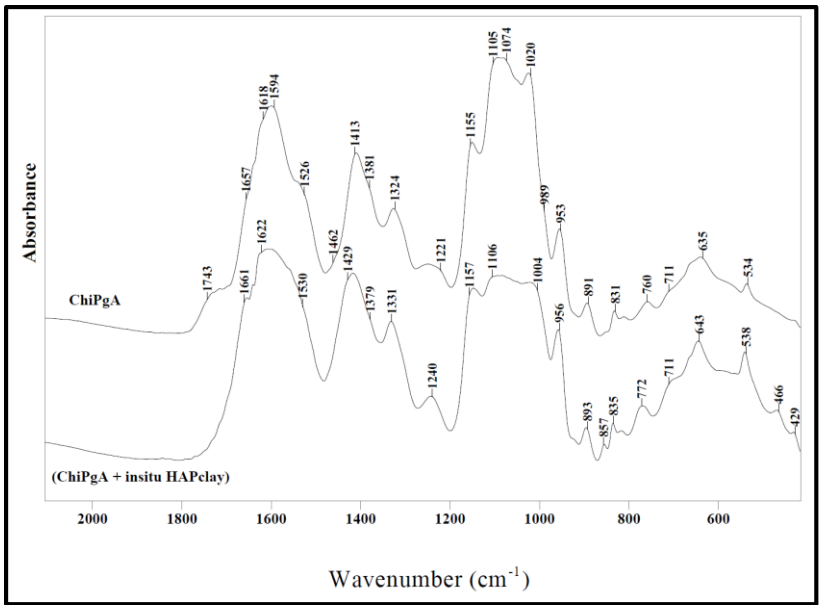

Figure 4.9. Transmission FTIR spectra of ChiPgA film and ChiPgA film containing *in situ* HAPclay in the 1950-400 cm^{-1} range

Table 4.1. FTIR band assignments for modified MMT clay

Band position (cm^{-1})	Band assignment	Reference
3738,3697,3631	OH stretching vibrations	[44-46]
1702	C=O stretching of undissociated carboxyl group	[47]
1618	H-O-H bending vibration of interlayer in modified MMT	[46, 48]
1499	NH_3^+ vibration	[47]
1465, 1437, 1409	$-CH_2-$ deformation vibration	[47]
1287	-OH deformation of the carboxylic group	[47]
1222	Si-O out-of-plane stretching	[46]
1130	Si-O stretching	[45, 46]
1066	Si-O stretching	[45, 46]
1001	OH deformation linked to the cation	[49]
918	Al-OH deformation	[45, 46, 50]
879	Fe-OH deformation	[45, 46]
842	Mg-OH deformation	[45, 46]
799,777	Si-O stretching of quartz and silica	[17, 45, 46]
689	Si-O deformation	[45, 46]
630	Coupled Al-O and Si-O vibration	[45, 46]
526	Al-OSi deformation	[45]
470	Si-OSi deformation	[45]

Table 4.2. FTIR band assignments for *in situ* HAPclay

Band position (cm^{-1})	**Band assignment**	**Reference**
3739	H-O-H asymmetric stretching of water in HAP	[51]
3697	H-O-H symmetric stretching of water in HAP	[52]
3568	OH stretching of hydroxyl group in HAP	[37, 51, 52]
1623	H-O-H bending vibration of adsorbed water in HAP	[53]
1541	Asymmetric C=O stretching in dissociated carboxylic group	[38]
1499	symmetric NH_3^+ deformation vibration	[47]
1458, 1417	$-CH_2-$ deformation vibration	[47]
1347	symmetric C=O stretching in dissociated carboxylic group	[47]
1154	γ_6 vibration of phosphate ion of HPO_4^{2-}	[53, 54]
1016	γ_3 phosphate vibration	[37]
965	γ_1 P-O stretching vibration of phosphate	[36, 37]
920	Al-OH deformation	[45, 46]
877	Fe-OH deformation	[45, 46]
783	Si-O stretching of quartz and silica	[45, 46]
730	Si-O deformation perpendicular to optical axis	[45]
600	γ_4 phosphate vibration	[37]
551	γ_4 phosphate vibration	[36, 37]

Table 4.3. FTIR band assignments for hydroxyapatite (HAP)

Band position (cm^{-1})	**Band assignment**	**Reference**
3739	H-O-H asymmetric stretching of water in HAP	[51]
3696	H-O-H symmetric stretching of water in HAP	[52]
3571	OH stretching of hydroxyl group in HAP	[37, 51, 52]
1634	H-O-H bending vibration of adsorbed water in HAP	[53]
1144	γ_6 vibration of phosphate ion of HPO_4^{2-}	[53, 54]
1027	γ_3 phosphate vibration	[37]
951	γ_1 P-O stretching vibration	[36, 37]
860	P-O(H) stretching vibration	[36, 37]
603	γ_4 phosphate vibration	[37]
570	γ_4 phosphate vibration	[36, 37]
470	γ_2 phosphate vibration	[36]

Table 4.4. FTIR band assignments for ChiPgA and ChiPgA *in situ* HAPclay composite film

Band position (cm^{-1})	Band assignment	Reference
2937,2933	Asymmetric C-H stretching	[47]
2880,2877	Symmetric C-H stretching	[47]
1743	C=O stretching of undissociated carboxylic groups in PgA	[34, 47]
1657,1661	Amide I bands from chitosan	
1618,1622	Asymmetric stretching vibration of dissociated carboxyl group	[34, 47]
1530,1526	Asymmetric NH_3^+ deformation vibration	[47]
1413,1429	Symmetric stretching of dissociated carboxylic group	[34, 47]
1324,1331	CH bending vibrations of the rings from ChiPgA	[47]
760,772	Pyranose ring vibration	[47]
643,645	OH out of plane bending	[47]
429	Mg-O vibration from modified MMT clay	[45]

4.3.2. X-ray Diffraction Studies

Figure 4.10. (a, b) shows the XRD plots of modified MMT clay, *in situ* HAPclay and hydroxyapatite (HAP). A distinct peak corresponding to (001) plane is seen in case of modified MMT clay at 2θ position of 6.896° (d_{001}=12.81 A°). In case of *in situ* HAPclay (Figure 4.10.b), this peak appears to have shifted to a higher 2θ position of 7.182° (d_{001}=12.3 A°) that indicates a decrease of 0.51 A° in the d_{001} spacing of the modified MMT clay. This may be attributed to change in the interaction of the modifier molecules with the MMT clay sheets due to possible nucleation of apatite at the functional groups of the modifier. In the transmission FTIR spectra of *in situ* HAPclay, it was observed that the undissociated carboxylic group seen in case of modified MMT clay is absent in case of *in situ* HAPclay. FTIR spectra also indicated that these carboxylic groups had dissociated. The possible reason for the dissociation of carboxylic group was the dispersion of modified MMT clay in the basic sodium phosphate solution during preparation of *in situ* HAPclay. Therefore, the change in the interactions of modifier molecules

with the MMT clay sheets due to this dissociation can be supposed to be initiated when the modified clay is dispersed in sodium phosphate solution and continue during the nucleation of apatite after the addition of calcium chloride solution to the sodium phosphate solution. The involvement of carboxylic groups in chelation with the carboxylic groups as observed by FTIR studies also implies a change in the conformation of the carboxylic group. This can also contribute to the change in the interactions between the modifier and the MMT clay sheets. Moreover, our previous experimental and simulation studies have shown that the functional groups of the modifier have an effect on the d-spacing of MMT clay [18]. During the process of preparation of *in situ* HAPclay, changes in the undissociated carboxylic group of modified MMT clay due to dissociation and chelation is likely to contribute to the observed change in the d-spacing of MMT clay.

In Figure 4.10. (a), it is observed that there are similarities in the XRD plots of *in situ* HAPclay and HAP. Peaks seen in case of XRD plot of hydroxyapatite (HAP) are also seen in of *in situ* HAPclay. This gives an indication of presence of apatite in *in situ* HAPclay. Peak positions 25.95°, 28.33°, 31.74°, 32.29°, 45.44°, 49.47° corresponding to planes (002), (102), (211), (112), (203) and (213) seem to have shifted to different 2θ positions in case of *in situ* HAPclay that indicates that the apatite in *in situ* HAPclay has different lattice parameters as compared to hydroxyapatite (HAP). Peak shift observed in XRD studies can be attributed to several factors such as dislocations, stacking faults, twinning, microstresses, internal stresses, grain boundaries, point defects, chemical heterogeneity, precipitates and inclusions [55]. Residual stresses that include internal stresses and microstresses have also been known to be responsible for peak shifts observed in XRD studies [56]. Mechanical, thermal and chemical factors can contribute to the residual stresses. In case of preparation of *in situ* HAPclay, chemical

factors such as the precipitation of apatite may contribute to the residual stress generation that results in the observed peak shifts of HAP. Also, the presence of a different chemical environment for nucleation of apatite in modified MMT clay can have an effect on the kinetics and growth of apatite that can also contribute to the difference in peak positions of apatite seen in case of *in situ* HAPclay. The peak positions seen at 27.52° and 19.86° in case of modified MMT clay appear to be shifted to a lower 2θ position to 26.58° and 19.77° respectively in case of *in situ* HAPclay. These shifts indicate a change in the lattice parameters of modified MMT clay. The difference in the positions of the peaks from modified MMT clay and HAP in case of *in situ* HAPclay thus indicates changes in the crystal structure of modified MMT clay due to precipitation of apatite and also the differences in the lattice parameters of the apatite precipitated (formed) in *in situ* HAPclay.

4.3.3. Cell Culture Studies

The purpose of cell culture experiments involving the use of *in situ* HAPclay was to study the attachment and cluster/pattern formation by anchorage dependent cells such as osteoblasts on engineered ChiPgA films containing *in situ* HAPclay. As discussed earlier under section 4.2.5.3., ChiPgA films with different weight percentage composition (between 10 wt % to 20 wt %) of *in situ* HAPclay were prepared and human osteoblast cells were cultured on these films. Initially, the behavior (attachment and cluster/pattern formation) of human osteoblast cells on ChiPgA films containing 10 wt % and 20 wt % *in situ* HAPclay was observed under an inverted microscope for a cell culture period of 36 days. From the images shown in Figures 4.11. & 4.12., it can be seen that the human osteoblasts were able to adhere and form clusters on the ChiPgA films containing 10 wt % and 20 wt % *in situ* HAPclay. Observations related to culture period required for cluster formation and size of clusters are described in further paragraphs.

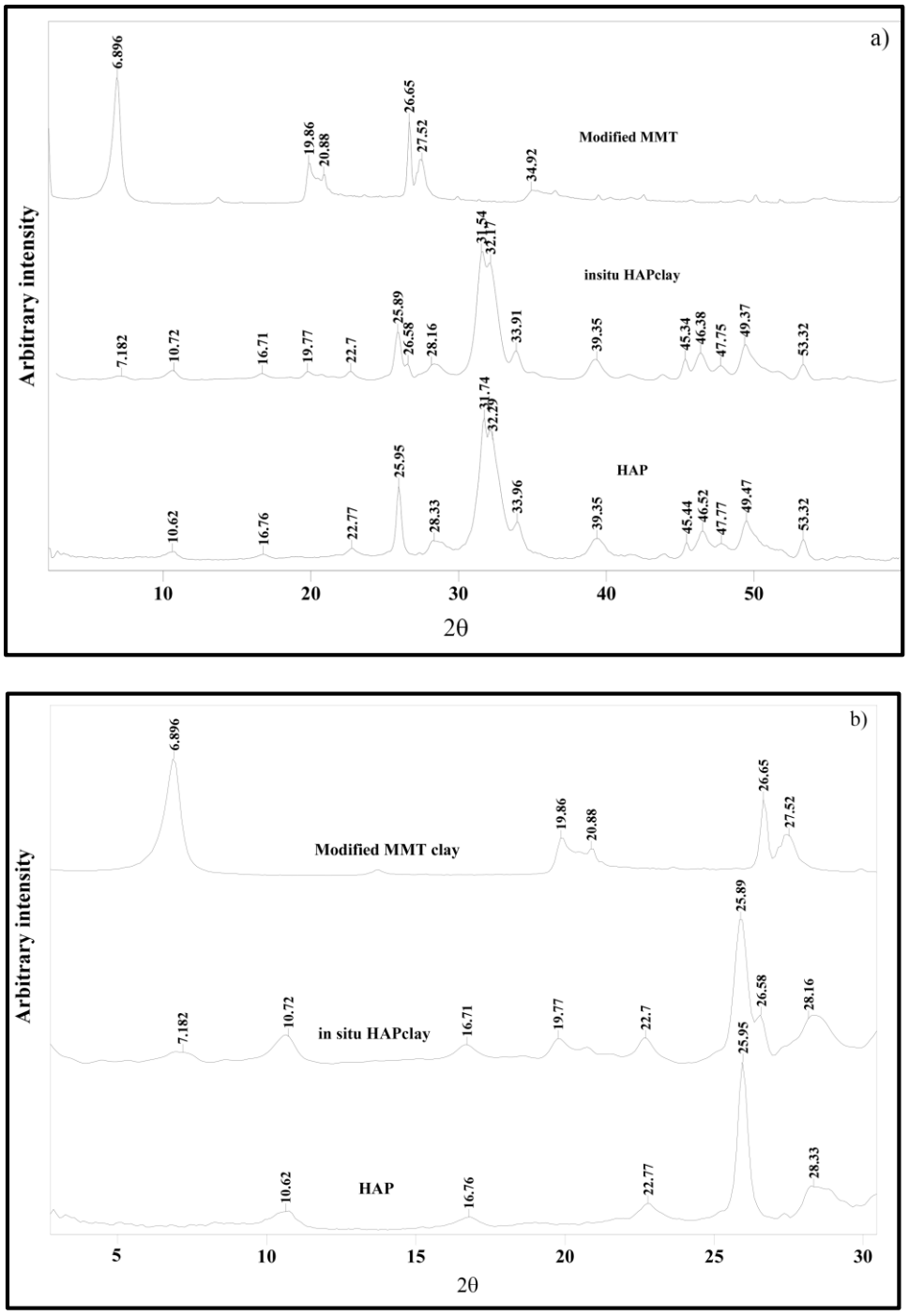

Figure 4.10. X-ray diffraction plots of modified MMT clay, *in situ* HAPclay (*in situ* HAP prepared using modified MMT clay), mixture of HAP and modified MMT clay and hydroxyapatite (HAP). a) in the range 2θ = 2° to 60°, b) in the range 2θ = 2° to 30°

Cluster formation was observed after 8 days and 4 days on ChiPgA films containing 10 wt % *in situ* HAPclay and ChiPgA films containing 20 wt % *in situ* HAPclay respectively. Clusters of size approximately 80 µm-800 µm were observed in case of ChiPgA films containing 10 wt % *in situ* HAPclay. In case of ChiPgA films with 20 wt % *in situ* HAPclay, clusters were in approximately 80 µm-1470 µm size range. The size of clusters on ChiPgA/*in situ* HAPclay composite films appeared to increase during cell culture. Clusters of size ~ 500 µm and greater were also observed after 24 days in case of ChiPgA films with 10 wt % *in situ* HAPclay and after 20 days for ChiPgA films with 20 wt % *in situ* HAPclay. Considering the prospects of tailoring the properties of ChiPgA composites by varying the *in situ* HAPclay content, osteoblasts were cultured on ChiPgA films containing 12.5 wt % and 15 wt % *in situ* HAPclay. Since it was intended to observe if similar cellular events (attachment, cluster formation) occurred in case of ChiPgA films containing 12.5 wt % and 15 wt % *in situ* HAPclay, cell culture experiments of duration less than 36 days were performed. Besides this osteoblast cluster formation was observed after 4-8 days culture as discussed previously in case of films with 10 wt % and 20 wt % *in situ* HAPclay. Osteoblast adhesion and cluster formation was also observed (figures 4.13. and 4.14.) in case of ChiPgA films with 12.5 wt % and 15 wt % *in situ* HAPclay. Size of osteoblast clusters observed during 16 days culture in case of films with 12.5 wt % *in situ* HAPclay was approximately in 80 µm-500 µm range and cluster formation was observed after 4 days. In case of films with 15 wt % *in situ* HAPclay, cluster formation was observed after 8 days and size of clusters observed was approximately in 80 µm-1370 µm range during 12 days of culture. Also, it was observed that relatively larger clusters (close to 1340 µm) were formed after 4 days. Events such as cell adhesion and clustering are known to play an important role in formation and mineralization of a bone nodule [57]. Therefore, it appears that ChiPgA films

containing *in situ* HAPclay provide a favorable environment for the events involved in the formation of a bone nodule. It can be thus said that the ChiPgA films containing *in situ* HAPclay are biocompatible and also appear to show potential for bone tissue regeneration. Moreover, it was observed that the human osteoblast cells were able to adhere and form clusters on ChiPgA films with composition of *in situ* HAPclay from 10 wt % to 20 wt %. This indicates that the percentage composition of *in situ* HAPclay can be varied while fabricating ChiPgA composite films and scaffolds to control mechanical properties and the architecture in case of three dimensional scaffolds.

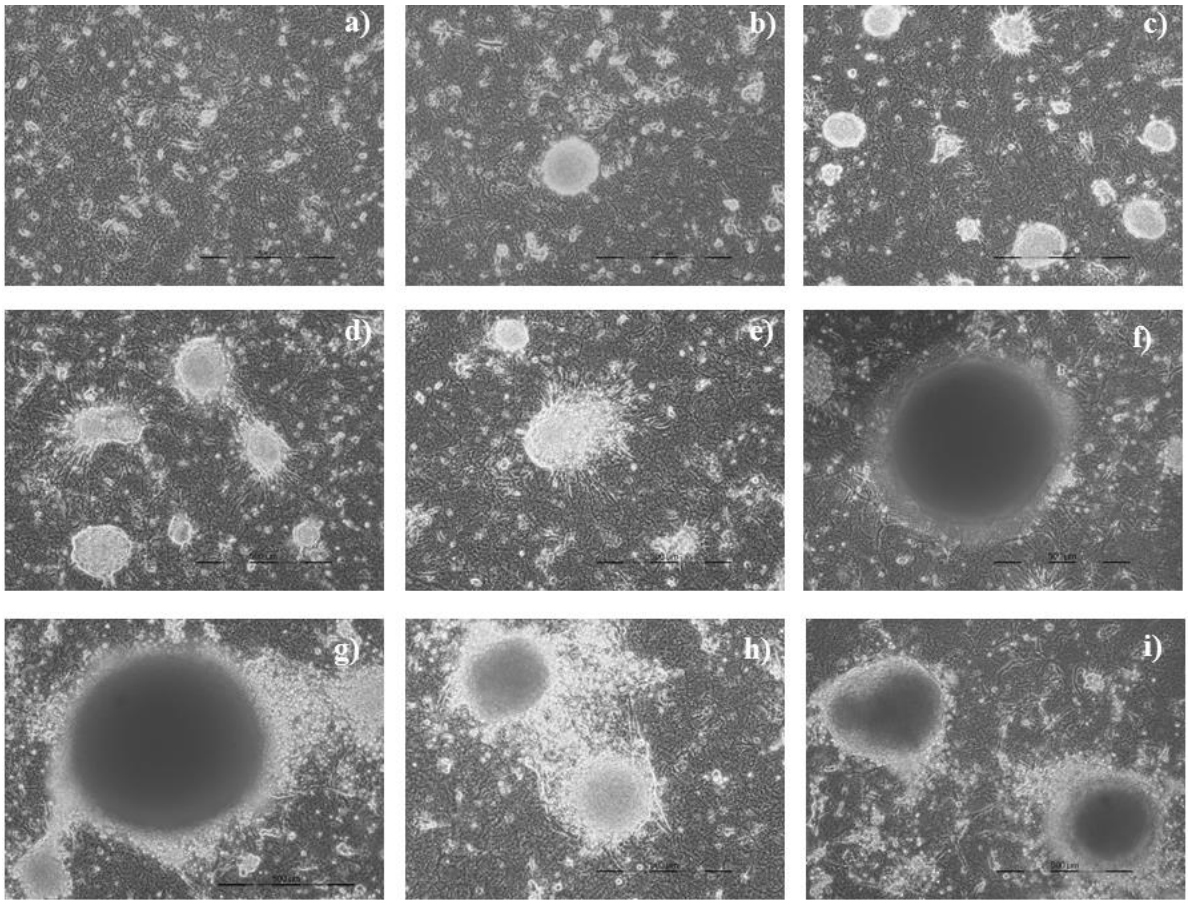

Figure 4.11. Inverted microscope images of human osteoblast cells cultured on ChiPgA films containing 10 wt % *in situ* HAPclay after a) 4 days, b) 8 days, c) 12 days, d) 16 days, e) 20 days, f) 24 days, g) 28 days, h) 32 days, i) 36 days (scale bar on lower right hand side – 500 µm)

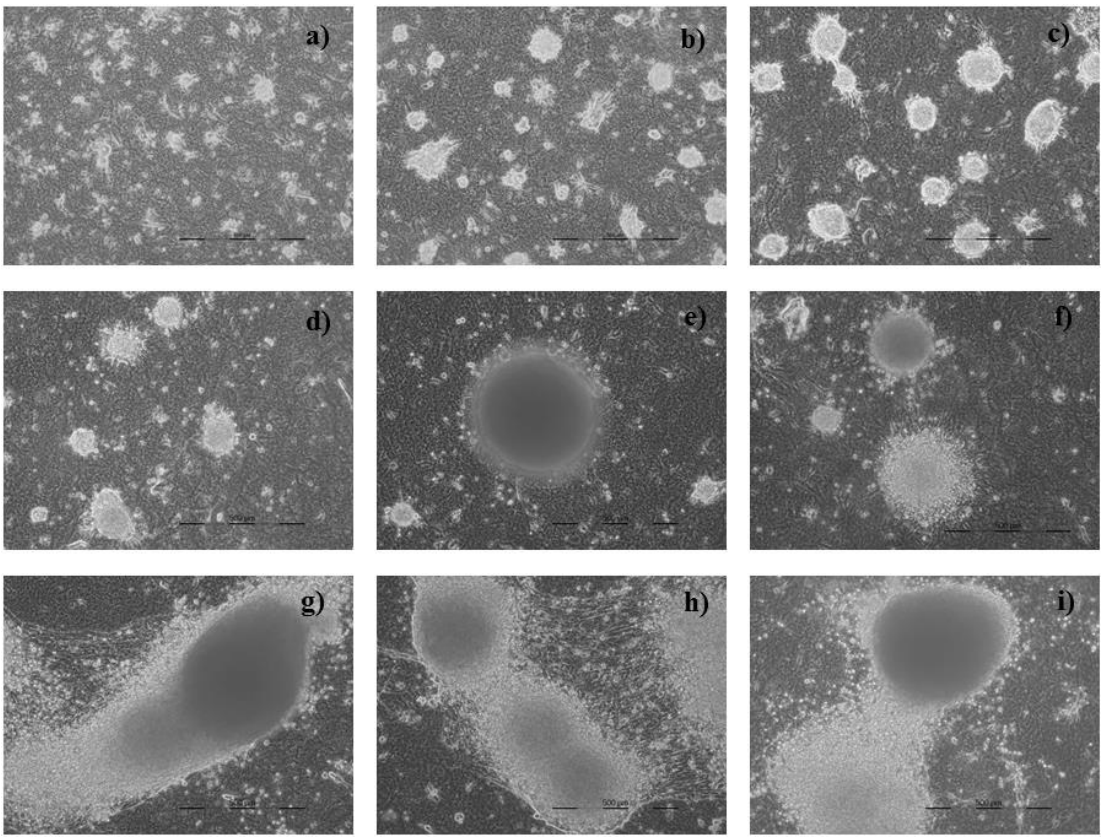

Figure 4.12. Inverted microscope images of human osteoblast cells cultured on ChiPgA films containing 20 wt % *in situ* HAPclay after a) 4 days, b) 8 days, c) 12 days, d) 16 days, e) 20 days, f) 24 days, g) 28 days, h) 32 days, i) 36 days (scale bar on lower right hand side – 500 µm)

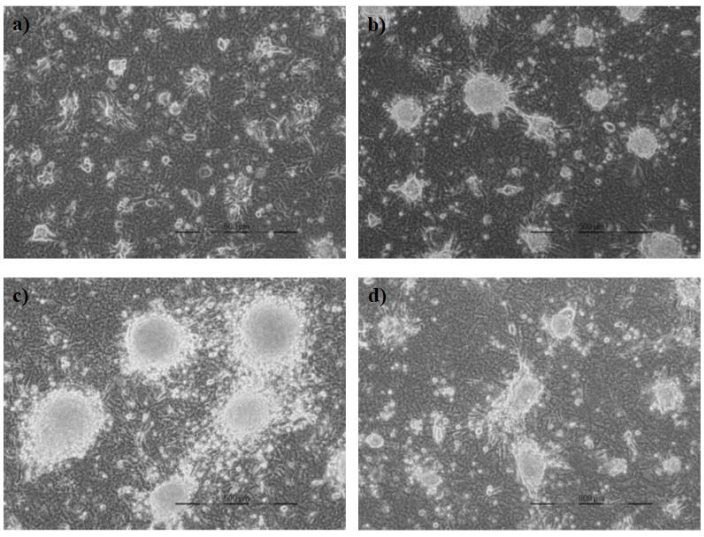

Figure 4.13. Inverted microscope images of human osteoblast cells cultured on ChiPgA films containing 12.5 wt % *in situ* HAPclay after a) 4 days, b) 8 days, c) 12 days, d) 16 days (scale bar on lower right hand side – 500 µm)

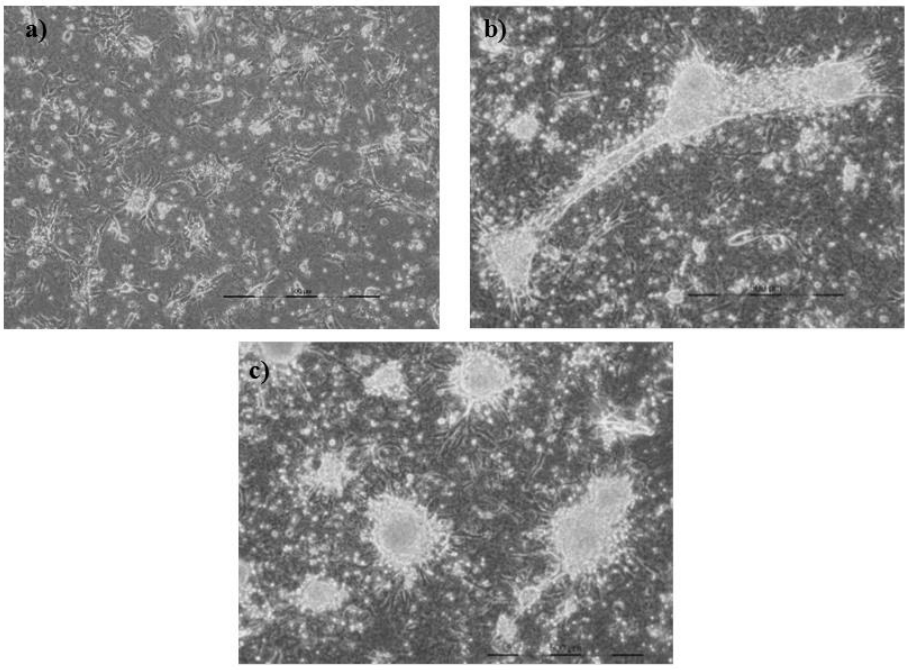

Figure 4.14. Inverted microscope images of human osteoblast cells cultured on ChiPgA films containing 15 wt % *in situ* HAPclay after a) 4 days, b) 8 days, c) 12 days (scale bar on lower right hand side – 500 µm)

4.4. Conclusions

A novel method of mineralizing hydroxyapatite using the functional groups of the modifier that serve as possible sites of mineralization in MMT clay modified with 5-aminovaleric acid was developed. Transmission FTIR experiments on *in situ* HAPclay indicated chelation of the dissociated carboxylate groups with the calcium ions suggesting the mechanism for nucleation of HAP. FTIR spectroscopy studies also indicated the presence of phosphate vibrations similar to those observed in HAP. The phosphate vibrations observed in case of *in situ* HAPclay were at different wavenumber positions as compared to those present in HAP and mixture of HAP with the modified MMT clay. This indicated that there were interactions between the modified MMT clay and the ions present in the apatite that was possibly mineralized in the modified MMT clay. Difference in the wavenumber positions of phosphate vibrations in case of *in situ* HAPclay also indicated possible differences in the symmetry of the apatite

possibly mineralized in modified MMT clay. XRD studies indicated the presence of apatite in *in situ* HAPclay and also the differences in the lattice structure of this apatite precipitated (formed) in *in situ* HAPclay. Also, XRD data for *in situ* HAPclay showed that there were changes in the crystal structure of the modified MMT clay due to precipitation of apatite. ChiPgA films containing *in situ* HAPclay were prepared and characterized by transmission FTIR experiments. These experiments showed that molecular level interactions existed between the ChiPgA polyelectrolyte and the *in situ* HAPclay. Cell culture experiments were carried out by culturing human osteoblast cells on the ChiPgA films containing *in situ* HAPclay and it was observed through inverted microscope images that the osteoblasts were able to adhere and form clusters on these films. Thus, the ChiPgA films containing *in situ* HAPclay was biocompatible and also favored events that are supposed to play an important role in the process of bone nodule formation. It was also found that the osteoblast cells were able to adhere on ChiPgA films containing different weight percent compositions of *in situ* HAPclay that can prove useful for tailoring properties of ChiPgA films and scaffolds for bone tissue engineering studies.

4.5. References

[1] Langer R, Vacanti JP. Tissue Engineering. Science. 1993;260:920-6.

[2] Chan CK, Kumar TSS, Liao S, Murugan R, Ngiam M, Ramakrishman S. Biomimetic nanocomposites for bone graft applications. Nanomedicine. 2006;1:177-88.

[3] Patel N, Best SM, Bonfield W, Gibson IR, Hing KA, Damien E, et al. A comparative study on the in vivo behavior of hydroxyapatite and silicon substituted hydroxyapatite granules. Journal of Materials Science:Materials in Medicine. 2002;13:1199-206.

[4] Xynos I, Edgar A, Buttery L, Hench L, Polak J. Ionic Products of Bioactive Glass Dissolution Increase Proliferation of Human Osteoblasts and induce Insulin-like Growth Factor II mRNA Expression and Protein Synthesis Biochemical and Biophysical Research Communications. 2000;276:461-5.

[5] Botelho CM, Brooks RA, Best SM, Lopes MA, Santos JD, Rushton N, et al. Human osteoblast response to silicon-substituted hydroxyapatite. Journal of Biomedical Materials Research Part A. 2006;79A:723-30.

[6] Vallet-Regi M. Revisiting ceramics for medical applications. Dalton Transactions. 2006:5211-20.

[7] Okada A, Kawasumi M, Usuki A, Kojima Y, Kurauchi T, Kamigaito O. Synthesis and properties of nylon-6/clay hybrids. In Polymer based molecular composites MRS SymposiumProceedings (eds D W Schaefer & J E Mark). 1990;171:45-50.

[8] Giannelis EP. Polymer Layered Silicate Nanocomposites. Advanced Materials. 1996;8:29-35.

[9] Chen GX, Hao GJ, Guo TY, Song MD, Zhang BH. Structure and mechanical properties of poly(3-hydroxybutyrateco-3-hydroxyvalerate) (PHBV)/clay nanocomposites. Journal of Materials Science Letters. 2002;21:1587-9.

[10] Pramanik M, Srivastava SK, Samantaray BK, Bhowmick AK. Rubber-clay nanocomposite by solution blending. Journal of Applied Polymer Science. 2003;87:2216-20.

[11] Yano K, Usuki A, Okada A, Kurauchi T, Kamigaito O. Synthesis and properties of polyimide-clay hybrid. Journal of Polymer Science Part A: Polymer Chemistry. 1993;31:2493-8.

[12] Messersmith PB, Giannelis EP. Synthesis and barrier properties of poly(ϵ-caprolactone)-layered silicate nanocomposites. Journal of Polymer Science Part A: Polymer Chemistry. 1995;33:1047-57.

[13] Bharadwaj RK. Modeling the Barrier Properties of Polymer-Layered Silicate Nanocomposites. Macromolecules. 2001;34:9189-92.

[14] Gilman JW. Flammability and thermal stability studies of polymer layered-silicate (clay) nanocomposites. Applied Clay Science. 1999;15:31-49.

[15] Gilman JW, Jackson CL, Morgan AB, R. H. Flammability Properties of Polymer−Layered-Silicate Nanocomposites. Polypropylene and Polystyrene Nanocomposites. Chemistry of Materials. 2000;12:1866-73.

[16] Sikdar D, Pradhan SM, Katti DR, Katti KS, Mohanty B. Altered Phase Model for Polymer Clay Nanocomposites. Langmuir. 2008;24:5599-607.

[17] Sikdar D, Katti DR, Katti KS. The role of interfacial interactions on the crystallinity and nanomechanical properties of clay-polymer nanocomposites: A molecular dynamics study. Journal of Applied Polymer Science. 2008;107:3137-48.

[18] Sikdar D, Katti D, Katti K, Mohanty, Bedabibhas. Influence of backbone chain length and functional groups of organic modifiers on crystallinity and nanomechanical properties of intercalated clay-polycaprolactam nanocomposites. International Journal of Nanotechnology. 2009;6:468-92.

[19] Viseras C, Aguzzi C, Cerezo P, Lopez-Galindo A. Uses of clay minerals in semisolid health care and therapeutic products. Applied Clay Science. 2007;36:37-50.

[20] Forni F, Iannuccelli V, Coppi G, Bernabei MT. Effect of Montmorillonite on Drug Release from Polymeric Matrices. Archiv der Pharmazie. 1989;322:789-93.

[21] Dong Y, Feng S-S. Poly(d,l-lactide-co-glycolide)/montmorillonite nanoparticles for oral delivery of anticancer drugs. Biomaterials. 2005;26:6068-76.

[22] Wen-Fu Lee, Yao-Tsung Fu. Effect of montmorillonite on the swelling behavior and drug-release behavior of nanocomposite hydrogels. Journal of Applied Polymer Science. 2003;89:3652-60.

[23] Lin K-F, Hsu C-Y, Huang T-S, Chiu W-Y, Lee Y-H, Young T-H. A novel method to prepare chitosan/montmorillonite nanocomposites. Journal of Applied Polymer Science. 2005;98:2042-7.

[24] Marras SI, Kladi KP, Tsivintzelis I, Zuburtikudis I, Panayiotou C. Biodegradable polymer nanocomposites: The role of nanoclays on the thermomechanical characteristics and the electrospun fibrous structure. Acta Biomaterialia. 2008;4:756-65.

[25] Zheng JP, Wang CZ, Wang XX, Wang HY, Zhuang H, Yao KD. Preparation of biomimetic three-dimensional gelatin/montmorillonite-chitosan scaffold for tissue engineering. Reactive and Functional Polymers. 2007;67:780-8.

[26] Katti KS, Katti DR, Dash R. Synthesis and characterization of a novel chitosan/montmorillonite/hydroxyapatite nanocomposite for bone tissue engineering. Biomedical Materials. 2008;3:12.

[27] Depan D, Kumar AP, Singh RP. Cell proliferation and controlled drug release studies of nanohybrids based on chitosan-g-lactic acid and montmorillonite. Acta Biomaterialia. 2009;5:93-100.

[28] Katti KS, Ambre AH, Peterka N, Katti DR. Use of unnatural amino acids for design of novel organomodified clays as components of nanocomposite biomaterials. Philosophical Transactions of The Royal Society A 2010;368:1963-80.

[29] Ambre AH, Katti KS, Katti DR. Nanoclay Based Composite Scaffolds for Bone Tissue Engineering Applications. Journal of Nanotechnology in Engineering and Medicine. 2010;1:031013-9.

[30] Christenson EM, Anseth KS, van den Beucken L, Chan CK, Ercan B, Jansen JA, et al. Nanobiomaterial applications in orthopedics. Journal of Orthopaedic Research. 2007;25:11-22.

[31] Murugan R, Ramakrishna S. Development of nanocomposites for bone grafting. Composites Science and Technology. 2005;65:2385-406.

[32] Verma D, et al. Osteoblast adhesion, proliferation and growth on polyelectrolyte complex-hydroxyapatite nanocomposites. Philosophical Transactions of The Royal Society A Mathematical Physical and Engineering Sciences. 2010;368:2083.

[33] Verma D, Katti KS, Katti DR. Polyelectrolyte-complex nanostructured fibrous scaffolds for tissue engineering. Materials Science and Engineering: C. 2009;29:2079-84.

[34] Verma D, Katti KS, Katti DR. Effect of Biopolymers on Structure of Hydroxyapatite and Interfacial Interactions in Biomimetically Synthesized Hydroxyapatite/Biopolymer Nanocomposites. Annals of Biomedical Engineering. 2008;36:1024-32.

[35] Verma D, Katti KS, Katti DR, Mohanty B. Mechanical response and multilevel structure of biomimetic hydroxyapatite/polygalacturonic/chitosan nanocomposites. Elsevier Science Bv; 2008. p. 399-405.

[36] Verma D, Katti K, Katti D. Experimental investigation of interfaces in hydroxyapatite/polyacrylic acid/polycaprolactone composites using photoacoustic FTIR spectroscopy. Journal of Biomedical Materials Research Part A. 2006;77A:59-66.

[37] Fowler BO. Infrared studies of apatites. I. Vibrational assignments for calcium, strontium, and barium hydroxyapatites utilizing isotopic substitution. Inorganic Chemistry. 1974;13:194-207.

[38] Hu H, Saniger J, Garcia-Alejandre J, Castano VM. Fourier Transform Infrared Spectroscopy Studies of the reaction between polyacrylic acid and metal oxides. Material Letters. 1991;12:281-5.

[39] Deacon GB, Phillips RJ. Relationships between the carbon-oxygen stretching frequencies of carboxylato complexes and the type of carboxylate coordination. Coordination Chemistry Reviews. 1980;33:227-50.

[40] Bhowmik R, Katti KS, Verma D, Katti DR. Probing molecular interactions in bone biomaterials: Through molecular dynamics and Fourier transform infrared spectroscopy. Materials Science and Engineering: C. 2007;27:352-71.

[41] Zhang W, Huang Z-L, Liao S-S, Cui F-Z. Nucleation Sites of Calcium Phosphate Crystals during Collagen Mineralization. Journal of the American Ceramic Society. 2003;86:1052-4.

[42] Bailey RA, Clark HM, Ferris JP, Krause S, Strong RL. Chemistry of the Environment. California: Academic Press; 2002.

[43] Rhee S-H, Lee JD, Tanaka J. Nucleation of Hydroxyapatite Crystal through Chemical Interaction with Collagen. Journal of the American Ceramic Society. 2000;83:2890-2.

[44] Viscarra Rossel RA, Lark RM. Improved analysis and modelling of soil diffuse reflectance spectra using wavelets. European Journal of Soil Science. 2009;60:453-64.

[45] Katti KS, Sikdar D, Katti DR, Ghosh P, Verma D. Molecular interactions in intercalated organically modified clay and clay-polycaprolactam nanocomposites: Experiments and modeling. Polymer. 2006;47:403-14.

[46] Amarasinghe PM, Katti KS, Katti DR. Molecular Level Hydraulic Properties of Montmorillonite:A Polarized Fourier Transform Infrared Spectroscopy Study. Applied Spectroscopy. 2008;62:1303-13.

[47] Socrates G. Infrared and Raman Characteristic Group Frequencies. Third Edition ed: John Wiley & Sons Ltd.; 2001.

[48] Amarasinghe PM, Katti KS, Katti DR. Nature of organic fluid-montmorillonite interactions: An FTIR spectroscopic study. Journal of Colloid and Interface Science. 2009;337:97-105.

[49] Katti KS, Katti DR. Relationship of Swelling and Swelling Pressure on Silicaâˆ’Water Interactions in Montmorillonite. Langmuir. 2005;22:532-7.

[50] Katti KS, Katti DR. Relationship of Swelling and Swelling Pressure on Silicaâˆ’Water Interactions in Montmorillonite. Langmuir. 2005;22:532-7.

[51] Reyes-Gasga J, et al. Structural and thermal behaviour of human tooth and three synthetic hydroxyapatites from 20 to 600 Â°C. Journal of Physics D: Applied Physics. 2008;41:225407.

[52] Chang M, Douglas W, Tanaka J. Organic-inorganic interaction and the growth mechanism of hydroxyapatite crystals in gelatin matrices between 37 and 80 Â°C. Journal of Materials Science: Materials in Medicine. 2006;17:387-96.

[53] Koutsopoulos S. Synthesis and characterization of hydroxyapatite crystals: A review study on the analytical methods. Journal of Biomedical Materials Research. 2002;62:600-12.

[54] Pleshko N, Boskey A, Mendelsohn R. Novel infrared spectroscopic method for the determination of crystallinity of hydroxyapatite minerals. Biophysical Journal. 1991;60:786-93.

[55] Ungar T. Microstructural parameters from X-ray diffraction peak broadening. Scripta Materialia. 2004;51:777-81.

[56] Cullity BD. Elements of X-ray Diffraction. 2nd Edition ed: Addison Wesley; 1978.

[57] Bellows CG, Aubin JE, Heersche JNM, Antosz ME. Mineralized Bone Nodules Formed In Vitro From Enzymatically Released Rat Calvaria Cell Populations. Calcified Tissue International. 1986;38:143-54.

CHAPTER 5. USE OF NANOCLAYS FOR MEDIATING MESENCHYMAL STEM CELL DIFFERENTIATION

This chapter presents the use of nanoclay-hydroxyapatite (HAP) hybrid also known as *in situ* HAPclay for the fabrication of biopolymer composites (scaffolds and films) and the response of human mesenchymal stem cells (hMSCs) to these composites. The contents of this chapter have been published in Ambre, A.H., Katti, D.R., Katti, K.S. Nanoclays Mediate Stem Cell Differentiation and Mineralized ECM formation on Biopolymer Scaffolds. Journal of Biomedical Materials Research Part A. 2013; 101 A: 2644-2660.

5.1. Introduction

Tissue engineering introduced by Langer and Vacanti [1] is one of the most promising approaches in regenerative medicine to rectify tissue defects arising from pathological conditions and injuries sustained. In addition, tissue engineering strategies present relatively less invasive routes and capability to cure tissue defects by natural processes, compared with conventional treatment methods. Scaffolds, cells, and growth factors used for supplementing cell culture media are vital components that can be modulated for successful tissue regeneration in tissue engineering. Scaffolds can be designed to provide the required biophysical and biochemical signals to the cells for tissue formation in a three dimensional environment similar to the in vivo environment. The limited availability of autologous tissue biopsies restricts the number of cells available for regeneration in case of large tissue defects. Also, cells obtained from such tissue biopsies exhibit limited proliferation and tissue formation abilities [2] in addition to improper phenotype expression for certain cell types [3]. Cells for tissue engineering need to be obtainable through existing cell isolation techniques with low donor site morbidity, show “immunological compatibility” and maintain a stable phenotype while being receptive to signals from the

surrounding environment [3-5]. Mesenchymal stem cells (MSCs) can proliferate in an undifferentiated state and also maintain their capability to differentiate into different cell lineages. The differentiation of MSCs is non-spontaneous unlike the embryonic stem cells and can be controlled by using appropriate stimuli (chemical, mechanical and electrical). MSCs also have also been reported for their "immunosuppressive" effects [6-8] although research related to this property of MSCs continues to evolve. These cells exert suppressive effects on cells (e.g. T, B and natural killer cells) involved in the immune system [6, 9]. This makes possible the use of allogeneic MSCs for regenerating a defective tissue in a host using tissue engineering principles. Although bone marrow has been the major source of MSCs, these cells are also found in different tissues. Thus, the important attributes of MSCs and their potential to be a major cell source for tissue engineering has stimulated research focused on the behavior of MSCs seeded on engineered scaffolds.

Materials synthesis and materials processing for developing scaffolds that satisfy tissue engineering requirements (biocompatibility, biodegradability, porosity, pore size and adequate mechanical properties) have been the focus of several studies. Biodegradable polymers (natural and synthetic) and ceramics have been used as major components for preparing scaffolds in such studies. The brittleness of ceramics, relatively inadequate mechanical properties of natural polymers, and inadequacy of biodegradable polymers for tissue formation in absence of appropriate stimuli despite favoring cell attachment restricts their independent use for preparing scaffolds. Difficulties in designing scaffolds with hierarchical organization similar to the extracellular matrix necessitate consideration of feasible strategies for preparing scaffolds. One of them is combining polymeric materials with fillers that impart tissue formation abilities and provide adequate mechanical properties to the resulting polymer scaffolds. Hydroxyapatite

(HAP) has been used in studies related to bone tissue engineering due to its biocompatibility, non-immunogenicity and osteoconductivity [10-12]. Ions such as carbonate, sodium, magnesium and silicon present in bone along with apatite have been reported for their effect on processes related to bone mineralization and formation [10, 13, 14]. Silicon-substituted HAP was used in some studies to study in vivo bioactivity [14, 15] and its effect on osteoblasts [16]. Studies related to silicon based materials such as bioactive glass suggested effect of silicon on osteoblast proliferation, bone metabolism and bioactivity shown by bioactive glass [14]. Introducing elements such as silicon, magnesium etc. in HAP and subsequent use of this substituted HAP for preparing engineered biomaterials is one of the methods used for influencing cell behavior and tissue formation. Another approach can be the use of silicate minerals such as montmorillonite (MMT) clay for preparing polymer composite scaffolds that can influence cellular events involved in bone formation and possibly have suitable mechanical properties for bone regeneration at the defective site.

MMT clay belongs to the family of 2:1 phyllosilicates, and is a layered silicate with one octahedral alumina sheet between two tetrahedral silica sheets [17]. Nanometer thickness of each layer in MMT clay gives it a high aspect ratio and can also be useful for obtaining cellular response favoring tissue formation since nanoscale features favor cell adhesion and protein adsorption [18-20]. High aspect ratio and its capacity to be intercalated with small organic molecules known as modifiers by exchanging the interlayer alkali metal ions such as sodium have contributed to the extensive use of MMT for preparing polymer-clay nanocomposites (PCNs) since their introduction by Toyota research group in 1990 [21]. PCNs have shown improvement in mechanical properties [17, 22-24], improvement in biodegradability [17],

reduced gas permeability [25-27] and flammability [28, 29] due to presence of MMT clay. Investigation of PCNs by our group through several experimental and simulation studies led to development of ‘‘Altered Phase Theory of PCNs’’ that postulates that molecular interactions between polymer, clay, and modifier lead to formation of an ‘‘altered phase’’ around clay particles in PCNs of the scale of 10 s of nanometers, which has significantly different physical properties the polymer [30]. In another study, interaction energies evaluated between different components of polymer and modifier in PCNs using molecular dynamics simulation showed that molecular interactions affect crystallinity and nanomechanical properties of PCNs [31]. Also, one of our previous studies showed that a modifier's backbone chain length and its functional groups affect MMT clay d-spacing and nanomechanical properties of PCNs [32]. Our modeling studies have indicated the potential of amino acids to be intercalated into clay galleries [33]. Further, medicinal properties [34], reported use for pharmaceutical applications [35-40] and ability to be excreted from the body [41] seem to make MMT suitable for use in tissue engineering studies.

PCNs based on chitosan [42], polycaprolactone [43] and gelatin [44] have been studied for their mechanical properties as potential biomaterials. Few studies showing the effect of PCNs on cell behavior [45-47] have been reported with one of them focused on drug release applications [45]. Bone tissue engineering applications require use of cells such as osteoblasts or MSCs. Understanding the effect of an engineered biomaterial on cellular behavior is crucial for its progress towards its application as a scaffold that can overcome difficulty of achieving mechanical properties adequate to withstand the load at the defective site in vivo. Studying the behavior of osteoblasts and MSCs on biomaterials containing MMT clay can improve our understanding related to the optimal use of MMT clay for modulating cell behavior.

Our prior studies related to use of MMT clay for bone tissue engineering applications involved use of three unnatural amino acids for modifying MMT clay [48]. Longer backbone chain length of these acids as compared to the natural amino acids [33] based on our previous study showing the effect of backbone chain length of modifiers on mechanical behavior [32] and their reported antimicrobial activity were considered as the selection criteria. MMT clays modified with these unnatural amino acids showed an increase in interlayer spacing and were found to be biocompatible with human osteoblasts. Improved biocompatibility and interlayer spacing increase were observed in case of MMT clay modified with 5-aminovaleric acid compared to MMT clays modified with the other two unnatural amino acids. In further studies, MMT clay modified with 5-aminovaleric acid was used for preparing chitosan/polygalacturonic acid (ChiPgA) composite scaffolds [49]. These scaffolds supported proliferation of osteoblasts and were able to satisfy basic tissue engineering requirements. In subsequent studies, a novel biomimetic nanoclay-HAP hybrid (*in situ* HAPclay) based on biomineralization concept reported for bone was prepared by mineralizing HAP on MMT clay intercalated with 5-aminovaleric acid to further improve the osteoconductive properties of MMT clay and extend its usefulness for bone tissue engineering [50]. Fourier Transform infrared (FTIR) spectroscopy studies indicated that the carboxyl group in 5-aminovaleric acid was involved in mineralization of HAP in modified clay. Cell culture experiments were performed by culturing human osteoblasts on ChiPgA films containing different loadings of *in situ* HAPclay. Adhesion and cluster formation by human osteoblasts was observed on these films that are important events involved in formation of bone nodules. Thus the biomimetic nanoclay-HAP hybrid (*in situ* HAPclay) was found to provide a favorable environment for growth and proliferation of osteoblasts and impart osteogenic characteristics to the resulting composites.

Here, we report investigation related to the use of biomimetic *in situ* HAPclay for preparation of chitosan/polygalacturonic (ChiPgA) composite scaffolds and films. It is hypothesized that the biomimetic HAP-nanoclay hybrid (*in situ* HAPclay) is capable of enhancing osteoinductive and osteoconductive abilities along with mechanical properties of resulting polymer composite based scaffolds. Preparation of ChiPgA/*in situ* HAPclay composite films and scaffolds, characterization of ChiPgA/*in situ* HAPclay composite scaffolds and films and studying the behavior (attachment, viability, differentiation) of MSCs on ChiPgA/*in situ* HAPclay composite films and scaffolds were the objectives of this study. For this purpose, behavior of undifferentiated MSCs derived from human bone marrow was studied on these ChiPgA composite scaffolds and films in the absence of any osteogenic supplements or soluble differentiation factors commonly used in cultures for differentiation of MSCs. Cell culture assays and staining methods were used for studying MSC behavior. Microscopy techniques (phase contrast microscopy, scanning electron microscopy (SEM), atomic force microscopy) were used to study MSC adhesion on ChiPgA composite scaffolds and films, microstructure of the fabricated composite scaffolds and nanoscale morphology of composite films. The primary goal was to investigate the osteoinductive and osteoconductive response and potential of the biomimetic nanoclay-HAP system to influence differentiation of MSCs.

Strategies to enhance the amount of tissue formed under in vitro conditions through experiments involving tissue engineering principles can be useful for approaching the difficulties related to repair of large tissue defects. Optimization of cell numbers and also the concentration of soluble factors (for growth and differentiation) in cell culture medium are some of the strategies that are being investigated in several studies related to tissue engineering for enhancing

tissue formation. MSCs can undergo events such as proliferation and differentiation when cultured on engineered biomaterials. MSCs are known to deposit ECM as they differentiate toward an osteogenic lineage. Proteins such as collagen, fibronectin, elastin, and laminin present in the ECM can have an effect on the proliferation and differentiation of MSCs. Also, proliferation and differentiation of MSCs involve complex sequence of events. Murine MSCs have been reported to undergo a ‘‘predifferentiation growth arrest’’ stage in the process of differentiation where the MSCs acquire the ability to differentiate and at the same time can regain their ability to proliferate if provided with appropriate amount of growth factors [51]. Human MSCs have also been reported to undergo ‘‘growth arrest’’ during differentiation [52]. Considering factors such as the potential of the ECM proteins to assist cell proliferation and differentiation along with the “growth arrest” stage of MSCs during differentiation, a two-stage cell seeding experiment was performed in the present work. MSCs were seeded at two different stages (time points) on ChiPgA/*in situ* HAPclay films during cell culture experiments. Observations indicating ECM formation made during SEM studies on MSC-seeded ChiPgA composite scaffolds and Alizarin Red S staining experiments on MSC-seeded ChiPgA composite films (method A) were also considered for performing the two-stage cell seeding experiments.

5.2. Materials and Methods

5.2.1. Materials

Sodium-montmorillonite (Na-MMT) clay used for experiments, SWy-2 (Crook County, Wyoming), was obtained from the Clay Minerals Repository at the University of Missouri, Columbia. This clay has a cation exchange capacity (CEC) of 76.4 mequiv/100 g according to the specifications provided by the supplier. 5-aminovaleric from Sigma Aldrich, sodium phosphate (Na_2HPO_4) from J.T. Baker and calcium chloride ($CaCl_2$) from EM Sciences were

used for preparing *in situ* HAPclay. Chitosan (≥ 85 % deacetylated and molecular weight 190,000-310,000) and polygalacturonic acid (approx. 95 % enzymatic and molecular weight 25,000-50,000) both from Sigma Aldrich were used for preparing composite films and scaffolds used in these studies. MSCGM™ (mesenchymal stem cell growth medium) Bullekit™ (PT-3001) consisting of mesenchymal stem cell basal medium (MSCBM™, PT-3238) and MSCGM™ SingleQuots™ purchased from Lonza, Walkersville, MD was used as cell culture medium for human mesenchymal stem cells (MSCs). Human mesenchymal stem cells (PT-2501) obtained from bone marrow were purchased from Lonza for cell culture experiments.

5.2.2. Method for Preparing Modified MMT Clay

Procedure described in our previous studies was used for modifying Na-MMT clay [48-50]. Briefly, solution of 5-aminovaleric acid (pH 1.8, temperature 60°C) was added to Na-MMT clay suspension in DI water (pre-heated to 60°C). The resultant mixture at pH 1.8 and 60°C was stirred vigorously for an hour followed by centrifuging to remove deionized water, further washing to remove chloride ions, drying at 70°C, grinding and finally sieving that yielded a fine powder.

5.2.3. Preparation of *In Situ* HAPclay

In situ HAPclay was prepared according to procedure described in our previous work [50]. Modified MMT clay prepared as per the procedure described in the previous section was dispersed in Na_2HPO_4 solution (23.8 mM) and stirred for 2 hours. $CaCl_2$ solution (39.8 mM) was then added to the suspension obtained by mixing modified MMT clay with Na_2HPO_4 solution. The resultant mixture maintained at pH 7.4 was stirred for 8 hours. The precipitates obtained were then allowed to settle, which was followed by centrifuging to remove water from the settled

precipitates. After this the precipitates were dried at 70°C, subjected to grinding and sieved to get a fine powder.

5.2.4. Fabrication of Chitosan/Polygalacturonic Acid (ChiPgA) Composite Films and Scaffolds

Based on our previous studies [49, 50, 53, 54], polyelectrolyte complexation between polymers such as chitosan (Chi) and polygalacturonic acid (PgA) was used for preparing ChiPgA/*in situ* HAPclay composite films and scaffolds. Two different sequences were used while adding *in situ* HAPclay in this work for preparing the ChiPgA composite scaffolds and films. Accordingly, the methods of preparing ChiPgA/*in situ* HAPclay composite scaffolds and films were known as method A and method B. A schematic of these two methods is shown in Figure 5.1.

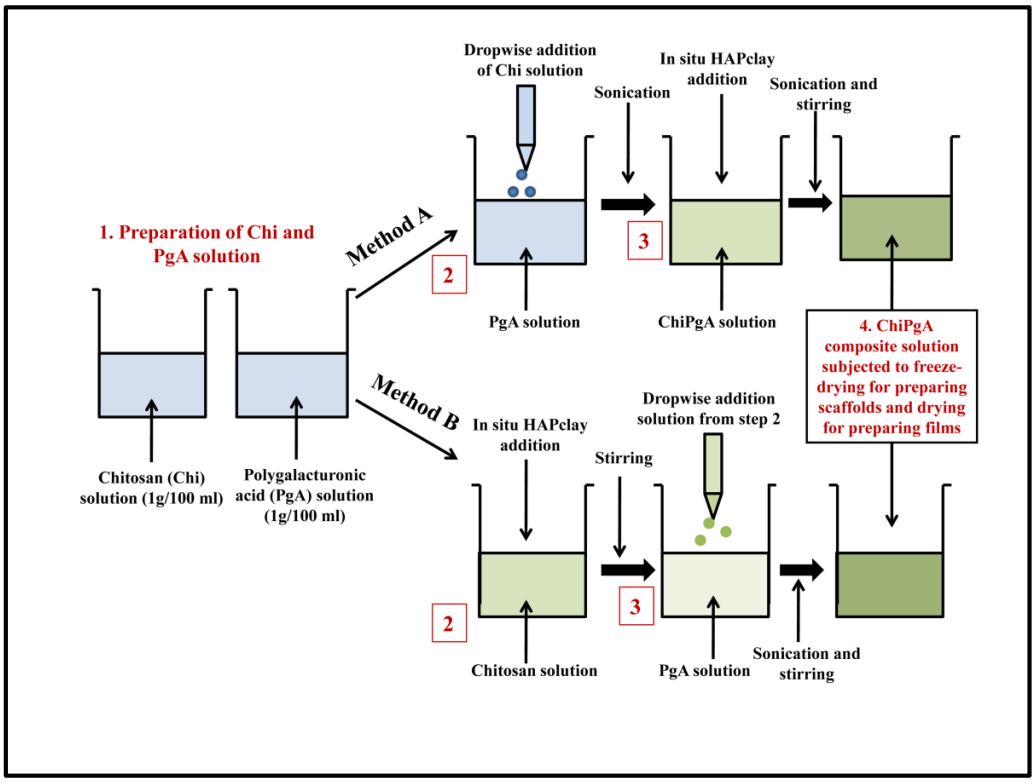

Figure 5.1. Schematic representing methods of preparation of ChiPgA/*in situ* HAPclay composite films and scaffolds

Preparation of chitosan and polygalacturonic acid solutions in deionized water by using acetic acid to dissolve chitosan and diluted sodium hydroxide solution to dissolve polygalacturonic acid were the initial steps in these methods. In method A, chitosan solution was added drop-wise to polygalacturonic acid solution and the resultant mixture was sonicated. *In situ* HAPclay dispersed in deionized water by sonication was then added to the sonicated mixture of Chi and PgA. Resultant mixture of Chi, PgA and *in situ* HAPclay was sonicated and further stirred to get a ChiPgA composite solution. For fabricating scaffolds, the ChiPgA composite solution was centrifuged, frozen at -20°C and then freeze-dried (at -85°C, 200 mTorr pressure). ChiPgA composite films were prepared by diluting (1:10) the ChiPgA composite solution obtained in deionized water and drying this diluted solution at room temperature in tissue culture Petri dishes and wells of 24-well polystyrene plates. Method B involved stages that were used for preparing ChiPgA/*in situ* HAPclay composite solution in our prior work [50]. This involved mixing of sonicated *in situ* HAPclay suspension in deionized water with chitosan solution. The chitosan-in situ HAPclay solution was then added dropwise to the PgA solution followed by sonication and further stirring to get a ChiPgA/*in situ* HAPclay solution. Scaffolds and films from this ChiPgA composite solution were prepared by following the methods described above. ChiPgA/*in situ* HAPclay composite films and scaffolds containing 20 wt % *in situ* HAPclay were thus prepared and used for further experiments.

5.2.5. Scanning Electron Microscopy (SEM) Studies

Microstructure of the fabricated ChiPgA/*in situ* HAPclay composite scaffolds was studied using JEOL JSM-7600F analytical high resolution field-emission scanning electron microscope. For studying the adhesion of MSCs to the ChiPgA composite scaffolds, SEM imaging was performed on the composite scaffolds seeded with MSCs using JEOL JSM-6490LV

scanning electron microscope. Scaffold samples (approx. 10mm diameter and 3mm thickness) seeded with MSCs were washed with PBS after incubation and then fixed using glutaraldehyde (2.5 %). Ethanol series (10 % v/v, 30 % v/v, 50 % v/v, 70 % v/v and 100 %) was used for dehydrating the fixed scaffold samples, which were dried subsequently after replacing 100 % ethanol with hexamethyldisilazane. The fixed and dried MSC-seeded scaffold samples were then coated with gold, mounted and imaged. Similar procedure was used for imaging the fabricated ChiPgA composite scaffold samples except the fixing and dehydration steps.

5.3. Cell Culture Studies

5.3.1. Phase Contrast Microscopy and Atomic Force Microscopy

ChiPgA/*in situ* HAPclay composite films prepared in 24-well polystyrene plates and Petri dishes were sterilized under ultraviolet (UV) light for 1.5 hours. The sterilized films were incubated at 37°C, 5 % CO_2 in cell culture medium overnight. Subsequently, 4.4 x 10^4 human MSCs were seeded in each well on the composite films and these MSC seeded films were incubated at 37°C, 5 % CO_2 under humidified conditions up to 31 days. During this cell culture period, phase contrast images were taken using Axiovert 40, Zeiss phase contrast/inverted microscope to study the behavior (cell attachment, cell clustering) of MSCs on the ChiPgA composite films. The films seeded with MSCs in 24-well polystyrene plates were also used for MTT assay (described later). Human MSCs (5.78 x 10^4) were also seeded on ChiPgA composite films in Petri dishes and the Petri dishes were then incubated at 37°C, 5 % CO_2 for 26 days. Media was changed after every 3 days. Phase contrast imaging was performed to study behavior (cell attachment, clusters or any patterns formed by cells) of MSCs on the films in Petri dishes (60 mm outer diameter x 15 mm height, actual growth area 19.5 cm^2) and these MSC seeded film samples were subsequently used for Alizarin Red S staining (described later). Human MSCs

up to passage 5 were used for all cell culture experiments. ChiPgA composite films containing *in situ* HAPclay prepared for cell culture experiments were also imaged using an atomic force microscope (AFM). Phase imaging under laboratory conditions was performed using MultimodeTM atomic force microscope having a Nanoscope III a controller and J-type piezo scanner from Veeco Metrology Group, Santa Barbara, CA. for this purpose. Tapping Mode™ mode of AFM and tips made from antimony (n) doped Si were used for imaging the samples.

5.3.2. MTT Assay

MTT assay was performed for studying the viability of MSCs seeded on ChiPgA composite films and scaffolds. MTT (3-(4, 5 dimethylthiazol-2)-2, 5-diphenyltetrazolium bromide) reagent used for performing MTT assay is reduced by mitochondrial dehydrogenase enzyme in live cells to formazan. This reduction causes formation of MTT purple colored formazan that is further solubilized and the intensity of solubilized formazan indicates the number of live cells. Human MSCs were seeded on ChiPgA/*in situ* HAPclay films in 24-well polystyrene plates as described earlier. MTT assay was performed on these cell seeded films after a period of 14, 21 and 31 days. Briefly, 75 µL MTT solution (5mg/ml PBS) and 500 µL serum-free DMEM were added to each well after washing the MSC seeded films with phosphate buffer saline (PBS). Remaining solution from the wells was aspirated after incubation for 12 hours and 500 µL DMSO was added to solubilize the formazan crystals. Absorbance values of the supernatant (400 µL) at 570 nm were then read using a microplate spectrophotometer (Bio-Rad, Benchmark Plus). Readings were thus obtained for quadruplicate sample sets.

Separate MTT assay experiments were carried out on ChiPgA/*in situ* HAPclay scaffolds prepared by method A and method B. The scaffold samples sterilized under UV light were incubated at 37°C, 5 % CO_2 in cell culture medium overnight prior to cell seeding. In case of

ChiPgA composite scaffolds prepared by method A, 4.8 x 10^4 human MSCs were seeded in each of the scaffold containing wells and the scaffold samples were then incubated at 37°C, 5 % CO_2 under humidified conditions up to 25 days. Scaffolds samples were then washed with PBS and 90 µL MTT solution (5mg/ml PBS) along with 600 µL serum-free DMEM was added to each well. After incubation for 12 hours, scaffold samples were carefully transferred to unused wells of the 24-well plates and 600 µL DMSO was added to solubilize the formazan crystals. Absorbance values of the supernatant (500 µL) were then read using a microplate spectrophotometer (Bio-Rad, Benchmark Plus) for quadruplicate sample sets. In a separate experiment, 3.4 x 10^4 human MSCs were seeded in each of the wells containing composite scaffolds prepared by method B followed by incubation of the scaffolds at 37°C, 5 % CO_2 up to 28 days. MTT assay was performed using the same method as the one used for scaffolds prepared by Method A.

5.3.3. Alizarin Red S Staining

ChiPgA composite film samples (prepared by Method A) seeded with human MSCs were washed with PBS after incubation for 26 days and fixed by immersing them overnight in 2.5 % glutaraldehyde. Samples fixed with 2.5 % glutaraldehyde were then washed with PBS and then stained with Alizarin Red S dye (2 grams/100 ml deionized water, pH=4.10-4.15). Further, the samples were washed with cell culture grade water to remove excess dye and images were captured using a phase contrast/inverted microscope (Axiovert 40, Zeiss).

5.3.4. Alkaline Phosphatase (ALP) Assay

Separate ALP assay experiments to study differentiation of MSCs were performed on MSC seeded ChiPgA composite scaffolds prepared by Method A and Method B. In case of experiments involving scaffolds prepared by Method A, 7.7 x 10^4 MSCs were seeded in each of

the scaffold containing wells. In a separate experiment, 4.67 x 10^4 MSCs were seeded in each of the wells containing composite scaffolds prepared by Method B. MSC seeded scaffold samples were washed with PBS after incubation for 15 and 22 days. Subsequently 850 µL Triton X-100 (1 v/v % solution) was added to each of the scaffold containing wells. This was followed by two cycles of freezing-thawing (-70°C-37°C) of the scaffold samples immersed in Triton X-100 (1 v/v % solution). Cell lysates (250 µL) were transferred to new 24-well plate and 250 µL p-Nitrophenyl Phosphate (pNPP) was added to the cell lysates. The plates were incubated for 45 minutes at room temperature and 3N NaOH (70 µL) was added to the wells. Absorbance readings at 405 nm were then read using a microplate spectrophotometer (Bio-Rad, Benchmark Plus).

5.3.5. Two-stage Cell Seeding Experiment

ChiPgA/*in situ* HAPclay films were prepared by method A as mentioned previously in petri dishes and seeded with 9.3 x 10^4 MSCs. After incubation for 22 days, fresh MSCs (9 x 10^4) from a different passage were again seeded on the films. The MSC seeded films were further incubated up to 39^{th} day and were then stained with Alizarin Red S dye as described earlier. Images of the stained samples were taken with a phase contrast microscope.

5.4. Swelling Studies

ChiPgA/*in situ* HAPclay scaffolds were weighed, immersed in PBS (pH=7.2) and then incubated at 37°C for 7hrs, 13 hrs and 27 hrs. Scaffold samples were then removed from PBS, weighed and swelling ratio was calculated according to the following formula:

Swelling ratio = (W1-W0)/W0 x 100

W0 = dry weight of the scaffold

W1= wet weight of the scaffold

5.5. Scaffold Porosity

The porosity of scaffolds was calculated by determining the apparent density and solid density of the material constituting the scaffolds. Apparent density was determined by considering the mass and volume of the scaffolds. The solid density was determined by using a pycnometer. Following formula was used for calculating the percentage porosity of scaffolds:

% porosity = $(1-\rho_a/\rho_s) \times 100$

ρ_a = apparent density of scaffold

ρ_s = solid density of scaffold material

5.6. Statistical Analysis

Student's t-test performed using Minitab software was used for data analysis. Experiments were performed in quadruplicate except for swelling studies and porosity studies (where experiments were performed in triplicate). One-way ANOVA was used performing statistical analysis for comparing more than two different samples. Probability values less than 0.05 ($p < 0.05$) were considered statistically significant.

5.7. Results and Discussion

5.7.1. Scanning Electron Microscopy (SEM)

SEM micrographs of ChiPgA and ChiPgA/*in situ* HAPclay scaffolds fabricated by using the freeze-drying technique are shown in Figures 5.2. (a-f). All the scaffolds appear to be porous and have pore size near to 100 μm and above. The microstructure of ChiPgA/ *in situ* HAPclay scaffolds prepared by method A appears to be more similar to the ChiPgA scaffolds not containing any *in situ* HAPclay. In case of ChiPgA/ *in situ* HAPclay scaffolds prepared by method B, the microstructure appears to have compartmentalized features not seen in ChiPgA and ChiPgA composite scaffolds prepared by method A.

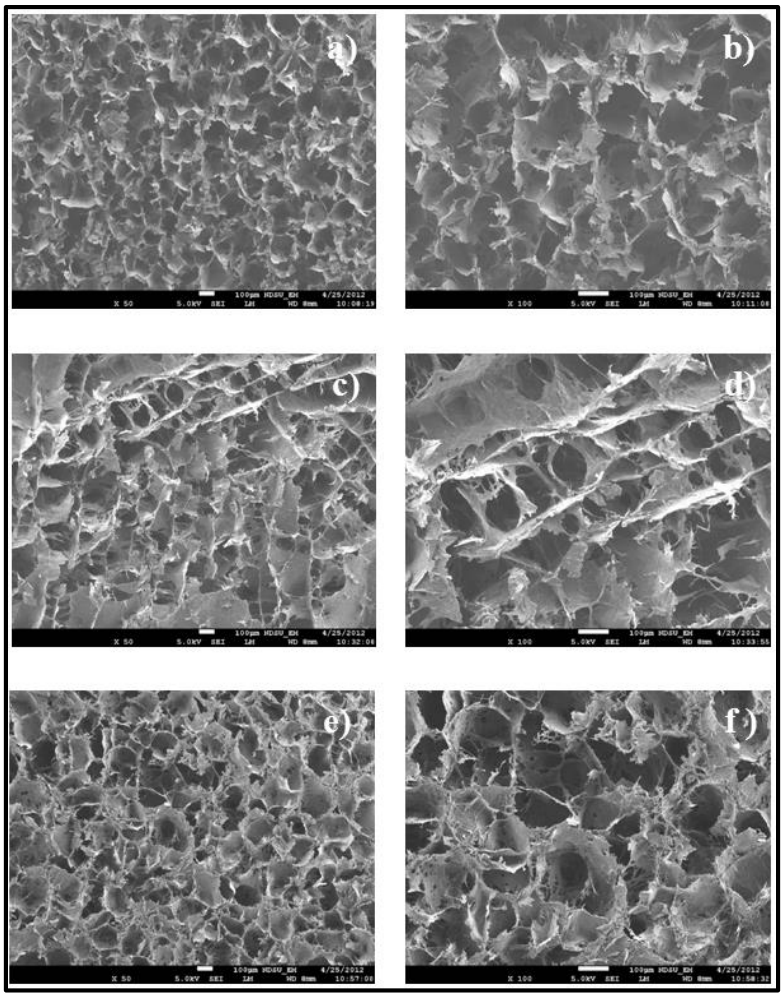

Figure 5.2. SEM micrographs of ChiPgA scaffolds with *in situ* HAPclay (20 wt %): a) & b) – scaffolds prepared by Method A, c) & d) scaffolds prepared by Method B and ChiPgA scaffolds without *in situ* HAPclay [e) & f)]. Images b), d), f) are magnifications of regions shown in images a), c), e)

The sequence of preparing the ChiPgA composite solutions in method A and method B seems to have an effect on the differences in the microstructure between the fabricated scaffolds. One of the possible reasons for these differences between the microstructure of scaffolds is that the *in situ* HAPclay has more opportunity to interact with chitosan (Chi) and polygalacturonic acid (PgA) in case of ChiPgA composite solution prepared by following the sequence in method A. Polyelectrolyte formation between Chi and PgA is a consequence of interactions between – NH_3^+ and –COO^- groups of Chi and PgA. Addition of *in situ* HAPclay to Chi prior to mixing of

Chi with PgA (using sonication) increases the possibility of interactions between *in situ* HAPclay with Chi and PgA. This can be possible through the available phosphate and calcium ions of *in situ* HAPclay interacting with unmixed Chi and PgA respectively. In our previous studies, it was observed that factors such as polymer concentration and freezing temperature used for scaffold fabrication have an effect on their microstructure [54]. SEM studies in present work suggest that the microstructure of the ChiPgA composite scaffolds is influenced by the order of mixing of *in situ* HAPclay with the polymers used and can be one of the methods to modify the microstructure of the ChiPgA composite scaffolds maintaining the same processing (freezing and freeze drying) conditions.

Figures 5.3. (a-f) and 5.4. (a-d) show SEM micrographs of ChiPgA/*in situ* HAPclay composite scaffolds seeded with human MSCs. Viability of cells and their attachment to engineered scaffolds is an indicator of their suitability for tissue engineering applications. The SEM micrographs indicate that human MSCs are able to survive and attach to the ChiPgA/*in situ* HAPclay composite scaffolds. In case of ChiPgA/*in situ* HAPclay composite scaffolds prepared by method A, SEM micrographs taken after 7 days of culture indicate presence of human MSCs having both flat and spherical morphology. The SEM micrographs also seem to indicate that most of the MSCs have flat morphology after 19 days of culture. SEM micrographs taken after 27 days of culture indicate formation of mineralized extracellular matrix by MSCs in the ChiPgA/*in situ* HAPclay scaffolds. For ChiPgA/*in situ* HAPclay composite scaffolds prepared by method B, SEM micrographs [Figure 5.4. (a-d)] show human MSCs with a flat morphology attached to the scaffolds. These micrographs taken after 18 days of culture indicate good attachment and spreading of the MSCs on the scaffolds (prepared by method B). Also, signs of formation of mineralized ECM by MSCs are visible on these scaffolds [Figure 5.4. (d)].

ChiPgA/*in situ* HAPclay scaffolds prepared by both methods (method A and method B) appear to favor attachment and viability of human MSCs. In case of ChiPgA/*in situ* HAPclay films prepared by both methods, differences in MSC behavior (attachment) were observed. These observations are described under section 5.7.2.

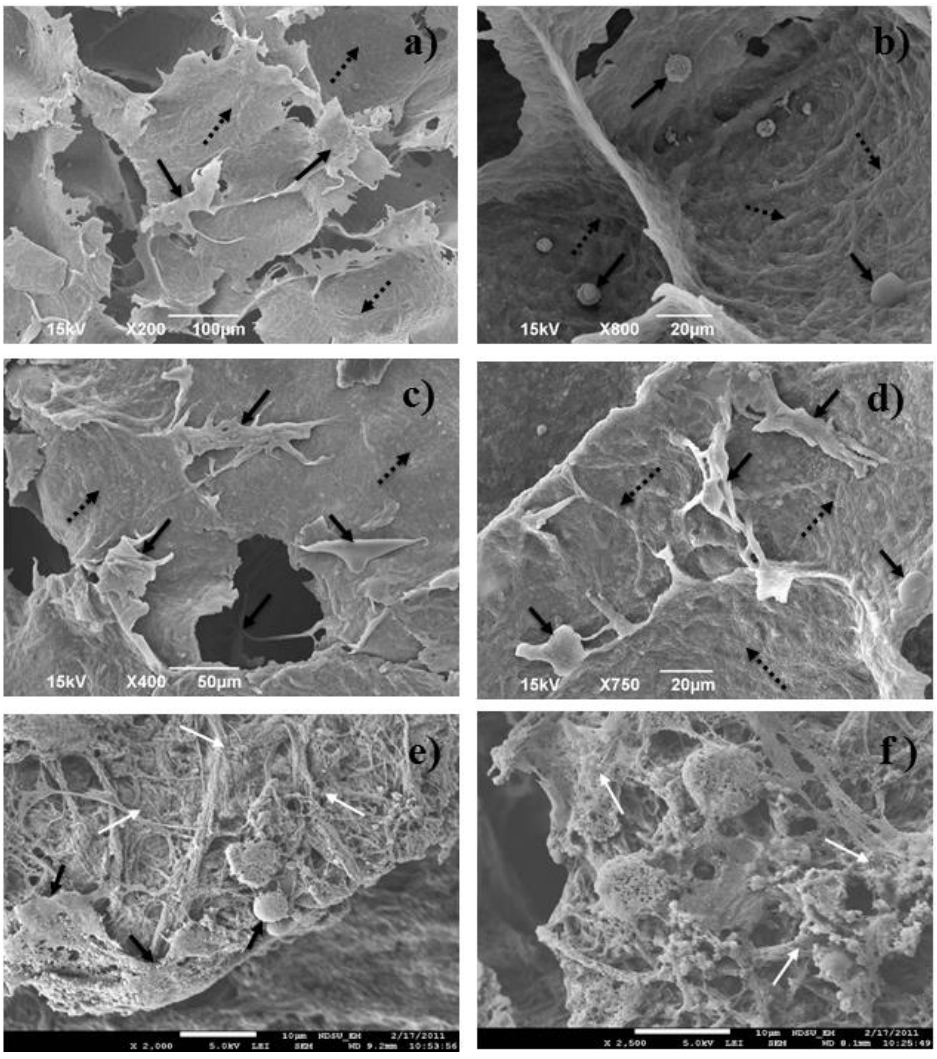

Figure 5.3. (a-f) SEM micrographs of human MSCs on ChiPgA/*in situ* HAPclay scaffolds (prepared by Method A) after a) & b) – 7 days, c) & d) – 19 days, e) & f) 27 days of culture. Solid black arrows indicate cells and dotted black arrows indicate regions of scaffold pore walls/scaffold material. Solid white arrows represent extracellular matrix (ECM)

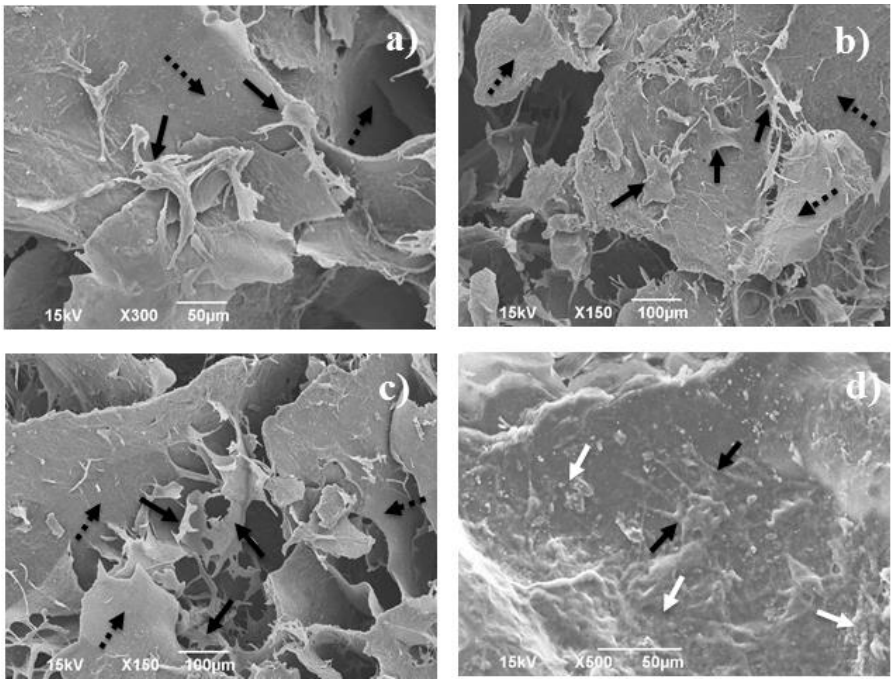

Figure 5.4. (a-d) SEM micrographs of human MSCs on ChiPgA/*in situ* HAPclay scaffolds (prepared by Method B) after 18 days of culture. Solid black arrows indicate cells and dotted black arrows indicate regions of scaffold pore walls/scaffold material. Solid white arrows represent extracellular matrix (ECM)

5.7.2. Phase Contrast Microscopy

Phase contrast images taken to study the behavior of human MSCs on ChiPgA/*in situ* HAPclay composite films are shown in Figures 5.5.(a-f), 5.6.(a-f) and 5.7.(a-h). Numerous studies in tissue engineering have suggested the cellular behavior is affected by scaffold microstructure, chemical composition of the scaffold, mechanical properties and biodegradability of the scaffold. Scaffolds are designed to present the cells with necessary but complex microenvironment similar to the one existing in vivo. The interdependency of the factors related to scaffolds affecting cellular behavior can make it difficult to develop our understanding of individual roles of these factors on cell behavior. Studying cell behavior on 2D substrates (films) can be helpful to understand the effect of materials used for preparing scaffolds on cell behavior.

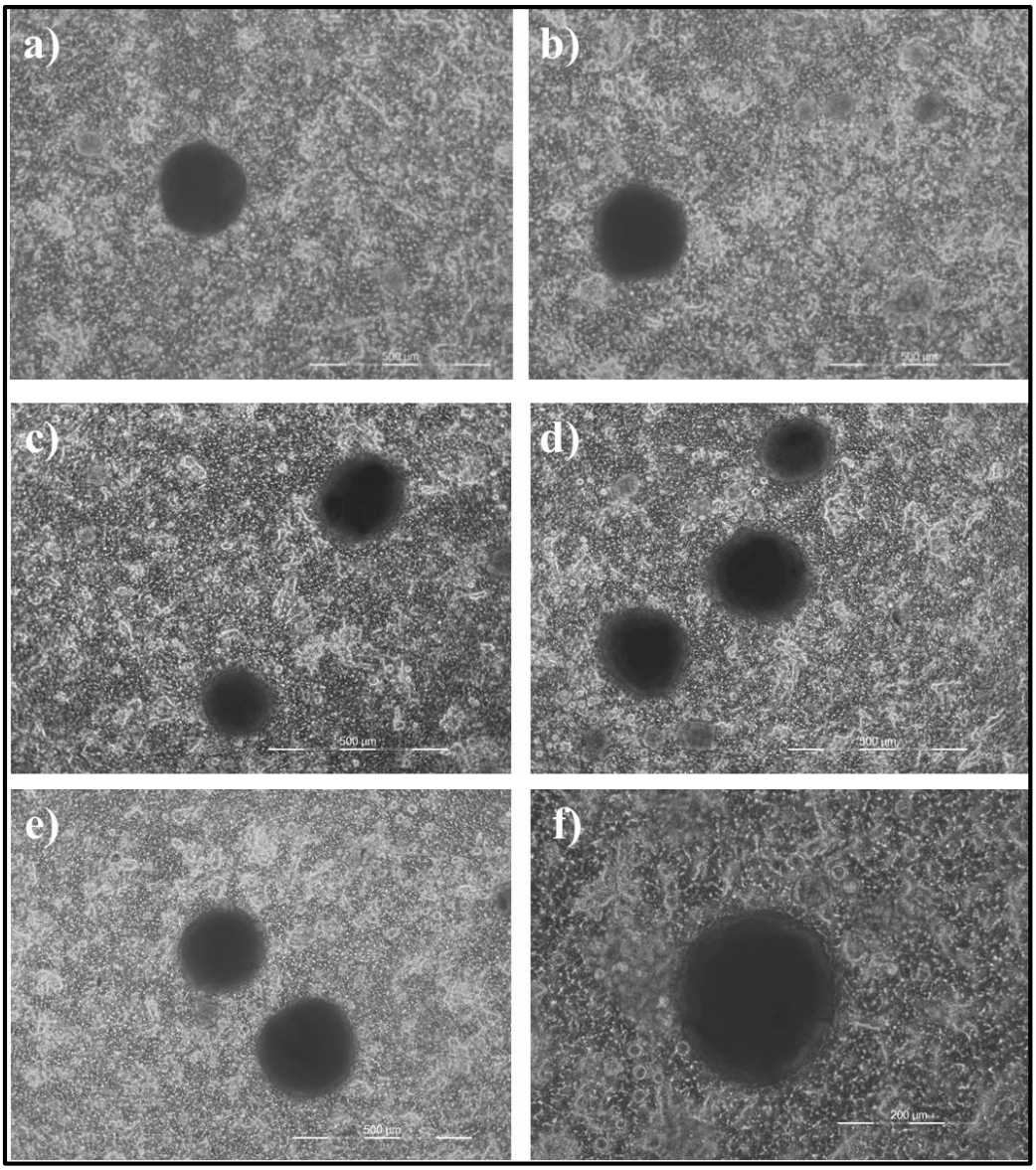

Figure 5.5. (a-f) Phase contrast images of human MSCs on ChiPgA/*in situ* HAPclay films prepared by Method A over a culture time of 21 days: a), b) – 4 days, c), d) – 8 days and e), f) – 21 days indicating formation of MSC clusters of similar shape and similar size range (~100-250 µm)

Figure 5.5. (a-f) shows MSCs on ChiPgA/*in situ* HAPclay films prepared by method A in wells of 24-well plates. Formation of cell clusters (appearing to be nodules) by MSCs adhered to these films was seen from day 4 of cell culture and such clusters were seen consistently over a cell culture time of 21 days. Figure 5.6. (a-f) shows phase contrast images of MSCs on

ChiPgA/*in situ* HAPclay films prepared by method B. Also, in this case formation of cell clusters by MSCs was seen from day 4 and consistently over a culture time of 21 days. Cluster formation by MSCs from day 4 was thus observed in case of ChiPgA composite films prepared by both methods.

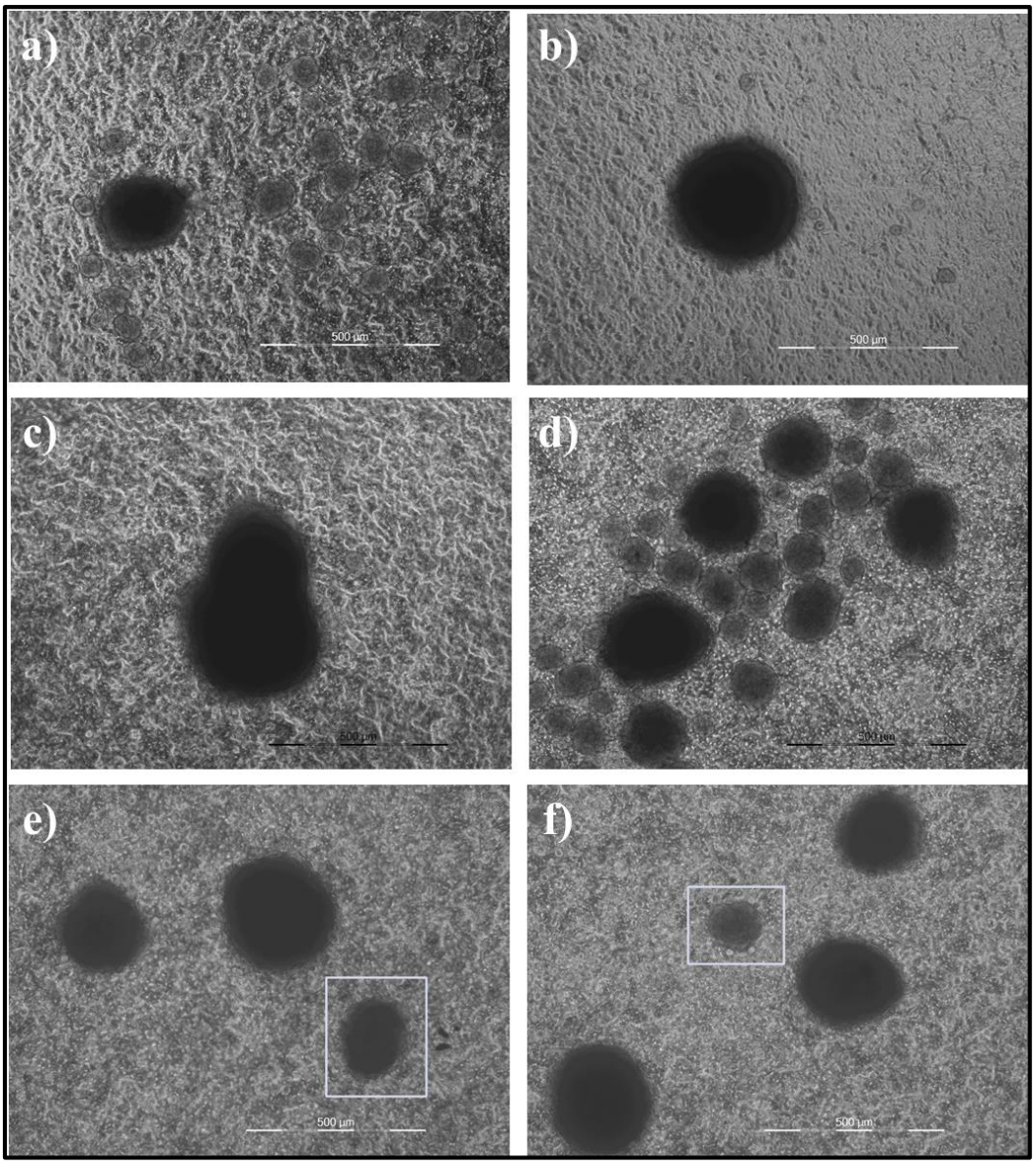

Figure 5.6. (a-f) Phase contrast images of human MSCs on ChiPgA/*in situ* HAPclay films prepared by Method B over a culture time of 21 days: a), b) – 4 days, c), d) – 8 days and e), f) – 21 days. Enclosed white squares indicate clusters/nodules that appeared to be attached to ChiPgA/*in situ* HAPclay films

Interestingly, in case of ChiPgA/*in situ* HAPclay films prepared by method B the cell clusters (appearing to be nodules) formed were floating/detached clusters unlike those seen in case of MSCs seeded on ChiPgA/*in situ* HAPclay films prepared by method A where they were adhered on the films. These floating/detached clusters were in the size range of 100μm to 500μm. Formation of detached nodules during osteogenic differentiation has been reported in case of rat bone marrow stem cells exposed to differentiation medium containing dexamethasone [55]. Chitosan particles did not affect attachment of human marrow stem cells in this study. Detached/floating nodules were alsoseen in our previous studies where human osteoblasts were seeded on ChiPgA/hydroxyapatite composite films [53]. During late stages of cell culture some of the nodules (indicated by enclosing square brackets in Figure 5.6.(e,f) appeared to be attached to the ChiPgA/*in situ* HAPclay films (prepared by Method B). The reasons for the formation of these floating MSC clusters (appearing to be nodules) have not been yet completely understood. One of the possible reasons can be attributed to the difference in the method of preparing ChiPgA/*in situ* HAPclay films. In case of films prepared by method B, the number of sites on *in situ* HAPclay available to the cells for interaction may be less due to mixing of *in situ* HAPclay with chitosan prior to mixing of chitosan with polygalacturonic acid achieved during sonication. Also, some of the nodules seen after 14 days of culture appeared to be attached, which may be attributed to increased exposure of the *in situ* HAPclay particles at some regions of the surface due to effect of cell culture media on the ChiPgA/*in situ* HAPclay films. Increased exposure of hydroxyapatite (HAP) particles at the surface has been reported through our previous studies in case of ChiPgA/HAP films with increase of soaking time in cell culture medium [56]. Increased exposure of *in situ* HAPclay particles at some regions of the film surface with increase in cell culture time may provide opportunities to the MSC clusters for attachment to the ChiPgA/*in situ*

HAPclay films (prepared by method B). At present this possible reasoning for the observation of floating MSC clusters is restricted to 2D substrates (films) made from ChiPgA/*in situ* HAPclay.

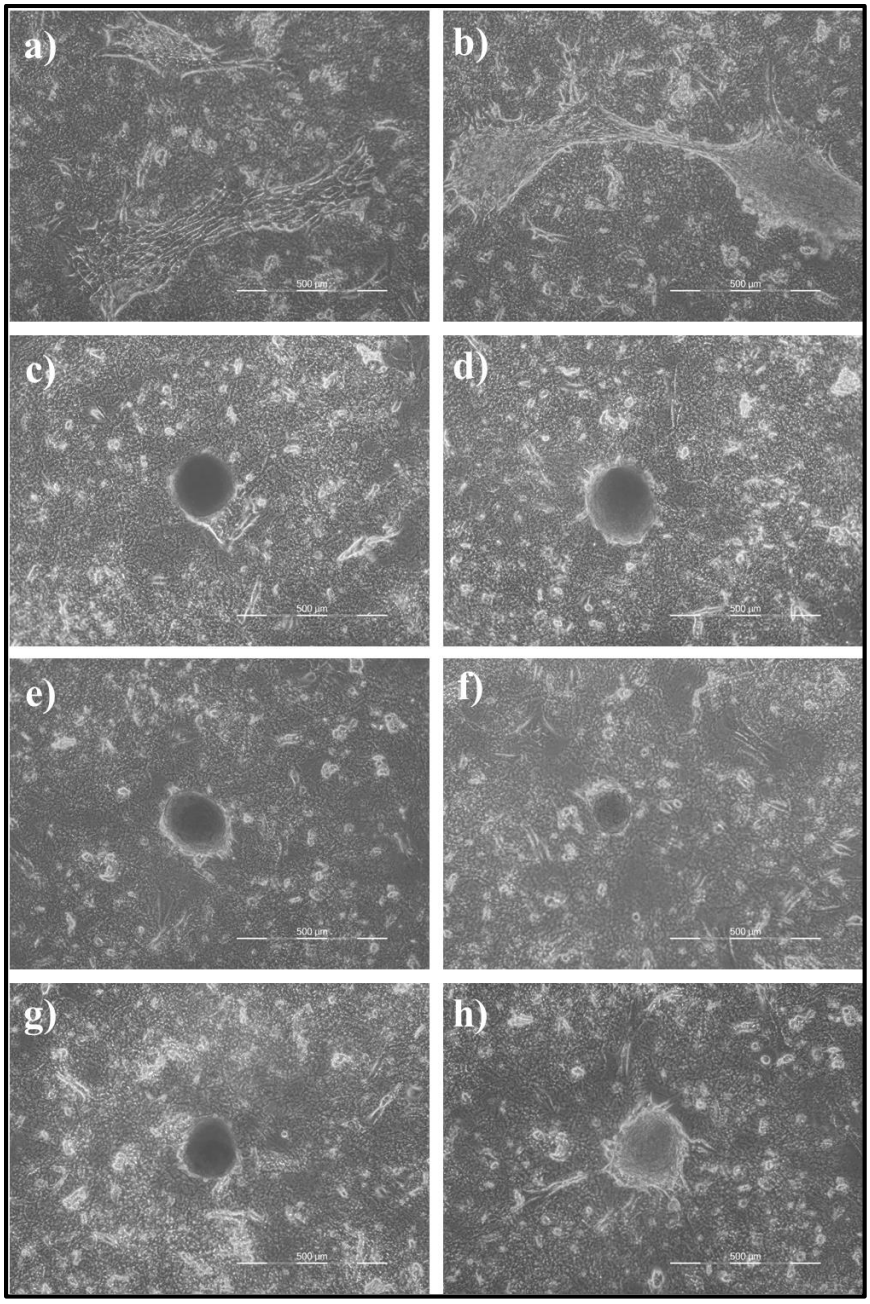

Figure 5.7. (a-h) Phase contrast images of human MSCs on ChiPgA/*in situ* HAPclay films prepared by Method A over a culture time of 26 days in tissue culture Petri dishes: a), b) - 3days, c), d) - 10 days, e),f) – 22 days, g), h) – 26 days

5.7.3. Alizarin Red S Staining

Human MSCs were also seeded on ChiPgA/*in situ* HAPclay films (prepared by method A) in a petri dish. Films prepared by method A were used for Alizarin Red S staining experiment due to formation of adhered cell clusters (appearing to be nodules) by MSCs on these films as seen in the phase contrast images discussed earlier. Before performing the staining experiment, the behavior of MSCs seeded on the films was studied by phase contrast microscopy over a cell culture period of 26 days. Figure 5.7. (a-h) shows that MSCs were able to attach and form clusters (appearing to be clusters) on the films. It can be seen that the MSCs show flat morphology indicating good attachment and appear to organize themselves. MSC clusters (appearing to be nodules) seen in Figure 5.7.(c-h) were observed from 10^{th} day of cell culture. Such clusters were observed till 26^{th} day of cell culture. Similar events of cell clustering were also observed in case of human osteoblasts cultured on ChiPgA/*in situ* HAPclay films from 8th day of cell culture in our previous studies [50]. Figure 5.8. (a-d) shows Alizarin Red S stained nodules formed by MSCs on the ChiPgA/*in situ* HAPclay films. Alizarin Red S is known to form complex with calcium and red color development indicates presence of calcium. Red color seen in stained nodules [Figure 5.8. (a-d)] thus indicates presence of calcium in the nodules formed by MSCs and thereby formation of mineralized nodules. Alizarin Red S positive staining of nodules formed by MSCs also suggests differentiation of the MSCs towards osteogenic lineage. Also, formation of mineralized nodules in the absence of osteogenic supplements indicated the osteoconductive and osteoinductive capabilities of ChiPgA/*in situ* HAPclay composites. Formation of nodules during in vitro culture has been reported in case of osteoblasts [57, 58]. These nodules formed by osteoblasts are considered to have multiple cell layers and mineralized extracellular matrix. Mineralization of the extracellular matrix is accompanied by changes in

morphology (change to round, small morphology) of osteoblasts to facilitate cellular communication and nutrition to the mineralized extracellular matrix. The changes in morphology of osteoblasts are also suggestive of changes in gene expression taking place during the development and mineralization of the extracellular matrix. Rounded cells along the periphery of the nodules are visible in some of the phase contrast images. Formation of mineralized extracellular matrix is also considered as an indicator of last stage of differentiation of osteoblasts [58, 59].

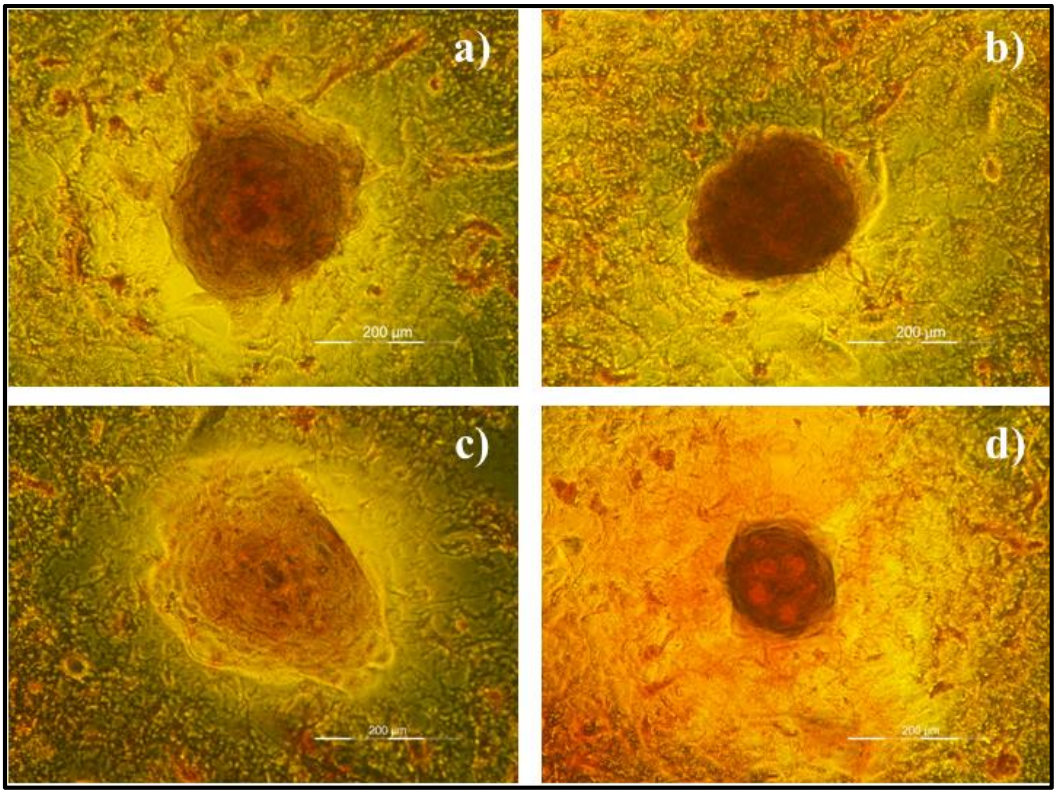

Figure 5.8. (a-d) Alizarin Red S stained nodules formed by MSCs after 26 days on ChiPgA/*in situ* HAPclay films prepared by Method A

In case of ChiPgA/*in situ* HAPclay films (prepared by Method A), the presence of Alizarin Red S stained nodules also suggests possibilities of similar events involving MSCs differentiated towards an osteogenic lineage. Positive Alizarin Red S staining of the nodules formed by MSCs during the two-stage cell seeding experiment after 39 days of culture can be

seen in Figure 5.9. (a-d). The calcified nodules (indicated by bright red color) having irregular shape in this case appear to consist of relatively dense extracellular matrix (ECM) as compared to those seen in Figure 5.8. (a-d). Besides this the nodules formed appear to have a relatively larger size (~500 microns) and more organized structure. Areas of the substrate covered by less dense ECM as compared to the denser matrix of the nodules (interpreted from intense red color) can also be seen surrounding these nodules.

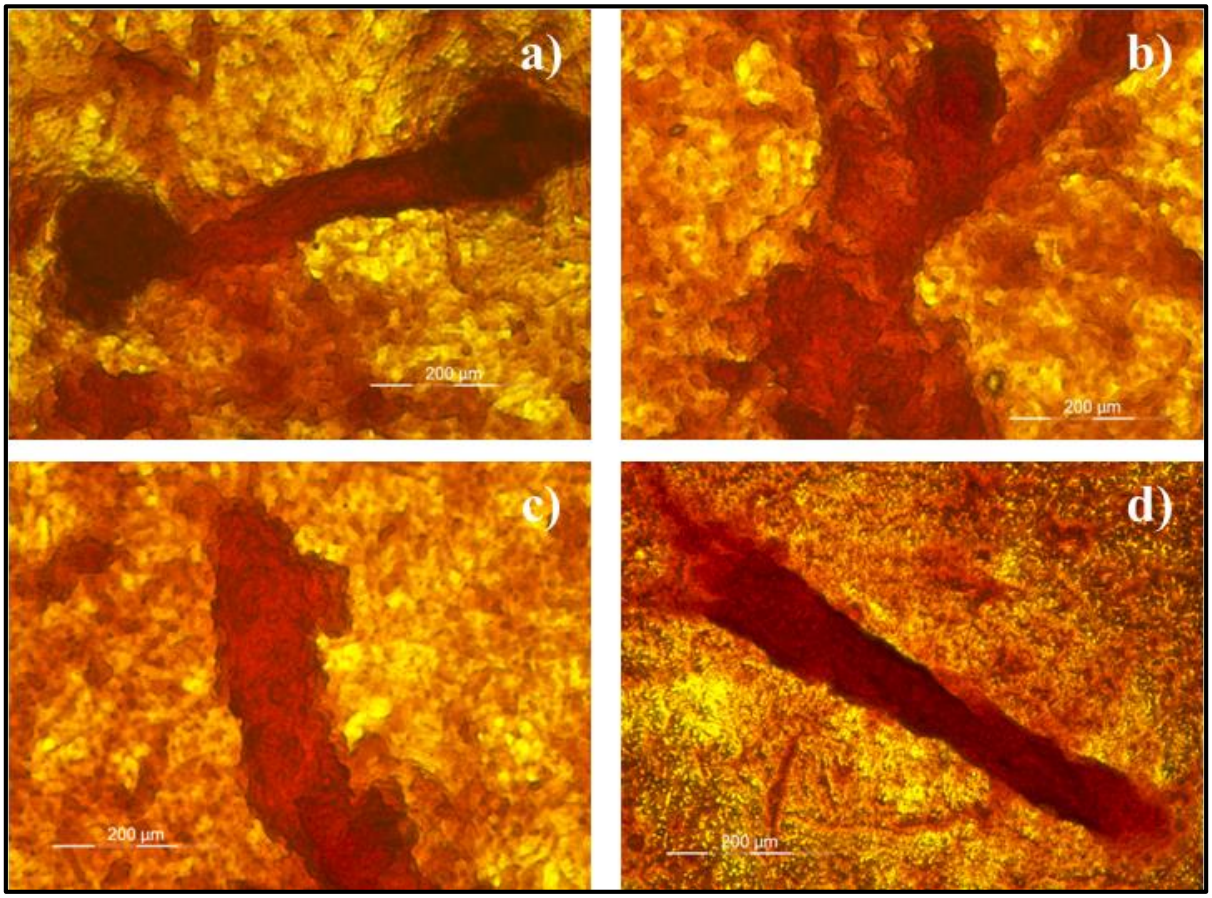

Figure 5.9. (a-d) Alizarin Red S stained nodules (indicated by relatively intense red color) of irregular shape (~ 500 µm) formed by MSCs after 39 days on ChiPgA/*in situ* HAPclay films prepared by Method A during two-stage cell seeding experiment. Mineralized extracellular matrix indicated by relatively less intense red color compared to the nodules appears to surround the irregularly shaped nodules and spread over ChiPgA/*in situ* HAPclay films

5.7.4. MTT Assay to Study MSC Viability

MTT assay results for MSCs seeded on ChiPgA/*in situ* HAPclay films (shown in Figure 5.10.) indicate that the MSCs remain viable on these films. Statistically significant differences in absorbance values (proportional to the number of live cells) are seen between ChiPgA/*in situ* HAPclay films prepared by method A and ChiPgA films without *in situ* HAPclay. In case of ChiPgA/*in situ* HAPclay films prepared by method B, significant differences in absorbance values were not observed compared to the ChiPgA films without *in situ* HAPclay. Floating clusters (appearing to be nodules) were formed by MSCs seeded on ChiPgA/*in situ* HAPclay films prepared by method B. Therefore, medium aspiration and washing prior to performing the MTT assay had to be performed carefully so that the floating nodules remained in the wells. In case of ChiPgA/*in situ* HAPclay films an increase in number of cells is observed with cell culture time with decrease after 21 days.

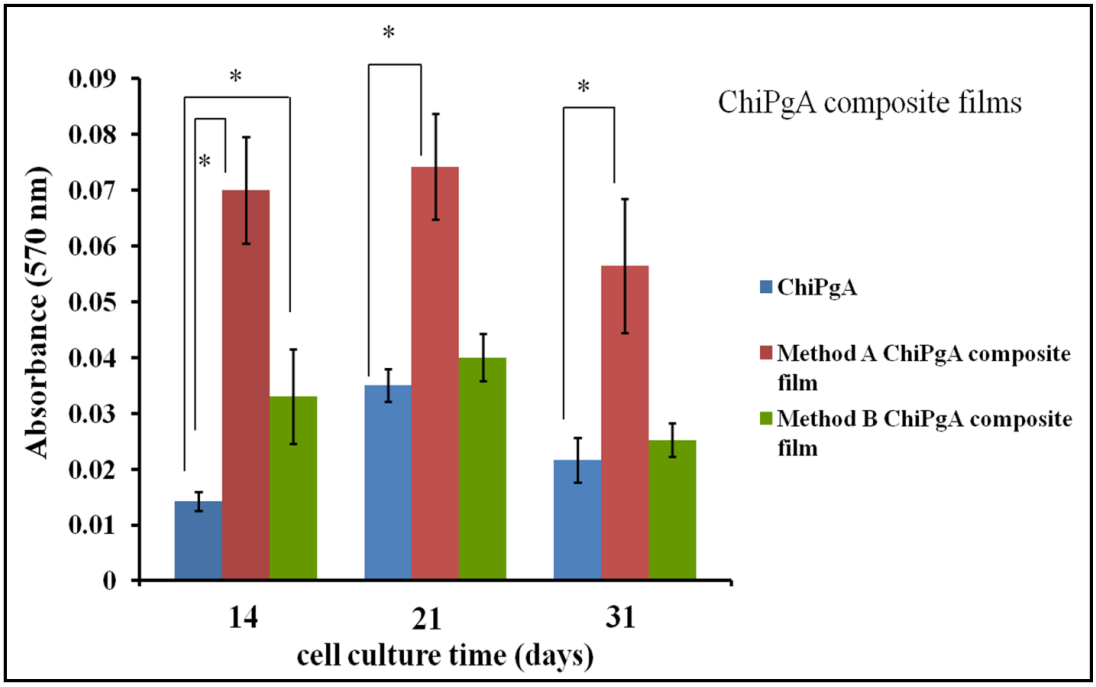

Figure 5.10. MTT assay results for MSCs seeded on ChiPgA/*in situ* HAPclay films

Similarly, in case of ChiPgA/*in situ* HAPclay scaffolds MTT assay results [shown in Figure 5.11. (a,b)] indicate viability of MSCs in these scaffolds. Significant differences in absorbance values is seen between ChiPgA/*in situ* HAPclay scaffolds prepared by method A and ChiPgA scaffolds without clay on day 20. MSCs showed an increase in cell number till day 20 in case of ChiPgA/*in situ* HAPclay scaffolds prepared by method A and till day 22 in case of ChiPgA/*in situ* HAPclay scaffolds prepared by method B. MSCs are specialized cells capable of differentiation into different lineages. Reciprocal relationship between proliferation and differentiation has been reported in case of osteoblasts [57, 60]. In case of mesenchymal stem cells, the relationship between proliferation and differentiation is not yet properly understood. This makes it difficult to make inferences from the observations made during MTT assay. Besides this possible events such as formation of extracellular matrix and its mineralization affecting cellular behavior present additional complexities. Also, films and scaffolds containing *in situ* HAPclay were studied as separate systems having potential to support MSC viability. Differences between 2D substrates (films) and scaffolds with respect to cell attachment, cell spreading, cell morphology, physical constraints to cell migration and deformation were some of the reasons considered for assaying the composite films and scaffolds in separate independent experiments. In case of scaffolds prepared by two different methods (A and B), the extent of difference in surface area available for cell attachment can be more due to differences in pore size, pore shape and pore interconnectivity. Therefore, scaffolds prepared by different methods were assayed in separate experiments. Since the MTT assay experiments performed were independent of each other where the ChiPgA composites containing *in situ* HAPclay were compared to ChiPgA without *in situ* HAPclay, different parameters such as cell numbers and culture time were used during these experiments. Figure 5.12. (a-f) represents phase contrast

images of MSC seeded scaffolds after formation of formazan crystals while performing MTT assay. Signs of cluster formation by MSCs in ChiPgA/*in situ* HAPclay scaffolds prepared by method A are seen in Figure 5.12. (c & d). Also, it appears from these images that the MSCs are distributed in the ChiPgA/*in situ* HAPclay scaffolds.

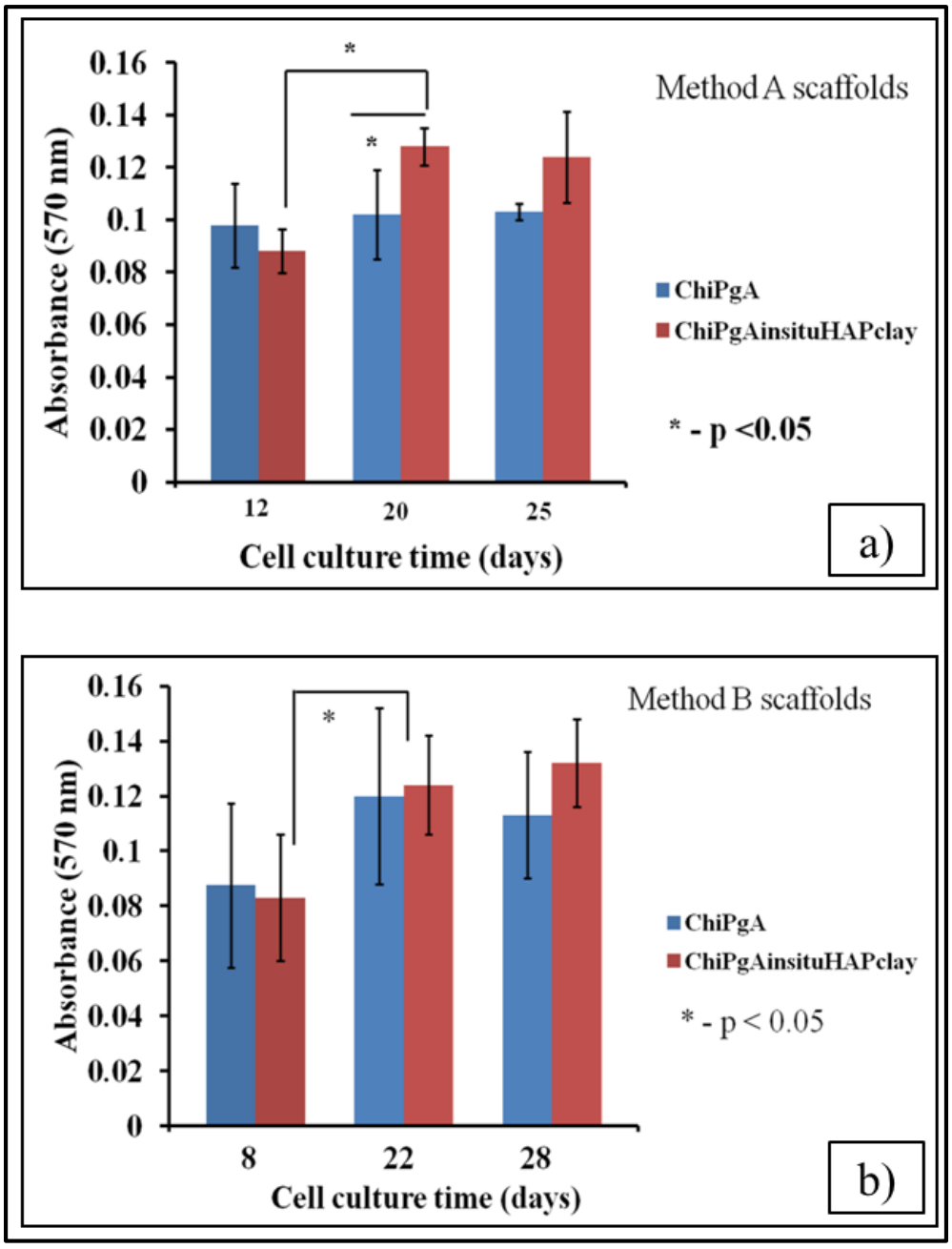

Figure 5.11. MTT assay results for MSCs seeded on ChiPgA/*in situ* HAPclay scaffolds: a) – Method A, b) – Method B

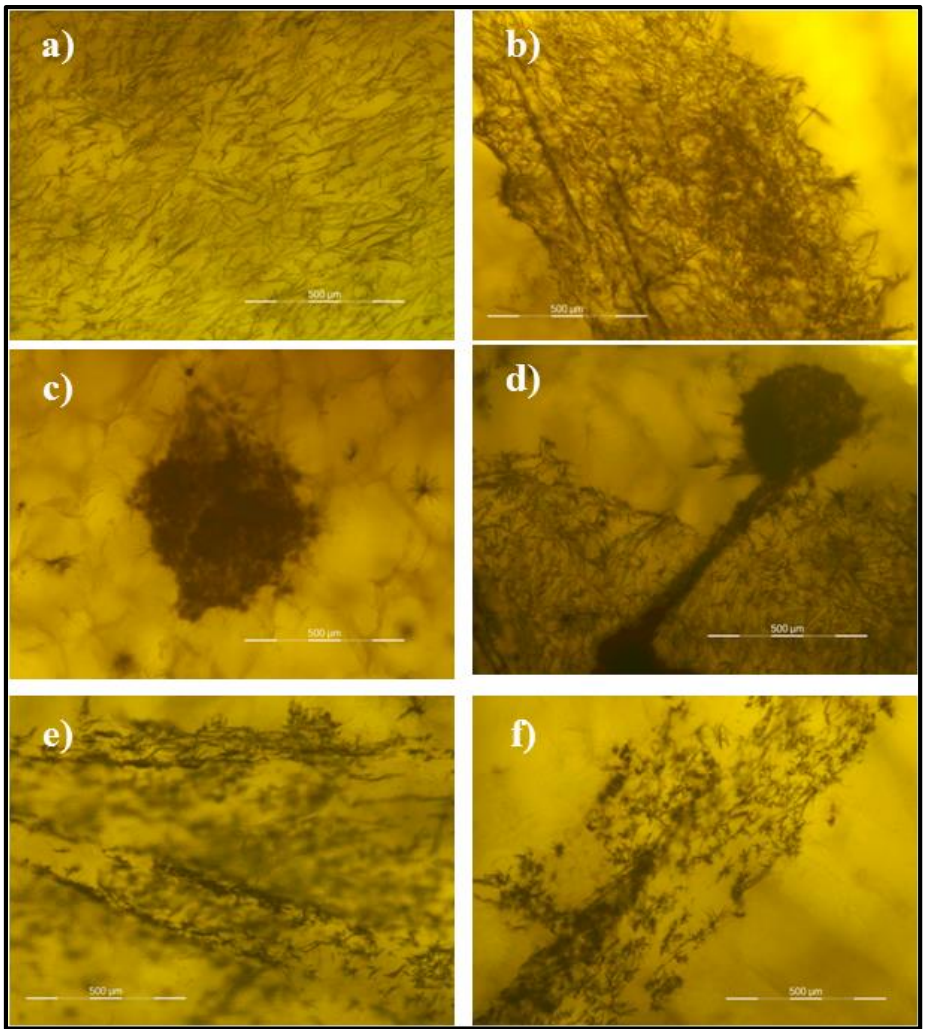

Figure 5.12. Formazan crystals formed in MSC seeded ChiPgA/*in situ* HAPclay scaffolds prepared by Method A during MTT assay after a), b)- 20 days and c), d)-25 days and by Method B during MTT assay after e), f) – 28 days. Formation of formazan crystals suggests viability of cells seeded on ChiPgA/*in situ* HAPclay scaffolds and indicates the distribution of cells, cluster formation by cells seeded on scaffolds

5.7.5. Alkaline Phosphatase (ALP) Assay

ALP experiments were performed to know whether ChiPgA/*in situ* HAPclay scaffolds were capable of supporting the differentiation of human MSCs. Alkaline phosphatase is considered as a marker for osteoblast phenotype and indicates the differentiation of MSCs in to osteogenic lineage. Results obtained from ALP assay (Figure 5.13.) show that MSCs seeded on ChiPgA/*in situ* HAPclay scaffolds were able to differentiate and their ALP activity (indicated by

absorbance values) increased as the cell culture time increased. ALP activity on day 22 was less in case of ChiPgA/*in situ* HAPclay scaffolds (prepared by Method A) compared to the ChiPgA scaffolds without *in situ* HAPclay.

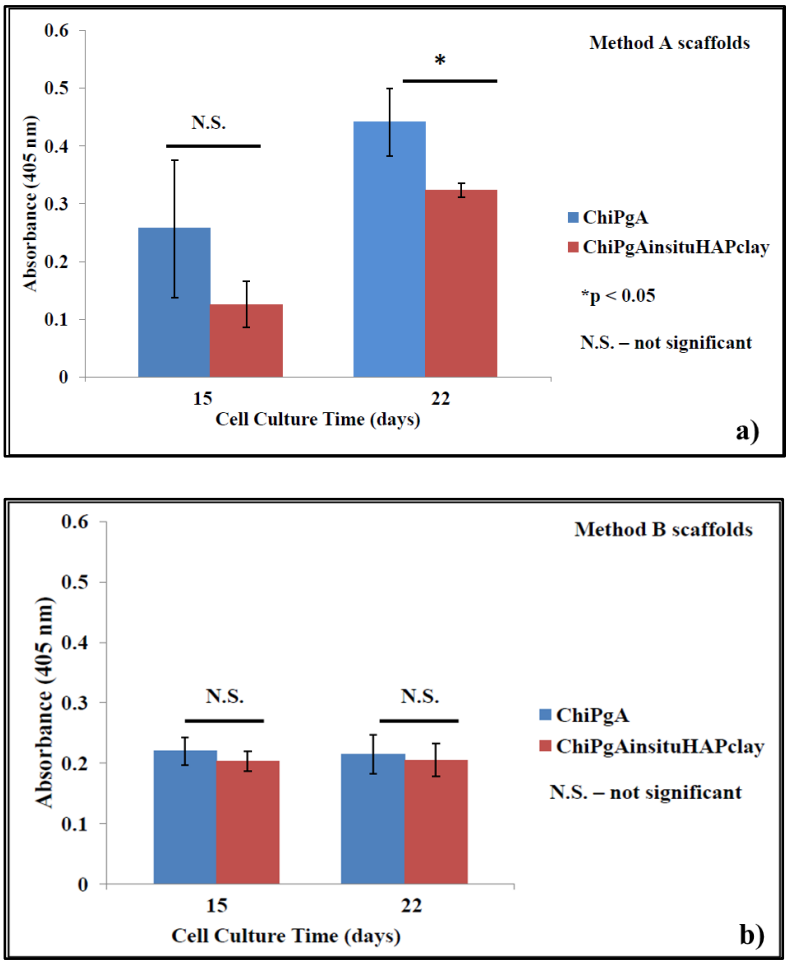

Figure 5.13. Alkaline Phosphatase (ALP) assay results for MSCs seeded on ChiPgA/*in situ* HAPclay scaffolds: a) - Method A, b) - Method B

Although ALP activity indicates differentiation of MSCs, it is difficult to relate increase in ALP activity to the extent of differentiation. Decrease in ALP activity has been associated with mineralization [61, 62] and differentiation stage of MSCs to osteoblasts [62-64]. ALP has been reported to have a higher expression in preosteoblasts that represent a transitional stage of MSC differentiation to osteoblasts. These factors make it difficult to relate ALP activity to the

extent of MSC differentiation. Decrease in ALP levels with the mineralization of the extracellular matrix has been reported for the osteoblast phenotype [57]. This can be one of the possible reasons for the lesser ALP activity seen in case of ChiPgA/*in situ* HAPclay scaffolds due to formation of mineralized ECM. SEM micrographs [Figure 5.3.(e,f)] of MSC seeded ChiPgA/*in situ* HAPclay scaffolds suggest formation of mineralized extracellular matrix with increase in cell culture time. No significant difference in ALP activity was observed between the ChiPgA/*in situ* HAPclay scaffolds prepared by Method B and ChiPgA scaffolds without *in situ* HAPclay.

5.7.6. Swelling Studies

Figure 5.14. shows swelling ratios of ChiPgA/*in situ* HAPclay scaffolds obtained after immersion in PBS over a time of 27 hours. It is seen that the ChiPgA scaffolds including those without *in situ* HAPclay are able to swell. Swelling of scaffolds is considered useful for tissue engineering applications since it allows the cells and nutrients to enter the interior of the scaffolds. It can be useful for in vivo applications where the body fluids (blood, plasma) need to be taken up by the scaffolds while implanting the scaffolds at the defective sites [65]. Swelling can be useful to properly fix the scaffolds at the defective site, maintain appropriate pressure and achieve adequate contact with the surrounding tissue (reference). However continuous swelling can lead to decrease in mechanical properties and exert excess pressure on the surrounding tissue [66]. Controlling swelling of scaffolds can be considered as one of the factors while designing scaffolds for tissue engineering. The swelling ratios of ChiPgA/*in situ* HAPclay scaffolds prepared by method A do not differ considerably as compared to those without *in situ* HAPclay. Differences in swelling ratios are significant in ChiPgA/*in situ* HAPclay scaffolds prepared by method B compared to those without *in situ* HAPclay. Swelling of scaffolds can depend on

factors such as its chemical composition, microstructure, wetting capability and pH value of the soaking medium. The differences observed in microstructure of the scaffolds through SEM micrographs can be considered as one of the possible factors responsible for the observed differences in swelling ratios of the scaffolds. Also, change in swelling ratios of the scaffolds appears to be more from 7 to 13 hours of immersion time as compared to immersion time from 13 hours to 27 hours. Besides the statistically significant differences between ChiPgA and ChiPgA scaffolds shown in figure 5.14. , statistically significant differences in swelling ratios with time were observed in case of ChiPgA scaffolds from 7 to 13 hours and in case of ChiPgA/*in situ* HAPclay composite scaffolds prepared by Method B from 13 to 27 hours. Immersion times extending up to several days can be used but there are possibilities that the swelling ratios may be affected by deposition of salts/minerals from the soaking medium and degradation of scaffolds in the soaking medium.

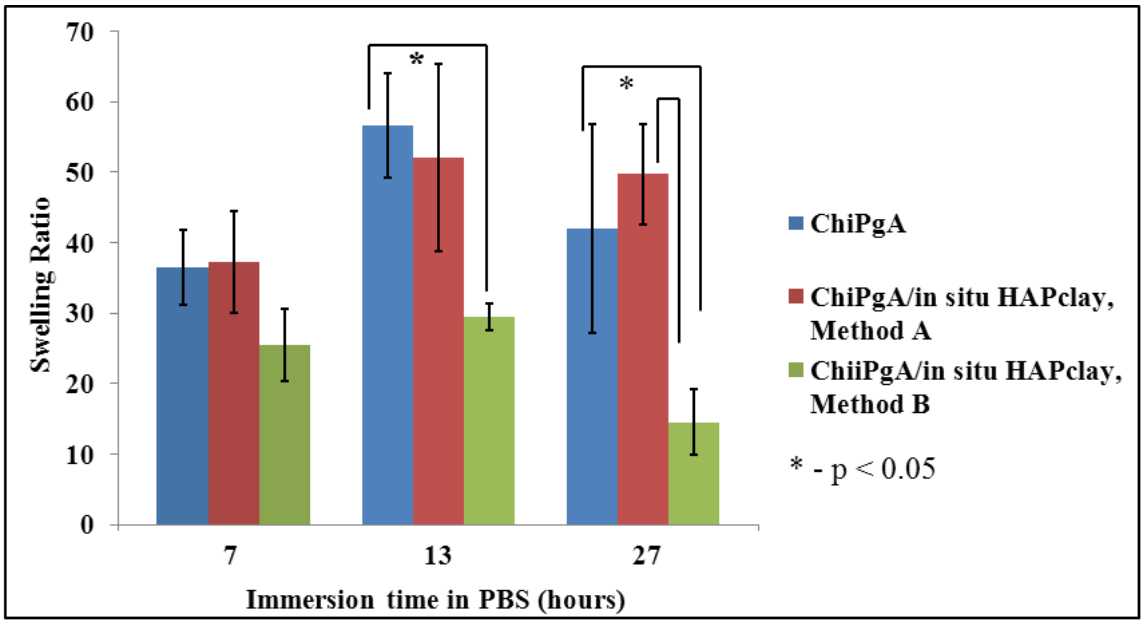

Figure 5.14. Swelling ratios of ChiPgA/*in situ* HAPclay scaffolds.

5.7.7. Porosity of Scaffolds

Figure 5.15. shows the percentage porosity of ChiPgA based scaffolds. It shows that the porosity of all the scaffolds is above 90 percent. Percentage porosity calculations showed that the porosity of all scaffolds was near to 97 percent. Porosity represents void space in scaffolds and is known to have effect on cell migration, vascularization, tissue formation etc. It is also known that porosity has an effect on the mechanical properties of the scaffolds and designing scaffolds with porosity suitable for tissue formation as well as for obtaining adequate mechanical properties is one of the significant challenges of bone tissue engineering.

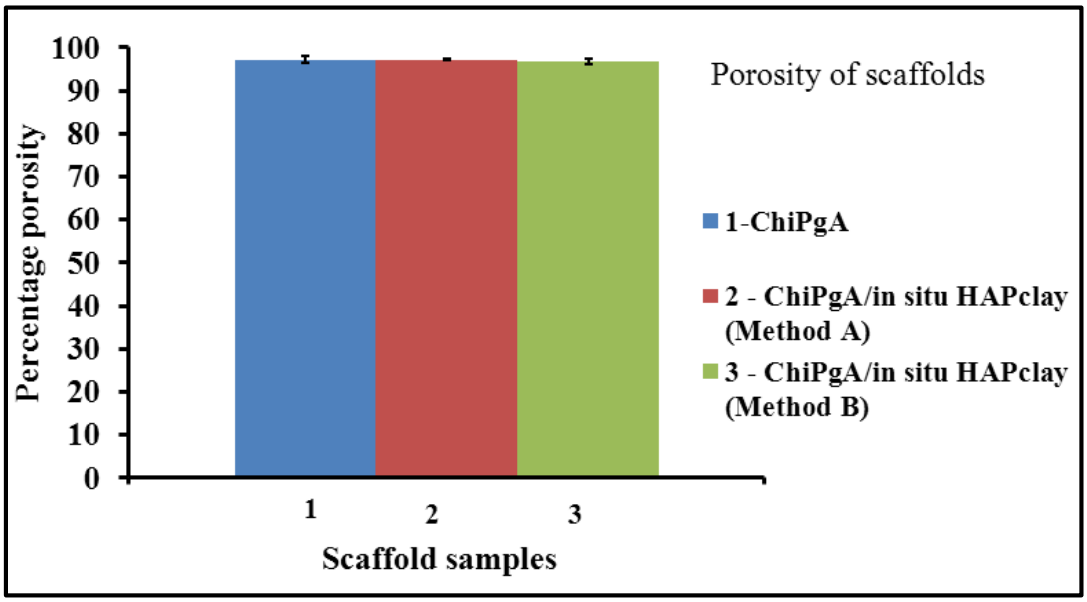

Figure 5.15. Porosity of ChiPgA/*in situ* HAPclay scaffolds

5.7.8. Atomic Force Microscopy

Figure 5.15 (a-d) shows AFM phase images of ChiPgA/*in situ* HAPclay films. Nanoscale features are clearly observed in these images. In case of films prepared by Method A, the size of these features appears to be less uniform than in case of films prepared by Method B. In case of films prepared by method A, the interspersed larger features appear to be made up of smaller features. These differences can possibly be attributed to the differences in processing resulting

from sequence of mixing the components while preparing these composites. Nanoscale morphology is one of the factors known to affect protein adsorption and cell adhesion.

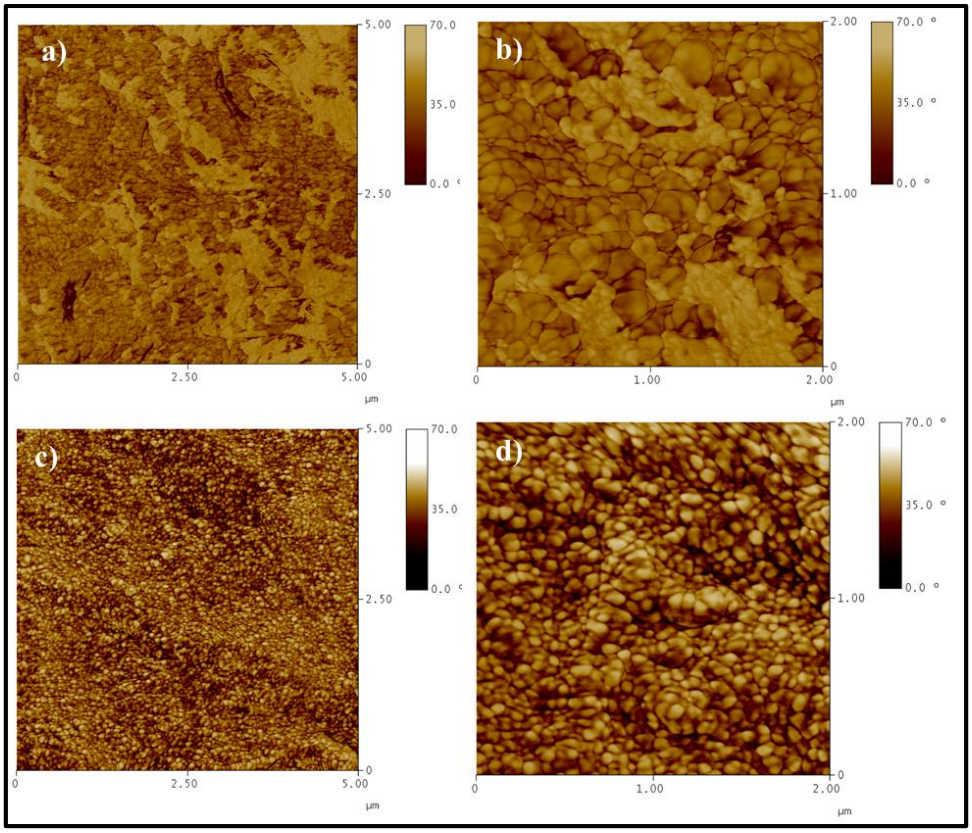

Figure 5.16. AFM phase images of ChiPgA/*in situ* HAPclay films prepared by Method A [a), b)] and Method B [c), d)]. Differences in phase images indicate possible differences in surface phase distribution, surface stiffness and sample topography. Features seen in images b), d) are in the submicron and nanoscale range. Relatively large (~ 500-790 nm) interspersed features can be seen in case of films prepared by Method A [images a), b)]

5.8. Conclusions

Biomimetically prepared HAP (*in situ* HAPclay) on intercalated nanoclays containing organomodified MMT clay with hydroxyapatite (HAP) was successfully used for the fabrication of biopolymer (ChiPgA) scaffolds and films. Formation of mineralized nodules by MSCs on ChiPgA/*in situ* HAPclay films in the absence of osteogenic supplements demonstrated the osteoconductive and osteoinductive potential of ChiPgA/*in situ* HAPclay composites. Thus the

biomimetic nanoclay-HAP material system represents a new viable system for design of scaffolds. Cell culture assays showed that the ChiPgA/*in situ* HAPclay scaffolds and films were able to support MSC viability and differentiation (in case of scaffolds). Formation of mineralized nodules on ChiPgA/*in situ* HAPclay films by MSCs was also an indicator of differentiation of MSCs on ChiPgA/*in situ* HAPclay composites. Two-stage cell seeding experiment was successfully performed as a strategy to enhance tissue formation by MSCs on ChiPgA/*in situ* HAPclay composite films. It was also observed that changes in the sequence of addition of *in situ* HAPclay with ChiPgA biopolymer system had considerable influence on the microstructure of the scaffolds. Swelling capabilities of the fabricated ChiPgA/*in situ* HAPclay composites and their porosity indicated their suitability for tissue engineering applications.

5.9. References

[1] Langer R, Vacanti JP. Tissue Engineering. Science. 1993;260:920-6.

[2] Elisseeff J, Ferran A, Hwang S, Varghese S, Zhang Z. The role of biomaterials in stem cell differentiation: Applications in the Musculoskeletal System. Stem Cells and Development. 2006;15:295-303.

[3] Polak JM, Bishop AE. Stem Cells and Tissue Engineering: Past, Present, and Future. Annals of the New York Academy of Sciences. 2006;1068:352-66.

[4] Leo AJ, Grande DA. Mesenchymal Stem Cells in Tissue Engineering. Cells Tissues Organs. 2006;183:112-22.

[5] Marolt D, Knezevic M, Vunjak-Novakovic G. Bone tissue engineering with human stem cells. Stem Cell Research & Therapy. 2010;1:10.

[6] Chen F, Tuan R. Mesenchymal stem cells in arthritic diseases. Arthritis Research & Therapy. 2008;10:223.

[7] Shi Y, Hu G, Su J, Li W, Chen Q, Shou P, et al. Mesenchymal stem cells: a new strategy for immunosuppression and tissue repair. Cell Res. 2010;20:510-8.

[8] Otto W, Wright N. Mesenchymal stem cells: from experiment to clinic. Fibrogenesis & Tissue Repair. 2011;4:20.

[9] Uccelli A, Pistoia V, Moretta L. Mesenchymal stem cells: a new strategy for immunosuppression? Trends in immunology. 2007;28:219-26.

[10] Bose S, Tarafder S. Calcium phosphate ceramic systems in growth factor and drug delivery for bone tissue engineering: A review. Acta Biomaterialia. 2012;8:1401-21.

[11] Zhou H, Lee J. Nanoscale hydroxyapatite particles for bone tissue engineering. Acta Biomaterialia. 2011;7:2769-81.

[12] Vallet-Regi M. Ceramics for medical applications. Journal of the Chemical Society, Dalton Transactions. 2001:97-108.

[13] Chan CK, Kumar TSS, Liao S, Murugan R, Ngiam M, Ramakrishman S. Biomimetic nanocomposites for bone graft applications. Nanomedicine. 2006;1:177-88.

[14] Patel N, Best SM, Bonfield W, Gibson IR, Hing KA, Damien E, et al. A comparative study on the in vivo behavior of hydroxyapatite and silicon substituted hydroxyapatite granules. Journal of Materials Science:Materials in Medicine. 2002;13:1199-206.

[15] Vallet-Regi M. Revisiting ceramics for medical applications. Dalton Transactions. 2006:5211-20.

[16] Botelho CM, Brooks RA, Best SM, Lopes MA, Santos JD, Rushton N, et al. Human osteoblast response to silicon-substituted hydroxyapatite. Journal of Biomedical Materials Research Part A. 2006;79A:723-30.

[17] Sinha Ray S, Okamoto M. Polymer/layered silicate nanocomposites: a review from preparation to processing. Progress in Polymer Science. 2003;28:1539-641.

[18] Goldberg M, Langer R, Jia XQ. Nanostructured materials for applications in drug delivery and tissue engineering. Journal of Biomaterials Science-Polymer Edition. 2007;18:241-68.

[19] Christenson EM, Anseth KS, van den Beucken L, Chan CK, Ercan B, Jansen JA, et al. Nanobiomaterial applications in orthopedics. Journal of Orthopaedic Research. 2007;25:11-22.

[20] Stevens MM, George JH. Exploring and Engineering the Cell Surface Interface. Science. 2005;310:1135-8.

[21] Okada A, Kawasumi M, Usuki A, Kojima Y, Kurauchi T, Kamigaito O. Synthesis and properties of nylon-6/clay hybrids. In Polymer based molecular composites MRS SymposiumProceedings (eds D W Schaefer & J E Mark). 1990;171:45-50.

[22] Giannelis EP. Polymer Layered Silicate Nanocomposites. Advanced Materials. 1996;8:29-35.

[23] Chen GX, Hao GJ, Guo TY, Song MD, Zhang BH. Structure and mechanical properties of poly(3-hydroxybutyrateco-3-hydroxyvalerate) (PHBV)/clay nanocomposites. Journal of Materials Science Letters. 2002;21:1587-9.

[24] Pramanik M, Srivastava SK, Samantaray BK, Bhowmick AK. Rubber-clay nanocomposite by solution blending. Journal of Applied Polymer Science. 2003;87:2216-20.

[25] Messersmith PB, Giannelis EP. Synthesis and barrier properties of poly(ϵ-caprolactone)-layered silicate nanocomposites. Journal of Polymer Science Part A: Polymer Chemistry. 1995;33:1047-57.

[26] Yano K, Usuki A, Okada A, Kurauchi T, Kamigaito O. Synthesis and properties of polyimide-clay hybrid. Journal of Polymer Science Part A: Polymer Chemistry. 1993;31:2493-8.

[27] Bharadwaj RK. Modeling the Barrier Properties of Polymer-Layered Silicate Nanocomposites. Macromolecules. 2001;34:9189-92.

[28] Gilman JW. Flammability and thermal stability studies of polymer layered-silicate (clay) nanocomposites. Applied Clay Science. 1999;15:31-49.

[29] Gilman JW, Jackson CL, Morgan AB, R. H. Flammability Properties of Polymer−Layered-Silicate Nanocomposites. Polypropylene and Polystyrene Nanocomposites. Chemistry of Materials. 2000;12:1866-73.

[30] Sikdar D, Pradhan SM, Katti DR, Katti KS, Mohanty B. Altered Phase Model for Polymer Clay Nanocomposites. Langmuir. 2008;24:5599-607.

[31] Sikdar D, Katti DR, Katti KS. The role of interfacial interactions on the crystallinity and nanomechanical properties of clay-polymer nanocomposites: A molecular dynamics study. Journal of Applied Polymer Science. 2008;107:3137-48.

[32] Sikdar D, Katti D, Katti K, Mohanty, Bedabibhas. Influence of backbone chain length and functional groups of organic modifiers on crystallinity and nanomechanical properties of intercalated clay-polycaprolactam nanocomposites. International Journal of Nanotechnology. 2009;6:468-92.

[33] Katti DR, Ghosh P, Schmidt S, Katti KS. Mechanical Properties of the Sodium Montmorillonite Interlayer Intercalated with Amino Acids. Biomacromolecules. 2005;6:3276-82.

[34] Viseras C, Aguzzi C, Cerezo P, Lopez-Galindo A. Uses of clay minerals in semisolid health care and therapeutic products. Applied Clay Science. 2007;36:37-50.

[35] Forni F, Iannuccelli V, Coppi G, Bernabei MT. Effect of Montmorillonite on Drug Release from Polymeric Matrices. Archiv der Pharmazie. 1989;322:789-93.

[36] Lee W-F, Fu Y-T. Effect of montmorillonite on the swelling behavior and drug-release behavior of nanocomposite hydrogels. Journal of Applied Polymer Science. 2003;89:3652-60.

[37] Lin F-H, Chen C-H, Cheng WTK, Kuo T-F. Modified montmorillonite as vector for gene delivery. Biomaterials. 2006;27:3333-8.

[38] Takahashi T, Yamada Y, Kataoka K, Nagasaki Y. Preparation of a novel PEG-clay hybrid as a DDS material: Dispersion stability and sustained release profiles. Journal of Controlled Release. 2005;107:408-16.

[39] Wang X, et al. Biopolymer/montmorillonite nanocomposite: preparation, drug-controlled release property and cytotoxicity. Nanotechnology. 2008;19:065707.

[40] Sun B, Ranganathan B, Feng S-S. Multifunctional poly(d,l-lactide-co-glycolide)/montmorillonite (PLGA/MMT) nanoparticles decorated by Trastuzumab for targeted chemotherapy of breast cancer. Biomaterials. 2008;29:475-86.

[41] Carretero MI. Clay minerals and their beneficial effects upon human health. A review. Applied Clay Science. 2002;21:155-63.

[42] Lin K-F, Hsu C-Y, Huang T-S, Chiu W-Y, Lee Y-H, Young T-H. A novel method to prepare chitosan/montmorillonite nanocomposites. Journal of Applied Polymer Science. 2005;98:2042-7.

[43] Marras SI, Kladi KP, Tsivintzelis I, Zuburtikudis I, Panayiotou C. Biodegradable polymer nanocomposites: The role of nanoclays on the thermomechanical characteristics and the electrospun fibrous structure. Acta Biomaterialia. 2008;4:756-65.

[44] Zheng JP, Wang CZ, Wang XX, Wang HY, Zhuang H, Yao KD. Preparation of biomimetic three-dimensional gelatin/montmorillonite-chitosan scaffold for tissue engineering. Reactive and Functional Polymers. 2007;67:780-8.

[45] Depan D, Kumar AP, Singh RP. Cell proliferation and controlled drug release studies of nanohybrids based on chitosan-g-lactic acid and montmorillonite. Acta Biomaterialia. 2009;5:93-100.

[46] Katti KS, Katti DR, Dash R. Synthesis and characterization of a novel chitosan/montmorillonite/hydroxyapatite nanocomposite for bone tissue engineering. Biomedical Materials. 2008;3:12.

[47] Mieszawska AJ, Llamas JG, Vaiana CA, Kadakia MP, Naik RR, Kaplan DL. Clay enriched silk biomaterials for bone formation. Acta Biomaterialia. 2011;7:3036-41.

[48] Katti KS, Ambre AH, Peterka N, Katti DR. Use of unnatural amino acids for design of novel organomodified clays as components of nanocomposite biomaterials. Philosophical Transactions of The Royal Society A 2010;368:1963-80.

[49] Ambre AH, Katti KS, Katti DR. Nanoclay Based Composite Scaffolds for Bone Tissue Engineering Applications. Journal of Nanotechnology in Engineering and Medicine. 2010;1:031013-9.

[50] Ambre A, Katti KS, Katti DR. In situ mineralized hydroxyapatite on amino acid modified nanoclays as novel bone biomaterials. Materials Science and Engineering: C. 2011;31:1017-29.

[51] Filipak M, Estervig DN, Tzen C-Y, Minoo P, Hoerl BJ, Maercklein PB, et al. Integrated Control of Proliferation and Differentiation of Mesenchymal Stem Cells. Environmental Health Perspectives. 1989;80:117-25.

[52] Plaisant M, Giorgetti-Peraldi S, Gabrielson M, Loubat A, Dani C, Peraldi P. Inhibition of Hedgehog Signaling Decreases Proliferation and Clonogenicity of Human Mesenchymal Stem Cells. PLoS ONE. 2011;6:e16798.

[53] Verma D, et al. Osteoblast adhesion, proliferation and growth on polyelectrolyte complex-hydroxyapatite nanocomposites. Philosophical Transactions of The Royal Society A Mathematical Physical and Engineering Sciences. 2010;368:2083.

[54] Verma D, Katti KS, Katti DR. Polyelectrolyte-complex nanostructured fibrous scaffolds for tissue engineering. Materials Science and Engineering: C. 2009;29:2079-84.

[55] Asumda F, Chase P. Age-related changes in rat bone-marrow mesenchymal stem cell plasticity. BMC Cell Biology. 2011;12:1-11.

[56] Khanna R, Katti KS, Katti DR. In Situ Swelling Behavior of Chitosan-Polygalacturonic Acid/Hydroxyapatite Nanocomposites in Cell Culture Media. International Journal of Polymer Science. 2010;2010.

[57] Lian JB, Stein GS. Concepts of Osteoblast Growth and Differentiation: Basis for Modulation of Bone Cell Development and Tissue Formation. Critical Reviews in Oral Biology & Medicine. 1992;3:269-305.

[58] Hauschka PV, Lian JB, Cole DE, Gundberg CM. Osteocalcin and matrix Gla protein: vitamin K-dependent proteins in bone. Physiological Reviews. 1989;69:990-1047.

[59] Kim E-K, Lim S, Park J-M, Seo JK, Kim JH, Kim KT, et al. Human mesenchymal stem cell differentiation to the osteogenic or adipogenic lineage is regulated by AMP-activated protein kinase. Journal of Cellular Physiology. 2012;227:1680-7.

[60] Stein GS, Lian JB. Molecular Mechanisms Mediating Proliferation/Differentiation Interrelationships During Progressive Development of the Osteoblast Phenotype. Endocrine Reviews. 1993;14:424-42.

[61] Genge BR, Sauer GR, Wu LN, McLean FM, Wuthier RE. Correlation between loss of alkaline phosphatase activity and accumulation of calcium during matrix vesicle-mediated mineralization. Journal of Biological Chemistry. 1988;263:18513-9.

[62] Aubin J. Regulation of Osteoblast Formation and Function. Reviews in Endocrine and Metabolic Disorders. 2001;2:81-94.

[63] Malaval L, Liu F, Roche P, Aubin JE. Kinetics of osteoprogenitor proliferation and osteoblast differentiation in vitro. Journal of Cellular Biochemistry. 1999;74:616-27.

[64] Turksen K, Aubin JE. Positive and negative immunoselection for enrichment of two classes of osteoprogenitor cells. The Journal of Cell Biology. 1991;114:373-84.

[65] Vallet-Regí JRaMVCaJPaM. Control of the pore architecture in three-dimensional hydroxyapatite-reinforced hydrogel scaffolds. Science and Technology of Advanced Materials. 2011;12:045003.

[66] Jana S, Florczyk SJ, Leung M, Zhang M. High-strength pristine porous chitosan scaffolds for tissue engineering. Journal of Materials Chemistry. 2012;22:6291-9.

CHAPTER 6. NANOCLAYS WITH BIOMINERALIZED HYDROXYAPATITE FOR DESIGN OF POLYCAPROLACTONE SCAFFOLDS FOR STEM CELL BASED BONE TISSUE ENGINEERING

Use of nanoclays with biomineralized hydroxyapatite (*in situ* HAPclay) for fabrication of synthetic polycaprolactone (PCL) composite scaffolds and studies showing their suitability for mesenchymal stem cell based bone tissue engineering are presented in this chapter. The contents of this chapter are included in a manuscript cited as Ambre, A.H., Katti, D.R., Katti, K.S. (2014) Biomineralized Hydroxyapatite Nanoclay Composite Scaffolds with Polycaprolactone for Stem Cell Base Bone Tissue Engineering, Journal of Biomedical Materials Research Part A. 00A:000-000, DOI: 10.1002/jbm.a.35342 (online version before inclusion in an issue)

6.1. Introduction

The tremendous potential of tissue engineering as an alternative to conventional treatment methods for repairing tissue defects has spurred research efforts in recent years towards developing improved/new strategies capable of overcoming the multiple challenges in tissue engineering. Tissue engineering introduced in the early 1990s [1] involves cell-scaffold (material) interactions eliciting natural tissue regeneration processes and has posed challenges concerning scaffolds that need to provide appropriate three-dimensional environment to the cells for new tissue formation. Studies till date have indicated that besides the basic requirements which a scaffold needs to satisfy it is also important to consider the emerging challenge of integrating and optimizing different properties of a scaffold from nanoscale to macroscale. Such integration and optimization can assist in satisfying an ensemble of properties responsible for making a scaffold capable of providing necessary biophysical and biochemical cues to the cells

for tissue regeneration. In addition to this the type of cells used can also contribute to the success of tissue regeneration strategies based on tissue engineering principles.

Bone can be considered as a nanocomposite consisting of a complex hierarchical structure extending from nanoscale to macroscale [2]. The mechanical properties of bone attributed to this hierarchical structure enables it provide the required structural support and facilitate movement. Designing scaffolds for bone regeneration that have structural hierarchy as observed in bones is a difficult task considering the existing methods for scaffold fabrication. However, it can be possible to incorporate important features similar to bone extracellular matrix (ECM) in scaffolds using the existing fabrication methods. Regeneration of hard tissues such as bone necessitates the use of scaffolds having mechanical properties capable of presenting appropriate mechanical cues to the cells in the porous microenvironment of scaffolds and also adequate to support the regenerating bone or biomechanical loads at the defect site. Reinforcing polymeric materials with inorganic fillers to fabricate composite scaffolds has emerged as a useful strategy which imparts scaffolds with organic-inorganic nature similar to bone and can also satisfy the necessities of bone tissue engineering.

The nature of inorganic fillers used for preparing polymer composite scaffolds can affect multiple aspects such as cell-scaffold interactions, subsequent tissue formation and mechanical properties of scaffolds. The known role of hydroxyapatite (HAP) in influencing biomechanical properties of bone and its characteristics such as biocompatibility, osteoconductivity, non-immunogenecity [3-6] are some of the important reasons for its extensive use in scaffold preparation for bone tissue engineering. The use of calcium phosphate based fillers such as HAP has also been attributed to the possible role of calcium and phosphate ions released from them under physiological environment in influencing cellular behavior [7]. Trace elements such as

carbonate, sodium, magnesium, silicon, zinc etc. [4] present in bone besides apatite influence bone formation and mineralization processes [8, 9]. This has been the basis of studies where such trace elements were used for preparing substituted HAP and its effect was studied on osteoblasts [10, 11] and in vivo bioactivity [9, 12]**.** Studies involving bioactive glass composed of oxides of some these trace elements had an effect on attachment [13] and genetic expression of osteoblasts [14, 15]. Silicon present in silicates has been also shown to affect differentiation and cell signaling routes of bone marrow stromal cells [16]**.** Although most studies involving HAP, substituted HAP and bioactive glass scaffolds emphasize their effect on cell behavior the low fracture toughness of these materials can limit their use for bone tissue engineering. Sodium montmorillonite (Na-MMT) clay, a layered silicate with ionic constituents, is known for its reinforcing capability in case of polymer-clay nanocomposites (PCNs) [17, 18] along with few studies showing its effect on cell behavior [19-22]. This suggests the utility of MMT clay as a filler for fabricating biodegradable composites that can be useful for bone tissue engineering.

MMT clay is a 2:1 phyllosilicate with its each nanometer thick layer having one octahedral alumina sheet between two tetrahedral silica sheets [17, 18]. High aspect ratio of MMT results from nanometer thickness of its each layer. Favorable effect of nanoscale features on cell behavior and protein adsorption [23-25] implies potential of MMT to affect cell behavior. The exchangeability of interlayer ions in MMT clay with organic molecules and cations in addition to its ability to be dispersed in to individual layers has been responsible for its use in several studies for preparing PCNs [18]. These studies since the first reported use of MMT clay for preparing PCNs in 1990 by Toyota research group [26] have shown that MMT clay improves mechanical properties [17, 18, 27, 28] and also affects biodegradability [18], gas permeability [29-31] and flammability [32, 33] of PCNs. The strengthening effect of MMT clay observed in

case of PCNs has led to studies exploring the mechanisms for enhancement in mechanical properties of PCNs. “Altered Phase Model” for PCNs [34] developed in our group based on molecular dynamics and experimental studies premises that molecular interactions between the PCN constituents (polymer, modifier and clay) are responsible for formation of an “altered phase” around clay particles in PCNs, which has considerably different mechanical properties than the polymer. Another simulation study involving evaluation of interaction energies between different components of PCN constituents elucidated the effect of molecular interactions on crystallinity and nanomechanical properties [35]. Our simulation studies also showed the effect of a modifier’s backbone chain length and its functional groups on clay d-spacing and nanomechanical properties of PCNs [36]. Besides the role of molecular interactions in enhanced mechanical properties of PCNs our simulation studies also indicate that designing PCNs at the molecular level can lead to better control of their physical properties across higher length scales.

The strengthening effect of MMT clay in case of PCNs combined with its medicinal properties [37, 38], ability to be excreted from the body [37] and known pharmaceutical applications [39-44] seems to make its use promising for tissue engineering. Optimal use of inorganic fillers for fabricating composite scaffolds useful for their desired application requires an understanding of the influence of such composite scaffolds on cellular events favoring tissue formation. For bone tissue engineering, it can thus be useful to study the response of mesenchymal stem cells or osteoblasts to polymer-clay based composite substrates (films and scaffolds). Past few studies have shown enhancement in mechanical properties of PCNs based on polymers such as chitosan [45], polycaprolactone [46] and gelatin [47] that were considered as potential materials for tissue engineering. Cellular behavior on PCNs has been reported in few

studies mentioned earlier with one of them related to pharmaceutical applications. This emphasizes the scope for further studies focused on cell-material interactions in case of PCNs.

Natural polymers known for promoting favorable cell responses are limited by their inadequate mechanical strength, batch-to-batch variation in properties and difficulties in controlling their degradation rate. Synthetic polymers though lacking the biomolecule sequences promoting desired cell responses as in case of natural polymers seem to have optimizable mechanical and degradation properties along with better processability. Polycaprolactone (PCL), a synthetic and aliphatic polyester, has re-emerged as a polymer with huge scope for tissue engineering applications. Good processability, compatibility with different polymers to form blends, broad molecular weight range, solubility in common organic solvents and its excellent potential for offering desired mechanical properties via its blends, copolymers, composites have contributed to this re-emergence of PCL in the biomedical field [48]. The versatility of PCL and the reinforcing ability of MMT clay may thus prove beneficial for fabricating composite scaffolds that can satisfy the complex bone tissue engineering requirements.

Mesenchymal stem cells (MSCs) have emerged as a promising alternative cell source for tissue engineering applications and continue to be studied further due to several factors. Important among these are their ability to proliferate in an undifferentiated state while maintaining the ability to differentiate in to different cell lineages when provided with appropriate stimuli, relatively controllable differentiation compared to embryonic stem cells, accessibility and possibilities of allogeneic use due to their "immunosuppressive effects [49-55]." The evolving understanding about the role of MSCs in wound healing [56] and their recruitment through peripheral blood to sites of bone injury [57] has extended the scope of their use in bone tissue engineering. Studying the behavior of MSCs in 3D scaffold microenvironment

resembling the in vivo environment can be helpful for understanding the complex mechanisms related to wound healing and tissue repair besides the cell-material interactions.

MMT clay was modified in our previous work [58] with three unnatural amino acids known for their antibacterial activity and having a longer backbone chain length compared to natural amino acids. Effect of a modifier's backbone chain length on mechanical properties [36] was considered while using these unnatural amino acids in addition to the intercalation potential of amino acids in clay interlayer as indicated by our previous simulation studies [59]. Based on its relatively better biocompatibility with human osteoblasts 5-aminovaleric acid modified MMT clay was chosen among the modified clays for preparing biopolymer polyelectrolyte (chitosan/polygalacturonic acid) composite scaffolds [60]. Osteoblast proliferation in case of biopolymer scaffolds containing modified clay was similar to those scaffolds containing HAP and these modified clay based scaffolds also satisfied basic requirements for tissue engineering. Biomimetic strategy was used in further studies to prepare a unique three-component nanoclay-HAP hybrid (*in situ* HAPclay) by mineralizing HAP in modified MMT clay to improve osteoconductive properties of MMT clay [61]. Infrared spectroscopy studies indicated involvement of the intercalated modifier's carboxylic groups in HAP mineralization through chelation and thus suggested a molecular level organic-inorganic association. Also, cluster formation by human osteoblasts observed on biopolymer (chitosan/polygalacturonic)/*in situ* HAPclay composite films indicated the osteogenic potential of *in situ* HAPclay. Similar behavior of osteoblasts leading to formation of bone nodules on biopolymer/HAP composites in the presence of cell culture medium without osteogenic supplements was seen in our previous studies [62, 63].

Based on our hypothesis that *in situ* HAPclay has potential to impart bone formation ability along with desirable mechanical properties to the resulting composites we studied the response of human MSCs to biopolymer/*in situ* HAPclay composite films and scaffolds. These MSCs formed bone nodules on composite films and mineralized extracellular matrix (ECM) in composite scaffolds in the absence of osteogenic supplements that indicated the mediatory effect of *in situ* HAPclay in MSC differentiation and bone nodule formation [22]. In this work, we extend our hypothesis about *in situ* HAPclay to a synthetic polymer composite system and attempt to evaluate it through studies involving PCL/*in situ* HAPclay composites. PCL was used in this work considering its immense prospects for tissue engineering due to its versatility and its lesser complexities compared to polymers obtained from natural sources. Besides the fabrication of PCL/*in situ* HAPclay composite films and scaffolds this work involves investigation of viability and differentiation of MSCs on these composites through appropriate assays. Atomic force microscopy (AFM) was used to characterize the surface of PCL composite films and study the morphology of mineralized ECM formed by MSCs on these films. Phase contrast microscopy was used to assay the formation of mineralized ECM formed by MSCs seeded on PCL composite films after Alizarin Red S staining. Scanning electron microscopy (SEM) was used to study scaffold microstructure and MSC infiltration in the PCL composite scaffolds. Attachment, spreading of MSCs on PCL/*in situ* HAPclay composites (films and scaffolds) and formation of mineralized ECM by MSCs on PCL composite films was also studied using SEM. Nanoindentation was used to evaluate the nanomechanical properties of the composite films. Photoacoustic FTIR (PA-FTIR) spectroscopy was used to study molecular level effect of accelerated in vitro degradation on PCL/*in situ* HAPclay composite scaffolds and the

morphological changes in these scaffolds resulting from such degradation were studied by SEM. Thus, the objectives of this work were as follows:

1. Fabrication of PCL/*in situ* HAPclay composites (films and scaffolds)
2. Studying MSC response (viability, differentiation, attachment and spreading, mineralized ECM formation) to the fabricated PCL/*in situ* HAPclay composites were the objectives of this study.
3. Investigating scaffold microstructure and micron to sub-micron scale characterization of surface morphology of PCL/*in situ* HAPclay composite films.
4. Sub-micron scale characterization of mineralized ECM formed by MSCs on PCL/*in situ* HAPclay composite films.
5. Nanomechanical characterization of PCL/*in situ* HAPclay composite films
6. Degradation studies of PCL/*in situ* HAPclay composite scaffolds.

6.2. Materials and Methods

6.2.1. Materials

Sodium-montmorillonite (Na-MMT) clay used for preparing modified clay, Swy-2 (Crook County, Wyoming), had a cation exchange capacity (CEC) of 76.4 mequiv./100 g and was sourced from the Clay Minerals Repository at the University of Missouri, Columbia. 5-aminovaleric acid, polycaprolactone (PCL) (average M_n = 80,000) and 1, 4 dioxane (anhydrous, 99.8 %) from Sigma Aldrich were used for experiments. Materials for preparing *in situ* HAPclay such as sodium phosphate (Na_2HPO_4) and calcium chloride ($CaCl_2$) were obtained from J.T. Baker and EM Sciences respectively. Human MSCs from bone marrow (PT-2501, Lonza,Walkersville, MD) were cultured in cell culture medium made by adding MSCGM^{TM}

SingleQuots™ (PT-4105) to mesenchymal stem cell basal medium (MSCBM™, PT-3238). These two components of cell culture medium were purchased as MSCGM™ (mesenchymal stem cell growth medium) Bullekit™ from Lonza, Walkersville.

6.2.2. Procedure for Preparation of Amino Acid Modified MMT Clay

Na-MMT was modified with 5-aminovaleric acid (unnatural amino acid) according to the procedure described in our previous studies [22, 58, 60, 61]. In short, mixture obtained by adding 5-aminovaleric acid solution (pH=1.8 & temperature = 60°C) prepared in DI water to Na-MMT clay suspension in DI water (pre-heated to 60°C) was stirred vigorously for an hour. The stirred mixture was then centrifuged for removal of DI water and washed further for removal of chloride ions followed by drying at 70°C, grinding and sieving to obtain a fine powder.

6.2.3. Procedure for Preparing *In Situ* HAPclay

In situ HAPclay was prepared according to procedure described in our earlier studies [22, 61]. Modified MMT clay was dispersed and further stirred for 2 hours in Na_2HPO_4 solution (23.8 mM) at room temperature to obtain modified MMT clay-Na_2HPO_4 suspension. $CaCl_2$ solution (39.8 mM) was then added to this suspension and the resulting mixture (at pH=7.4) was stirred for 8 hours. Precipitates obtained were allowed to settle, centrifuged to remove water, dried at 70°C and subsequently sieved after grinding to obtain a fine powder.

6.2.4. Preparation of Polycaprolactone (PCL)/ *In Situ* HAPclay Films and Scaffolds

Figure 6.1. represents a schematic for preparing PCL/*in situ* HAPclay films and scaffolds respectively. For preparing composite films with different (10 wt % and 20 wt %) *in situ* HAPclay concentrations, PCL (0.09 grams/ml dioxane) was dissolved in 1, 4 dioxane at room temperature. Thus for preparing PCL films with 10 wt% *in situ* HAPclay, 3.6 grams PCL was

dissolved in 40 ml 1, 4 dioxane and a sonicated suspension of *in situ* HAPclay in 1, 4 dioxane (0.4 grams in 16 ml dioxane) was added to the PCL solution. The resulting solution was stirred for 2 hours and then transferred to glass Petri dishes. The composite solution in Petri dishes was subjected to drying for 72 hours at room temperature to get films. Samples having ~12.7 mm diameter were punched out from these dried films (~85 mm diameter) for further experiments. Similar procedure was followed for preparing PCL composite film containing 20 wt % *in situ* HAPclay by using appropriate proportion of constituents accordingly. PCL films without *in situ* HAPclay were also prepared similarly with the difference being absence of addition of *in situ* HAPclay suspension to the PCL solution.

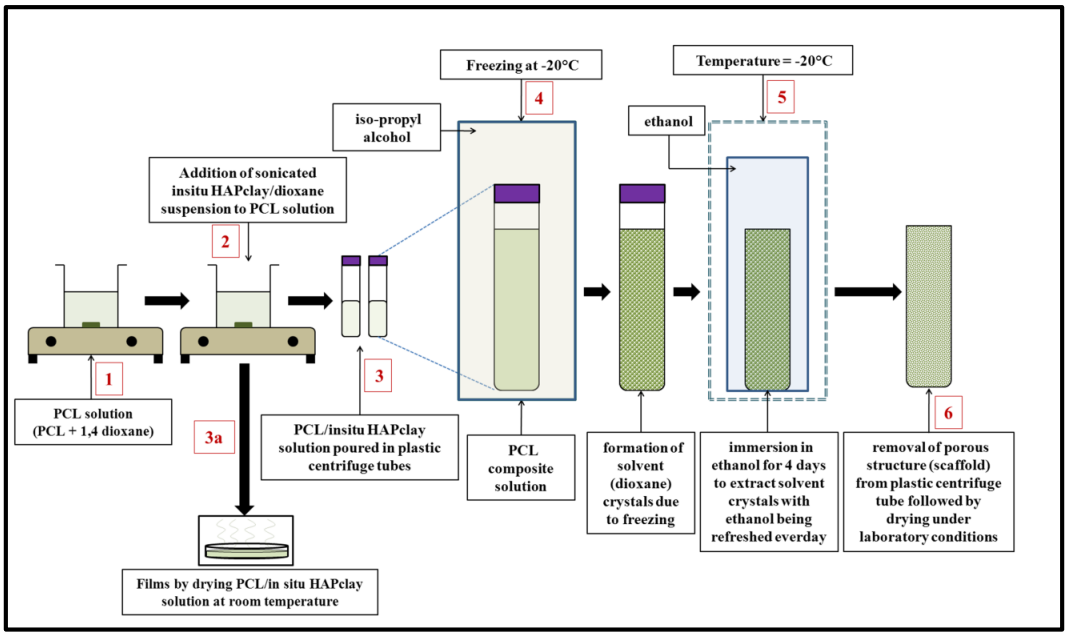

Figure 6.1. Representative schematic showing methods for preparation of polycaprolactone (PCL)/*in situ* HAPclay composite films and scaffolds

For preparing scaffolds, the PCL/*in situ* HAPclay composite solution was frozen at -20°C in an iso-propyl alcohol bath overnight. Cylindrical shaped frozen samples of the composite solution were then carefully removed from polypropylene (PP) centrifuge tubes and further immersed in absolute ethanol (cooled to -20°C) for solvent extraction. Immersion in absolute

ethanol was continued for 4 days with absolute ethanol being refreshed every day. After 4 days the cylindrical shaped porous samples known as scaffolds were removed and dried at room temperature. PCL composite scaffolds with 10 wt % and 20 wt % *in situ* HAPclay were thus prepared using freeze extraction method.

6.2.5. Scanning Electron Microscopy (SEM) studies

SEM was used to study microstructure of fabricated PCL/*in situ* HAPclay composite scaffolds (~12 mm diameter and ~ 3 mm thickness) using JEOL JSM-6490LV scanning electron microscope. The same SEM instrument was also used for studying MSC adhesion to both PCL/in situ HAPclay composite scaffolds and films. For this purpose, PCL/*in situ* HAPclay composite scaffolds seeded with human MSCs (9.16×10^4 cells in each scaffold containing well) were removed from culture, washed with phosphate buffer saline (PBS), fixed using glutaraldehyde (2.5%), subsequently dehydrated using ethanol series (10 % v/v, 30 % v/v, 50 % v/v, 70 % v/v and 100 %) and then dried after 100 % ethanol was replaced with hexamethyldisilazane. These scaffold samples were then used for SEM imaging after coating them with gold using sputter coater and mounting them on a SEM sample stub. Similarly, fixed and dried MSC seeded **(**7.36×10^4 cells in each sample containing well) PCL/*in situ* HAPclay composite film samples were imaged using SEM. Fabricated PCL/*in situ* HAPclay composite scaffolds did not require fixing and dehydration before imaging. SEM was also used to study the effect of accelerated degradation (described later) on the microstructure and surface morphology of PCL/*in situ* HAPclay composite scaffolds.

6.2.6. Cell Culture

6.2.6.1. Cell Viability Using MTT Assay

MSC viability was studied in the fabricated PCL composite scaffolds and also on the PCL composite films using MTT assay. Purple colored formazan obtained after reduction of MTT (3-(4, 5 dimethylthiazol-2)-2, 5-diphenyltetrazolium bromide) reagent by mitochondrial dehydrogenase enzyme in live cells is solubilized and intensity of this solubilized formazan read using a spectrophotometer indicates number of live cells. PCL/*in situ* HAPclay (10 wt %) composite film samples (~12.7 mm as mentioned earlier) in sterile 24-well polystyrene plates (Falcon®, Corning®) were UV sterilized and then immersed in 70 % alcohol overnight to ensure wetting of these hydrophobic polyester (PCL) based films [64-67]. The PCL composite film samples were then washed with PBS twice and further incubated in PBS (6 hours) for removal of alcohol. PBS was then removed and after 24 hours of subsequent incubation at 37°C, 5 % CO_2 in cell culture medium human MSCs (3.96×10^4) were seeded in each well on these composite film samples (quadruplicates) and these seeded samples were incubated at 37°C, 5 % CO_2 under humidified conditions for 10, 16 and 23 days. Media was refreshed after every two days. After incubation the MSC seeded PCL composite film samples were washed with PBS and transferred to unused wells of the 24-well plates. 75 µL MTT solution (5 mg/ml PBS) along with 500 µL serum-free DMEM was added further to each well. After subsequent incubation for 12 hours, remaining solution was aspirated from the wells and 500 µL DMSO was added to these wells. Microplate spectrophotometer (Bio Rad, Benchmark Plus) was then used to read the absorbance values of the supernatant (400 µL) at 570 nm of quadruplicate sample sets. PCL film samples containing 10 wt % *in situ* HAPclay and 20 wt % *in situ* HAPclay were assayed in two separate

experiments. 3.1 x 10^4 human MSCs were seeded in each well of 24-well polystyrene plates on PCL composite film samples (quadruplicates) containing 20 wt % *in situ* HAPclay.

For performing MTT assay in case of PCL composite scaffolds containing 10 wt% *in situ* HAPclay, scaffold samples (quadruplicates) in sterile 24-well polystyrene plates (Falcon®, Corning®) were UV sterilized, immersed in 70 % alcohol overnight, subsequently washed with PBS twice and incubated in PBS (7 hours). Further, PBS was removed and after 24 hours of incubation in cell culture medium at 37°C, 5 % CO_2, 5.66 x 10^4 cells human MSCs were seeded in each of the scaffold containing wells. Incubation of seeded scaffold samples was carried out at 37°C, 5 % CO_2 under humidified conditions for 10, 16 and 23 days. Seeded scaffold samples were then washed with PBS after incubation and transferred to unused wells of 24-well plates. This was followed by addition of 90 µL MTT (5 mg/ml PBS) along with 600 µL serum-free DMEM to each well. After further incubation for 12 hours, remaining solution was aspirated and 600 µL DMSO was added to these wells. Absorbance readings of the supernatant (400 µL) were then obtained at 570 nm using a microplate spectrophotometer (Bio Rad, Benchmark Plus) for quadruplicate sample sets. Separate MTT assay experiment was also performed using the same procedure in case of PCL composite scaffolds containing 20 wt% *in situ* HAPclay with 4.7 x 10^4 human MSCs seeded in each of the scaffold containing wells of 24-well polystyrene plates. Human MSCs up to passage 5 were used during MTT assay experiments and all other cell culture experiments conducted during this work.

Presence of micron to sub-micron surface features in case of PCL and PCL composite films (discussed later under section 6.3.5.2) makes it difficult to estimate the surface area available for cell attachment and growth. The actual surface area available for cell attachment, growth can be different or more than the area calculated using external dimensions (e.g.

diameter, length, breadth) due to the presence of such micron to sub-micron scale features on PCL/PCL composite films. There is also a possibility that change in *in situ* HAPclay content (weight percentage) may lead to change in the surface area of the PCL composite films. This change caused due to relative change in the dimensions of the surface features may be an effect of *in situ* HAPclay on polymer crystallization during fabrication of PCL composite films and scaffolds. Similarly, it is difficult to estimate the surface area for cell attachment, growth in case of scaffolds due to different features associated with its microstructure such as pore shape, pore size, pore interconnectivity and topography of pore walls. PCL composite films and scaffolds with different weight percentage of *in situ* HAPclay were assayed in separate experiments due to possible differences in their surface areas and to make interpretation of experimental results less difficult. Since one of the important objectives of this work was to study the effect of addition of *in situ* HAPclay to PCL (by using PCL composite films and scaffolds) on MSC proliferation and differentiation, PCL/*in situ* HAPclay composite films/scaffolds were compared with PCL films/scaffolds without *in situ* HAPclay in these separate experiments. Also, since PCL composites with different weight percent composition of in situ HAPclay were being investigated as different systems in separate experiments, it was deemed that use of different cell numbers in these independent experiments was appropriate since the important objective was to study the effect of in situ HAPclay addition in PCL on MSC behavior (proliferation, differentiation). Although it may be possible to determine the surface area of films using AFM, Brunauer-Emmett-Teller (BET) methods and those of scaffolds possibly by BET method, further investigation may be needed to determine the suitability, consistency of these methods in case of scaffolds and films. Besides this, current experimental assay protocols developed for cells

cultured in standard polystyrene well plates may not address the difficulty in using samples having different surface areas with same external dimensions.

6.2.6.2. Alizarin Red S Staining

PCL/*in situ* HAPclay (10 wt %) film samples seeded with human MSCs were incubated at 37°C, 5 % CO_2 under humidified conditions for 41 days and were then washed with PBS before fixing with 2.5 % glutaraldehyde overnight. PBS was further used to wash the fixed samples and this was followed by staining of the samples with Alizarin Red S dye (EMD Chemicals Inc., USA, 2 g/100 ml, deionized water and pH = 4.10-4.15). After washing the stained samples with cell culture grade water to remove excess dye, images were captured using a phase contrast microscope (Axiovert 40, Zeiss).

6.2.6.3. Alkaline Phosphatase (ALP) Assay

PCL composites containing *in situ* HAPclay (film samples and scaffolds) were subjected to similar sterilization, wetting, washing and immersion (in cell culture medium) steps as those in case of MTT assay prior to seeding them with human MSCs. 4×10^4 human MSCs were seeded in each well on the PCL composite film samples containing 10 wt % *in situ* HAPclay. In a separate experiment, same number of human MSCs were seeded in each well on PCL composite film samples containing 20 wt % *in situ* HAPclay. The cell-seeded film samples were further incubated at 37°C, 5 % CO_2 under humidifed conditions for 10, 16 and 23 days. Media was refreshed after every two days. These samples were washed with PBS after incubation, transferred to unused wells of 24-well plates and 500 µL Triton X-100 (1 v/v % solution) was then added to each of the well containing the film samples. Cell lysates (250 µL) obtained after subjecting the immersed film samples to two freeze-thaw cycles (-70°C to 37°C) were transferred to new 24-well plates and incubated with p-nitrophenyl phosphate (250 µL) at room

temperature for 60 minutes. 3N NaOH (70 µL) was further added to the wells and absorbance readings were taken at 405 nm using a microplate spectrophotometer (Bio Rad, Benchmark Plus) for quadruplicate sample sets.

In case of PCL composite scaffolds containing 10 wt % in situ HAPclay, 4.77×10^4 human MSCs were seeded in each of the scaffold containing wells. PCL composite scaffolds containing 20 wt % in situ HAPclay were assayed in a separate experiment with 4×10^4 human MSCs seeded in each of the scaffold containing wells. The MSC seeded scaffold samples were incubated at 37°C, 5 % CO_2 under humidified conditions for 10,16 and 23 days, further washed with PBS after incubation and then transferred to unused wells of 24-well plates. 850 µL Triton X-100 (1 v/v % solution) was added to each of the scaffold containing wells. Cell lysates (250 µL) obtained after two cycles of freezing-thawing (-70°C to 37°C) of scaffold samples immersed in Triton X-100 were incubated in a new 24-well plate with p-nitrophenyl phosphate (250 µL) at room temperature for 60 minutes. Absorbance values were measured at 405 nm for quadruplicate sample sets after further addition of 3N NaOH (70 µL) to the wells.

6.2.6.4. MSC Infiltration in PCL/*In Situ* HAPclay Composite Scaffolds

PCL composite scaffolds (dimensions ~ 12 mm diameter and 12 mm thickness/height) containing 10 wt % *in situ* HAPclay were sterilized, wetted in alcohol, washed using PBS and incubated in cell culture media as mentioned earlier (section 2.6.1) before seeding them with human MSCs. 1×10^5 MSCs were seeded in each of the scaffold containing wells. MSC seeded scaffolds were further incubated under humidified conditions at 37°C, 5 % CO_2 for 20 days. These MSC seeded scaffolds were then washed with PBS, fixed and dried using glutaraldehyde (2.5%), ethanol series and hexamethyldisilazane as mentioned earlier in section 2.5. After cutting

the fixed scaffolds at depths of 3.5 mm and 6 mm from the scaffold surfaces, upper surface regions of the remaining portions of the scaffolds were imaged using SEM.

6.2.6.5. Two Stage Cell Seeding

Two-stage cell seeding experiment was performed as a possible approach to increase tissue formation under in vitro conditions based on the experimental method reported in our previous work [22]. Potential of proteins present in the extracellular matrix (ECM) produced by the MSCs, complexities related to proliferation and differentiation of MSCs such as "growth arrest" during their differentiation [68] were considered while using this approach. Following sterilization, wetting, washing and incubation (in cell culture media) prior to cell seeding as mentioned earlier for PCL/*in situ* HAPclay composite film samples, 7.36×10^4 human MSCs were seeded in each well (of 24-well plate) on PCL composite film samples containing 10 wt % *in situ* HAPclay. After incubating these MSC seeded composite films for 24 days at 37°C, 5 % CO_2, human MSCs (7.36×10^4) were again seeded on these films. Incubation of the PCL composite films thus seeded two times with human MSCs was continued further up to 41^{st} day. The composite film samples were then stained with Alizarin Red S dye and were also imaged using SEM and AFM (described later). Similarly, in a separate two-stage cell seeding experiment PCL films containing 20 wt % *in situ* HAPclay seeded with MSCs were incubated for 42 days and then imaged using SEM.

6.2.7. Atomic Force Microscopy (AFM) studies

AFM was used to study the sub-micron scale morphology of PCL/*in situ* HAPclay composite films and mineralized ECM formed by human MSCs on PCL/*in situ* HAPclay (10 wt %) composite films. Multimode™ AFM equipped with Nanoscope IIIa controller and J-type piezo scanner (Veeco Metrology Group, Santa Barbara, CA) was used to perform AFM imaging

in TappingMode™ . Antimony (n) doped Si tips were used to image the samples under laboratory conditions.

6.2.8. Nanoindentation

Nanoindentation experiments were performed using a Hysitron Triboscope nanomechanical testing instrument (Minneapolis, MN) to measure nanomechanical properties of PCL/*in situ* HAPclay films. The nanomechanical testing instrument was used along with Multimode™ AFM mentioned earlier to perform load-controlled nanoindentation tests. This instrument has a diamond Berkovich tip (100-200 nm diameter) operated by a three-plate capacitive transducer that is used to apply desired load on the sample. Load-displacement curves obtained by loading and unloading the sample were used to calculate the elastic modulus (E) and hardness (H) using the Oliver-Pharr method [69]. In this work, a 5-5-5 trapezoidal load function was used to perform load-controlled indentation tests at 1000 μN and 5000 μN loads. Elastic moduli and hardness values obtained from a total 31 indents made at different sites on the sample surface were used to calculate the average E and H values represented in Table 1**.**

6.2.9. In Vitro Degradation Studies

Accelerated degradation studies were performed on PCL composite scaffolds using sodium hydroxide solution (0.1 M). Scaffold samples (~12 mm diameter and ~ 3 mm thickness) were UV sterilized, immersed in 70 % alcohol overnight and then washed with PBS. The scaffold samples were then transferred to glass vials containing the degradation media (0.1 M NaOH). Each scaffold sample was thus immersed in separate vials containing the degradation media with the caps of these vials tightened properly. These scaffold containing vials were maintained at 37°C during the degradation period with degradation media being refreshed after every 7 days. After each degradation period (time point), the scaffolds were removed from the

vials, washed carefully with deionized water and dried at room temperature. The percentage weight loss for the scaffold samples was calculated using the following formula:

% weight loss = $(w_i-w_d)/w_i$ x 100

w_i = initial weight of scaffold before degradation

w_d = weight of degraded scaffold

Data was obtained for quadruplicate sample sets after each time point in these experiments.

6.2.10. Fourier Transform Infrared (FTIR) Spectroscopy Studies

Photoacoustic FTIR (PA-FTIR) spectroscopy experiments were performed on PCL and PCL composite scaffolds containing *in situ* HAPclay. Degraded PCL/*in situ* HAPclay composite scaffold samples obtained during accelerated in vitro degradation studies were also characterized using PA-FTIR spectroscopy for comparative studies. PA-FTIR experiments were performed using ThermoNicolet Nexus 870 spectroscopy instrument accessorized with MTEC Model 300 photoacoustic detector. Spectra were collected in the 4000-400 cm^{-1} range at a mirror velocity of 0.15 cm/s.

6.2.11. Porosity Evaluation

Apparent density of the scaffolds was calculated by considering their mass and volume. Solid density of the scaffold material was determined using a pycnometer. Porosity of the PCL/*in situ* HAPclay composite scaffolds was then calculated using the following formula:

% porosity = $(1- \rho_a/\rho_s)$

ρ_a = apparent density of scaffold and ρ_s=solid density of scaffold material

6.2.12. Mechanical Properties

Compressive mechanical properties of scaffold samples (~ 13 mm diameter and 13 mm length) were determined using MTS 858 materials testing servo mechanical test frame (Materials

Testing Solutions, Eden Prairie, MN). Quadruplicate sample sets were used while performing during this experiment. Slope of the initial linear region of stress-strain curve was used for calculating the compressive elastic moduli of scaffold samples.

6.2.13. Statistical Analysis

Student's t-test was performed using Minitab to analyze the data acquired during experiments. One-way ANOVA was used in case of comparison between more than two different samples. Data was considered significantly different when probability values were less than 0.05 ($p < 0.05$).

6.3. Results and Discussion

6.3.1. Scanning Electron Microscopy

6.3.1.1 Scaffold Morphology

SEM micrographs in Figure 6.2. (a-c) show that the PCL and PCL composite scaffolds containing *in situ* HAPclay prepared using freeze-extraction method have a porous microstructure. These scaffolds seem to have pore sizes in the 100 µm-300 µm range and also below 100 µm. Pore size is known to have an effect on cell migration and proliferation, diffusion of nutrients and oxygen, vascularization and bone formation [70]. Also, other morphological features (pore shape, internal geometry, macro and micro porosities, surface concavities) of the scaffold can affect bone formation [71-73] and also have an effect on the osteoinductivity of scaffolds [6]. Microporosities (pore size < 10 µm) along with few pores in the 10 µm-30 µm range can be seen in the walls of larger (100 µm-300µm range) pores [Figure 6.3. (a-c)]. Such micropores can result in increase of protein adsorption due to increase in surface area, assist in ion-exchange along with apatite formation via dissolution-reprecipitation on pore surfaces [74] and can be useful to allow effective nutrient-waste exchange [75]. These processes (protein

adsorption and apatite formation) are known to promote bone formation and also induce favorable response of bone forming cells through the roughened pore surface. The PCL composite scaffolds containing *in situ* HAPclay also show interspersed lamellar features [Figure 6.3. (d, e)]. Presence of such features in PCL/*in situ* HAPclay composite scaffolds can thus possibly affect bone formation and may contribute to enhance their osteoinductivity in case of in vivo applications.

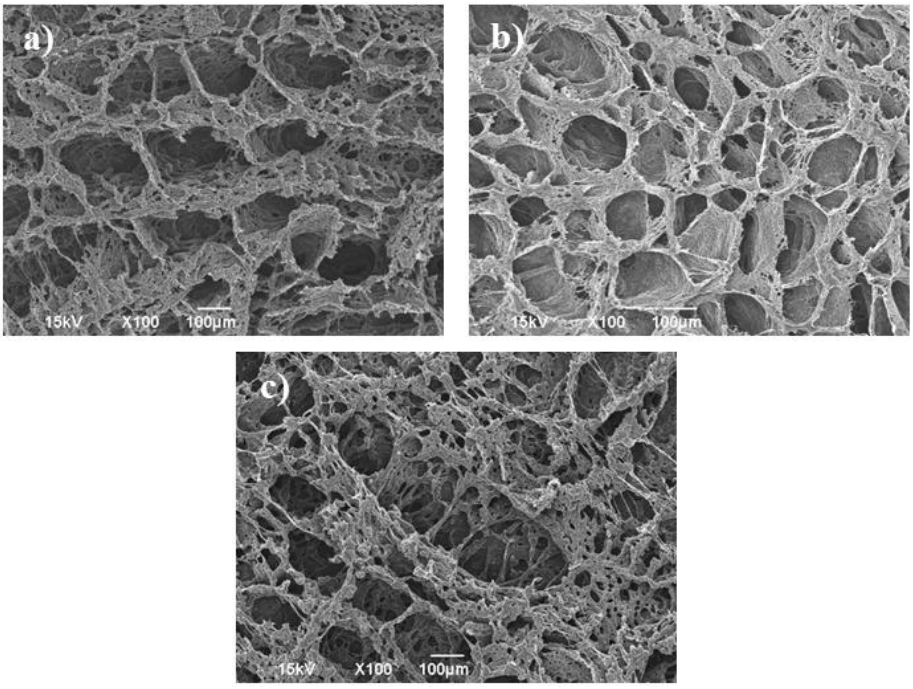

Figure 6.2. SEM micrographs of PCL scaffolds [a)], PCL scaffolds containing 10 wt % *in situ* HAPclay [b)] and PCL scaffolds containing 20 wt % *in situ* HAPclay [c)]

Consideration of the complexities of in vivo environment such as the inflammatory/foreign body response to implanted biomaterials while designing scaffolds can be useful to improve the in vivo performance of scaffolds. Macrophages involved in foreign body reaction to conventional biomaterials (solid implants) undergo “frustrated phagocytosis” and eventually the implanted biomaterial gets enclosed in a collagenous capsule [76]. Degrading substances released during this reaction affect the performance of the implanted biomaterial [77].

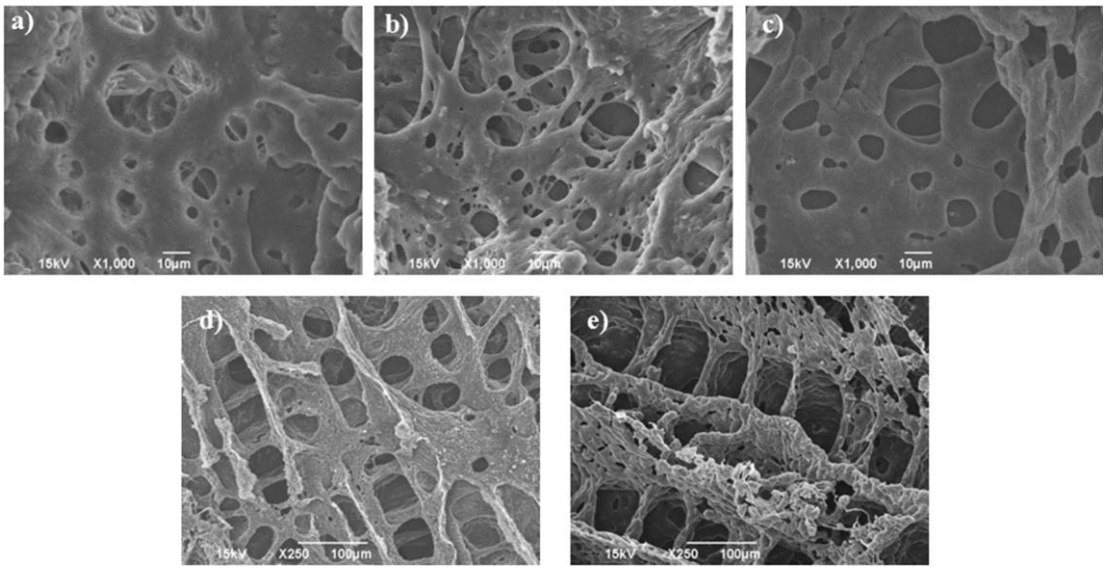

Figure 6.3. SEM micrographs showing micropores (<10 µm and 10 µm-30 µm range) in PCL scaffolds [a)], PCL scaffolds containing 10 wt % *in situ* HAPclay [b)], PCL scaffolds containing 20 wt % *in situ* HAPclay [c)] and lamellar features in PCL scaffolds containing 10 wt % *in situ* HAPclay [d)], PCL scaffolds containing 20 wt % *in situ* HAPclay [e)]

Studies over the past few years have suggested that porous scaffolds can be useful to evade the foreign body reaction in case of in vivo applications [78, 79]**.** It has been hypothesized that the pore size of scaffolds can be used to induce the M2 phenotypic expression of the macrophages. M2 phenotype of macrophages is considered to be immunosuppressive, anti-inflammatory and has healing properties as opposed to the pro-inflammatory M1 phenotype [78]. Recent studies have reported scaffolds having pore size below 50 µm capable of inducing M2 phenotypic expression in macrophages [79, 80] and reducing the thickness of the collagenous capsule formed under in vivo conditions [81, 82]. Several studies have proposed pore size of 100-500 µm for bone regeneration taking in to account factors such as cell attachment, proliferation and infiltration in scaffolds, capillary formation, nutrient diffusion and waste removal [70, 83, 84]. Importance of graded pore size in scaffolds to mimic the structural complexities of natural tissues was also emphasized in some of these studies [75, 85]. The two different pore size ranges seen in PCL/*in situ* HAPclay scaffolds seem to satisfy the criteria for

use in bone tissue engineering and were used for in vitro experiments in this work. Differences in pore size/pore size range required for bone regeneration and avoidance of adverse in vivo response makes synergizing tissue regeneration with in vivo immune response a difficult task and needs further investigation.

6.3.1.2. Human MSC seeded PCL/*In Situ* HAPclay Composite Films and Scaffolds

Figure 6.4. (a-l) shows SEM micrographs of PCL/*in situ* HAPclay composite films seeded with human MSCs. These images indicate attachment, spreading of MSCs on the composite films and formation of mineralized extracellular matrix (ECM) by MSCs on these composite films. The attached MSCs also seem to conform to substrate geometry and formation of cell layers by MSCs on the PCL composite films can also be observed in some of these SEM micrographs. These cell layers can be a result of membrane fusion events or formation of special types of intercellular adherens junctions such as “processus adhaerentes” or “recessus adhaerentes” between the MSCs [86]. A closer inspection of some of these SEM micrographs also gives an indication of intercellular communication in MSCs through cell protrusions such as lamellipodia (sheet-like) and a few filopodia (long & thin processes). The mineralized ECM formed by the MSCs appears to be composed of matrix vesicles. Matrix vesicles have been implicated in cell-dependent bone mineral formation mechanisms where such vesicles may either emerge from the cell plasma membrane [87] or may be transported from inside of the cell to the extracellular space [88]. Matrix vesicles observed in the SEM micrographs also appear to be associated with surface of the cell layers with a few of them seeming to be embedded in the cell layers. This suggests the delivery of these vesicles from the cells along the routes involved in bone mineral formation mentioned earlier. Moreover, cell layers formed due to intercellular associations or junctions observed in the SEM micrographs also suggests movement of

substances/particles across cell membranes. However, further detailed investigation using different types of available microscopy techniques is needed to confirm the transport of particles/substances across cell membranes.

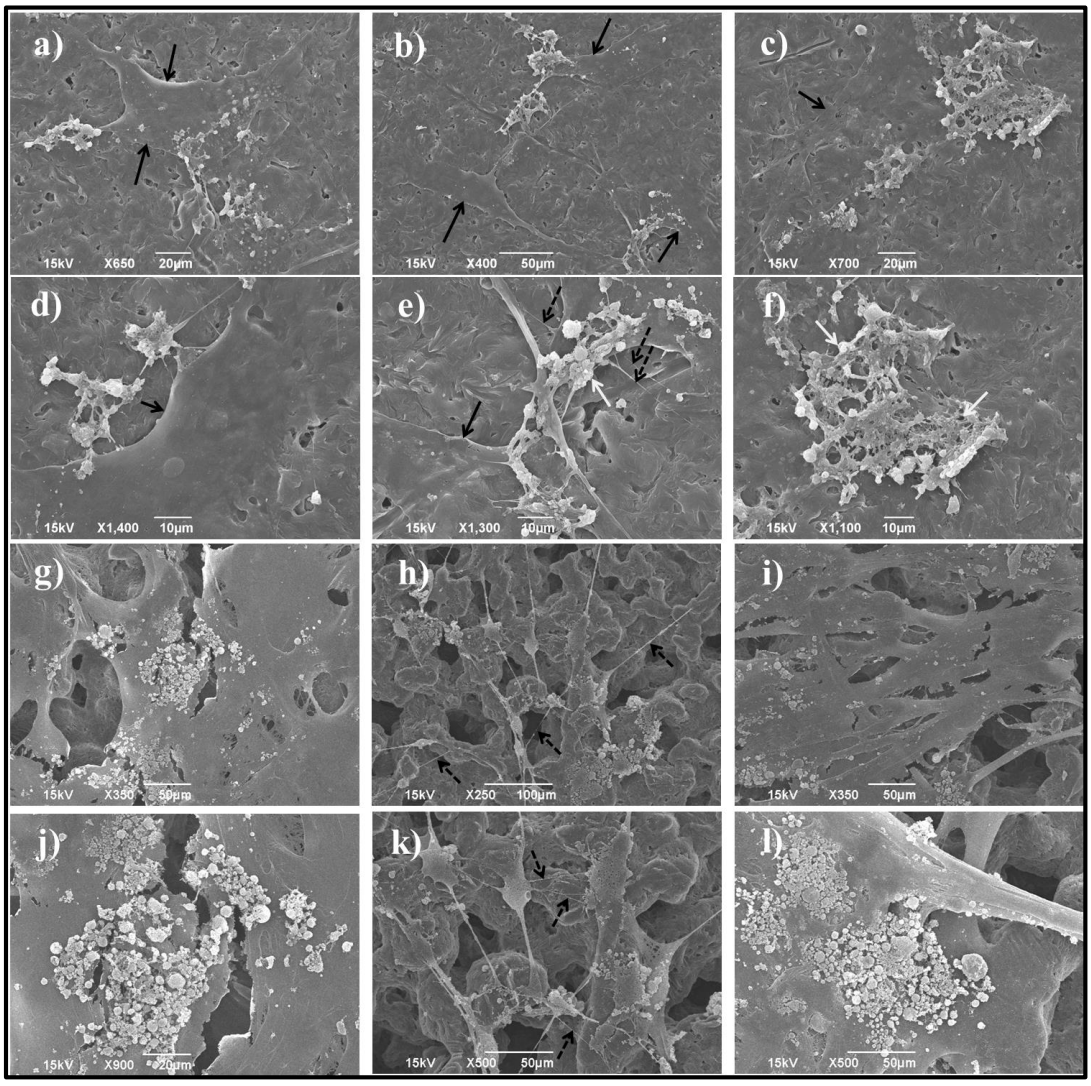

Figure 6.4. SEM micrographs of human MSCs cultured on PCL composite films containing 10 wt % *in situ* HAPclay [a) -f)] after 41 days, PCL composite films containing 20 wt % *in situ* HAPclay [g) -l)] after 42 days indicating cell attachment, spreading and mineralized extracellular matrix (ECM) formation. Solid black arrows indicate sheet-like cell protrusions known as lamellipodia and dotted black arrows indicate long, thin cell processes known as filopodia. White arrows in image f) indicate mineralized ECM

SEM micrographs in Figure 6.5. (a-h) represent qualitative data from the two-stage cell seeding experiment involving MSCs. These micrographs show formation of MSC cell layers on the PCL/*in situ* HAPclay composites. The MSC cell layers also appear to exhibit some stacking (indicated by arrows) along with possibilities of membrane fusion and formation of cell junctions mentioned earlier. Formation of dense mineralized ECM is also observed in some of the micrographs which indicates differentiation of MSCs towards an osteogenic lineage. Besides this, "stacked cells" (possibly osteoprogenitor cells) consisting a layer of four to six cells surrounding a "prechondrogenic" core of cells and known to differentiate in to ostoeblasts are considered to be involved in initial stages of embryonic bone formation [89].

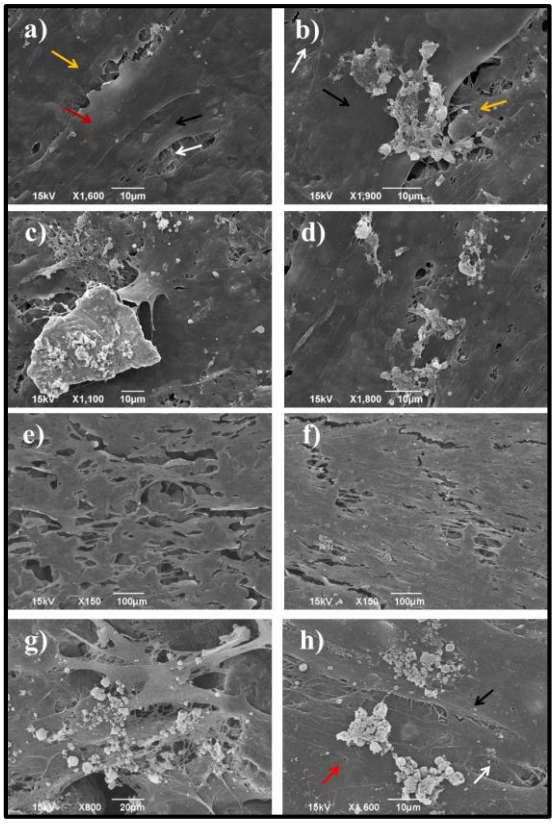

Figure 6.5. SEM micrographs of human MSCs cultured on PCL composite films containing 10 wt % *in situ* HAPclay [a) -d)] after 41 days, PCL composite films containing 20 wt % *in situ* HAPclay [e) -h)] after 42 days indicating stacking of cell layers and mineralized extracellular matrix (ECM) formation during two-stage cell seeding experiment. Different colored arrows in a), b) and h) indicate different cell layers

In case of two-stage cell seeding experiment, the observed stacking in cell layers may be an effect of experimental procedure where the cells seeded initially form the initial cell layer on the substrate and cells seeded second time form the following cell layers. Moreover, it may also be possible that the cells (MSCs) in the initial layer on the substrate may be at an advanced stage of differentiation compared to the cells in the successive layers and needs further studies. This implies the possible utility of two-stage cell seeding experiment in creating an in vitro environment similar to the one known to exist during embryonic stages of bone formation. MSCs were also able to attach to the PCL/*in situ* HAPclay composite scaffolds [Figure 6.6. (a-h)] and showed both spherical and flat morphology. Some of the SEM micrographs in Figure 6.6. also indicate MSCs having interdigitated membrane features possibly containing adhering junctions [86]. In a separate experiment to study the infiltration of MSCs in the PCL/*in situ* HAPclay composite scaffolds, it was observed that the MSCs were able to infiltrate the scaffolds at depths of 3.5 mm and 6 mm from the scaffold surface [Figure 6.7. (a-i)]. SEM micrographs in Figure 6.7. (a-i) also indicate differences in morphology of the infiltrated MSCs and those attached to the scaffold surface. MSCs attached on the scaffold surface appear to have a flat morphology along with the interdigitated membrane features. MSCs that infiltrated the interior regions of the scaffold seem to have longer filopodia and also appear to be clustered while exhibiting relatively complex cellular configurations. Differences in microenvironment at the surface and in the interior regions of the PCL composite scaffolds may be one of the factors that can be attributed to the observed differences in morphology of the MSCs. Cell morphology is known to be affected by dynamic reorganization of cytoskeletal filaments and also related to cell signaling cascades, protein synthesis along with other vital cellular functions. Thus, the MSCs in the interior regions of the PCL composite scaffolds possibly experience different signaling cascades

compared to the MSCs at the scaffold surface with this further having an effect on their protein synthesis and other functions.

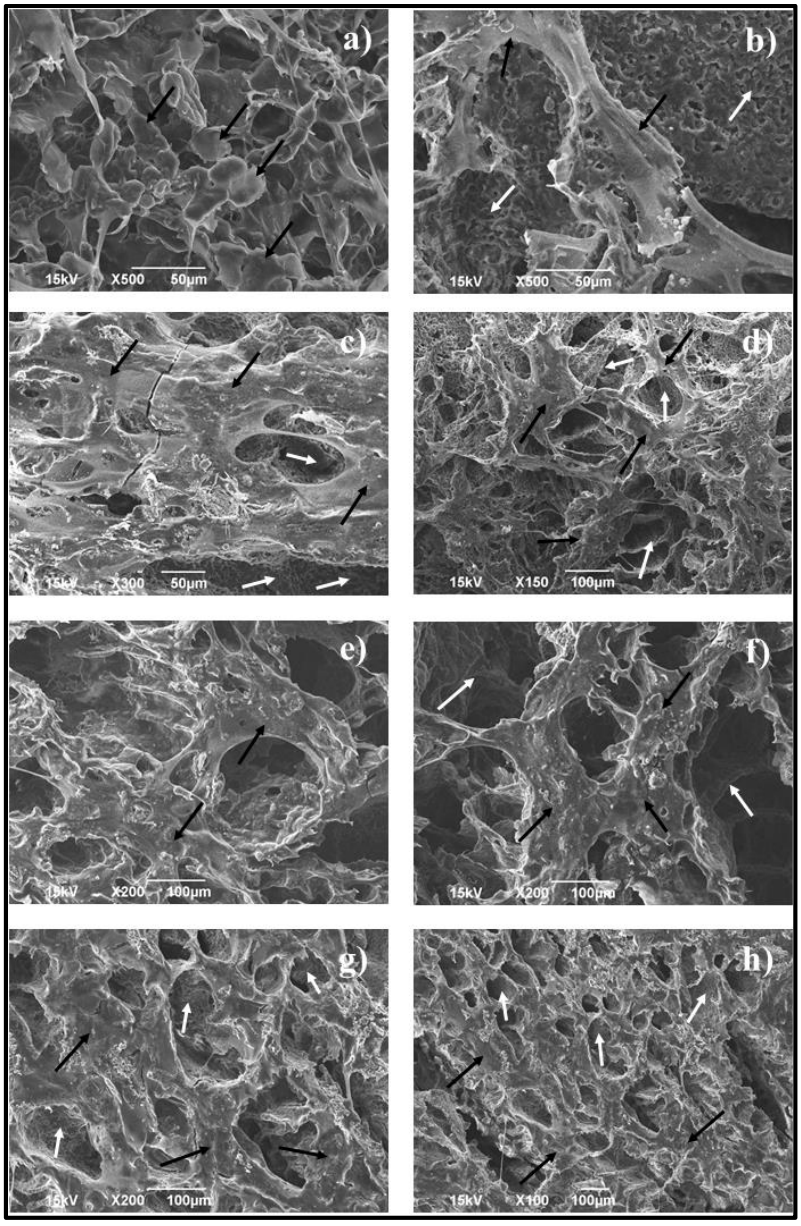

Figure 6.6. SEM micrographs of human MSCs cultured on PCL composite scaffolds after 11 days: PCL scaffolds containing 10 wt % *in situ* HAPclay [a),b)], PCL scaffolds containing 20 wt % *in situ* HAPclay [c),d)] and after 34 days: PCL scaffolds containing 10 wt % *in situ* HAPclay [e), f)], PCL scaffolds containing 20 wt % *in situ* HAPclay [g),h)]. Black arrows indicate cells that appear to have spherical morphology and flat morphology (either conforming to scaffold pore walls or bridging the pores). White arrows indicate regions of scaffold pore walls/material

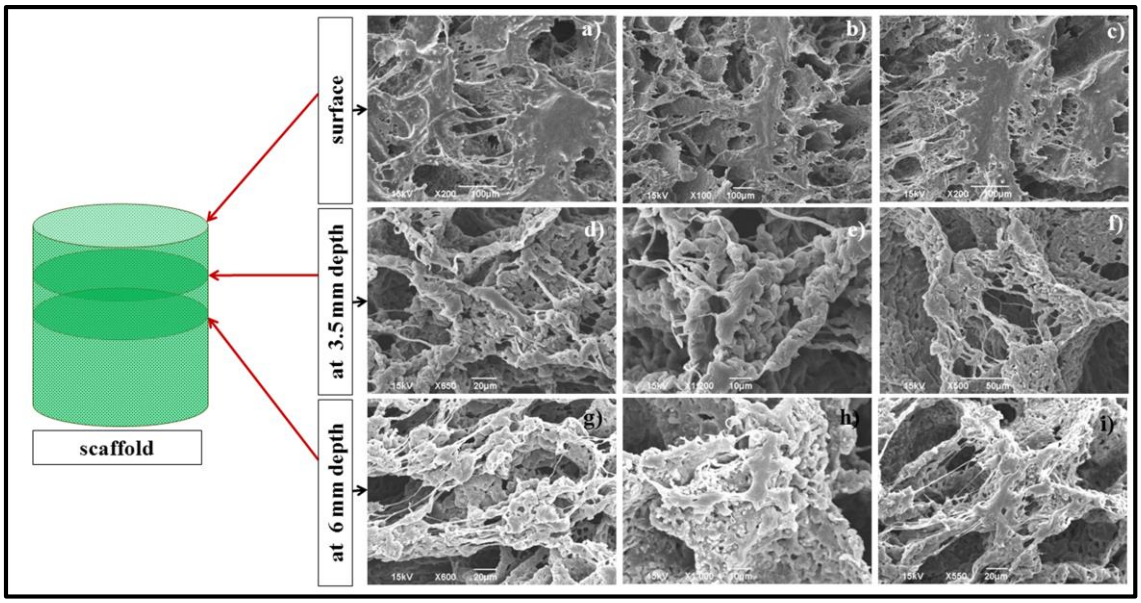

Figure 6.7. SEM micrographs of human MSCs on scaffold surface [a) - c)], at 3.5 mm depth from scaffold surface [d) – f)] and at 6 mm depth from scaffold surface [g) – i)] in case of PCL scaffolds containing 10 wt % *in situ* HAPclay after 20 days of culture. Images d) - h) indicate MSC infiltration in PCL/*in situ* HAPclay scaffolds and also show that the infiltrated cells appear to be clustered and have relatively complex cellular configuration compared to the cells on scaffold surface

6.3.2. Cell Viability

MTT assay indicated the viability of human MSCs on PCL/*in situ* HAPclay composite films [Figure 6.8.] and scaffolds [Figure 6.9.]. Statistical similarity (insignificant differences) between the absorbance values (;live cells) can be seen in case of PCL films containing 10 wt % in *situ* HAPclay and PCL films without *in situ* HAPclay. In case of PCL films containing 20 wt % *in situ* HAPclay and PCL films without *in situ* HAPclay, significant differences in absorbance values can be observed (after 10 days and 23 days). Insignificant differences can be seen between absorbance values for PCL scaffolds containing 10 wt % *in situ* HAPclay and PCL scaffolds without *in situ* HAPclay except for data obtained after 10 days culture. Significant differences between absorbance values are observed for PCL scaffolds containing 20 wt % *in situ* HAPclay and PCL scaffolds without *in situ* HAPclay. PCL composite scaffolds containing

20 wt % *in situ* HAPclay also show lower mean absorbance values compared to PCL scaffolds without clay at all data points. Studies have suggested that MSCs can go through complex cellular events such as "predifferentiation growth arrest," "nonterminal" and "terminal" differentiation that are involved in their unified control process of proliferation and differentiation [68, 90]. Recently it has been reported that a considerable heterogeneity exists in the division capabilities of MSCs in a single passage constituted of multiple generations [91]. A smaller fraction of the original cell numbers is mostly responsible for the increase in cell numbers in a single passage and a large fraction of the original cells do not undergo cell division. It was also reported that a size heterogeneity exists between MSCs in a single passage where the larger cells do not divide or self-replicate. The numerous complexities associated with MSCs along with yet incomplete understanding about the interrelationship between their proliferation and differentiation makes it difficult to conclude about the effect of material (PCL/*in situ* HAPclay composites) on cell proliferation from MTT assay results.

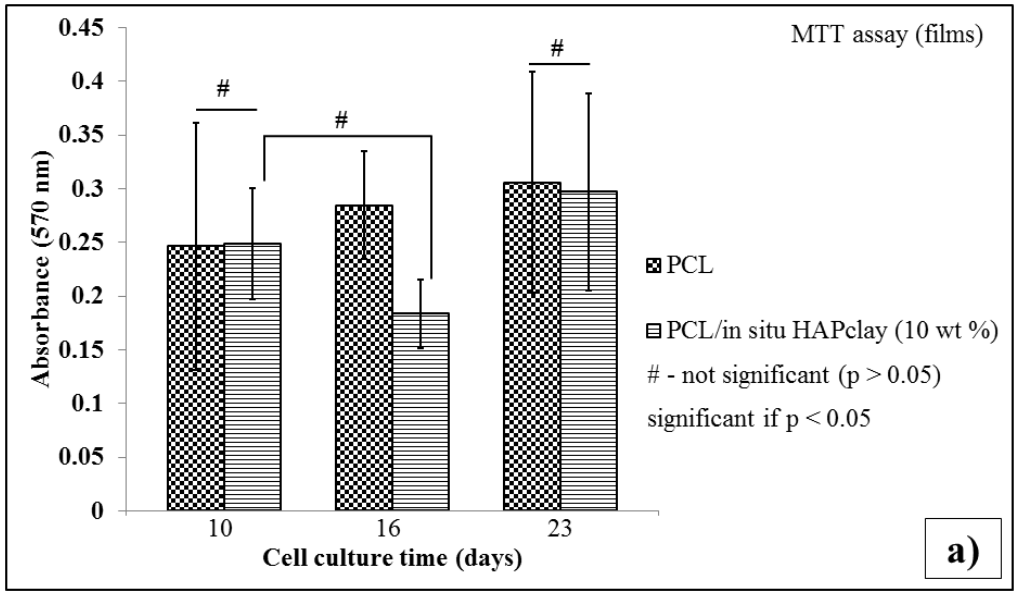

Figure 6.8. Comparative results from MTT assay [a)], ALP assay [b)] for PCL composite films containing 10 wt % *in situ* HAPclay and MTT assay [c)], ALP assay [d)] for PCL composite films containing 20 wt % *in situ* HAPclay

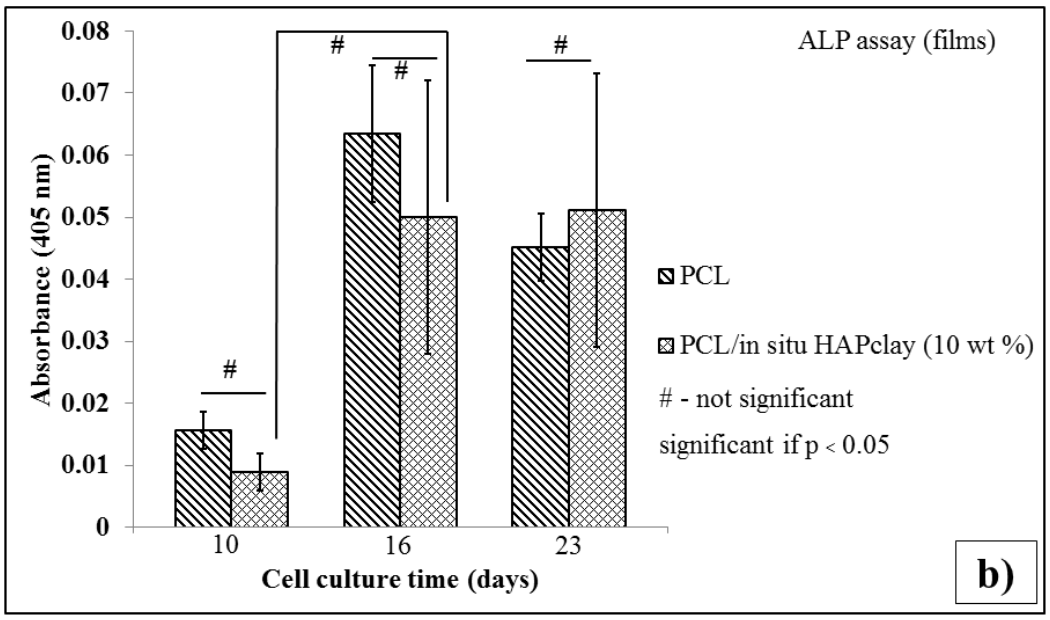

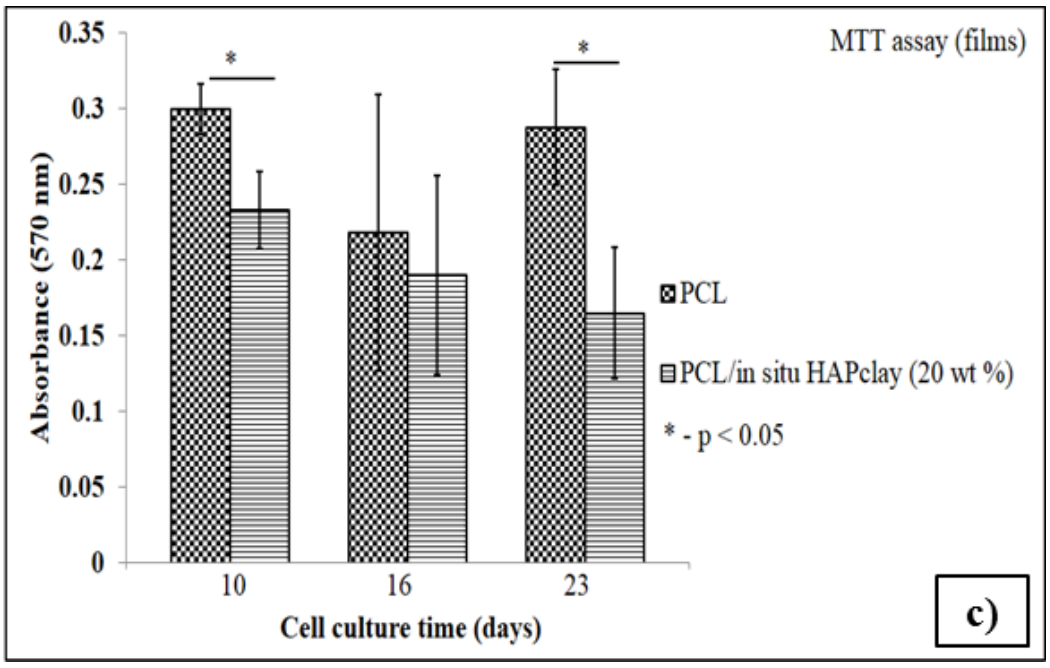

Figure 6.8. Comparative results from MTT assay [a)], ALP assay [b)] for PCL composite films containing 10 wt % *in situ* HAPclay and MTT assay [c)], ALP assay [d)] for PCL composite films containing 20 wt % *in situ* HAPclay (continued)

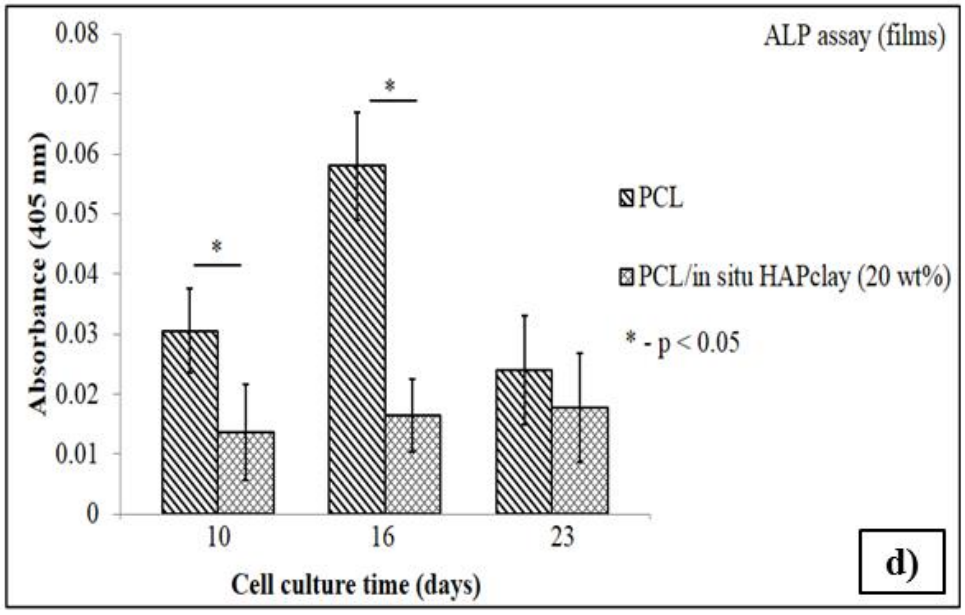

Figure 6.8. Comparative results from MTT assay [a)], ALP assay [b)] for PCL composite films containing 10 wt % *in situ* HAPclay and MTT assay [c)], ALP assay [d)] for PCL composite films containing 20 wt % *in situ* HAPclay (continued)

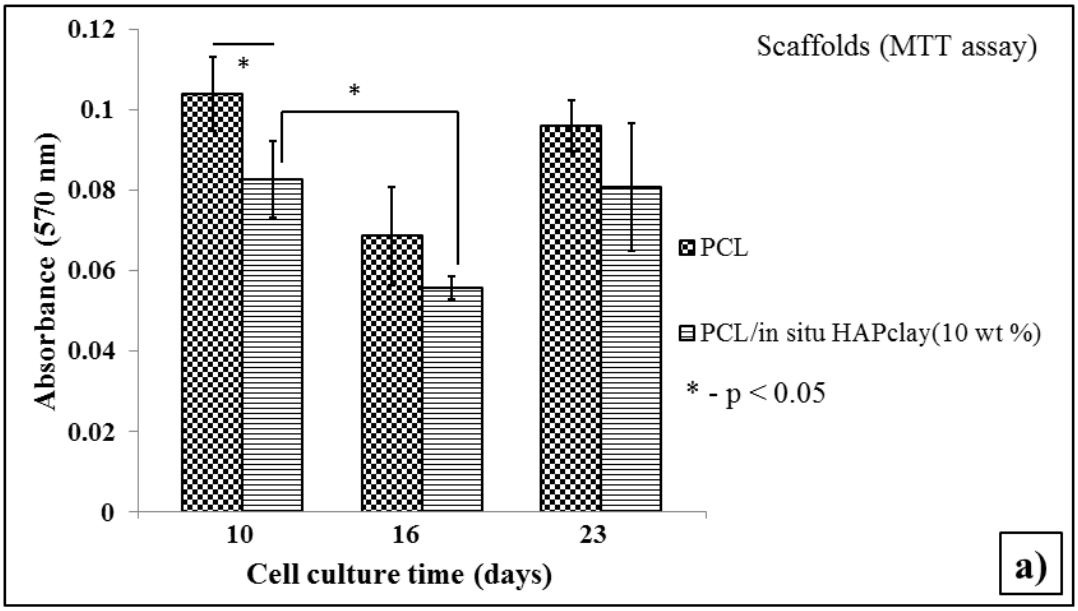

Figure 6.9. Comparative results from MTT assay [a)], ALP assay [b)] for PCL composite scaffolds containing 10 wt % *in situ* HAPclay and MTT assay [c)], ALP assay [d)] for PCL composite scaffolds containing 20 wt % *in situ* HAPclay

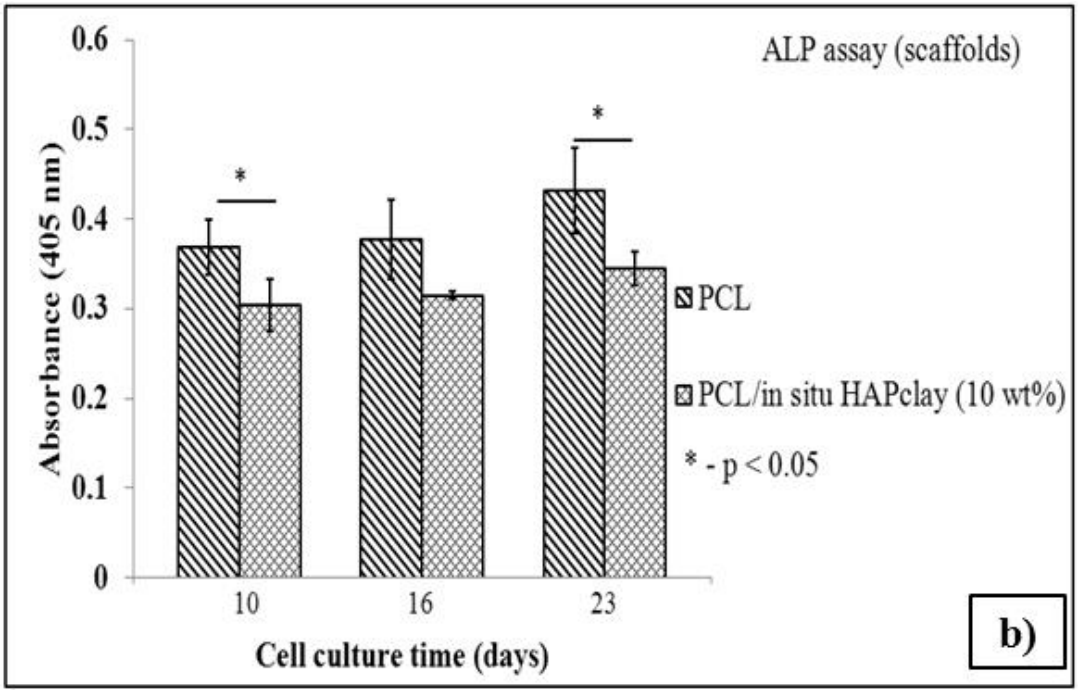

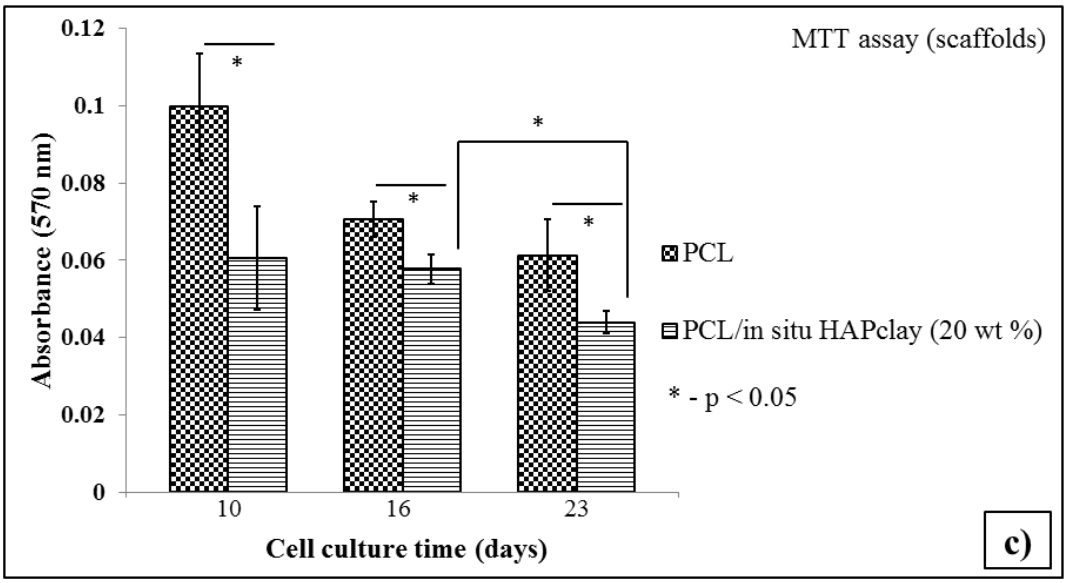

Figure 6.9. Comparative results from MTT assay [a)], ALP assay [b)] for PCL composite scaffolds containing 10 wt % *in situ* HAPclay and MTT assay [c)], ALP assay [d)] for PCL composite scaffolds containing 20 wt % *in situ* HAPclay (continued)

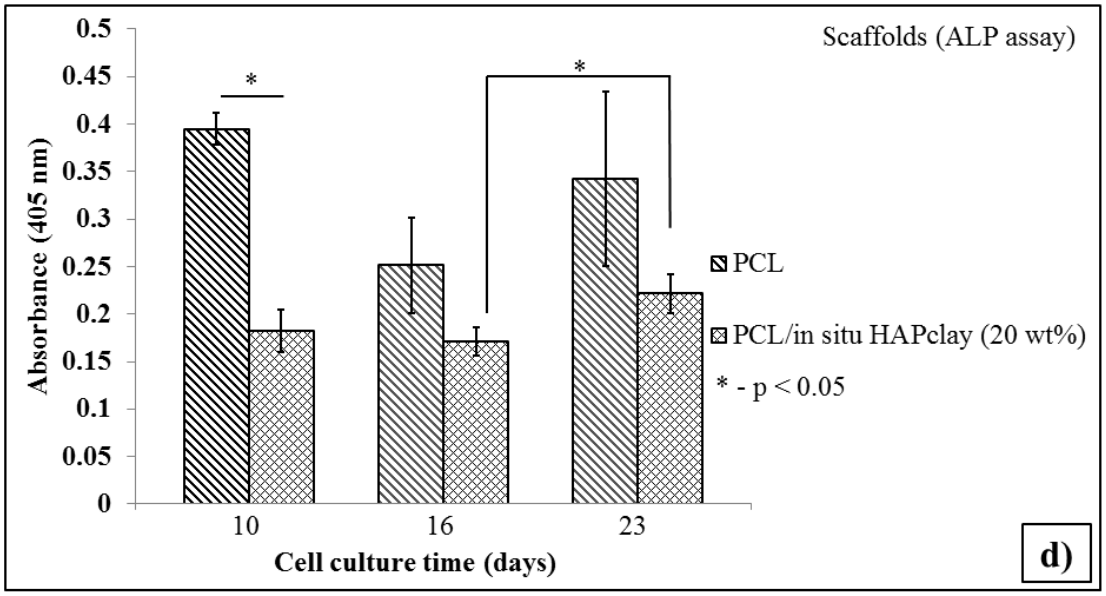

Figure 6.9. Comparative results from MTT assay [a)], ALP assay [b)] for PCL composite scaffolds containing 10 wt % *in situ* HAPclay and MTT assay [c)], ALP assay [d)] for PCL composite scaffolds containing 20 wt % *in situ* HAPclay (continued)

6.3.3. Cell Differentiation

Alkaline phosphatase (ALP), a metalloenzyme present in plasma membrane, is known as biochemical marker of osteoblast phenotype and used to study the differentiation of MSCs towards osteogenic lineage. ALP assay indicated the differentiation of MSCs on PCL/*in situ* HAPclay films [Figure 6.8.] and scaffolds [Figure 6.9.]. ALP activity was not normalized to the total protein content. Due to the possibility of extracellular matrix (ECM) formation on PCL/*in situ* HAPclay films and scaffolds (also indicated by figures 6.4., 6.5 and 6.7) seeded with MSCs during cell culture, the proteins present in the ECM may get included while estimating the total protein content. There are uncertainties whether the current methods (such as RC DC assay) to estimate protein content specifically quantify the intracellular proteins or both intracellular and extracellular proteins. Inclusion of ECM proteins in the total protein content may affect the results since total intracellular protein content (proportional to cell numbers) is required for data normalization. Insignificant differences between absorbance values obtained from MTT assay

for PCL/*in situ* HAPclay (10 wt %) films and PCL films without *in situ* HAPclay at the same time points (e.g. 16 and 23 days) suggest that the ALP activity is unlikely to be significantly affected by cell numbers in case of PCL films containing 10 wt % *in situ* HAPclay. Increase in mean absorbance values was observed in case of these films after 10 days of culture but the differences in mean values were not statistically significant ($p > 0.05$). ALP activity was lower in case of PCL films containing 20 wt % *in situ* HAPclay compared to PCL films without *in situ* HAPclay and is more likely to be affected by the differences in absorbance values (;cell numbers) obtained from MTT assay at this time point. Though lower ALP activity was observed in case of PCL/*in situ* HAPclay (20 wt %) films compared to the PCL films after 16 days culture, insignificant differences in absorbance values (;cell numbers) at this time point obtained from MTT assay suggests that the ALP activity is more likely to be affected by other factors (explained later) rather than the cell numbers. Similar observation about ALP activity can also be made in case of PCL/*in situ* HAPclay scaffolds containing 10 wt % *in situ* HAPclay for comparative data obtained at time point of 23 days. Insignificant differences between ALP activity of PCL scaffolds with 20 wt % *in situ* HAPclay and PCL scaffolds (at days 16 and 23) with higher mean absorbance values (ALP activity) for PCL scaffolds. This can be attributed to a combination of statistically higher absorbance values (proportional to cell numbers) from MTT assay for PCL scaffolds and other factors affecting ALP activity.

ALP known to be associated with cell membrane and matrix vesicles is considered to be involved in the initiation of mineralization by hydrolyzing organic phosphates to release inorganic phosphates at mineralization sites [92] and may also cause increase in local pH to precipitate apatite [93]. Decrease in ALP activity has been associated with mineralization due to its adsorption to the mineral being formed and loss of metal ions from its active site [94]. This

may be one of the factors for the comparatively lower ALP activity observed in case of PCL/*in situ* HAPclay films and scaffolds mentioned earlier. ALP is also considered as a marker for early stage of osteogenic differentiation and has higher expression in pre-osteoblasts that represent one of the transitional stages of differentiation of stem cells to osteoblasts capable of synthesizing extracellular matrix (ECM). Other factors affecting ALP activity can thus include the differences in differentiation stage of MSCs (e.g., ALP negative osteoprogenitor cells and ALP positive pre-osteoblasts [95, 96] cultured on composites (scaffolds and films) with and without *in situ* HAPclay.

6.3.4 Alizarin Red S Staining

Alizarin Red S, a dye known to develop red color on forming a complex with calcium, was used to stain the PCL/*in situ* HAPclay (10 wt %) films seeded with MSCs. Figure 6.10. (b,c) indicates appearance of red color with some regions in these images showing relatively intense red color. Appearance of red color indicates presence of calcium and thereby formation of mineralized extracellular matrix (ECM) by the MSCs. The irregularly shaped regions (100-200 μm) of relatively intense red color seen in the images may possibly be cell clusters/nodules with higher calcium concentration. Considering the presence of calcium in *in situ* HAPclay incorporated in the PCL composite film and for making the formation of mineralized ECM more evident in case of PCL composite films, unseeded PCL/*in situ* HAPclay (10 wt %) film was stained with Alizarin Red S. Red colored spots (~ 80 μm and below) seen in Figure 6.10. (a) indicate the presence of calcium in these films. On comparison with PCL/*in situ* HAPclay (10 wt %) films seeded with MSCs, it was observed that irregularly shaped regions (similar to one delineated in Figure 9.10. (b) with relatively intense red color are absent in case of unseeded PCL/*in situ* HAPclay (10 wt %) films. Besides this, red color seen in Figure 6.10.(b, c) for MSC

seeded PCL composite films appears to be well dispersed over the region of images compared to the relatively discrete red colored spots seen in case of image for unseeded PCL composite film. The relatively large and bright yellow colored regions interspersed among these red spots possibly indicate absence of calcium and such regions appear to be less in case of images for MSC seeded PCL composite films. The formation of mineralized ECM on MSC seeded PCL/*in situ* HAPclay (10 wt %) films also indicated differentiation of MSCs towards osteogenic lineage and possibly the last stage of osteoblast differentiation [97, 98]. Also, mineralized ECM formation indicated the osteoinductive and osteoconductive properties of PCL/*in situ* HAPclay composites due to the absence of osteogenic supplements in the cell culture medium used for experiments.

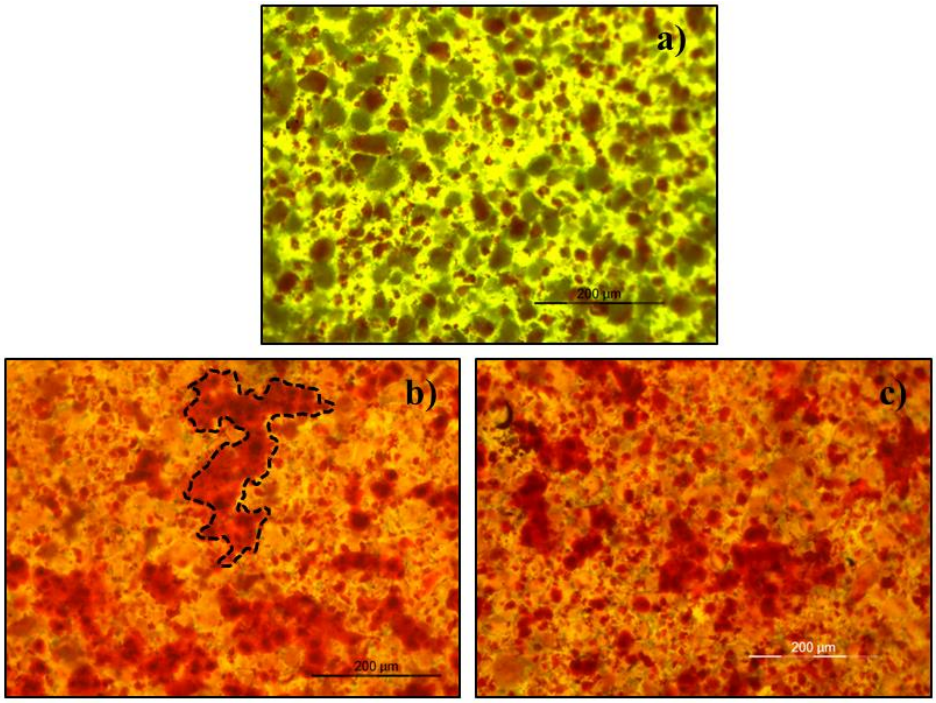

Figure 6.10. Phase contrast images of a) Alizarin Red S stained PCL/*in situ* HAPclay (10 wt %) film, b) PCL/*in situ* HAPclay films seeded with human MSCs after Alizarin Red S staining (culture time 41 days) indicating mineralized extracellular matrix (ECM) formation. One of the irregularly shaped regions of intense red color in image b) delineated by dotted line may possibly be mineralized ECM in cell nodules/clusters having higher calcium concentration. Scale bar -200 µm

6.3.5. Atomic Force Microscopy (AFM)

6.3.5.1 Sub-micron Scale Structure of Mineralized ECM

Lower levels of structural hierarchy arising from arrangement of hydroxyapatite (HAP) with self-assembled collagen at the nanoscale level and interaction between these two components (viz., HAP and collagen) across different scales contribute to the high mechanical properties of bone. Studying the sub-micron scale structure of engineered bone or mineralized ECM generated from cell-material interactions in vitro can be useful for comparative assessment of their nano/microstructural components with their natural bone counterparts. Figure 6.11. (a-f) shows 3D AFM height and phase images of mineralized ECM formed on PCL/*in situ* HAPclay (10 wt %) composite films by human MSCs (also discussed earlier under section 3.4). Alizarin Red S staining was performed prior to AFM imaging to confirm positive staining and thus mineralization of ECM formed by MSCs. Collagen fibrils having a width/diameter in the 70-100 nm range are visible in the phase images [Figure 6.11. (b, d)] and also appear to have banded features similar to collagen fibrils in natural bone. These banded features represent gap (hole) and overlap zones resulting from characteristic "quarter-staggered" arrangement of collagen fibrils in natural bone. Identification of collagen by different microscopy techniques (e.g. transmission electron microscopy, AFM) via presence of banded features has been reported in several studies [99-104]. Besides appearing to be arranged parallel to each other, the collagen fibrils also seem to be in the process of forming fibers by associating with each other. The associated fibrils seem to have formed bundles having width approximately in 0.85-1.00 μm range [indicated by black dotted arrows in Figure 6.11. (a)]. The AFM images also indicate considerable mineralization and presence of irregularly shaped mineral particles having size approximately in 20-330 nm range.

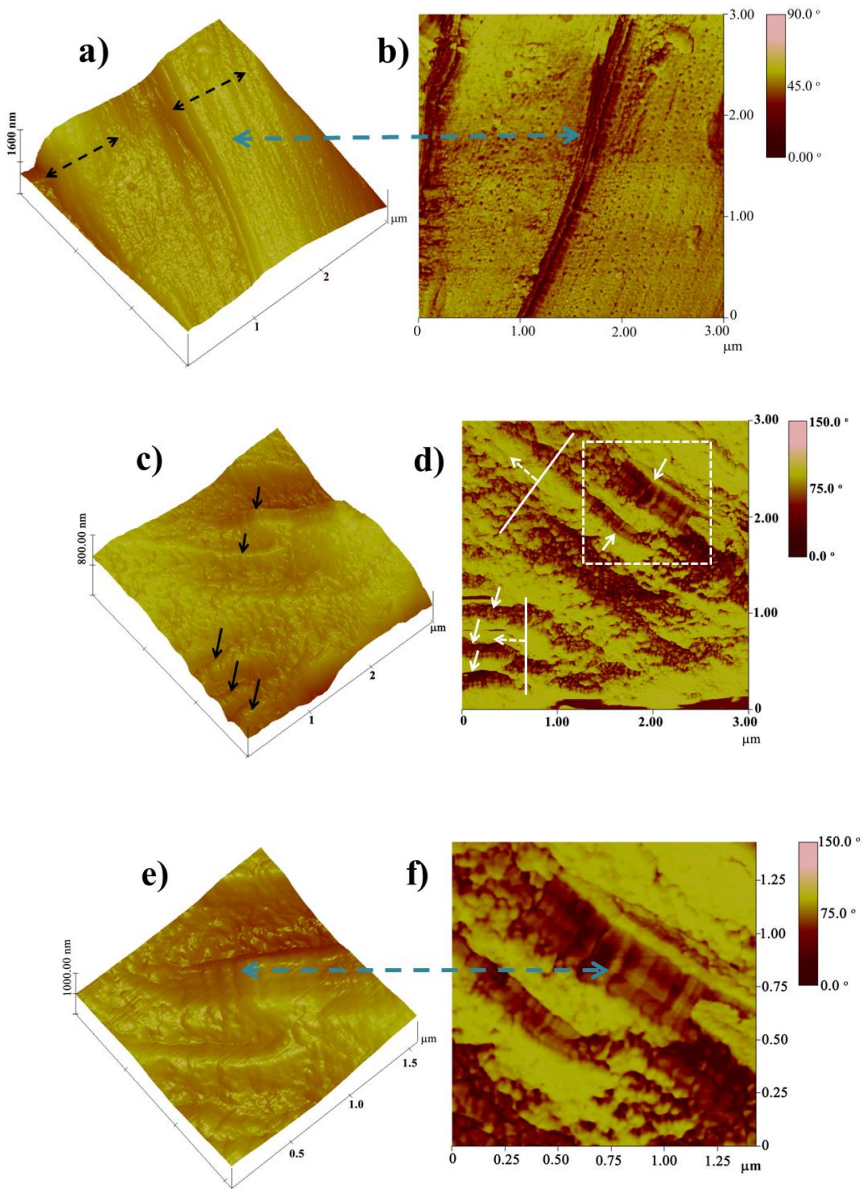

Figure 6.11. AFM 3D height images/surface plots [a), c), e)] and phase images [b), d), f)] showing sub-micron scale structure of mineralized ECM formed by MSCs on PCL/*in situ* HAPclay (10 wt %) films. Dotted black arrows in image a) indicate formation of collagen fibril bundles. Banded features observed in images b), d), f) (more evident in image f) indicate presence of collagen (explanation under section 6.3.5.1). Black arrows in image c) and smaller white arrows in image d) indicate "fish scale" packing of mineral particles over collagen fibrils. Solid white lines with dotted arrow at the center (image d) indicate orientations of different groups of collagen fibrils. Dotted square in image d) represents the zoomed region shown in images e) and f)

The mineral particles appear to overlay the collagen fibrils in some regions and are oriented both parallel and perpendicular to the long axis of collagen fibrils. Also, the mineral particles appear to be fused with each other to form mineral layers/sheets. Figure 6.11. (c, d) indicates presence of "fish scale" packing [101] of mineral particles over the collagen fibrils (indicated by black arrows in 3D height image and white arrows in phase image). This type of packing [more evident in zoomed regions shown in Figure 6.11. (e) & Figure 6.11. (f)] involves mineral platelets arranged along the long axis of collagen fibrils with the z-axis of these mineral platelets perpendicular to the fibril axis. Figure 6.11.(b) further indicates presence of groups of mineral overlaid fibrils with fibrils in the same group parallel to each other but fibrils in different groups oriented in different directions (indicated by white solid lines with dotted arrow at the center). The dimensions of banded features showing repetitive patterns in collagen fibrils at a few subportions of the fibrils were found to be approximately 64-70 nm. Considerable mineralization as indicated by the AFM images caused most of the collagen fibrils to be overlaid by mineral particles that led to insufficient demarcation of the gap/overlap banded pattern in AFM images of collagen fibrils. This made it difficult to measure the size of the morphological features along the length of collagen fibrils. Dependence of AFM Tapping Mode™ imaging mode on factors such as sample topography, sample-tip interactions, surface stiffness and experimental parameters may have further contributed to this insufficient demarcation of gap/overlap regions in the collagen fibrils. Presence of variation in dimensions of banding pattern (values greater or less than the widely reported 67 nm) observed in collagen fibrils can be attributed to several factors [105]. One of them is the difference in local mechanical stresses under in vitro (cell culture) and in vivo (in functional bone inside the body) conditions. Also, different cells participating in collagen fibrillogenesis via "fibropositors" may experience

different mechanical stresses that may further affect the dimensions of the banding pattern [105]. Additionally, cell-related factors such as expression levels of homotrimeric collagens and minor collagens (types V and XI) along with posttranslational modifications can further influence the dimensions of the banding pattern.

6.3.5.2 Surface Morphology of PCL/*In Situ* HAPclay Composite Films

Surface morphological features in the micron to sub-micron size range have been reported for their effect on cell adhesion, morphology, migration, proliferation, differentiation, contact guidance [106-108] and possible role in modulating foreign body response [109]. Figure 6.12. (a-d) shows AFM images (rotated 3D surface plots) of PCL and PCL/*in situ* HAPclay (10 wt %) films. Disordered morphological features in the micron to sub-micron scale were seen in case of PCL films without *in situ* HAPclay [Figure 6.12. (a, b)]. Shapes of these morphological features varied from elongated, globular to irregular. The size of most of these morphological features was in the sub-micron range (below 1µm-100 nm) with some of them being in the nanoscale range (< 100 nm). A few relatively larger, elongated features in 500 nm-1µm size range were also observed. Closer observation of the images showed some of these larger features to be composed of smaller globular morphological features. In case of PCL composite films containing 10 wt % *in situ* HAPclay surface morphological features had similar shapes to those observed in case of PCL films without *in situ* HAPclay [Figure 6.12.(c,d)]. In addition to the observation of some globular features in the 100 nm-200 nm, it was also seen that the elongated features of 1-2 µm size appeared to be formed by side-by-side arrangement of short, thick features of sub-micron size. Thus, a certain degree of order seems to exist in the substructure of the elongated features in case of PCL composite films. Such substructural arrangement of short, thick features was not observed in the elongated features present on surface of PCL films without

in situ HAPclay. Overall, the shorter dimension (width) of most of the elongated morphological features in case of PCL films with *in situ* HAPclay appeared to be larger (250 nm -1µm range) than those seen in case of PCL films (< 250 nm). Osteoinductive properties have been attributed to topography and geometry in previous studies involving biomaterials for bone formation [6]**.** The subtle differences between topographical features of PCL/*in situ* HAPclay composite films compared to PCL films among various other factors may thus have contributed to the osteoinductivity (inferred from SEM studies and Alizarin Red S staining) of PCL/*in situ* HAPclay composite films. Representative AFM phase images [Figure 6.13. (a, b)] of PCL and PCL/*in situ* HAPclay films indicate presence of lamellae known to form spherulites in semicrystalline polymers. These lamellae/lamellar features are polymer crystallites composed of folded polymer chains and are considered to radiate outward from the center of polymer spherulites. Existence of such lamellae in "flat-on" and "edge-on" orientations have been reported in case of polymer films prepared by solution casting and solvent evaporation [110, 111]. The lamellae seen in the phase images seem to have a "flat-on" orientation both in case of PCL and PCL/*in situ* HAPclay (10 wt %) films. Also, these lamellae appear to be made of short and discrete features due to which their substructure seems to have a granular appearance. Lamellae in case of PCL films had widths in the nanoscale (< 100 nm) range and 100-150 nm range whereas in case of PCL/*in situ* HAPclay (10 wt %) films most of the lamellar widths were approximately in the 100-500 nm range. Polymer crystallization involving nucleation and subsequent growth of lamellae may proceed in a different manner at the complex polymer (PCL) /inorganic (*in situ* HAPclay) interfaces during preparation of PCL/*in situ* HAPclay (10 wt %) films compared to the neat PCL films. The relatively larger lamellar widths observed in case of

PCL/*in situ* HAPclay (10 wt %) films may thus be an effect of *in situ* HAPclay particles on the nucleation and subsequent growth of polymer lamellae.

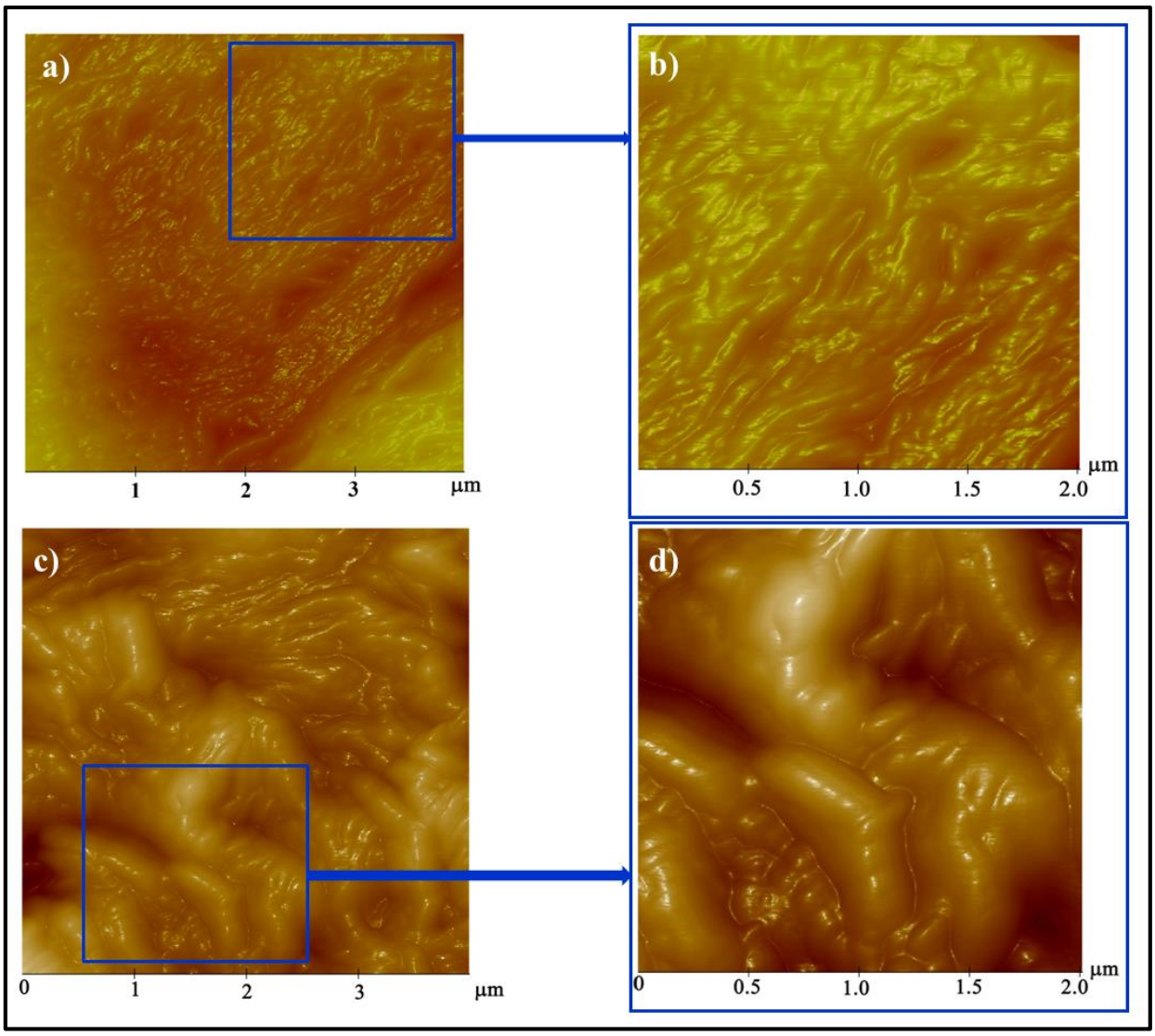

Figure 6.12. AFM images (rotated 3D surface plots) of PCL [a), b)] films, PCL composite films containing 10 wt % *in situ* HAPclay [c), d)]. PCL films appear to have morphological features of different shapes (elongated, globular, and irregular) in the sub-micron range and nanoscale range. PCL composite films also had similar morphological features in 100-200 nm range and 1-2 µm range. The elongated features in case of PCL composite films seem to consist of sub-micron sized features arranged side-by-side

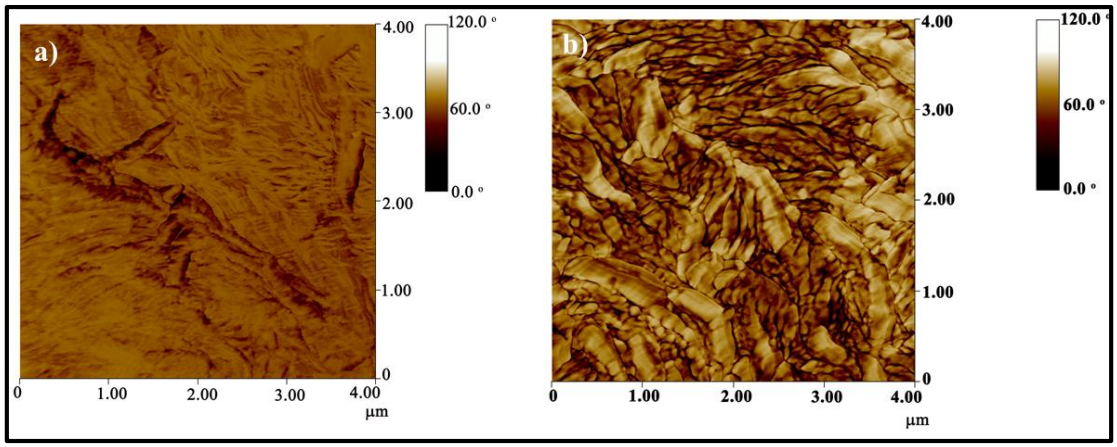

Figure 6.13. AFM phase images of PCL [a)], PCL composite films containing 10 wt % *in situ* HAPclay [b)]. Lamellar features observed in these phase images are polymer crystallites composed of folded polymer chains and appear to have a "flat-on" orientation. Widths of lamellar features in case of PCL films were in the nanoscale range and 100-150 nm range. Lamellar widths in case of PCL composite films were in 100-500 nm range

6.3.6. Nanomechanical Properties of PCL/*In Situ* HAPclay Composite Films

Table 6.1. shows comparative nanomechanical properties (average values of elastic moduli and hardness) of PCL composite films containing *in situ* HAPclay. It was observed that the average elastic moduli and hardness were significantly higher in case of PCL composites containing *in situ* HAPclay compared to PCL. At 1000 µN, the average elastic modulus increased by ~ 592 % and ~ 223 % in case of PCL films containing 10 wt % and 20 wt % *in situ* HAPclay respectively. Similarly, increase in average hardness at this load was ~ 798 % and ~ 290 % in case of PCL films containing 10 wt % and 20 wt % *in situ* HAPclay respectively. At a higher load of 5000 µN, similar trend of increase in nanomechanical properties was observed. For PCL films containing 10 wt % *in situ* HAPclay (at 5000 µN), the average elastic modulus increased by ~ 370 % and the average hardness increased by ~ 587 %. In case of PCL films containing 20 wt % *in situ* HAPclay (at 5000 µN), the average elastic modulus and hardness values increased by ~ 106 % and ~ 97 % respectively. Better dispersion of *in situ* HAPclay in PCL films containing 10 wt % *in situ* HAPclay may be one of the reasons for relatively higher

nanomechanical properties observed in case of PCL films containing 10 wt % *in situ* HAPclay compared to PCL films containing 20 wt% *in situ* HAPclay. Higher nanomechanical properties of the PCL/*in situ* HAPclay composite films compared to PCL can be attributed to several factors such as interfacial interactions between PCL and *in situ* HAPclay, size and distribution of *in situ* HAPclay particles along with the mechanical properties of PCL. The relative decrease in nanomechanical properties at higher load (5000 µN) compared to lower load (1000 µN) may be due to the failure of interfaces in the bulk of the film samples. Such decrease in nanomechanical properties of modified hydroxyapatite (HAP) at higher loads has been reported in one of our previous studies [112]. Cellular processes such as proliferation, migration and differentiation are known to be influenced by mechanical properties of the underlying substrate through complex mechanisms involving conversion of mechanical cues to biochemical signals [113, 114]. Considering the increase in nanomechanical properties of PCL films with the addition of *in situ* HAPclay, it may be possible that *in situ* HAPclay thus plays a role in influencing the behavior of human MSCs.

Table 6.1. Nanomechanical Properties of Polycaprolactone (PCL)/*In Situ* HAPclay composites

Sample	Maximum Load (µN)	Elastic Modulus (GPa)	Hardness (GPa)
Polycaprolactone (PCL) without *in situ* HAPclay	1000	0.406±0.115	0.0421
	5000	0.362±0.096	0.0328
PCL/10 wt % *in situ* HAPclay	1000	2.808±0.641	0.377
	5000	1.702±0.251	0.220
PCL/20 wt % *in situ* HAPclay	1000	1.310±0.413	0.164
	5000	0.745±0.113	0.0635

6.3.7. In Vitro Degradation of PCL/*In Situ* HAPclay Scaffolds

In vitro accelerated hydrolytic degradation of PCL/*in situ* HAPclay composite scaffolds was studied under alkaline conditions (0.1 M NaOH). Studies have shown that non-enzymatic hydrolysis of ester linkages in PCL constitutes the first stage of its in vivo degradation followed

by a second stage involving intracellular degradation of decreased molecular weight, hydrolytically cleaved PCL [48, 115]. Use of alkaline conditions during degradation studies helps to increase the hydrolytic degradation rate of PCL and thus simultaneously simulates the initial in vivo stage of PCL degradation. Possibilities of reversible hydrolytic degradation under acidic conditions [116], effect of temperature on polymer morphology during thermal degradation and lack of degrading enzymes under normal physiological conditions [117] were some of the other factors responsible for the preference of alkaline conditions for degradation studies. Figure 6.14. indicates increase in in vitro degradation of PCL and PCL/*in situ* HAPclay scaffolds over a period of 18 days. Mean weight percent loss values of PCL scaffolds containing *in situ* HAPclay were observed to be higher compared to PCL scaffolds without *in situ* HAPclay over the degradation period. Statistically significant difference in weight percent loss values was observed between PCL and PCL scaffolds containing 20 wt % *in situ* HAPclay after 14 days. Similarly, significant difference in weight percent loss values was also observed between PCL and PCL scaffolds containing 10 wt % *in situ* HAPclay after 18 days. Changes in rate of weight loss percentage were observed for scaffolds over the degradation period indicated by the changing slopes of lines connecting the data points (Figure 9.14. inset). PCL scaffolds without *in situ* HAPclay appear to have lost weight only after 7 days unlike PCL scaffolds with *in situ* HAPclay that appear to show weight loss before 7 days from the start of the experiment. It was also observed that the rate of weight loss percentage was more in case of PCL scaffolds without *in situ* HAPclay from 7 to 18 days compared to the rate of weight loss percentage observed in case of PCL scaffolds containing *in situ* HAPclay over the same time period. Rate of percentage weight loss was more in case of PCL scaffolds containing 10 wt % *in situ* HAPclay during time intervals of 0-7 days, 14-18 days and lower during 7-14 days time interval compared to the PCL

scaffolds containing 20 wt % *in situ* HAPclay. Weight loss during degradation of aliphatic polyesters such as PCL has been reported to occur when oligomeric species resulting from degradation become adequately small (also implying molecular weight decrease to a certain extent) to diffuse in to the surroundings from the bulk [115]. Also, weight loss may not be observed despite cleavage of ester bonds resulting in progressive decrease of molecular weight during the initial stage of degradation. Therefore in case of PCL scaffolds without *in situ* HAPclay though weight loss was not observed till 7 days, hydrolysis of ester linkages may have possibly started before 7 days (also supported by observations made from FTIR data described later). Weight loss observed in case of PCL scaffolds containing *in situ* HAPclay before 7 days can be a result of processes such as ester bond (polymer chain) cleavage, diffusion of oligomers formed by polymer chain cleavage in to the surroundings and erosion of *in situ* HAPclay particles. This also implies possibility of relatively faster reduction in molecular weight of PCL chains to an extent adequate for the diffusion of oligomers in case of PCL/*in situ* HAPclay composite scaffolds compared to PCL scaffolds without *in situ* HAPclay. Higher weight loss seen in case of PCL scaffolds containing *in situ* HAPclay compared to the PCL scaffolds without *in situ* HAPclay can be attributed to several factors. Our previous studies have shown that addition of organomodified clays decreases the crystallinity of PCNs and regions with disrupted crystallinity exist around the organomodified clay particles [35, 118]. Since the crystalline regions in semi-crystalline polymers are more resistant to water (degradation media) ingress than the amorphous regions, it may be possible that water ingress was comparatively higher in PCL scaffolds containing *in situ* HAPclay due to hypothesized presence of regions of disrupted crystallinity around the *in situ* HAPclay particles. Also, calcium phosphate based particles (e.g. tricalcium phosphate) incorporated in PCL based scaffolds have been reported for their effect on

the arrangement of polymer chains that further affects polymer chain hydrolysis. Also, these particles enhance water ingress since they act as "defects" in the polymer and serve as "conductors," "channels" assisting in water diffusion [119]. This indicates possibility of similar effect of *in situ* HAPclay particles on the surrounding polymer (PCL) and transport of water molecules during degradation of PCL/*in situ* HAPclay scaffolds. Taking in to account the mobility of PCL chains at 37°C (temperature used during degradation studies) due to its low Tg (-60°C) and ability to recrystallize [119], the *in situ* HAPclay particles may impede recrystallization of PCL chains in PCL/*in situ* HAPclay composite scaffolds that further affects their crystallinity and thereby their degradation. PCL scaffolds and PCL/*in situ* HAPclay composite scaffolds may also differ in porosity, pore size, pore interconnectivity that affect water (media) access and thus the degradation (extent of hydrolysis).

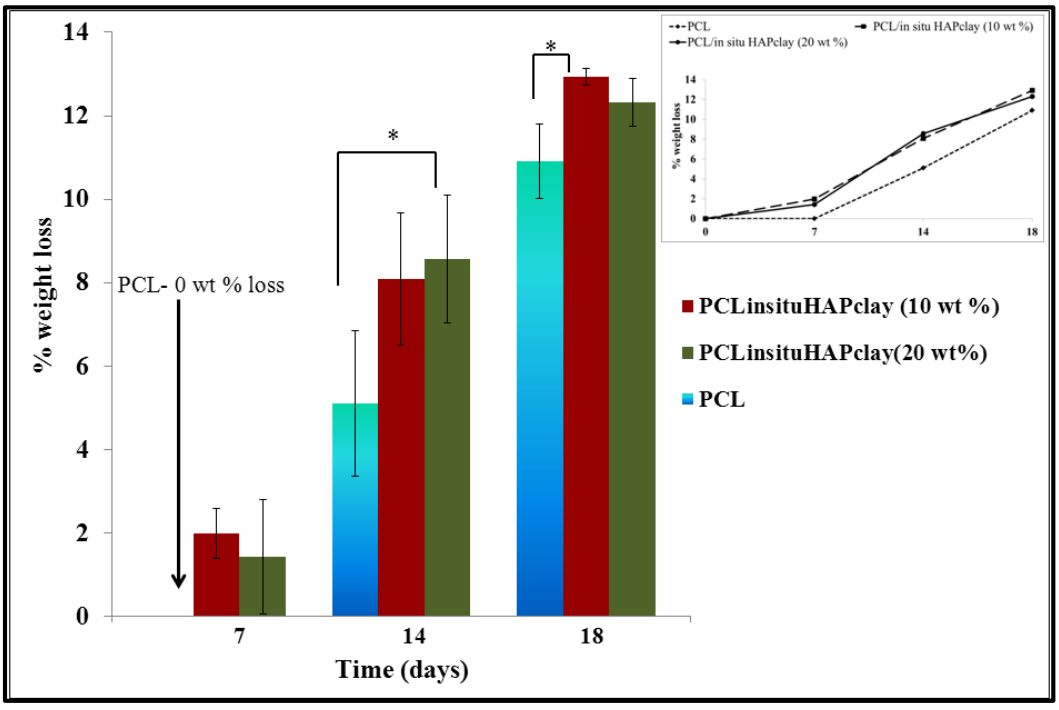

Figure 6.14. Comparative percentage weight loss of PCL composite scaffolds containing *in situ* HAPclay from in vitro degradation experiment under accelerated conditions

Comparative photoacoustic FTIR (PA-FTIR) spectra of in vitro degraded PCL and PCL scaffolds with *in situ* HAPclay are shown in Figure 6.15. and Table 6.2. shows the relevant band assignments. FTIR spectra for scaffolds within the 1860-1530 cm^{-1} wavenumber region show presence of bands close to/at 1558 cm^{-1} (7 days) and 1565 cm^{-1} (14 and 18 days) in case of in vitro degraded scaffold samples. This band not seen in case of undegraded scaffolds can be attributed to the asymmetric stretching of carboxylate groups formed due to the hydrolysis of ester bonds in PCL. It was also observed that in case of PCL scaffolds without *in situ* HAPclay, this band due to the stretching of carboxylate groups was present after 7 days of in vitro degradation though no weight loss was observed after 7 days (discussed earlier). This indicated that the process of PCL chain hydrolysis may have started prior to 7^{th} day during in vitro degradation and the oligomeric species formed were unable to diffuse in to the surroundings. Moreover, the intensity of this band representing carboxylate stretching appeared to increase with degradation time (7-18 days). Bands observed close to/at 1741 cm^{-1} and 1725 cm^{-1} in FTIR spectra of scaffolds (both degraded and undegraded) correspond to carbonyl stretching bands associated with amorphous and crystalline phases in PCL. Differences in widths and heights of these bands can be observed between overlaid FTIR spectra of undegraded and degraded scaffold samples [shown in Figure 6.15. (b, e, f)**]**. This implies changes in crystallinity of the scaffold samples during the degradation process due to the possible rearrangement of PCL chains having considerable mobility at 37°C. Similar differences were observed in widths and heights of bands close to/at 1295 cm^{-1} and 1194 cm^{-1} in overlaid FTIR spectra of scaffolds [Figure 6.15. (c, f, i)]. Bands close to/at 1295 cm^{-1} arise due to C-O and C-C stretching in the crystalline phase of PCL and those close to/at 1194 cm^{-1} have been reported for their sensitivity to orientation [120]. This further suggests rearrangement of PCL chains in the scaffolds during the degradation

process. FTIR spectra of PCL scaffolds containing 10 wt % *in situ* HAPclay within 795-420 cm^{-1} region [Figure 6.15. (j, k)] indicate minor changes (shape, intensity, width) in the band formed by the overlap of phosphate vibrations (close to/at 607 cm^{-1}, 565 cm^{-1}) and out of plane bending vibrations of carbonyl groups in PCL. Shoulder band at 473 cm^{-1} in undegraded PCL/*in situ* HAPclay (10 wt %) scaffold sample appears to show shifts over the degradation period with the highest shift (6 cm^{-1}) observed for scaffolds after 14 days degradation. Although difficulty exists in assigning this shoulder band since it can arise from either Si-O-Si bending vibration in MMT clay or from phosphate vibration in HAP, it can be presumed to be arising from molecular vibrations in *in situ* HAPclay having MMT clay and HAP both as its components. Similar shifts in this shoulder band were also seen in case of PCL/*in situ* HAPclay (20 wt %) scaffolds and it appeared to be absent in spectra of scaffold samples subjected to 18 days of in vitro degradation. The reasons for this apparent absence of the band are yet incompletely understood.

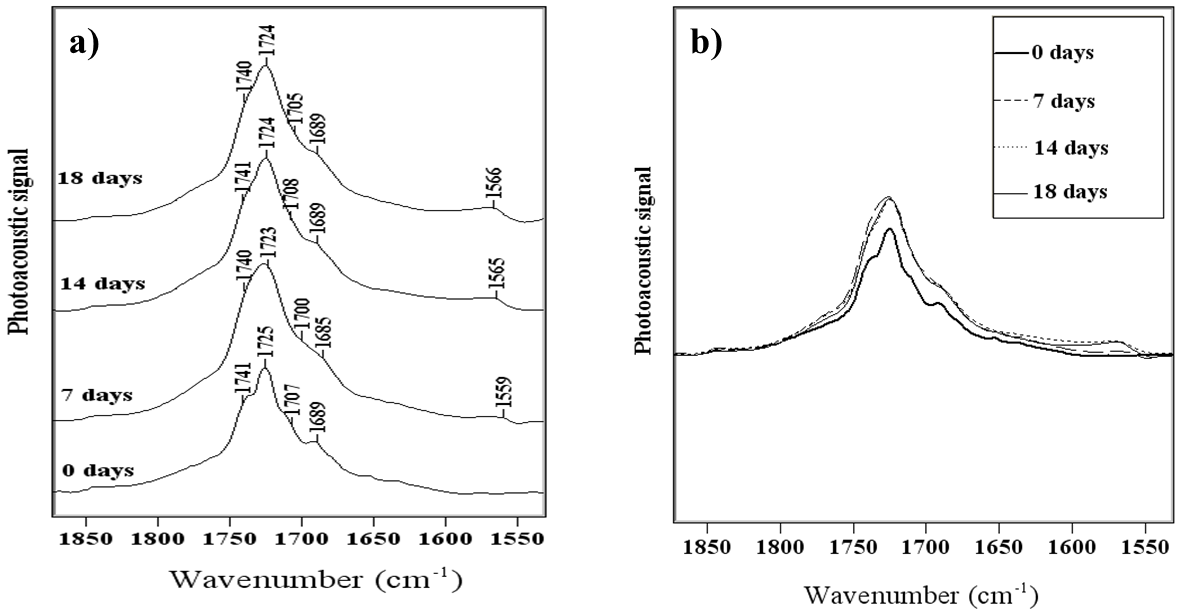

Figure 6.15. Comparative photoacoustic FTIR spectra of PCL scaffolds [a) – c)], PCL scaffolds with 10 wt % *in situ* HAPclay [d) – f), j)], PCL scaffolds with 20 wt % *in situ* HAPclay [g) – i), k)] over 18 days of in vitro degradation under accelerated conditions. Vertical lines a and b represent positions 1295 cm^{-1} and 1194 cm^{-1} in FTIR spectra

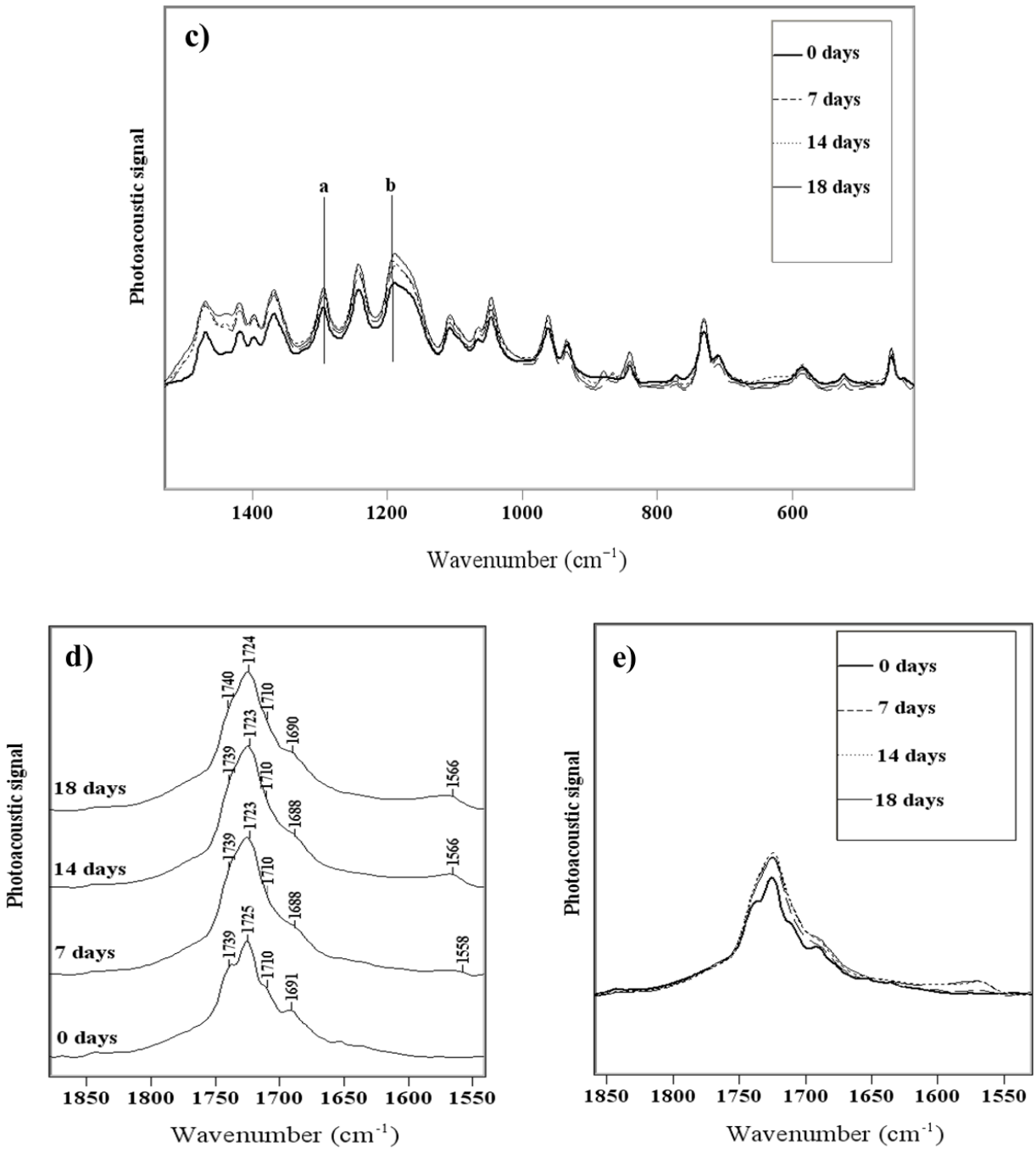

Figure 6.15. Comparative photoacoustic FTIR spectra of PCL scaffolds [a) – c)], PCL scaffolds with 10 wt % *in situ* HAPclay [d) – f), j)], PCL scaffolds with 20 wt % *in situ* HAPclay [g) – i), k)] over 18 days of in vitro degradation under accelerated conditions. Vertical lines a and b represent positions 1295 cm^{-1} and 1194 cm^{-1} in FTIR spectra (continued)

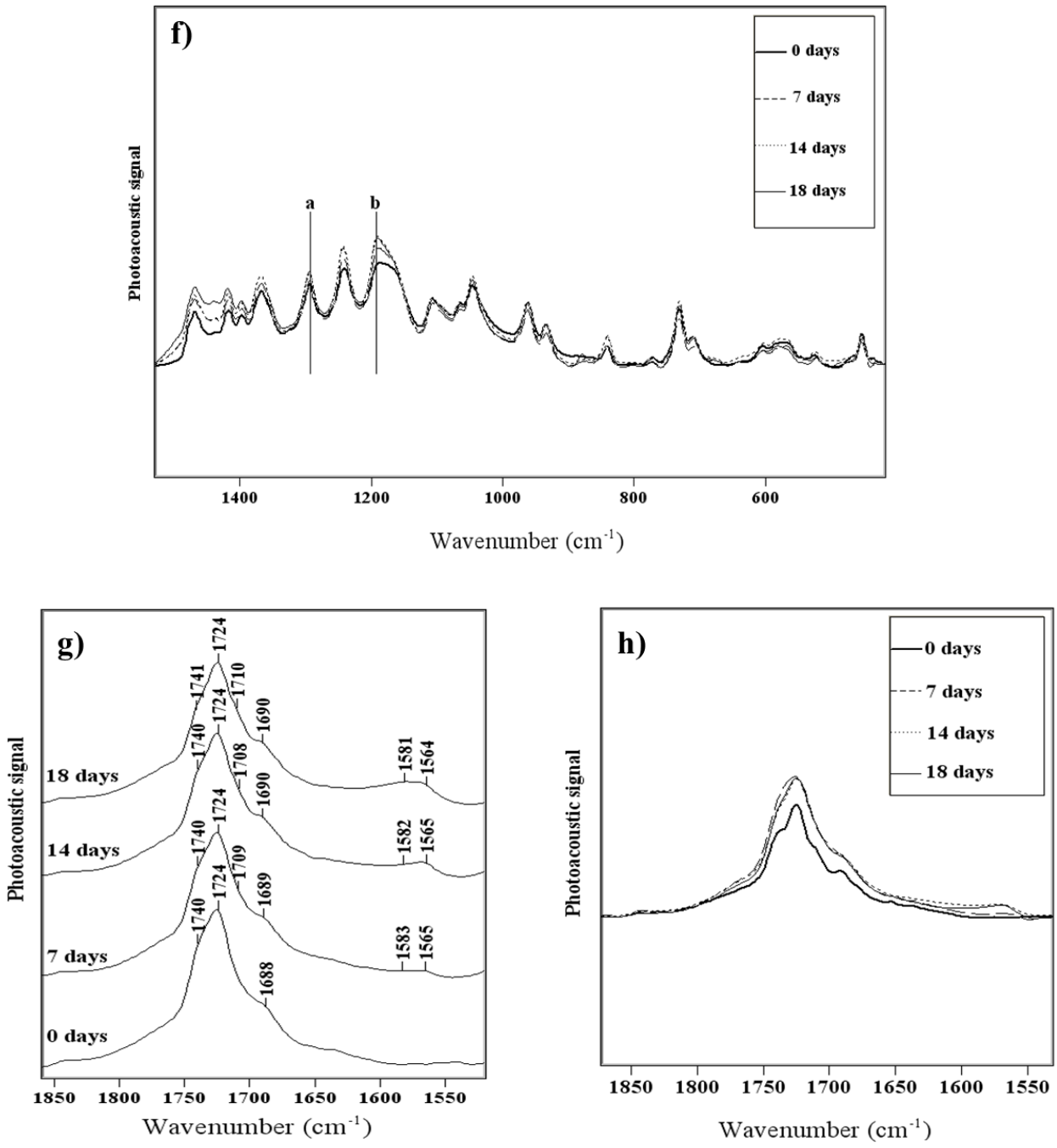

Figure 6.15. Comparative photoacoustic FTIR spectra of PCL scaffolds [a) – c)], PCL scaffolds with 10 wt % *in situ* HAPclay [d) – f), j)], PCL scaffolds with 20 wt % *in situ* HAPclay [g) – i), k)] over 18 days of in vitro degradation under accelerated conditions. Vertical lines a and b represent positions 1295 cm^{-1} and 1194 cm^{-1} in FTIR spectra (continued)

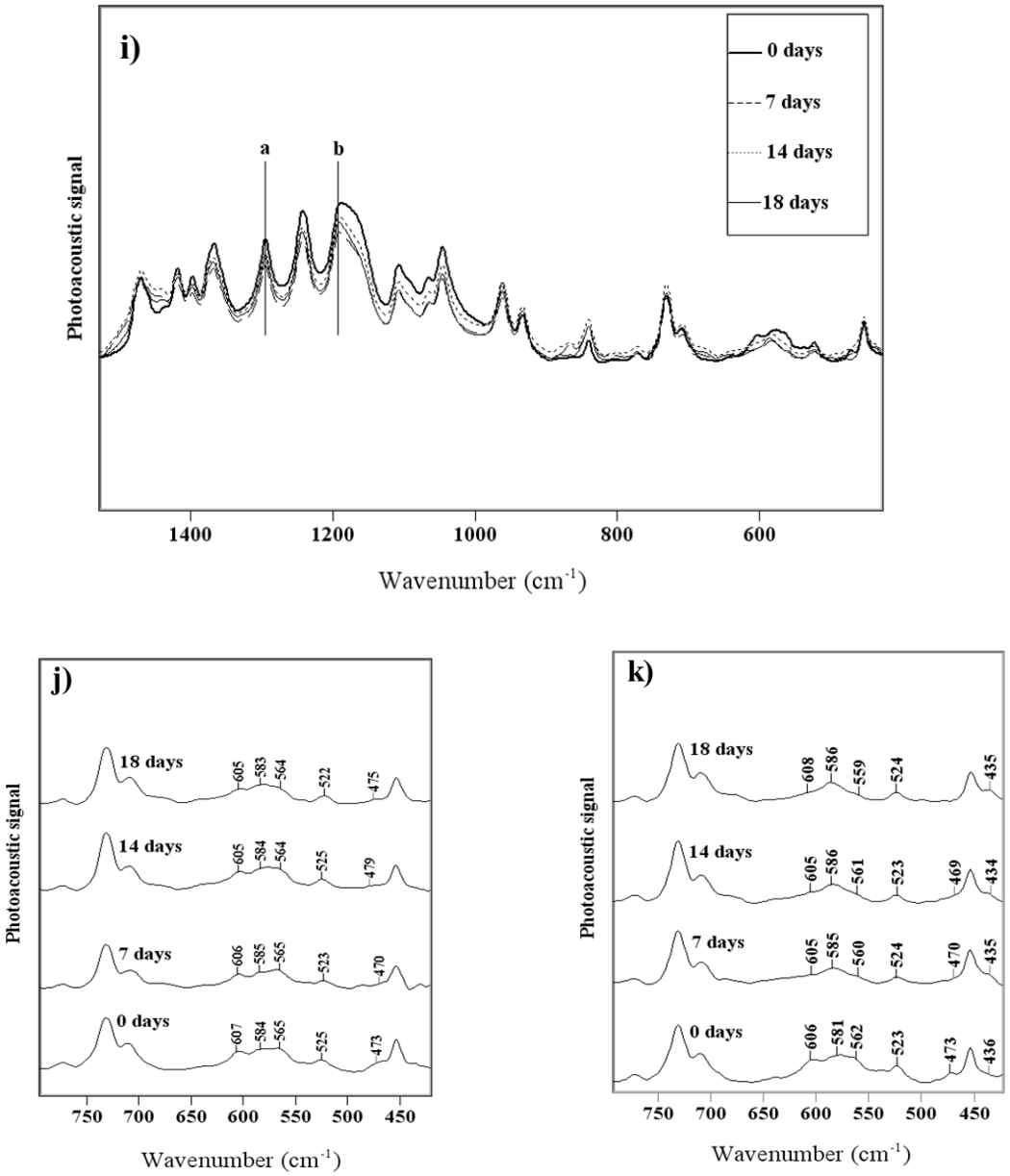

Figure 6.15. Comparative photoacoustic FTIR spectra of PCL scaffolds [a) – c)], PCL scaffolds with 10 wt % *in situ* HAPclay [d) – f), j)], PCL scaffolds with 20 wt % *in situ* HAPclay [g) – i), k)] over 18 days of in vitro degradation under accelerated conditions. Vertical lines a and b represent positions 1295 cm^{-1} and 1194 cm^{-1} in FTIR spectra (continued)

Figure 6.16. (m-r) shows SEM images of scaffolds after 14 days and 18 days of in vitro degradation. Although weight loss was observed in case of all scaffolds at these time points, the overall structure of these scaffolds appeared to remain intact and were retrievable. The effect of in vitro degradation is more evident in Figure 6.16. (a-l) representing SEM images of scaffold

surfaces over the degradation time. Filamentous features (~ 1-3 μm length and below 500 nm width) were observed on surfaces of the degraded scaffolds. These features seen only in case of degraded scaffolds appeared to sprout from the degraded scaffold surfaces either in bunches or individually. The degraded scaffold surfaces thus appeared to be rougher compared to the undegraded scaffold surfaces having a relatively smooth texture. In case of undegraded PCL scaffolds containing *in situ* HAPclay, the scaffold surfaces seemed to have bumps probably due to presence of *in situ* HAPclay particles close the scaffold surface and minuscule defects appeared to surround these *in situ* HAPclay particles. Such defects have been previously reported due to the presence of tricalcium phosphate particles in synthetic polymer matrix and are considered to assist in water ingress in the scaffolds [119]. Also, intactness of the overall structure of the scaffolds over the degradation period and changes observed in scaffold surface morphology due to degradation indicate that the scaffolds may have undergone a surface degradation pathway.

Table 6.2. FTIR band assignments for PCL/*In Situ* HAPclay composite scaffolds

Band position (cm^{-1})	**Band assignment**	**Reference**
1559-1566	Asymmetric COO^- stretching	[116, 121]
1581-1583	Symmetric COO^- stretching	[122, 123]
1707-1710	Hydrogen bonded carbonyl groups in PCL	[124]
1723-1725	C=O stretching related to crystalline regions in PCL	[120]
1739-1741	C=O stretching related to amorphous regions in PCL	[120]
1295	C-O and C-C stretching in crystalline phase	[120, 125]
1194	OC-O stretching	[125]
605-608	ν_4 phosphate vibration	[126]
559-565	ν_4 phosphate vibration	[126]
581-586	out of plane bending of carbonyl groups from PCL	[127]
469, 479	ν_2 phosphate vibration from HAP/ Si-OSi deformation	[126]

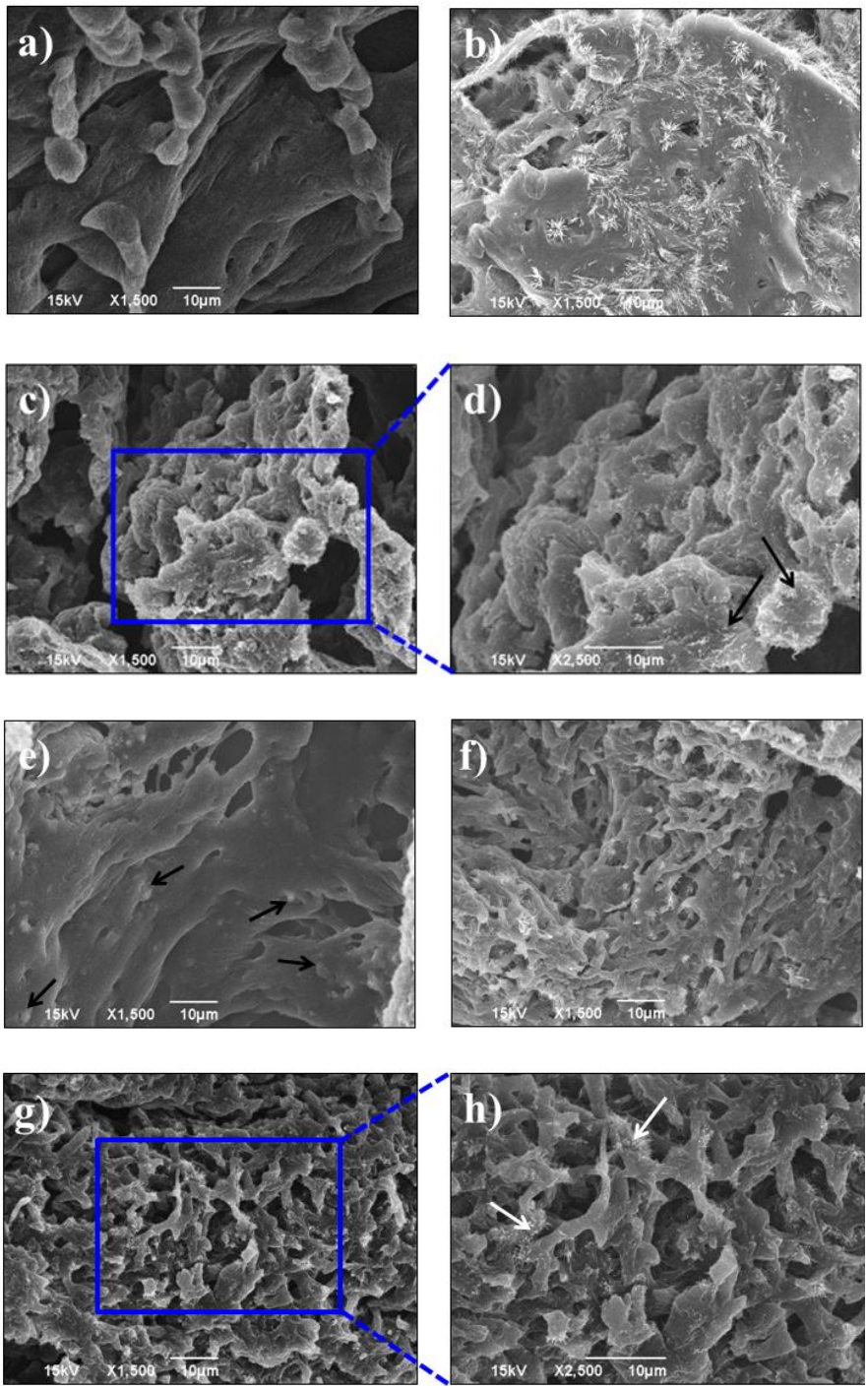

Figure 6.16. SEM micrographs of scaffolds from in vitro degradation experiments: PCL scaffolds – 0 days [a)], 14 days [b), m)], 18 days [c), d), n)], PCL scaffolds containing 10 wt % *in situ* HAPclay - 0 days [e)], 14 days [f), o)], 18 days [g), h), p)] and PCL scaffolds containing 20 wt % *in situ* HAPclay - 0 days [i)], 14 days [j), q)], 18 days [k), l), r)]. Arrows in image d) show filamentous features (~1-3 µm length, < 500 nm diameter) sprouted from degraded scaffold surfaces

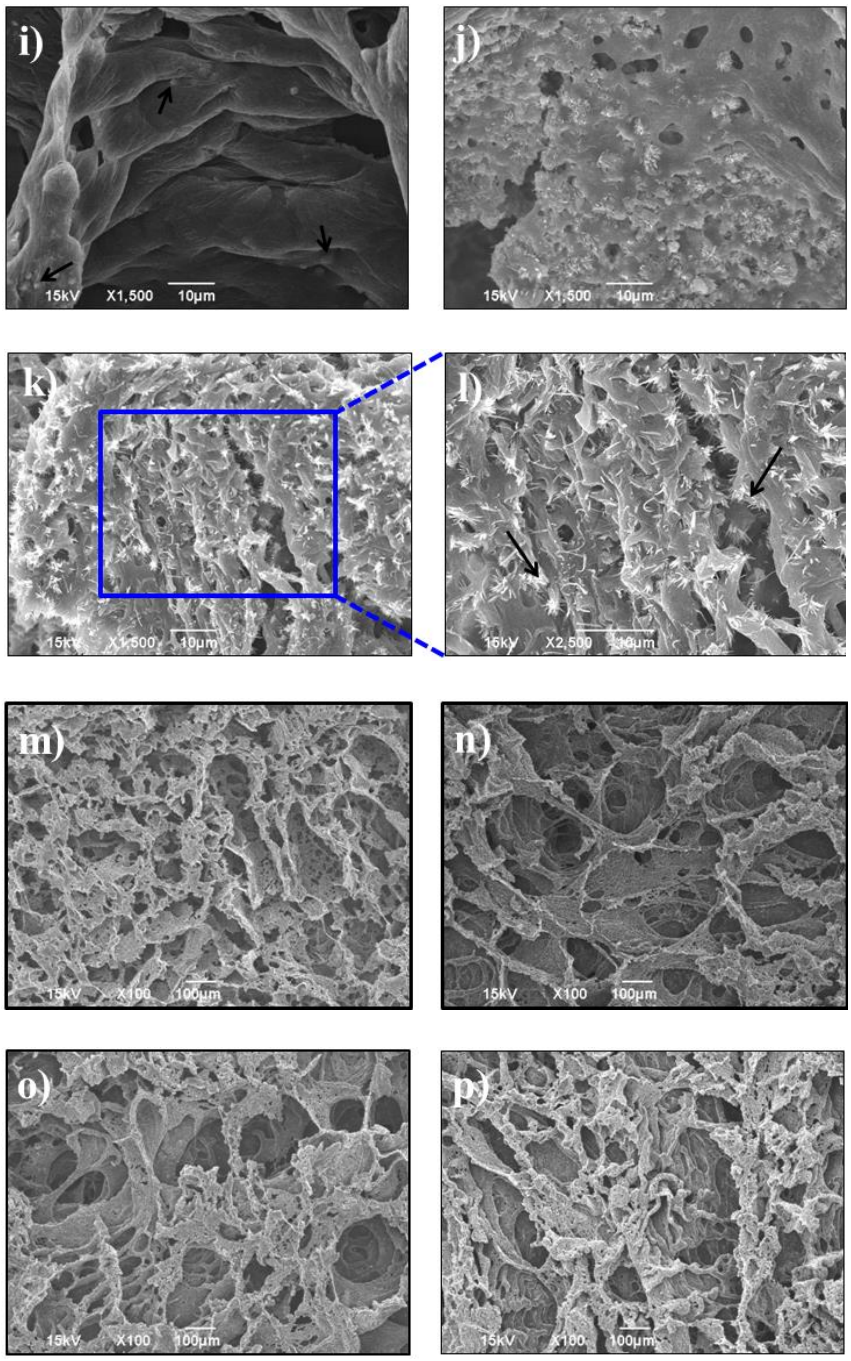

Figure 6.16. SEM micrographs of scaffolds from in vitro degradation experiments: PCL scaffolds – 0 days [a)], 14 days [b), m)], 18 days [c), d), n)], PCL scaffolds containing 10 wt % *in situ* HAPclay - 0 days [e)], 14 days [f), o)], 18 days [g), h), p)] and PCL scaffolds containing 20 wt % *in situ* HAPclay - 0 days [i)], 14 days [j), q)], 18 days [k), l), r)]. Arrows in image d) show filamentous features (~1-3 µm length, < 500 nm diameter) sprouted from degraded scaffold surfaces (continued)

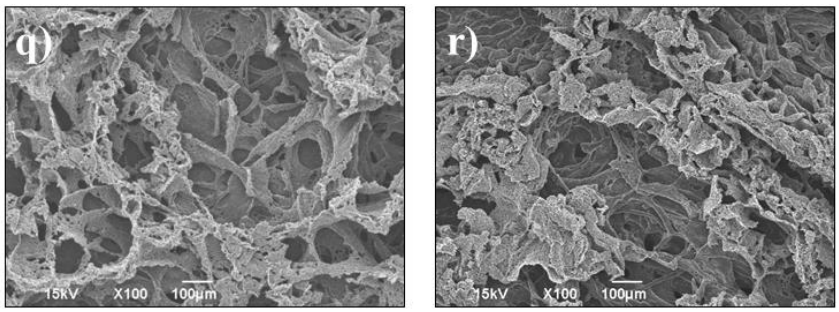

Figure 6.16. SEM micrographs of scaffolds from in vitro degradation experiments: PCL scaffolds – 0 days [a)], 14 days [b), m)], 18 days [c), d), n)], PCL scaffolds containing 10 wt % *in situ* HAPclay - 0 days [e)], 14 days [f), o)], 18 days [g), h), p)] and PCL scaffolds containing 20 wt % *in situ* HAPclay - 0 days [i)], 14 days [j), q], 18 days [k), l), r)]. Arrows in image d) show filamentous features (~1-3 µm length, < 500 nm diameter) sprouted from degraded scaffold surfaces (continued)

6.3.8. Scaffold Porosity

Mean values of percentage porosity evaluated for PCL and PCL/*in situ* HAPclay (10 wt %) scaffolds were 88.83 % and 86.06 % respectively (Figure 6.17.). The difference between the percentage porosity values was found to be statistically significant. Porosity of scaffolds has been reported for its effect on biological processes such as cell migration, vascularization, tissue formation along with nutrient transport, degradation and mechanical properties of the scaffold. Percentage porosity above 85 percent for PCL/*in situ* HAPclay scaffolds further indicates the suitability of these scaffolds for bone tissue engineering applications.

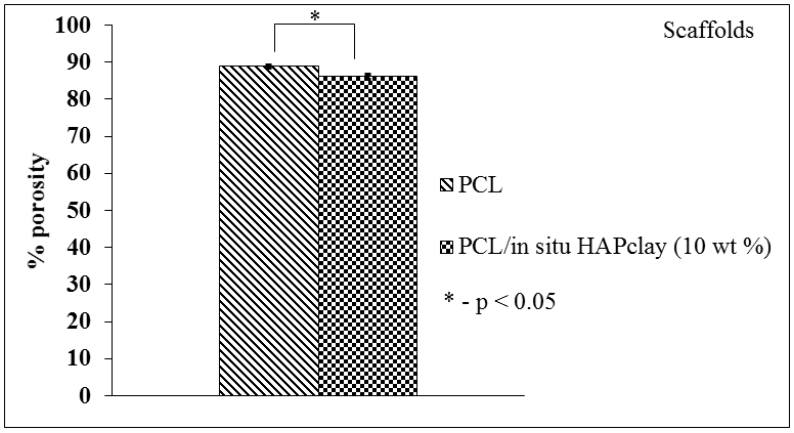

Figure 6.17. Porosity of PCL/*In Situ* HAPclay composite scaffolds

6.3.9. Compressive Mechanical Properties

Figure 16.18 shows comparative plot of elastic moduli of PCL scaffolds without in situ HAPclay and PCL/in situ HAPclay (10 wt %) composite scaffolds. PCL scaffolds containing in situ HAPclay (10 wt %) showed ~ 94 % increase in elastic modulus compared to the PCL scaffolds without in situ HAPclay (table 6.3.). Mechanical properties of scaffolds can be affected by factors such as porosity, pore size, interconnections between the scaffold pores apart from the interfacial interactions between the components used to fabricate scaffolds (e.g. PCL and in situ HAPclay in this case). The interdependency of these factors makes it difficult to attribute the change in mechanical properties of scaffolds to one of these factors. Mechanical properties including elastic modulus values of PCL composite scaffolds containing in situ HAPclay higher (>) than 10 wt % in situ HAPclay can depend on dispersion of in situ HAPclay in PCL and the extent of change in the polymer nucleation process, freezing kinetics during scaffold fabrication. Representative stress-strain curve for PCL composite scaffolds containing 10 wt % in situ HAPclay comprising of elastic region (a), plateau region (b) and densification (c) regions is shown in figure 16B. Presence of such regions have been reported to be observed in case of stress-strain curves of porous (cellular) materials [128]. Similar stress-strain curve is also observed for PCL scaffolds. The elastic region of stress-strain curve for PCL composite scaffolds containing 10 wt % in situ HAPclay appears to have a relatively steeper slope that indicates a higher elastic modulus compared to PCL scaffolds without in situ HAPclay.

Table 6.3. Compressive mechanical properties of PCL/*In Situ* HAPclay composite scaffolds

Sample	Elastic Modulus (MPa)	Standard deviation (MPa)	% increase
Polycaprolactone (PCL)	1.285	0.212	-
PCL with 10 wt % in situ HAPclay	2.495	0.146	94.16

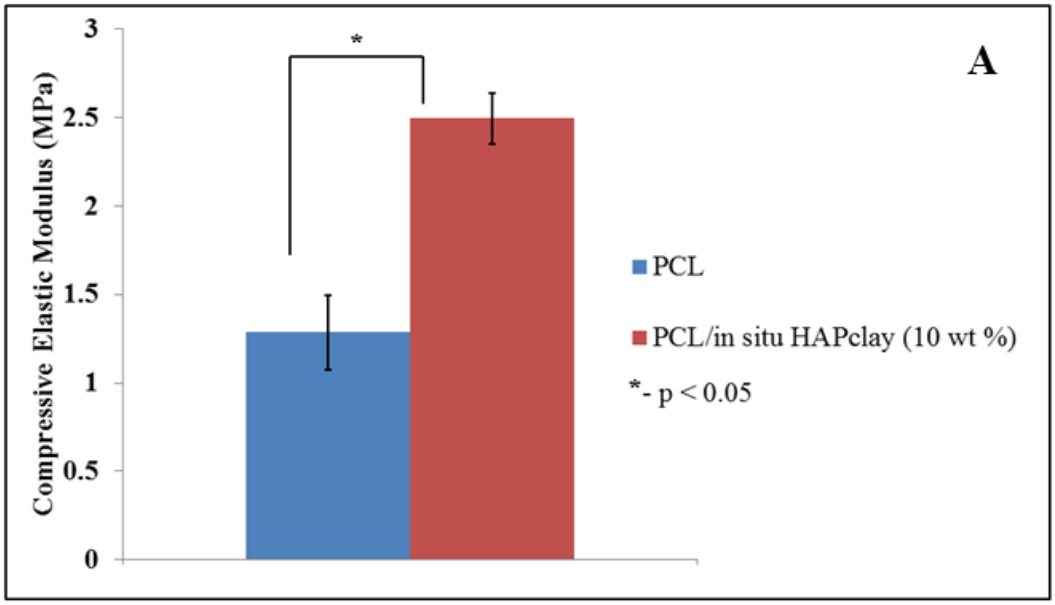

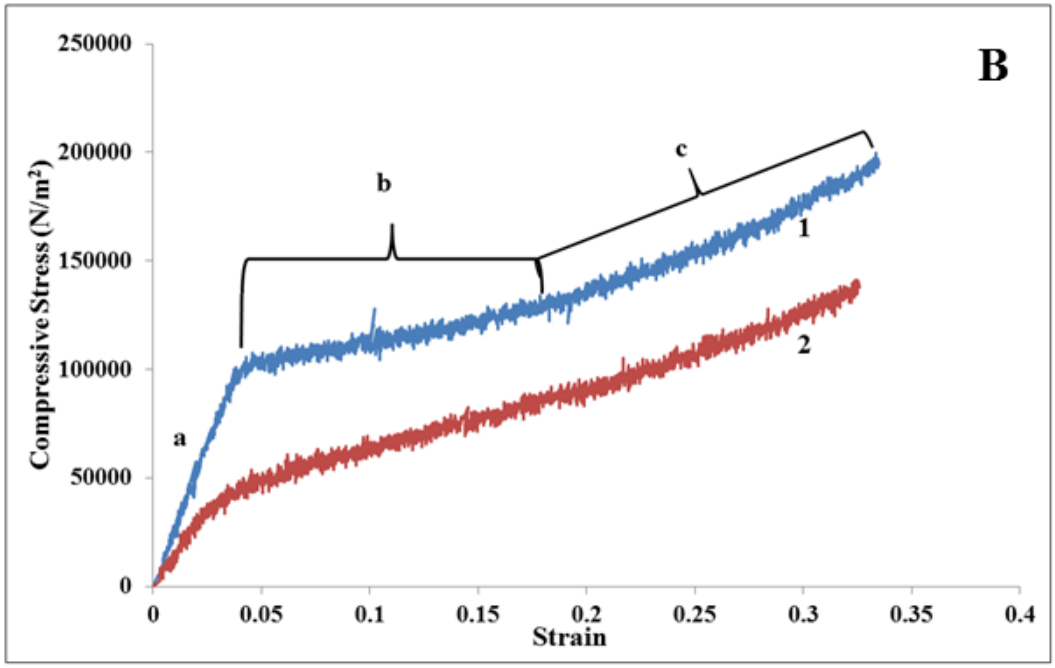

Figure 6.18. Compressive mechanical properties: A) compressive elastic moduli of PCL/*in situ* HAPclay (10 wt %) composite scaffolds, B) Representative stress-strain curves obtained for PCL and PCL/*in situ* HAPclay scaffolds- elastic region (a), plateau region (b) and densification region (c), Curves 1 and 2 represent stress-strain curves for PCL/*in situ* HAPclay (10 wt%) composite scaffolds and PCL scaffolds respectively

6.4. Conclusions

In situ HAPclay prepared based on biomineralization process and containing organomodified MMT clay associated with HAP was used to fabricate synthetic polycaprolactone (PCL) composite films and scaffolds. Incorporation of *in situ* HAPclay imparted osteoinductive and osteoconductive properties to PCL/*in situ* HAPclay films evidenced by formation of mineralized ECM by MSCs on these films in the absence of osteogenic supplements. Significant improvement in nanomechanical properties and subtle effects on sub-micron scale surface morphology were observed due to addition of *in situ* HAPclay in case of PCL/*in situ* HAPclay composite films. PCL/*in situ* HAPclay scaffolds showed a microstructure suitable for bone bone regeneration and their interior seemed to provide appropriate microenvironment for MSC attachment and their spatial organization. Cell culture assays indicated that PCL/*in situ* HAPclay composites (both scaffolds and films) provided suitable environment for MSC viability and influenced MSC differentiation. Increased degradation of PCL/*in situ* HAPclay composite scaffolds observed during accelerated in vitro degradation experiments suggested a role of *in situ* HAPclay in influencing degradation of slow degrading PCL (or polyester based) scaffolds. Also, considering these effects of *in situ* HAPclay on PCL/*in situ* HAPclay composites (films and scaffolds) extending from nanoscale to microscale suggests the potential of scaffold systems containing *in situ* HAPclay to satisfy multiple requirements of bone tissue engineering and also the ability of *in situ* HAPclay to impart multifunctional properties to resulting composites. AFM imaging experiments revealed that mineralized ECM formed by MSCs on PCL/*in situ* HAPclay composite films consisted of components of hierarchical organization known to exist in natural bone. These components (collagen and mineral) showed similarities with their natural bone counterparts with respect to their structure,

dimensions and arrangement. Formation of dense mineralized ECM and stacking of MSCs was observed on PCL/*in situ* HAPclay films during two-stage cell seeding experiment indicating its potential as a strategy to enhance tissue (bone) formation under in vitro conditions through cellular events similar to those observed in vivo during bone formation.

6.5. References

[1] Langer R, Vacanti JP. Tissue Engineering. Science. 1993;260:920-6.

[2] Murugan R, Ramakrishna S. Development of nanocomposites for bone grafting. Composites Science and Technology. 2005;65:2385-406.

[3] Zhou H, Lee J. Nanoscale hydroxyapatite particles for bone tissue engineering. Acta Biomaterialia. 2011;7:2769-81.

[4] Bose S, Tarafder S. Calcium phosphate ceramic systems in growth factor and drug delivery for bone tissue engineering: A review. Acta Biomaterialia. 2012;8:1401-21.

[5] Vallet-Regi M. Ceramics for medical applications. Journal of the Chemical Society, Dalton Transactions. 2001:97-108.

[6] LeGeros RZ. Calcium Phosphate-Based Osteoinductive Materials. Chemical Reviews. 2008;108:4742-53.

[7] Chai YC, Carlier A, Bolander J, Roberts SJ, Geris L, Schrooten J, et al. Current views on calcium phosphate osteogenicity and the translation into effective bone regeneration strategies. Acta Biomaterialia. 2012;8:3876-87.

[8] Chan CK, Kumar TSS, Liao S, Murugan R, Ngiam M, Ramakrishman S. Biomimetic nanocomposites for bone graft applications. Nanomedicine. 2006;1:177-88.

[9] Patel N, Best SM, Bonfield W, Gibson IR, Hing KA, Damien E, et al. A comparative study on the in vivo behavior of hydroxyapatite and silicon substituted hydroxyapatite granules. Journal of Materials Science:Materials in Medicine. 2002;13:1199-206.

[10] Thian ES, Huang J, Best SM, Barber ZH, Brooks RA, Rushton N, et al. The response of osteoblasts to nanocrystalline silicon-substituted hydroxyapatite thin films. Biomaterials. 2006;27:2692-8.

[11] Botelho CM, Brooks RA, Best SM, Lopes MA, Santos JD, Rushton N, et al. Human osteoblast response to silicon-substituted hydroxyapatite. Journal of Biomedical Materials Research Part A. 2006;79A:723-30.

[12] Vallet-Regi M. Revisiting ceramics for medical applications. Dalton Transactions. 2006:5211-20.

[13] Roether JA, Gough JE, Boccaccini AR, Hench LL, Maquet V, Jérôme R. Novel bioresorbable and bioactive composites based on bioactive glass and polylactide foams for bone tissue engineering. Journal of Materials Science: Materials in Medicine. 2002;13:1207-14.

[14] Xynos ID, Edgar AJ, Buttery LDK, Hench LL, Polak JM. Gene-expression profiling of human osteoblasts following treatment with the ionic products of Bioglass® 45S5 dissolution. Journal of Biomedical Materials Research. 2001;55:151-7.

[15] Xynos I, Edgar A, Buttery L, Hench L, Polak J. Ionic Products of Bioactive Glass Dissolution Increase Proliferation of Human Osteoblasts and induce Insulin-like Growth Factor II mRNA Expression and Protein Synthesis Biochemical and Biophysical Research Communications. 2000;276:461-5.

[16] Han P, Wu C, Xiao Y. The effect of silicate ions on proliferation, osteogenic differentiation and cell signalling pathways (WNT and SHH) of bone marrow stromal cells. Biomaterials Science. 2013;1:379-92.

[17] Giannelis EP. Polymer Layered Silicate Nanocomposites. Advanced Materials. 1996;8:29-35.

[18] Sinha Ray S, Okamoto M. Polymer/layered silicate nanocomposites: a review from preparation to processing. Progress in Polymer Science. 2003;28:1539-641.

[19] Depan D, Kumar AP, Singh RP. Cell proliferation and controlled drug release studies of nanohybrids based on chitosan-g-lactic acid and montmorillonite. Acta Biomaterialia. 2009;5:93-100.

[20] Katti KS, Katti DR, Dash R. Synthesis and characterization of a novel chitosan/montmorillonite/hydroxyapatite nanocomposite for bone tissue engineering. Biomedical Materials. 2008;3:12.

[21] Mieszawska AJ, Llamas JG, Vaiana CA, Kadakia MP, Naik RR, Kaplan DL. Clay enriched silk biomaterials for bone formation. Acta Biomaterialia. 2011;7:3036-41.

[22] Ambre AH, Katti DR, Katti KS. Nanoclays mediate stem cell differentiation and mineralized ECM formation on biopolymer scaffolds. Journal of Biomedical Materials Research Part A. 2013;101:2644-60.

[23] Goldberg M, Langer R, Jia XQ. Nanostructured materials for applications in drug delivery and tissue engineering. Journal of Biomaterials Science-Polymer Edition. 2007;18:241-68.

[24] Christenson EM, Anseth KS, van den Beucken L, Chan CK, Ercan B, Jansen JA, et al. Nanobiomaterial applications in orthopedics. Journal of Orthopaedic Research. 2007;25:11-22.

[25] Stevens MM, George JH. Exploring and Engineering the Cell Surface Interface. Science. 2005;310:1135-8.

[26] Okada A, Kawasumi M, Usuki A, Kojima Y, Kurauchi T, Kamigaito O. Synthesis and properties of nylon-6/clay hybrids. In Polymer based molecular composites MRS SymposiumProceedings (eds D W Schaefer & J E Mark). 1990;171:45-50.

[27] Chen GX, Hao GJ, Guo TY, Song MD, Zhang BH. Structure and mechanical properties of poly(3-hydroxybutyrateco-3-hydroxyvalerate) (PHBV)/clay nanocomposites. Journal of Materials Science Letters. 2002;21:1587-9.

[28] Pramanik M, Srivastava SK, Samantaray BK, Bhowmick AK. Rubber-clay nanocomposite by solution blending. Journal of Applied Polymer Science. 2003;87:2216-20.

[29] Messersmith PB, Giannelis EP. Synthesis and barrier properties of poly(ϵ-caprolactone)-layered silicate nanocomposites. Journal of Polymer Science Part A: Polymer Chemistry. 1995;33:1047-57.

[30] Yano K, Usuki A, Okada A, Kurauchi T, Kamigaito O. Synthesis and properties of polyimide-clay hybrid. Journal of Polymer Science Part A: Polymer Chemistry. 1993;31:2493-8.

[31] Bharadwaj RK. Modeling the Barrier Properties of Polymer-Layered Silicate Nanocomposites. Macromolecules. 2001;34:9189-92.

[32] Gilman JW. Flammability and thermal stability studies of polymer layered-silicate (clay) nanocomposites. Applied Clay Science. 1999;15:31-49.

[33] Gilman JW, Jackson CL, Morgan AB, R. H. Flammability Properties of Polymer−Layered-Silicate Nanocomposites. Polypropylene and Polystyrene Nanocomposites. Chemistry of Materials. 2000;12:1866-73.

[34] Sikdar D, Pradhan SM, Katti DR, Katti KS, Mohanty B. Altered Phase Model for Polymer Clay Nanocomposites. Langmuir. 2008;24:5599-607.

[35] Sikdar D, Katti DR, Katti KS. The role of interfacial interactions on the crystallinity and nanomechanical properties of clay-polymer nanocomposites: A molecular dynamics study. Journal of Applied Polymer Science. 2008;107:3137-48.

[36] Sikdar D, Katti D, Katti K, Mohanty, Bedabibhas. Influence of backbone chain length and functional groups of organic modifiers on crystallinity and nanomechanical properties of intercalated clay-polycaprolactam nanocomposites. International Journal of Nanotechnology. 2009;6:468-92.

[37] Carretero MI. Clay minerals and their beneficial effects upon human health. A review. Applied Clay Science. 2002;21:155-63.

[38] Viseras C, Aguzzi C, Cerezo P, Lopez-Galindo A. Uses of clay minerals in semisolid health care and therapeutic products. Applied Clay Science. 2007;36:37-50.

[39] Forni F, Iannuccelli V, Coppi G, Bernabei MT. Effect of Montmorillonite on Drug Release from Polymeric Matrices. Archiv der Pharmazie. 1989;322:789-93.

[40] Wen-Fu Lee, Yao-Tsung Fu. Effect of montmorillonite on the swelling behavior and drug-release behavior of nanocomposite hydrogels. Journal of Applied Polymer Science. 2003;89:3652-60.

[41] Lin F-H, Chen C-H, Cheng WTK, Kuo T-F. Modified montmorillonite as vector for gene delivery. Biomaterials. 2006;27:3333-8.

[42] Takahashi T, Yamada Y, Kataoka K, Nagasaki Y. Preparation of a novel PEG-clay hybrid as a DDS material: Dispersion stability and sustained release profiles. Journal of Controlled Release. 2005;107:408-16.

[43] Wang X, et al. Biopolymer/montmorillonite nanocomposite: preparation, drug-controlled release property and cytotoxicity. Nanotechnology. 2008;19:065707.

[44] Sun B, Ranganathan B, Feng S-S. Multifunctional poly(d,l-lactide-co-glycolide)/montmorillonite (PLGA/MMT) nanoparticles decorated by Trastuzumab for targeted chemotherapy of breast cancer. Biomaterials. 2008;29:475-86.

[45] Lin K-F, Hsu C-Y, Huang T-S, Chiu W-Y, Lee Y-H, Young T-H. A novel method to prepare chitosan/montmorillonite nanocomposites. Journal of Applied Polymer Science. 2005;98:2042-7.

[46] Marras SI, Kladi KP, Tsivintzelis I, Zuburtikudis I, Panayiotou C. Biodegradable polymer nanocomposites: The role of nanoclays on the thermomechanical characteristics and the electrospun fibrous structure. Acta Biomaterialia. 2008;4:756-65.

[47] Zheng JP, Wang CZ, Wang XX, Wang HY, Zhuang H, Yao KD. Preparation of biomimetic three-dimensional gelatin/montmorillonite-chitosan scaffold for tissue engineering. Reactive and Functional Polymers. 2007;67:780-8.

[48] Woodruff MA, Hutmacher DW. The return of a forgotten polymer—Polycaprolactone in the 21st century. Progress in Polymer Science. 2010;35:1217-56.

[49] Shi Y, Hu G, Su J, Li W, Chen Q, Shou P, et al. Mesenchymal stem cells: a new strategy for immunosuppression and tissue repair. Cell Res. 2010;20:510-8.

[50] Chen F, Tuan R. Mesenchymal stem cells in arthritic diseases. Arthritis Research & Therapy. 2008;10:223.

[51] Uccelli A, Pistoia V, Moretta L. Mesenchymal stem cells: a new strategy for immunosuppression? Trends in immunology. 2007;28:219-26.

[52] Otto W, Wright N. Mesenchymal stem cells: from experiment to clinic. Fibrogenesis & Tissue Repair. 2011;4:20.

[53] Han Z, Jing Y, Zhang S, Liu Y, Shi Y, Wei L. The role of immunosuppression of mesenchymal stem cells in tissue repair and tumor growth. Cell & Bioscience. 2012;2:8.

[54] Abumaree M, Jumah M, Pace R, Kalionis B. Immunosuppressive Properties of Mesenchymal Stem Cells. Stem Cell Reviews and Reports. 2012;8:375-92.

[55] Ghannam S, Bouffi C, Djouad F, Jorgensen C, Noel D. Immunosuppression by mesenchymal stem cells: mechanisms and clinical applications. Stem Cell Research & Therapy. 2010;1:2.

[56] Maxson S, Lopez EA, Yoo D, Danilkovitch-Miagkova A, LeRoux MA. Concise Review: Role of Mesenchymal Stem Cells in Wound Repair. Stem Cells Translational Medicine. 2012;1:142-9.

[57] Crha M, Necas A, Srnec R, Janovec J, Stehlik L, Rauser P, et al. Mesenchymal Stem Cells in Bone Tissue Regeneration and Application to Bone Healing. Acta Veterinaria Brno. 2009;78:635-42.

[58] Katti KS, Ambre AH, Peterka N, Katti DR. Use of unnatural amino acids for design of novel organomodified clays as components of nanocomposite biomaterials. Philosophical Transactions of The Royal Society A 2010;368:1963-80.

[59] Katti DR, Ghosh P, Schmidt S, Katti KS. Mechanical Properties of the Sodium Montmorillonite Interlayer Intercalated with Amino Acids. Biomacromolecules. 2005;6:3276-82.

[60] Ambre AH, Katti KS, Katti DR. Nanoclay Based Composite Scaffolds for Bone Tissue Engineering Applications. Journal of Nanotechnology in Engineering and Medicine. 2010;1:031013-9.

[61] Ambre A, Katti KS, Katti DR. In situ mineralized hydroxyapatite on amino acid modified nanoclays as novel bone biomaterials. Materials Science and Engineering: C. 2011;31:1017-29.

[62] Verma D, et al. Osteoblast adhesion, proliferation and growth on polyelectrolyte complex-hydroxyapatite nanocomposites. Philosophical Transactions of The Royal Society A Mathematical Physical and Engineering Sciences. 2010;368:2083.

[63] Khanna R, Katti KS, Katti DR. Bone nodules on chitosan–polygalacturonic acid–hydroxyapatite nanocomposite films mimic hierarchy of natural bone. Acta Biomaterialia. 2011;7:1173-83.

[64] Mikos AG, Lyman MD, Freed LE, Langer R. Wetting of poly(l-lactic acid) and poly(dl-lactic-co-glycolic acid) foams for tissue culture. Biomaterials. 1994;15:55-8.

[65] Mikos AG, Sarakinos G, Lyman MD, Ingber DE, Vacanti JP, Langer R. Prevascularization of porous biodegradable polymers. Biotechnology and Bioengineering. 1993;42:716-23.

[66] Chong EJ, Phan TT, Lim IJ, Zhang YZ, Bay BH, Ramakrishna S, et al. Evaluation of electrospun PCL/gelatin nanofibrous scaffold for wound healing and layered dermal reconstitution. Acta Biomaterialia. 2007;3:321-30.

[67] Xu CY, Inai R, Kotaki M, Ramakrishna S. Aligned biodegradable nanofibrous structure: a potential scaffold for blood vessel engineering. Biomaterials. 2004;25:877-86.

[68] Plaisant M, Giorgetti-Peraldi S, Gabrielson M, Loubat A, Dani C, Peraldi P. Inhibition of Hedgehog Signaling Decreases Proliferation and Clonogenicity of Human Mesenchymal Stem Cells. PLoS ONE. 2011;6:e16798.

[69] Oliver WC, Pharr GM. An improved technique for determining hardness and elastic modulus using load and displacement. Journal of Materials Research. 1992;7:1664-83.

[70] Karageorgiou V, Kaplan D. Porosity of 3D biomaterial scaffolds and osteogenesis. Biomaterials. 2005;26:5474-91.

[71] Simon JL, Roy TD, Parsons JR, Rekow ED, Thompson VP, Kemnitzer J, et al. Engineered cellular response to scaffold architecture in a rabbit trephine defect. Journal of Biomedical Materials Research Part A. 2003;66A:275-82.

[72] Scaglione S, Giannoni P, Bianchini P, Sandri M, Marotta R, Firpo G, et al. Order versus Disorder: in vivo bone formation within osteoconductive scaffolds. Sci Rep. 2012;2.

[73] Graziano A, d'Aquino R, Cusella-De Angelis MG, Laino G, Piattelli A, Pacifici M, et al. Concave Pit-Containing Scaffold Surfaces Improve Stem Cell-Derived Osteoblast Performance and Lead to Significant Bone Tissue Formation. PLoS ONE. 2007;2:e496.

[74] Yuan H, Kurashina K, de Bruijn JD, Li Y, de Groot K, Zhang X. A preliminary study on osteoinduction of two kinds of calcium phosphate ceramics. Biomaterials. 1999;20:1799-806.

[75] Zhang Q, Luo H, Zhang Y, Zhou Y, Ye Z, Tan W, et al. Fabrication of three-dimensional poly(ε-caprolactone) scaffolds with hierarchical pore structures for tissue engineering. Materials Science and Engineering: C. 2013;33:2094-103.

[76] Ratner B. Replacing and renewing: synthetic materials, biomimetics, and tissue engineering in implant dentistry. Journal of Dental Education. 2001;65:1340-7.

[77] Anderson JM, Rodriguez A, Chang DT. Foreign body reaction to biomaterials. Seminars in Immunology. 2008;20:86-100.

[78] Brown BN, Ratner BD, Goodman SB, Amar S, Badylak SF. Macrophage polarization: An opportunity for improved outcomes in biomaterials and regenerative medicine. Biomaterials. 2012;33:3792-802.

[79] Bryers JD, Giachelli CM, Ratner BD. Engineering biomaterials to integrate and heal: The biocompatibility paradigm shifts. Biotechnology and Bioengineering. 2012;109:1898-911.

[80] Garg K, Pullen NA, Oskeritzian CA, Ryan JJ, Bowlin GL. Macrophage functional polarization (M1/M2) in response to varying fiber and pore dimensions of electrospun scaffolds. Biomaterials. 2013;34:4439-51.

[81] Madden LR, Mortisen DJ, Sussman EM, Dupras SK, Fugate JA, Cuy JL, et al. Proangiogenic scaffolds as functional templates for cardiac tissue engineering. Proceedings of the National Academy of Sciences. 2010.

[82] Bota PCS, Collie AMB, Puolakkainen P, Vernon RB, Sage EH, Ratner BD, et al. Biomaterial topography alters healing in vivo and monocyte/macrophage activation in vitro. Journal of Biomedical Materials Research Part A. 2010;95A:649-57.

[83] Tsuruga E, Takita H, Itoh H, Wakisaka Y, Kuboki Y. Pore Size of Porous Hydroxyapatite as the Cell-Substratum Controls BMP-Induced Osteogenesis. The Journal of Biochemistry. 1997;121:317-24.

[84] Murphy CM, Haugh MG, O'Brien FJ. The effect of mean pore size on cell attachment, proliferation and migration in collagen–glycosaminoglycan scaffolds for bone tissue engineering. Biomaterials. 2010;31:461-6.

[85] Tang G, Zhang H, Zhao Y, Zhang Y, Li X, Yuan X. Preparation of PLGA Scaffolds with Graded Pores by Using a Gelatin-Microsphere Template as Porogen. Journal of Biomaterials Science, Polymer Edition. 2012;23:2241-57.

[86] Wuchter P, Boda-Heggemann J, Straub B, Grund C, Kuhn C, Krause U, et al. Processus and recessus adhaerentes: giant adherens cell junction systems connect and attract human mesenchymal stem cells. Cell and Tissue Research. 2007;328:499-514.

[87] Anderson HC. Molecular biology of matrix vesicles. Clinical orthopaedics and related research. 1995:266-80.

[88] Boonrungsiman S, Gentleman E, Carzaniga R, Evans ND, McComb DW, Porter AE, et al. The role of intracellular calcium phosphate in osteoblast-mediated bone apatite formation. Proceedings of the National Academy of Sciences. 2012.

[89] Bruder SP, Caplan AI. Cellular and Molecular Events During Embryonic Bone Development. Connective Tissue Research. 1989;20:65-71.

[90] Filipak M, Estervig DN, Tzen C-Y, Minoo P, Hoerl BJ, Maercklein PB, et al. Integrated Control of Proliferation and Differentiation of Mesenchymal Stem Cells. Environmental Health Perspectives. 1989;80:117-25.

[91] Whitfield MJ, Lee WCJ, Van Vliet KJ. Onset of heterogeneity in culture-expanded bone marrow stromal cells. Stem Cell Research. 2013;11:1365-77.

[92] Bellows CG, Aubin JE, Heersche JNM. Initiation and progression of mineralization of bone nodules formed in vitro: the role of alkaline phosphatase and organic phosphate. Bone and Mineral. 1991;14:27-40.

[93] Dorozhkin SV. Calcium orthophosphates. Journal of Materials Science. 2007;42:1061-95.

[94] Genge BR, Sauer GR, Wu LN, McLean FM, Wuthier RE. Correlation between loss of alkaline phosphatase activity and accumulation of calcium during matrix vesicle-mediated mineralization. Journal of Biological Chemistry. 1988;263:18513-9.

[95] Malaval L, Liu F, Roche P, Aubin JE. Kinetics of osteoprogenitor proliferation and osteoblast differentiation in vitro. Journal of Cellular Biochemistry. 1999;74:616-27.

[96] Turksen K, Aubin JE. Positive and negative immunoselection for enrichment of two classes of osteoprogenitor cells. The Journal of Cell Biology. 1991;114:373-84.

[97] Hauschka PV, Lian JB, Cole DE, Gundberg CM. Osteocalcin and matrix Gla protein: vitamin K-dependent proteins in bone. Physiological Reviews. 1989;69:990-1047.

[98] Kim E-K, Lim S, Park J-M, Seo JK, Kim JH, Kim KT, et al. Human mesenchymal stem cell differentiation to the osteogenic or adipogenic lineage is regulated by AMP-activated protein kinase. Journal of Cellular Physiology. 2012;227:1680-7.

[99] Olszta MJ, Cheng XG, Jee SS, Kumar R, Kim YY, Kaufman MJ, et al. Bone structure and formation: A new perspective. Materials Science & Engineering R-Reports. 2007;58:77-116.

[100] Revenko I, Sommer F, Minh DT, Garrone R, Franc J-M. Atomic force microscopy study of the collagen fibre structure. Biology of the Cell. 1994;80:67-9.

[101] Hassenkam T, Fantner GE, Cutroni JA, Weaver JC, Morse DE, Hansma PK. High-resolution AFM imaging of intact and fractured trabecular bone. Bone. 2004;35:4-10.

[102] Lin AC, Goh MC. Investigating the ultrastructure of fibrous long spacing collagen by parallel atomic force and transmission electron microscopy. Proteins: Structure, Function, and Bioinformatics. 2002;49:378-84.

[103] Fantner GE, Rabinovych O, Schitter G, Thurner P, Kindt JH, Finch MM, et al. Hierarchical interconnections in the nano-composite material bone: Fibrillar cross-links resist fracture on several length scales. Composites Science and Technology. 2006;66:1205-11.

[104] Paige MF, Rainey JK, Goh MC. Fibrous Long Spacing Collagen Ultrastructure Elucidated by Atomic Force Microscopy. Biophysical Journal. 1998;74:3211-6.

[105] Fang M, Holl MMB. Variation in type I collagen nanomorphology:the significance and origin. BoneKEy Reports International Bone and Mineral Society; 2013.

[106] Curtis A, Wilkinson C. Topographical control of cells. Biomaterials. 1997;18:1573-83.

[107] Chen W, Villa-Diaz LG, Sun Y, Weng S, Kim JK, Lam RHW, et al. Nanotopography Influences Adhesion, Spreading, and Self-Renewal of Human Embryonic Stem Cells. ACS Nano. 2012;6:4094-103.

[108] Meyle J, Gültig K, Brich M, Hämmerle H, Nisch W. Contact guidance of fibroblasts on biomaterial surfaces. Journal of Materials Science: Materials in Medicine. 1994;5:463-6.

[109] Chen S, Jones JA, Xu Y, Low H-Y, Anderson JM, Leong KW. Characterization of topographical effects on macrophage behavior in a foreign body response model. Biomaterials. 2010;31:3479-91.

[110] Wang T, Wang H, Li H, Gan Z, Yan S. Banded spherulitic structures of poly(ethylene adipate), poly(butylene succinate) and in their blends. Physical Chemistry Chemical Physics. 2009;11:1619-27.

[111] Yang P, Han Y. Crystal Growth Transition from Flat-On to Edge-On Induced by Solvent Evaporation in Ultrathin Films of Polystyrene-b-Poly(ethylene oxide). Langmuir. 2009;25:9960-8.

[112] Khanna R, Katti K, Katti D. Nanomechanics of Surface Modified Nanohydroxyapatite Particulates Used in Biomaterials. Journal of Engineering Mechanics. 2009;135:468-78.

[113] Discher DE, Janmey P, Wang Y-l. Tissue Cells Feel and Respond to the Stiffness of Their Substrate. Science. 2005;310:1139-43.

[114] Buxboim A, Ivanovska IL, Discher DE. Matrix elasticity, cytoskeletal forces and physics of the nucleus: how deeply do cells 'feel' outside and in? Journal of Cell Science. 2010;123:297-308.

[115] Woodward SC, Brewer PS, Moatamed F, Schindler A, Pitt CG. The intracellular degradation of poly(ε-caprolactone). Journal of Biomedical Materials Research. 1985;19:437-44.

[116] Raghavan D, Egwim K. Degradation of polyester film in alkali solution. Journal of Applied Polymer Science. 2000;78:2454-63.

[117] Htay AS, Teoh SH, Hutmacher DW. Development of perforated microthin poly(ε-caprolactone) films as matrices for membrane tissue engineering. Journal of Biomaterials Science, Polymer Edition. 2004;15:683-700.

[118] Sikdar D, Katti D, Katti K, Mohanty, Bedabibhas. Effect of Organic Modifiers on Dynamic and Static Nanomechanical Properties and Crystallinity of Intercalated Clay–Polycaprolactam Nanocomposites. Journal of Applied Polymer Science. 2007;105:790-802.

[119] Lam CXF, et al. Dynamics of in vitro polymer degradation of polycaprolactone-based scaffolds: accelerated versus simulated physiological conditions. Biomedical Materials. 2008;3:034108.

[120] Coleman MM, Zarian J. Fourier-transform infrared studies of polymer blends. II. Poly(ϵ-caprolactone)–poly(vinyl chloride) system. Journal of Polymer Science: Polymer Physics Edition. 1979;17:837-50.

[121] Partini M, Pantani R. FTIR analysis of hydrolysis in aliphatic polyesters. Polymer Degradation and Stability. 2007;92:1491-7.

[122] Socrates G. Infrared and Raman Characteristic Group Frequencies. Third Edition ed: John Wiley & Sons Ltd.; 2001.

[123] Medhat I, Nada A, Kamal DE. Density functional theory and FTIR spectroscopic study of carboxyl group. Indian Journal of Pure and Applied Physics. 2005;43:911-7.

[124] Kuo SW, Huang CF, Chang FC. Study of hydrogen-bonding strength in poly(ϵ-caprolactone) blends by DSC and FTIR. Journal of Polymer Science Part B: Polymer Physics. 2001;39:1348-59.

[125] Elzubair A, Elias CN, Suarez JCM, Lopes HP, Vieira MVB. The physical characterization of a thermoplastic polymer for endodontic obturation. Journal of Dentistry. 2006;34:784-9.

[126] Fowler BO. Infrared studies of apatites. I. Vibrational assignments for calcium, strontium, and barium hydroxyapatites utilizing isotopic substitution. Inorganic Chemistry. 1974;13:194-207.

[127] Tadokoro H, Kobayashi M, Yoshidome H, Tai K, Makino D. Structural Studies of Polyesters. II. Far-Infrared Spectra of Aliphatic Polyesters: Comparison with α-Polyamides. The Journal of Chemical Physics. 1968;49:3359-73.

[128] Gibson LJ, Ashby MF. Cellular solids : structure and properties. 2nd Edition ed. New York: Cambridge University Press; 1999.

CHAPTER 7. CELL DEPENDENT BONE MINERAL FORMATION ON TISSUE ENGINEERING COMPOSITES CONTAINING NANOCLAYS WITH BIOMINERALIZED HYDROXYAPATITE

This chapter presents a brief overview of bone mineral formation mechanisms and studies related to cell dependent bone mineral formation on polycaprolactone (PCL) composites containing nanoclays with biomineralized hydroxyapatite (*in situ* HAPclay). Observations made from scanning electron microscopy (SEM) studies on PCL composite composites containing *in situ* HAPclay seeded with human mesenchymal stem cells (MSCs) and results obtained from SEM-EDS (energy dispersive spectroscopy) experiments performed on these cell seeded composites constitute a major part of this chapter.

7.1. Introduction

Mineralization is considered an important process due to its fundamental relationship to human health, development and its proposed role in different types of bone diseases. The role of collagen and the associated non-collagenous proteins in extracellular mineralization of bone has been widely reported in literature. Understanding mechanisms responsible for bone mineral formation continue to be a part of several studies till date and it has been difficult to reach consensus on a specific mechanism being responsible for mineralization in bone. There seems to be a renewed interest in studies related to mineralization processes involving cells [1]. A major focus of such studies has been the role of matrix vesicles in bone mineral formation. Observations made during recent studies [1, 2] suggest relation between intracellular processes and bone mineral formation.

Matrix vesicles are “membrane-invested” particles released by “budding” and “pinching” of plasma membranes of cells such as osteoblasts, chondrocytes and odontoblasts [3, 4]. Their

diameter can vary from 30 nm to one micron or more [3] and have been reported to be located at the sites of initial mineralization (or where mineralization will commence) in the extracellular matrix (ECM). In case of bone, matrix vesicles are positioned in the developing osteoid under osteoblast surfaces. Matrix vesicles are composed of "vesicle sap" enclosed by a membrane and are considered as sites of initial appearance of bone mineral crystals. These crystals are closely associated with the inner layer of the vesicular membrane. Also, these crystalline mineral particles appear after the vesicles are released in the ECM and are further immobilized in collagenous matrix of the ECM [3]. Crystals in the matrix vesicles break the vesicular membrane and are known to guide crystal growth known to form mineral spherules. Bone mineralization involving matrix vesicles is considered biphasic. First stage involves formation of mineral crystals in matrix vesicles followed by breaking of vesicular membrane. Subsequently, the mineral crystals are exposed to extracellular fluid consisting of ions (calcium and phosphate), pH conditions of the extracellular fluid and molecules (e.g. proteoglycans, non-collagenous proteins) in the extracellular environment that are considered to affect mineral crystal growth. Initial stage of mineral formation is controlled by enzymes, proteins and phospholipid membrane of the matrix vesicle. Since all these factors affecting initial mineral formation originate from the cells that give rise to matrix vesicles, the initial stage of mineral formation is considered to be under cellular control.

The uncertainty over presence of mineral in the vesicles emerging from the cells in to the ECM has been discussed in several studies related to mineralization. The presence of amorphous calcium phosphate in intracellular matrix vesicles and the transport of such calcium phosphate containing vesicles from intracellular to extracellular space was suggested through experimental investigation involving electron microscopy, electron energy loss spectroscopy (EELS) in one of

the recent studies [1]. This study suggested involvement of simultaneously occurring processes/routes during bone mineralization. Similarly, presence of amorphous phosphate in intracellular vesicles and the involvement of these vesicles in bone mineralization was suggested in another study involving use of electron microscopy techniques. [2]. Most studies related to bone mineral formation have been performed using samples prepared using mineralized nodules formed by inducing cells with osteogenic supplements, tissue sections and tissue fragments. In this work, human mesenchymal stem cells (MSCs) seeded on a synthetic substrate composed of polycaprolactone (PCL) incorporated with *in situ* HAPclay (nanoclay with biomineralized hydroxyapatite) showed attachment and were also able to form mineralized ECM (discussed in Chapter 9). This synthetic substrate designed for bone regeneration applications was able to stimulate the human MSCs to form mineralized ECM without the use of osteogenic supplements or any externally applied stimuli. In this study, we hypothesize that bone mineral formation mechanism on an engineered substrate such as PCL/*in situ* HAPclay substrate (film) is similar to mineral formation mechanism proposed in case of natural bone. This similarity pertains to composition and transport of matrix vesicles involved in mineral formation in natural bone. Investigating the mineralized ECM and studying the morphology, composition, transport (delivery) of matrix vesicles present in the mineralized ECM were the objectives of this study. SEM imaging was used to perform qualitative studies related to cell dependent mineralization on these MSC seeded PCL/*in situ* HAPclay synthetic substrates and SEM-EDS (energy dispersive spectroscopy) was used to study the composition of matrix vesicles. Through these studies we attempt to understand the suitability of synthetic polymer composites containing *in situ* HAPclay for providing an environment assisting cellular processes involved in bone mineral formation.

7.2. Materials and Methods

7.2.1. Materials

Sodium-montmorillonite (Na-MMT) clay, Swy-2 (Crook County, Wyoming), having a cation exchange capacity (CEC) of 76.4 mequiv./100 g and sourced from the Clay Minerals Repository at the University of Missouri, Columbia was used to prepare modified MMT clay. 5-aminovaleric acid for modifying MMT clay, polycaprolactone (PCL) (average M_n = 80,000) and 1,4 dioxane (anhydrous, 99.8 %) for scaffold preparation were obtained from Sigma Aldrich. Sodium phosphate (Na_2HPO_4) and calcium chloride ($CaCl_2$) required for preparing *in situ* HAPclay were obtained from J.T. Baker and EM Sciences respectively. Human MSCs from bone marrow (PT-2501, Lonza,Walkersville, MD.) were cultured in cell culture medium made by adding MSCGM™ SingleQuots™ (PT-4105) to mesenchymal stem cell basal medium (MSCBM™, PT-3238). These two components of cell culture medium available as MSCGM™ (mesenchymal stem cell growth medium) Bullekit™ were purchased from Lonza, Walkersville, MD.

7.2.2. Preparation of Modified MMT Clay and *In Situ* HAPclay

Na-MMT was modified with 5-aminovaleric acid (unnatural amino acid) according to the procedure described in our previous studies [5-8]. Briefly, 5-aminovaleric acid solution (pH=1.8 & temperature = 60°C) prepared in DI water was added to Na-MMT clay suspension in DI water (pre-heated to 60°C) and the resultant mixture was stirred vigorously for an hour. The stirred mixture was centrifuged for removal of DI water, washed further for removal of chloride ions, subsequently dried at 70°C followed by grinding and sieving to obtain a fine powder.

In situ HAPclay was prepared according to procedure described in our earlier studies [7, 8]. A suspension of modified MMT clay in Na_2HPO_4 solution was prepared by dispersing

modified MMT clay in Na_2HPO_4 solution and further stirring it for 2 hours. $CaCl_2$ solution (39.8 mM) was further added to this suspension and the resulting mixture (at pH=7.4) was stirred for 8 hours. Precipitates formed were allowed to settle, centrifuged to remove water, dried at 70°C and then sieved after grinding to obtain a fine powder.

7.2.3. Preparation of Polycaprolactone (PCL)/*In Situ* HAPclay Films (Substrates)

PCL (0.09 grams/ml dioxane) was dissolved in 1, 4 dioxane at room temperature. For preparing PCL composite films containing 10 wt % in situ HAPclay, PCL (3.6 grams) was initially dissolved in 40 ml 1, 4 dioxane to obtain PCL solution. Further, a sonicated suspension of *in situ* HAPclay (0.4 grams in 16 ml dioxane) was added to the PCL solution. The resulting solution was stirred for 2 hours, further transferred to glass Petri dishes and then dried for 72 hours to obtain PCL/*in situ* HAPclay (10 wt %) composite films. Samples of ~12.7 mm diameter were punched out from these dried films (~85 mm diameter) for cell culture experiments.

7.2.4. Cell Culture

PCL/*in situ* HAPclay composite film samples (~12.7 mm diameter) in 24-well plates were UV sterilized and further immersed in 70 % alcohol overnight to wet these hydrophobic polyester (PCL) based film samples [9-12]. The wetted PCL composite film samples were washed with PBS twice and then incubated in PBS (6 hours) for removal of alcohol. PBS was then removed and after 24 hours of subsequent incubation at 37°C, 5 % CO_2 in cell culture medium 7.36×10^4 cells human MSCs were seeded in each well on the PCL/*in situ* HAPclay composite film samples. The cell seeded samples were incubated at 37°C, 5 % CO_2 under humidified conditions for 41 days.

A separate two-stage cell seeding experiment was performed using PCL/in situ HAPclay composite films. After sterilization, wetting, washing and incubation (in cell culture media), 7.36

x 10^4 human MSCs were seeded in each well (of 24-well plate) on PCL/10 wt% *in situ* HAPclay composite film samples. Following incubation of these MSC seeded composite films for 24 days at 37°C, 5 % CO_2, human MSCs (7.36 x 10^4) were again seeded on these films. PCL composite films thus seeded two times with human MSCs were incubated further up to 41^{st} day. MSCs up to passage 5 were used for all cell culture experiments.

7.2.5. Scanning Electron Microscopy (SEM) and SEM-EDS (Energy Dispersive Spectroscopy)

SEM was used to perform imaging on MSC seeded PCL/*in situ* HAPclay films. For this purpose, JEOL JSM-6490LV scanning electron microscope was used. After removing the MSC seeded film samples from culture, these samples were washed with phosphate buffer saline (PBS), fixed using glutaraldehyde (2.5%), subsequently dehydrated using ethanol series (10 % v/v, 30 % v/v, 50 % v/v, 70 % v/v and 100 %) and then dried after 100 % ethanol was replaced with hexamethyldisilazane. SEM imaging was then performed on the dried samples after coating them with gold and mounting them on a SEM sample stub. SEM-EDS experiments were also performed on these MSC seeded film samples after fixing, dehydration in ethanol series and drying. In SEM-EDS, a sample is bombarded with electrons (or electron beam) that causes emission of X-rays of characteristic energies to be emitted from the spots where the electron beam bombards the sample. An energy dispersive spectrometer consisting of a detector detects the X-rays having different energies. X-ray spectrum is then generated with y-axis showing the number of counts (corresponding to number of X-rays detected and processed by the detector) and x-axis showing the energy levels of these counts. Since each element has a unique atomic structure and characteristic X-ray energy, an X-ray spectrum consisting of elemental peaks is generated and is useful to know elemental composition of a sample. Number of counts

corresponding to these peaks are used to calculate the ratios of elements present in a sample. JEOL JSM-6490LV scanning electron microscope equipped with an energy dispersive spectrometer was used in this study. X-ray spectra were obtained from different spots corresponding to matrix vesicles formed at various locations on MSC seeded PCL composite films. These spectra were then used to determine the Ca and P composition (atom %) for different spots and Ca/P ratio for each of these spots was subsequently calculated. Number of points were then grouped according to the range of Ca/P ratio as shown in tables 7.1. and 7.2.

7.3. Results and Discussion

Figures 7.1. and 7.2. show SEM images of PCL/*in situ* HAPclay films seeded with human MSCs after 41 days of cell culture. SEM images obtained from two-stage cell seeding experiment are shown in Figure 7.2. In addition to the attachment of human MSCs, these images also indicate formation of mineralized ECM by the seeded MSCs. Magnified regions of images e), g), i), k) in Figure 7.1. outlined by green squares are represented by images f), h), j), l) in the same figure. These images indicate that the mineralized regions consist of smaller structures having spherical features. These spherical structures known as matrix vesicles appear to have different sizes. The size of most of these vesicles was in the sub-micron to below ten micrometers range. Some of these images also indicate that the vesicles fuse or aggregate to form complex structures having size above ten micrometers. SEM images in Figure 7.2. obtained from two-stage cell seeding experiment (described under section 7.2.4.) also indicate formation of matrix vesicles and these vesicles show similarity in size, organization with those shown in Figure 7.1. The vesicles appear to be closely associated with cellular protrusions (lamellipodia, filopodia) and thus seem to be emerging from the attached cells to the extracellular environment as observed in images c) and d) in Figure 7.1. The size of these vesicles emerging from the cells

was in 0.5 micrometer to 0.7 micrometer range, which is closer to the size of the vesicles reported in other studies [2, 3].

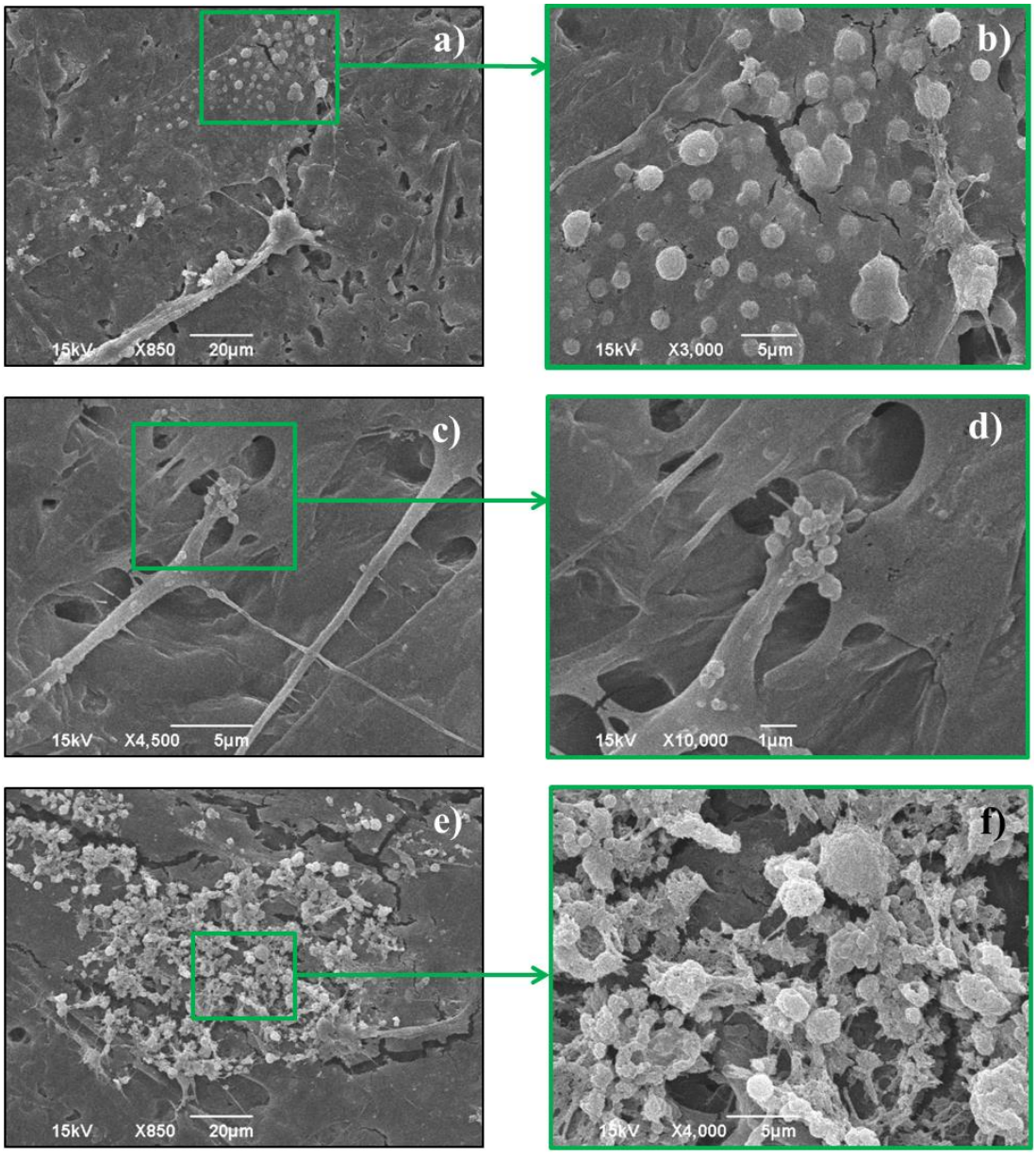

Figure 7.1. SEM images (a-r) of PCL/*in situ* HAPclay (10 wt %) films seeded with human MSCs showing presence of matrix vesicles after 41 days of culture. Images b, d, f, h, j, l represent magnified regions of images a, c, e, g, i, k (outlined by green squares) and indicate presence of structures with spherical features (also known as matrix vesicles) with size in the sub-micron to below ten micrometers range. Images c, d show vesicles to be associated with cellular protrusions. (Detailed explanation given under 7.3. Results and Discussion)

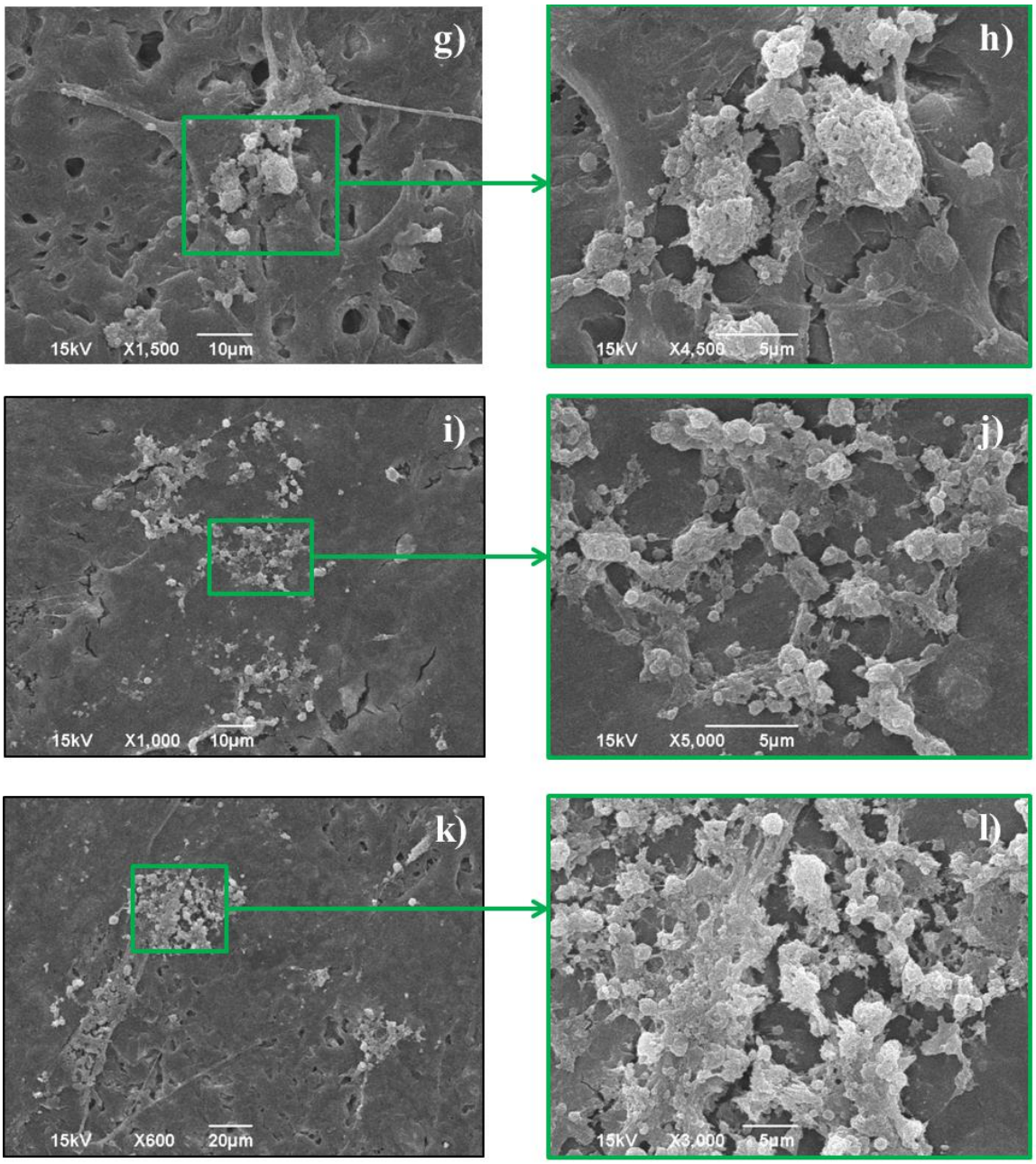

Figure 7.1. SEM images (a-r) of PCL/*in situ* HAPclay (10 wt %) films seeded with human MSCs showing presence of matrix vesicles after 41 days of culture. Images b, e, f, h, j, l represent magnified regions of images a, c, e, g, i, k (outlined by green squares) and indicate presence of structures with spherical features (also known as matrix vesicles) with size in the sub-micron to below ten micrometers range. Images c, d show vesicles to be associated with cellular protrusions. (Detailed explanation given under 7.3. Results and Discussion) (continued)

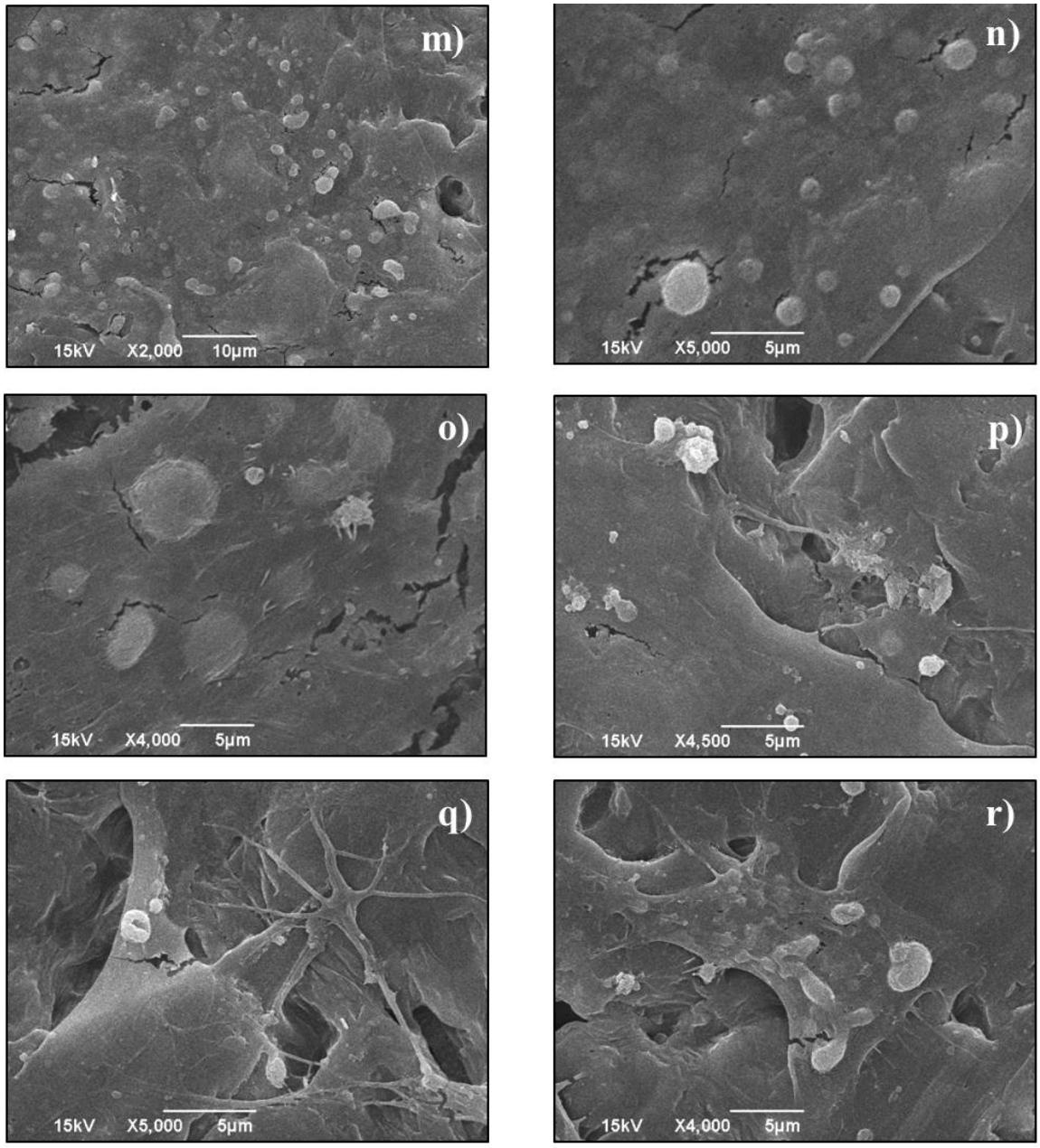

Figure 7.1. SEM images (a-r) of PCL/*in situ* HAPclay (10 wt %) films seeded with human MSCs showing presence of matrix vesicles after 41 days of culture. Images b, e, f, h, j, l represent magnified regions of images a, c, e, g, i, k (outlined by green squares) and indicate presence of structures with spherical features (also known as matrix vesicles) with size in the sub-micron to below ten micrometers range. Images c, d show vesicles to be associated with cellular protrusions. (Detailed explanation given under 7.3. Results and Discussion) (continued)

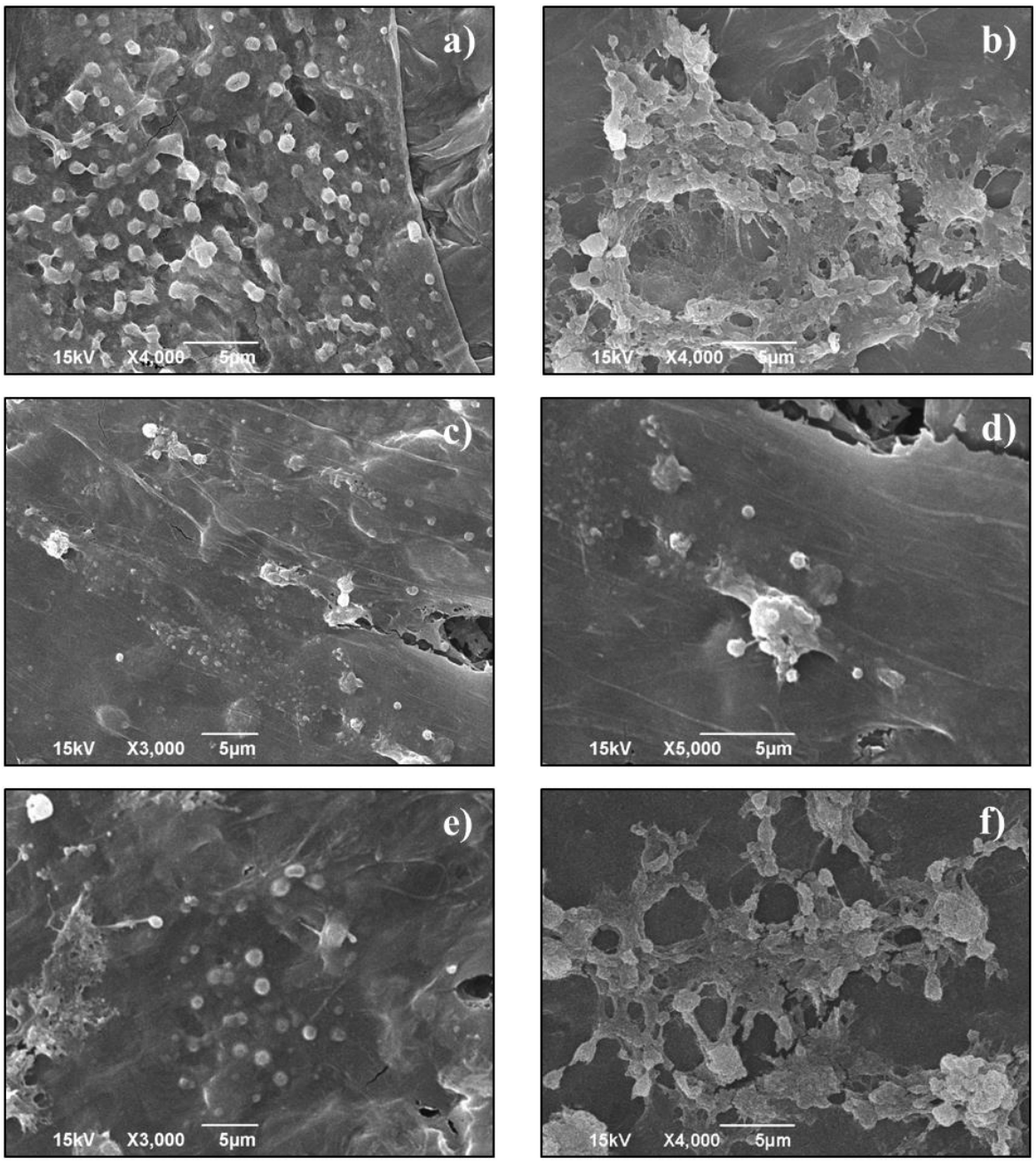

Figure 7.2. SEM images (a-h) of PCL/*in situ* HAPclay (10 wt %) films seeded twice with human MSCs during two-stage cell seeding experiment showing presence of matrix vesicles. Image h represents magnified region of image g. Structures with spherical features (also known as matrix vesicles) shown in these images have size in the sub-micron to below ten micrometers range. (Detailed explanation given under 7.3. Results and Discussion)

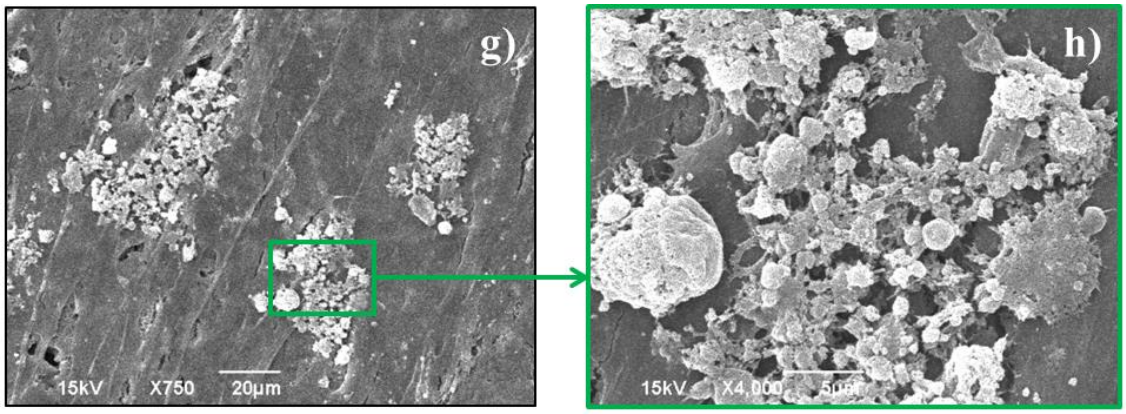

Figure 7.2. SEM images (a-h) of PCL/*in situ* HAPclay (10 wt %) films seeded twice with human MSCs during two-stage cell seeding experiment showing presence of matrix vesicles. Image h represents magnified region of image g. Structures with spherical features (also known as matrix vesicles) shown in these images have size in the sub-micron to below ten micrometers range. (Detailed explanation given under 7.3. Results and Discussion) (continued)

A closer observation of images shown in Figures 7.1. and 7.2. indicates the vesicles to be either embedded within the cells or closely associated with the surface of the cells. It can be possible that these vesicles are present under the surface of cells. Such vesicles are seen in images b), m) - r) in Figure 7.1. and images a) – e) in figure 7.2. The size of some of the vesicles observed in these images was closer to one micrometer and below that suggests that these can be intracellular vesicles. Similar observations were made in another study where cryo-SEM was used to study mouse bones and vesicles closer to one micrometer size were suggested to be intracellular vesicles containing bone mineral [2].

SEM-EDS experiments were also performed to detect the presence of calcium and phosphorus in the matrix vesicles formed on MSC seeded PCL/*in situ* HAPclay films. Figure 7.3. shows images indicating different sites/points (represented by numbers) on these samples used for obtaining EDS data. Similarly, images indicating data points are also shown in Figure 7.4. for SEM-EDS performed on samples seeded twice with MSCs (during two-stage cell seeding experiment). Tables 7.1. and 7.2. represent calcium to phosphorus (Ca/P) ratio obtained

from SEM-EDS experiments. Data presented in these tables is for points selected on matrix vesicles while performing SEM-EDS experiments. Localized elemental data (calcium and phosphorus percentage) was obtained from these points.

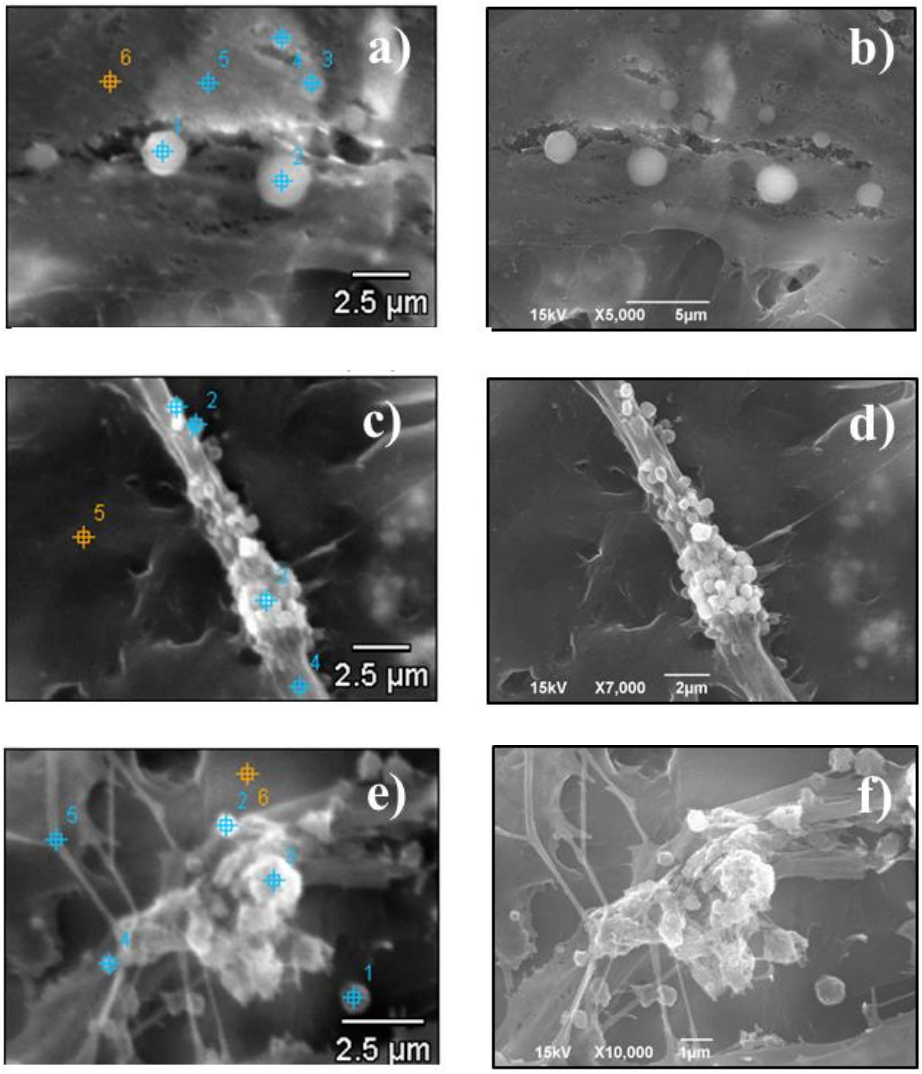

Figure 7.3. SEM images (a-l) obtained during SEM-EDS experiment indicating different points used for obtaining SEM-EDS data for matrix vesicles formed on MSC seeded PCL/*in situ* HAPclay (10 wt %) films. Blue and yellow points shown in left hand side images represent the spots from which localized elemental data (calcium and phosphorus percentage) was obtained during SEM-EDS experiments. Images on the right hand side [b), d), f), h), j), l)] are shown for better visualization of the features seen in images a), c), e), g), i), k)

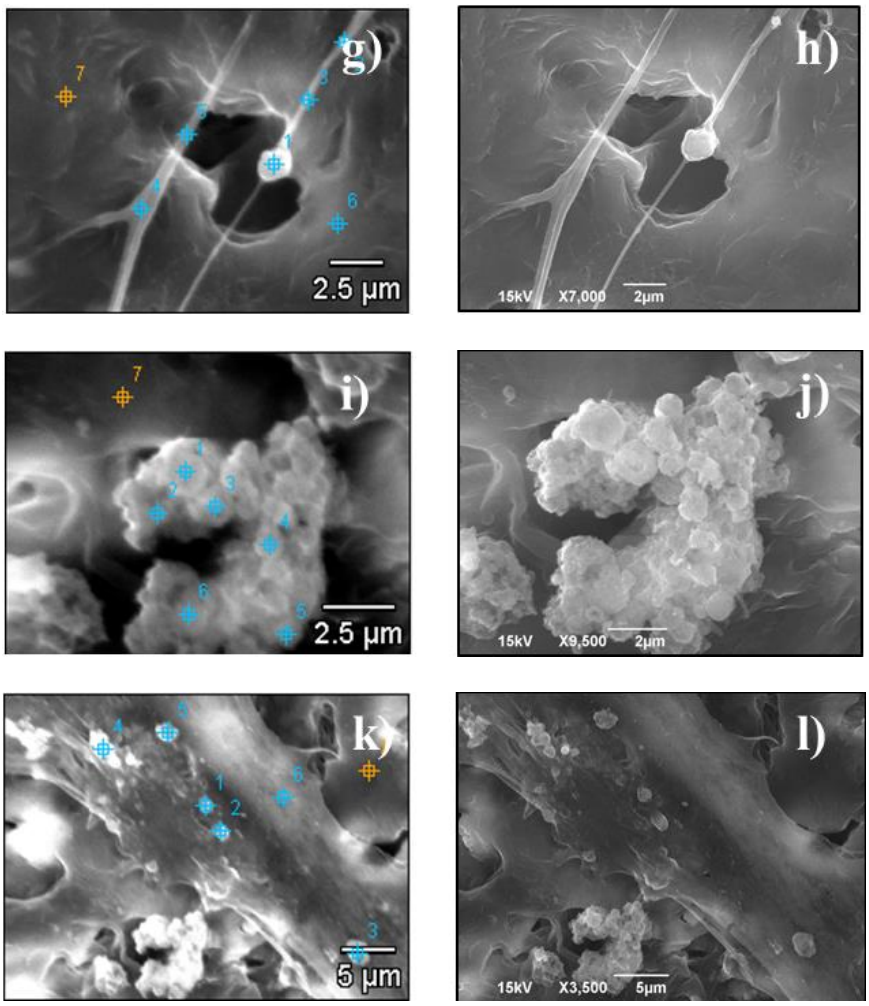

Figure 7.3. SEM images (a-l) obtained during SEM-EDS experiment indicating different points used for obtaining SEM-EDS data for matrix vesicles formed on MSC seeded PCL/*in situ* HAPclay (10 wt %) films. Blue and yellow points shown in left hand side images represent the spots from which localized elemental data (calcium and phosphorus percentage) was obtained during SEM-EDS experiments. Images on the right hand side [b), d), f), h), j), l)] are shown for better visualization of the features seen in images a), c), e), g), i), k) (continued)

Previous studies involving SEM-EDS analysis of matrix vesicles have implicitly suggested presence of calcium phosphate based minerals in matrix vesicles based on calcium and phosphorous detected during SEM-EDS experiments [1, 2]. Presence of calcium and phosphorus detected by SEM-EDS in this study is thus suggestive of calcium phosphate in the matrix vesicles. Hydroxyapatite (HAP) containing calcium and phosphorus constitutes approximately 60 weight percent of bone. Stoichiometric HAP with chemical formula $Ca_{10}(PO_4)_6(OH)_2$ has

Ca/P ratio of 1.67. However, in case of natural bone it is known that Ca/P ratio can be non-stoichiometric due to substitution of calcium, phosphate or hydroxyl ions by ions such as carbonate, zinc and silicon. The non-stoichiometric ratios have also been associated with bone maturity, bone site and bone disease [13, 14]. The Ca/P ratios obtained from SEM-EDS experiments vary from less than 1 to 1.8. Most of these ratios are non-stoichiometric (< 1.67 for stoichiometric hydroxyapatite). Studies have related Ca/P ratios of mineral containing matrix vesicles to polyphosphates present in matrix vesicles that increase the local concentration of phosphates in the vesicles that can be responsible for Ca/P ratios lower than 1.67 [2, 15]. Ca/P ratios lower than one have also been associated with new bone formation in these studies indicating the effect of polyphosphates on Ca/P ratios.

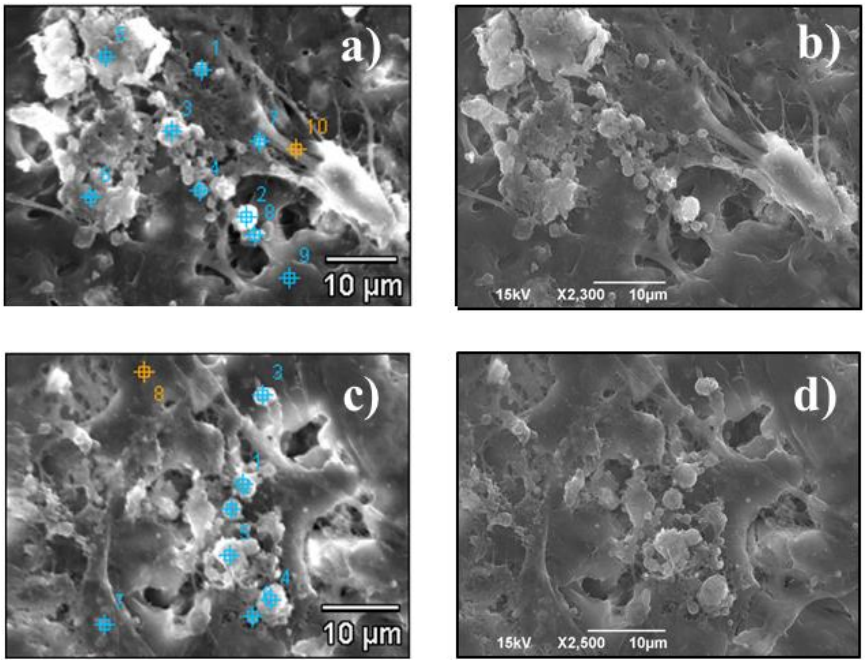

Figure 7.4. SEM images (a-j) obtained during SEM-EDS experiment indicating different points used for obtaining SEM-EDS data for matrix vesicles formed on MSC seeded PCL/*in situ* HAPclay (10 wt %) films during two-stage cell seeding experiment. Blue and yellow points represent the spots from which localized elemental data (calcium and phosphorus percentage) was obtained during SEM-EDS experiments. Images on the right hand side [b), d), f), h), j)] are shown for better visualization of the features seen in images a), c), e), g), i)

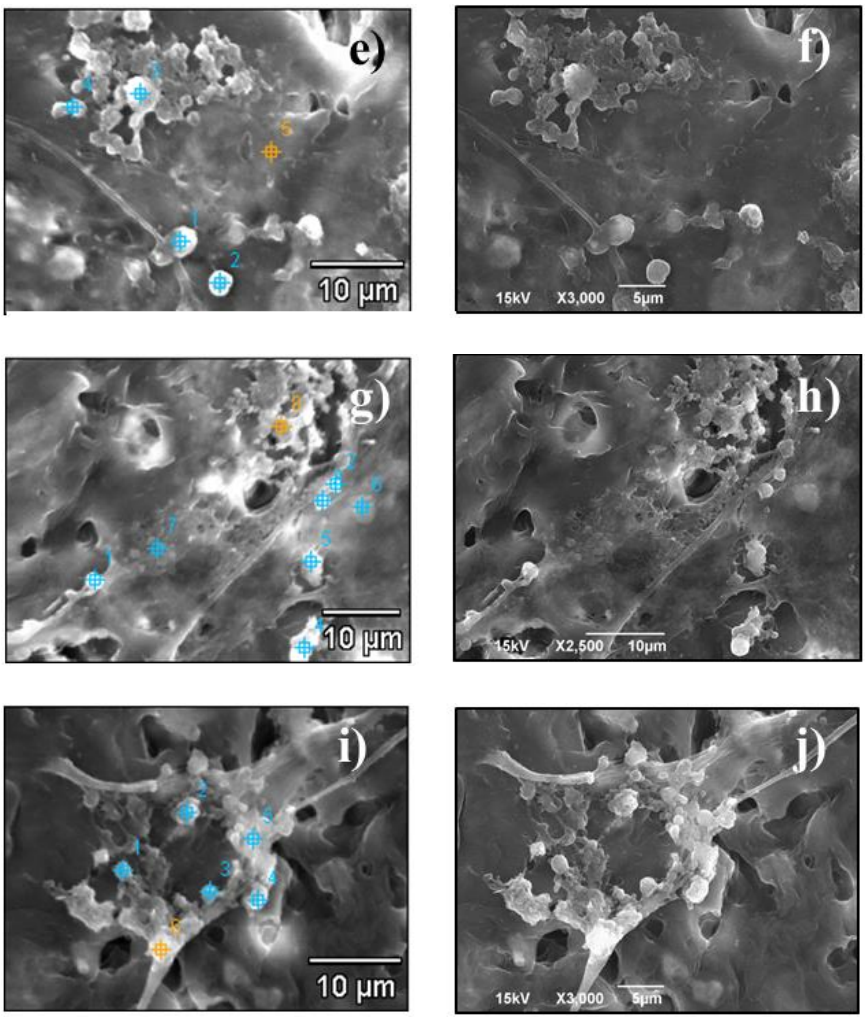

Figure 7.4. SEM images (a-j) obtained during SEM-EDS experiment indicating different points used for obtaining SEM-EDS data for matrix vesicles formed on MSC seeded PCL/*in situ* HAPclay (10 wt %) films during two-stage cell seeding experiment. Blue and yellow points represent the spots from which localized elemental data (calcium and phosphorus percentage) was obtained during SEM-EDS experiments. Images on the right hand side [b), d), f), h), j)] are shown for better visualization of the features seen in images a), c), e), g), i) (continued)

7.4. Conclusions

SEM imaging experiments performed on PCL/*in situ* HAPclay composite films seeded with human MSCs indicated formation of matrix vesicles. These vesicles appeared to be emerging from the cells attached to the PCL/*in situ* HAPclay composite films and also to be deposited in the extracellular space. SEM images also indicated presence of vesicles embedded

in the cells or under the surface of cells. This further suggested the presence of intracellular vesicles. Data obtained from SEM-EDS experiments showed presence of calcium and phosphate in the vesicles. Ca/P ratios calculated using EDS data showed values ranging from below 1 to those closer to the stoichiometric value of 1.67. These values suggested an ongoing process of mineralization and new bone formation. Also, these studies show that PCL/*in situ* HAPclay composites besides being osteinductive are also capable of providing a favorable micro-environment for cell dependent processes involved in bone mineral formation.

Table 7.1. Calcium to phosphorus (Ca/P) ratios for matrix vesicles obtained from SEM-EDS experiments performed on matrix vesicles formed on MSC seeded PCL/*in situ* HAPclay (10 wt %) composite films

Ca/P ratio	Number of Points
0.7 – 0.8	0
0.8 – 0.9	2
0.9 – 1.0	2
1.0 – 1.1	1
1.1 – 1.2	4
1.2 – 1.3	3
1.3 – 1.4	8
1.4 – 1.5	4
1.5 – 1.6	6
1.6 – 1.7	0
1.7 – 1.8	1

Table 7.2. Calcium to phosphorus (Ca/P) ratios for matrix vesicles obtained from SEM-EDS experiments performed on matrix vesicles formed on PCL/*in situ* HAPclay (10 wt %) films during two-stage cell seeding experiment

Ca/P Ratio	Number of Points
0.7 – 0.8	1
0.8 – 0.9	1
0.9 – 1.0	2
1.0 – 1.1	1
1.1 – 1.2	3
1.2 – 1.3	6
1.3 – 1.4	4
1.4 – 1.5	2
1.5 – 1.6	2
1.6 – 1.7	1
1.7 - 1.8	1

7.5. References

[1] Boonrungsiman S, Gentleman E, Carzaniga R, Evans ND, McComb DW, Porter AE, et al. The role of intracellular calcium phosphate in osteoblast-mediated bone apatite formation. Proceedings of the National Academy of Sciences. 2012.

[2] Mahamid J, Sharir A, Gur D, Zelzer E, Addadi L, Weiner S. Bone mineralization proceeds through intracellular calcium phosphate loaded vesicles: A cryo-electron microscopy study. Journal of Structural Biology. 2011;174:527-35.

[3] Anderson HC. Molecular biology of matrix vesicles. Clinical orthopaedics and related research. 1995:266-80.

[4] Anderson HC. Matrix vesicles and calcification. Current Rheumatology Reports. 2003;5:222-6.

[5] Katti KS, Ambre AH, Peterka N, Katti DR. Use of unnatural amino acids for design of novel organomodified clays as components of nanocomposite biomaterials. Philosophical Transactions of The Royal Society A 2010;368:1963-80.

[6] Ambre AH, Katti KS, Katti DR. Nanoclay Based Composite Scaffolds for Bone Tissue Engineering Applications. Journal of Nanotechnology in Engineering and Medicine. 2010;1:031013-9.

[7] Ambre A, Katti KS, Katti DR. In situ mineralized hydroxyapatite on amino acid modified nanoclays as novel bone biomaterials. Materials Science and Engineering: C. 2011;31:1017-29.

[8] Ambre AH, Katti DR, Katti KS. Nanoclays mediate stem cell differentiation and mineralized ECM formation on biopolymer scaffolds. Journal of Biomedical Materials Research Part A. 2013;101:2644-60.

[9] Mikos AG, Lyman MD, Freed LE, Langer R. Wetting of poly(l-lactic acid) and poly(dl-lactic-co-glycolic acid) foams for tissue culture. Biomaterials. 1994;15:55-8.

[10] Mikos AG, Sarakinos G, Lyman MD, Ingber DE, Vacanti JP, Langer R. Prevascularization of porous biodegradable polymers. Biotechnology and Bioengineering. 1993;42:716-23.

[11] Chong EJ, Phan TT, Lim IJ, Zhang YZ, Bay BH, Ramakrishna S, et al. Evaluation of electrospun PCL/gelatin nanofibrous scaffold for wound healing and layered dermal reconstitution. Acta Biomaterialia. 2007;3:321-30.

[12] Xu CY, Inai R, Kotaki M, Ramakrishna S. Aligned biodegradable nanofibrous structure: a potential scaffold for blood vessel engineering. Biomaterials. 2004;25:877-86.

[13] Gu C, Katti DR, Katti KS. Photoacoustic FTIR spectroscopic study of undisturbed human cortical bone. Spectrochimica Acta Part A: Molecular and Biomolecular Spectroscopy. 2013;103:25-37.

[14] Tzaphlidou M. Bone Architecture: Collagen Structure and Calcium/Phosphorus Maps. Journal of Biological Physics. 2008;34:39-49.

[15] Omelon S, Georgiou J, Henneman ZJ, Wise LM, Sukhu B, Hunt T, et al. Control of Vertebrate Skeletal Mineralization by Polyphosphates. PLoS ONE. 2009;4:e5634.

CHAPTER 8. CONCLUSIONS

Use of modified sodium montmorillonite (Na-MMT) clay for designing polymeric scaffolds useful for bone regeneration is a major focus of this work. Bone regeneration strategies based on tissue engineering principles that involve use of scaffolds are driven by multiple challenges associated with these scaffolds. Scaffolds need to be capable of eliciting favorable cell response and also provide enough mechanical support until the regenerating tissue can support itself or becomes capable of restoring function at the defect site. Requirements of osteoinductivity and osteoconductivity along with adequate mechanical properties enhances the complexity of designing scaffolds for bone regeneration. Na-MMT clay was used in this work considering its widely reported reinforcing ability in case of polymer-clay nanocomposites (PCNs). Two different types of polymer, both natural and synthetic, were used for designing polymeric scaffolds containing modified Na-MMT clay and investigated further for bone tissue engineering applications.

A molecular level materials design strategy was used in which Na-MMT clay was modified with three different unnatural amino acids. Unnatural amino acids were used considering the bicompatibility requirements for tissue engineering, longer backbone chain of these amino acids and their previously reported use for pharmaceutical applications. X-ray diffraction (XRD) experiments indicated that the unnatural amino acids were able to intercalate Na-MMT clay. Fourier Transform Infrared (FTIR) spectroscopy studies on these modified nanoclays suggested non-bonded molecular level interactions between the intercalated amino acids and Na-MMT clay. Previous molecular dynamics simulation studies of PCNs in our group had revealed that such non-bonded interactions between the constituents (modifier, clay and polymer) of PCNs have a significant effect on the mechanical properties of PCNs. This further

indicated the potential of Na-MMT clay modified with unnatural amino acids to influence the mechanical properties and their use for preparing PCNs. Cell culture experiments performed using the unnatural amino acid modified nanoclays indicated their biocompatibility with bone forming cells (osteoblasts).

Na-MMT clay modified with 5-aminovaleric acid was used to fabricate natural polymer based composite scaffolds. For this purpose, 5-aminovaleric modified nanoclay was incorporated in a polyelectrolyte complex formed between natural polymers such as chitosan (Chi) and polygalacturonic acid (PgA). The ChiPgA biopolymer based composite scaffolds containing 5-aminovaleric acid modified nanoclay satisfied the basic requirements of tissue engineering and showed bicompatibility with osteoblasts (bone cells). Similarities were also observed in proliferation of osteoblasts between ChiPgA scaffolds containing modified Na-MMT clay and ChiPgA scaffolds containing hydroxyapatite (HAP). HAP is known for its favorable cell response and similarity of modified clay containing scaffolds with HAP containing scaffolds with respect to cell proliferation indicated the potential of modified Na-MMT clay to elicit favorable cell response for tissue engineering applications.

Considering the requirements of osteoconductivity and osteoinductivity along with mechanical properties for scaffolds, HAP was mineralized in modified Na-MMT clay based on the process of biomineralization in bone. The nanoclay-HAP hybrid (*in situ* HAPclay) thus prepared was used to fabricate ChiPgA composites. FTIR studies indicated the role of functional groups of the intercalated modifier in nucleation of HAP along with molecular interactions between modified Na-MMT clay and mineralized HAP. Formation of osteoblast clusters considered to be an important event in bone formation was observed on ChiPgA/*in situ* HAPclay composites that suggested the osteoconductive properties of these composites.

Human mesenchymal stem cells (MSCs) were able to form mineralized ECM in ChiPgA/*in situ* HAPclay composite scaffolds and formed mineralized extracellular matrix (ECM) on ChiPgA/in situ HAPclay composite films. Formation of mineralized ECM and nodules in the absence of osteogenic supplements demonstrated the osteoinductive and osteoconductive potential of ChiPgA/*in situ* HAPclay composite systems. This also implied the ability of *in situ* HAPclay to impart osteoinductivity, osteoconductivity to the resulting polymer composites. During these studies, it was also observed that the order of mixing of *in situ* HAPclay with Chi and PgA had an effect on the microstructure of the fabricated scaffolds and also the response of human MSCs to the ChiPgA/*in situ* HAPclay composite films. ChiPgA/*in situ* HAPclay scaffolds also supported the viability and differentiation of MSCs.

Two-stage cell seeding experiment involving human MSCs was introduced as a strategy to enhance amount of bone tissue formation under in vitro conditions and approaching the difficulties related to repair of large tissue defects. Complexities related to MSC proliferation and differentiation, ability of ECM proteins to assist cell proliferation and differentiation were considered while performing two-stage cell seeding experiment involving MSCs. Qualitative data obtained from this experiment showed formation of relatively dense ECM and larger size nodules on the ChiPgA/*in situ* HAPclay composites.

Polycaprolactone (PCL), a synthetic polymer, was used to prepare PCL/*in situ* HAPclay composites (scaffolds and films) and these composites were investigated for their use in stem cell based bone regeneration. *In situ* HAPclay appeared to affect the microstructure of PCL composite scaffolds and these scaffolds showed pore size range considered useful for bone regeneration. Human MSCs seeded on PCL/*in situ* HAPclay films were able to form mineralized ECM in absence of osteogenic supplements and appeared to form cell layers on these composites

during two-stage cell seeding experiment. Formation of such cell layers indicated possible similarities with cellular events known to take place during embryonic stages of bone formation. ECM formation by MSCs in absence of osteogenic supplements indicated the osteoinductive and osteoconductive properties of PCL composites. MSCs were also able to infiltrate the interior of the PCL composite scaffolds and also appeared to be remain viable, differentiate in these scaffolds. Atomic force microscopy (AFM) imaging of mineralized ECM formed on PCL composites showed presence of collagen and mineral. Collagen and mineral are important constituents of hierarchical organization in bone and in case of in vitro generated ECM formed on PCL/*in situ* HAPclay composites these components showed similarities in their organization, dimensions with their natural bone counterparts. Addition of *in situ* HAPclay led to significant increase (~ 100 to 595 %) in nanomechanical properties of PCL composites and increase in degradation of PCL/*in situ* HAPclay composite scaffolds under accelerated conditions. The observed effects of *in situ* HAPclay on PCL/in situ HAPclay composites extending from nanoscale to micron scale suggests the potential of scaffold systems containing *in situ* HAPclay to meet the multiple requirements of bone tissue engineering.

Scanning electron microscopy (SEM) experiments showed vesicles emerging from the cells attached to the PCL/*in situ* HAPclay composites and being deposited in the extracellular space. SEM-EDS showed presence of calcium and phosphorous in these vesicles that suggested presence of calcium phosphate in these vesicles. PCL/*in situ* HAPclay thus also seemed to provide favorable environment for cellular processes involved in bone mineral formation.

In situ HAPclay was incorporated in two different polymer systems (natural and synthetic) to prepare polymeric composites for bone tissue engineering applications in this work. These polymer composite systems showed osteinductive and osteoinductive behavior that

emphasizes the ability of in situ HAPclay to impart osteinductivity, osteoconductivity to polymer composite scaffold systems. Along with the potential of *in situ* HAPclay to influence the mechanical properties of composites for bone tissue engineering, this work also puts forth the utility of Na-MMT clay as a promising cell-instructive material.

CHAPTER 9. FUTURE WORK

Polymeric composites (scaffolds and films) containing unnatural amino acid modified nanoclay and *in situ* HAPclay were fabricated for bone tissue engineering applications in this work. Investigations performed during this work showed that nanoclays can be useful for designing scaffolds with biomimetic environment for bone regeneration. Based on the understanding gained about biomaterials and their interactions with relevant cells for bone regeneration during this work, following suggestions can be made for future research:

1. As a step towards clinical application of the fabricated polymer composite scaffolds, it can be useful to investigate the response of immune/inflammatory cells to the fabricated scaffolds. Understanding gained from such investigation can lead to better design of scaffolds for avoiding foreign body reaction and increase the possibilities of their transition towards clinical applications.
2. Human mesenchymal stem cells (MSCs) were used in this work. These cells are known for their immunosuppressive effects. Polymer composite scaffolds fabricated in this work can be seeded with MSCs and used for understanding the interaction between MSCs and the cells of immune system.
3. Comparative studies can be performed between scaffolds having diversity in their structure at the sub-micron to microscale and scaffolds having a uniform structure at a similar scale with respect to their interactions with cells.
4. Tissue or bone defects can be of irregular shapes. Scaffolds in tissue engineering need to conform to the shape of these defects. Studies related to load transfer through such irregularly shaped scaffolds can lead to better design of scaffolds for in vivo bone

formation and improve understanding about the effect of mechanical loads on bone regeneration and remodeling.